Carbon Monoxide Hydrogenation using Ruthenium Catalysts

Jan Hendrik Blank

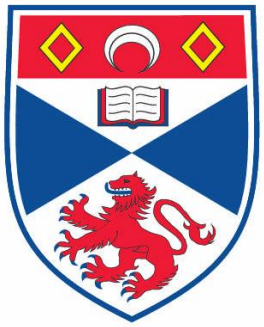

This thesis is submitted in partial fulfilment for the degree of PhD
at the
University of St Andrews

May 4th 2012

1. Candidate's declarations:

I, Jan Hendrik Blank, hereby certify that this thesis, which is approximately 75,000 words in length, has been written by me, that it is the record of work carried out by me and that it has not been submitted in any previous application for a higher degree.

I was admitted as a research student in January 2008 and as a candidate for the degree of PhD in January 2008; the higher study for which this is a record was carried out in the University of St Andrews between 2008 and 2012.

Date May 2nd 2012 Signature of Candidate

2. Supervisor's declaration:

I hereby certify that the candidate has fulfilled the conditions of the Resolution and Regulations appropriate for the degree of Doctor of Philisophy in the University of St Andrews and that the candidate is qualified to submit this thesis in application for that degree.

Date ...10th May, 2012 Signature of Supervisor .....

3. Permission for electronic publication: (*to be signed by both candidate and supervisor*)

In submitting this thesis to the University of St Andrews I understand that I am giving permission for it to be made available for use in accordance with the regulations of the University Library for the time being in force, subject to any copyright vested in the work not being affected thereby. I also understand that the title and the abstract will be published, and that a copy of the work may be made and supplied to any bona fide library or research worker, that my thesis will be electronically accessible for personal or research use unless exempt by award of an embargo as requested below, and that the library has the right to migrate my thesis into new electronic forms as required to ensure continued access to the thesis. I have obtained any third-party copyright permissions that may be required in order to allow such access and migration, or have requested the appropriate embargo below.

The following is an agreed request by candidate and supervisor regarding the electronic publication of this thesis:

Embargo on both all of printed copy and electronic copy for the same fixed period of five years on the following ground(s):

Publication would be commercially damaging to the researcher, or to the supervisor, or the University;

Date 10th May 2012 Signature of Candidate .....

Signature of Supervisor .....

University of St Andrews
from first to foremost

600 YEARS
1413 – 2013

School of Chemistry
Prof D. J. Cole-Hamilton

10th May, 2012

To whom it may concern
Request for embargo on publication of the Thesis of Jan H. Blank

I write in support of the request for a five year embargo on the publication of Jan Blank's Thesis, entitled:

Carbon monoxide hydrogenation using ruthenium catalysts in phosphonium ionic liquid media

Jan was sponsored by Eastman Chemical Company, a commercial organisation based in the United States. The terms of the contract under which we have carried out the work include a ban on publishing without specific permission from the company. Although some of the work has been cleared for publication, much of it has not. We, therefore, request the embargo so that we can obtain the necessary permissions for publication in the open literature.

David Cole-Hamilton
Irvine Professor of Chemistry
PhD Supervisor to Jan Blank

Purdie Building, North Haugh, St Andrews, Fife KY16 9ST
Direct Line: +44 (0) 1334 463805 School Office: +44 (0) 1334 463800 Fax: +44 (0) 1334 463808
e-mail: djc@st-andrews.ac.uk
WWW: http://ch-www.st-and.ac.uk/eastchem/profiles/sta/cole-hamilton.html

UNIVERSITY OF ST ANDREWS

REGISTRY – STUDENT OFFICE

EXAMINATION FOR THE DEGREE OF Ph.D
(by research thesis)

Special Circumstances Form

(*to be completed by the candidate*)

Name of Candidate: Jan Hendrik Blank

ID Number: 070014692

Department / School: School of Chemistry

Are there Special Circumstances? NO

Student's Signature:

Date: May 2nd 2012

N.B. The form should state any special circumstances that have affected the progress of the thesis or its final presentation e.g. ill health, bereavement or other temporary incapacity, and which should be brought to the attention of the examining committee and the Faculty Officer before the thesis is examined. Failure to report any special circumstances without good reason may affect any subsequent appeal. This form must be submitted with the thesis. It is expected that the form will normally be blank.

Details of Special Circumstances:-

Acknowledgement

Dear David, you have been a wonderful guide throughout this important part of my academic life. In St Andrews you were the only person that properly knew my work, and the only person I could turn to in St. Andrews for advice about my topic. Your keen observation, accurate assessment and very sharp comments were invaluable to the entire project. Literally up to the day before submitting this work you have supplied me with excellent comments, and proper, difficult questions. Invaluable.

Daily, have I barged into your office -without knocking- to share enthusiasm and frustration, news, to discuss problems, to raise issues or just to simply question everything. The door is always open, and you are never impatient. That is much better than I could do! You have been a supervisor to many students, some of them not even your own, and I am sure that without your help, many of them would have been lost, as I would have been. I have nothing in return for you but my sincerest gratitude, both for this great opportunity and for your help. At last, I wish to say that I think I have learned a great deal from your "management style". My current students would thank you if only they knew! I am proud to say I am a student of David Cole-Hamilton.

Now for the Americans (we agreed on that term in the third meeting). Doctors Jim Ponasik and Robert Hembre. We had such a close group of people for this project. Jim, thank you for the motivation. I have often gone into a meeting feeling completely useless and down, only to come out ready for action. That is the manager in you, and you are doing a great job. However, do not give up being a chemist yet. Whenever we were stuck, you would come with the best suggestions! You have clearly not forgotten any of your chemistry background, ready to teach us a lesson. Many thanks for making this possible. I truly appreciate it.

The same of course goes for Bob. Dear Bob, I am very sorry about confusing you so, so many times. You showed me that industrial chemistry is even better than I thought it would be. I loved doing chemistry with you, because you have the experience and knowledge to make everything tie together. David has that too. Great experimental experience, even better theoretical knowledge, a true master of your domain. I enjoy having a beer or two with

you whenever you are over and just talk chemistry. You are a great guy and a great inspiration. I hope I will get an opportunity to talk chemistry with you in the future.

Now Peter Pogorzelec. Peter, it was a definite pleasure working with you. Thank you for all your help in organizing the laboratory and help in solving experimental problems. Whenever I needed help, I could rely on you. Your help was also invaluable during the write-up of this project. I could call you any time to get data from our equipment. Many, many thanks.Further, I would like to give thanks to all the other members of the DCH group during my time in St Andrews. Lynzi, Simon, Nicolas, Ruben, Marc, Patrizia, Sergey, Bartel, Hanno, Juma, Jacqui, Jenny, Luke and the dynamic duo: Gregorio and Jacorien. I would also like to thank the people in our department for all the help I got, Melanja, Sylvia, Brian & Brian, Artur, Jim and I would like to especially mention Bobby, who was a particular saviour for a the problems I created. Thank you very much for all your efforts.

The good people in St Andrews, many thanks for making this time such a pleasure, especially Eleni, Gabe, Vivian, Wouter en Peter. Good times!

I wish extend a special thank-you towards my family for supporting me through my entire academic education. Mam, Pap, Bas, Daan en oma. Many thanks. In addition, a big thank-you to my friends in Holland, thanks guys, for always picking up the phone and many thanks for the great holidays, Pieter, David, Marieke, Didi, Viktor, Joris and Joey.

I wish to also thank my sponsor, the Eastman Chemical Company for taking the time and funding this wonderful project. I enjoyed all aspects of working with you. I truly appreciate it.

Finally, I reserved a special place for Marina, who has shared all of my frustration, excitement, joy and grumpiness. Thank you for being you and thank you for creating such a wonderful home in such demanding times.

With love,

Jan

Abstract

In this dissertation we investigate aspects of the Ru/[PBu_4]Br mixture in the homogeneous conversion of CO and H_2 as pioneered by Knifton, Dombek and Gresham. In chapter 1 we present a current overview of the literature on this subject.

In chapter 2 we establish benchmark reactions and a full analysis of the liquid products that are generated during catalysis. The product mixture consists primarily of small alcohols (linear), acetic acid ethers, esters, and ethylene glycol. Both methanol and EG are formed independently, but methanol is then converted into almost all other products that we find.

In chapter 3, the gas phase activity is assessed, and it is found that the Ru/[PBu_4]Br system is highly active for the WGS reaction, and as a result the reactor gas phase changes in composition over time. Following this, in chapter 4 the orders in p_{H2} and p_{CO} are determined for both the methanol formation reaction and the methanol homologation reaction. In order to achieve this, a simple kinetic model is developed to assess the relative reactivity of the system for each reaction. Using these orders and the knowledge of fast Water-Gas-Shift activity, we iteratively model the conditions in the reactor to closely fit and predict the methanol levels during the reaction.

In chapter 5 the discovery of a promoter, [$HPBu_3$]Br is discussed. The promoter dissociates under catalysis conditions into HBr and PBu_3. The HBr then proceeds to improve catalysis by changing the catalyst composition, while the PBu_3 inhibits the homologation reaction selectively.

In chapter 6 we proceed to test the activity of the system for a range of different promoters and solvents. The effect of bromide concentration, changing the halide, and using various acid promoters is tested. At last we attempt to expand on the scope of this reaction by using different ruthenium precursors and by using dimethyl ether as a reagent instead of methanol. Both seem effective.

Notably, the conversion of CO_2 to methanol in a one-pot reaction was observed.

Table of Contents

Chapter 1
Introduction

The heart of the chemical industry is based on converting one feedstock into a more valuable product. The benefit is highly dependent on the costs of the starting materials, but they can vary significantly over time. To safeguard against unexpected or expected increases in the price of these commodities, companies develop knowledge about processes that surround their core-business. If changing markets cause the price of certain feedstock to increase, the company may consider making products through a different route. This requires a significant investment to explore new pathways, better technology and human expertise even though some technology may never be used.

For the chemist there is a natural curiosity for developing unknown chemistry. It leads to an increase in fundamental knowledge and it may also lead to the development of new tools that can be applied in other processes or otherwise unexpected benefits.

There are some basic principles used in the development of catalytic systems. One of the first hurdles is to find a catalyst that performs the chemical conversion. After that, optimisation becomes relevant; which species are present during catalysis, what is the mechanistic cycle, what is the slowest step in this cycle and how can this part be improved? For this, there are many tools and of these, NMR, IR and kinetic information in particular lead to valuable insights. However, not every process can be elucidated using these techniques, often because of physical limitations of the equipment used. In this case, we can still obtain information about the system by changing the parameters of the process and observing the effects. For instance if a process is too fast to observe directly the active species, or if only resting state species are seen, the addition of promoters or additives may tell something about the catalytic cycle.

Because of increasing oil prices (Figure 1.1) the price of oil derived feedstocks and commodities has risen significantly. Oil is used as a source for energy, fuels and chemicals, and that is why we currently live in an oil-based economy. However, the oil reserves are finite and for political and economic reasons countries and companies may become interested in switching to other resources. Currently, there are many

investments into energy from wind, waves and sunlight. Furthermore, there is a large drive for chemicals from renewable sources. When employed on a large scale, chemicals and energy from renewable sources leads to a significant reduction in the so-called carbon footprint. Even though it is not a renewable source, coal and gas serve as good starting points for the development of renewable routes to chemicals.[1] As oil reserves dwindle, there will have to be a switch towards an alternative energy source. Despite the fact that it is not a particularly clean source and despite the drive towards renewable resources, coal is a probable resource that is currently being developed because it is the one of the few readily available carbon source sources that is abundant enough to satisfy our current demands. Besides coal, natural gas is also currently being developed on a large scale, for instance in Russia, Qatar and Iran. Both coal and gas can be utilised in the same way to produce fuels and chemicals as they both can be converted into the same basic materials.

As a resource for chemicals, coal has been used since the 1920's in a process called Fischer-Tropsch (F-T) chemistry. In this process the coal is gasified to form a mixture of CO and H_2 called syngas. The syngas is converted to fuels by leading it over an iron, ruthenium or cobalt catalyst. The conversion from syngas to liquid products is the actual Fischer-Tropsch process. The same chemistry can be used to convert biomass and natural gas to for instance, gasoline, diesels, waxes and mixed alcohols, so an improvement in F-T chemistry will, therefore, lead to an improvement in the use of these resources. Scheme 1.1 shows a number of reaction pathways from syngas to chemicals.

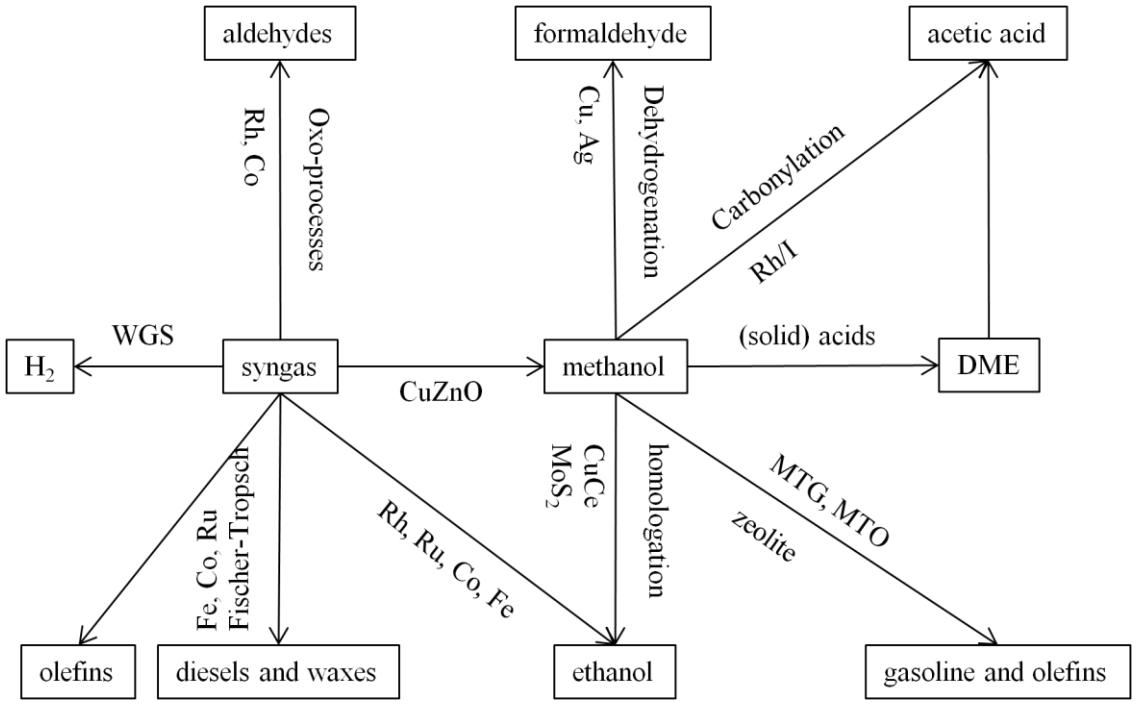

Scheme 1.1 A set of routes from syngas to chemicals. Most of the products formed by solid catalysts are unfunctionalised long-chained hydrocarbons. Reproduced from Subramani et al.[2]

As can be seen F-T chemistry leads to mixtures of compounds and, depending on the conditions used, there are different product types ranging from waxes, paraffins, olefins, diesel and gasoline to mixed alcohols. A separate process is the synthesis of methanol from syngas. This process is well developed and has high conversions, close to the thermodynamic equilibrium. From methanol a set of other products can be made, a good example is the carbonylation towards acetic acid or acetic anhydride. Homologation to ethanol is a reaction that is still underdeveloped. Compared to the range of chemicals that are routinely produced from oil, syngas utilisation could be expanded significantly. There is another interesting aspect to the use of syngas. Because the coal that is gasified contains high levels of impurities, the product gas needs to be scrubbed rigorously. The scrubbing is a very energy consuming process, which leads to very pure syngas streams, but also to large waste streams. Having pure syngas is often a necessity because sulphur is a notorious F-T catalyst poison. However, the benefit is that it also leads to very clean F-T products like high purity fuels. The waste is removed at the source rather than being contained in the end-product. Even though the levels of impurities in oil are lower in general than in coal, the removal of impurities from liquid streams is generally more difficult. This also applies to the case where coal is converted by direct liquefaction. This makes syngas an excellent source where clean fuels are needed. In addition to the removal of heteroatoms like sulphur and nitrogen from the

gaseous feed streams, the Fischer-Tropsch process leads to a relatively simple set of products, mainly straight chain hydrocarbons, whereas oil derived fuels contain high aromatics content that contribute to incomplete combustion. As mentioned before there will have to be multiple incentives to move from an oil based economy to a coal based economy. A large incentive is the price of oil. At the start of this project the price of oil was increasing significantly. Figure 1.1 shows the price of oil over time.

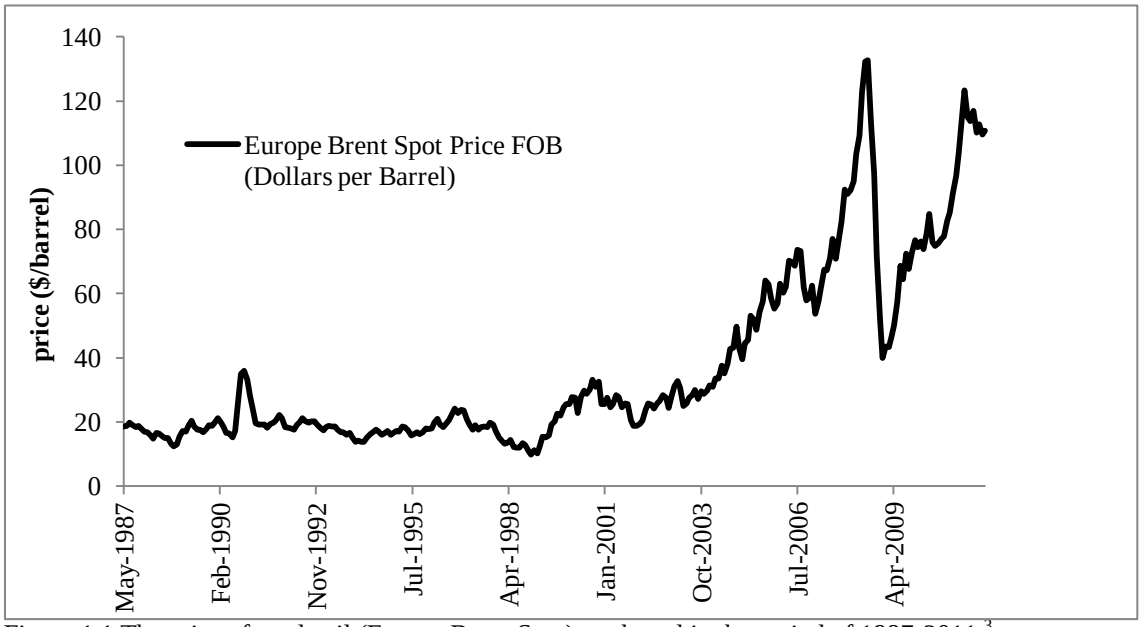

Figure 1.1 The price of crude oil (Europe Brent Spot) per barrel in the period of 1987-2011.[3]

This led to an increase in interest for developing new routes from syngas to chemicals. In our case there is particular interest in developing a route from syngas to C_{2+}-alcohols. F-T chemistry produces mainly long chained unfunctional hydrocarbons. This means that for every CO incorporated into the product, one H_2O is formed and this unattractive in terms of hydrogen usage. Even though the production of water is a strong thermodynamic driving force in F-T chemistry, the result is that the F-T product is rather inert from a chemical point of view, so difficult to functionalise. Furthermore, most of the carbons in the products are essentially the same, so chemo-selective conversion towards higher value products is also difficult. Therefore, if this oxygen functionality from CO could be retained in the product then this would be a good result. This is the case for methanol, but in generating methanol no C-C coupling takes place. Therefore, ethylene glycol is a more desirable product, or even ethanol, because they contain C-C bonds and also provide chemo-selective and functionalised precursors to higher products. Besides recent findings in selectively making ethanol from syngas using zeolites, the best system for making these types of products was using

homogeneous rhodium or ruthenium and halide promoters at very high temperatures and pressures. We will present a very general and quick overview of CO hydrogenation before we move to a more detailed overview of the chemistry in this field. The onset of homogeneous conversion of CO and H_2 to products was in the 1950's with work from Gresham et al. from DuPont. The conditions applied were very harsh and he used up to 3000 bar of pressure, high temperatures and large amounts of catalyst (cobalt) in solvents like water, acetic acid and butanol, and this yielded very interesting product mixtures containing poly-ols. Such conditions are economically not viable and, most likely because of this, research was discontinued, or at least not published. Later in the 1970's, the oil crisis lead to renewed interest into this chemistry and various groups pursued homogeneous syngas conversion. In this time much work was done by Bradley (Exxon)[4-6], Dombek and Pruett (Union Carbide)[7-10], Knifton (Texaco)[11] Masters (Shell) and some academics like Keim and Schlupp[12, 13] and Rathke and Feder[14]. Some of this work was reviewed by Blackborow et al. in 1982.[15] Notably, Knifton and Dombek made a lot of progress in the field, using halide promoters or solvents and managed to obtain good results using relatively, for that time, low pressures of between 430 and 860 bar. The efforts then, and in the following decade, form the basis for this type of chemistry, and most of the work that must still be done will be a continuation of their published work. After this time the oil price fell and there was not much need for alternative sources to chemicals so fewer publications appeared on the subject. However, in the mid 1980's the Japanese C_1 chemistry project was undertaken and this resulted in a few important advances concerning the use of phosphate and increasing the selectivity towards ethanol, but after this the subject has been relatively quiet in terms of published results. Only a few groups openly speculated about mechanisms for methanol formation and ethanol formation, and with the help of spectroscopic investigations with concurrent activity measurements the suggestion was made that methanol was formed via an intermolecular mechanism containing a hydride donor (H^-) and a hydride acceptor (CO) mechanism. This is a theory that was later not supported by the Japanese scientists who appear to be in favour of a single catalytic species for the synthesis of methanol. However, no direct evidence has been provided to verify any suggested mechanisms so far partly because of the unfavourable conditions necessary to achieve catalysis. Because of significant improvements in homogeneous catalysis research since then and the interest in further development of homogeneous syngas chemistry, we have

further investigated homogenous CO conversion and in particular Knifton's melt chemistry.

1.1 Early homogeneous Fischer-Tropsch chemistry

The first attempts at finding a homogeneous catalyst for the conversion of syngas into chemicals occurred in the 1950's. In these first attempts, the goal was to find a better tuneable homogeneous analogue for Fischer-Tropsch chemistry. A more selective reduction might result in better atom efficiency and cheaper routes to functional chemicals like polyhydroxy hydrocarbons which are enthalpy favoured products. For instance the work by Gresham for DuPont de Nemours and Co. examined the reactions of Cobalt acetate in the presence of acetic acid and/or water.[16] Under pressures of 2000-3000 atm and temperatures between 180 and 250 ^{o}C CO was reduced to monofunctional C_{1-3} alcohols and poly-ols, e.g. ethylene glycol (EG), ethylene glycol formates and the glycerol equivalents. Likewise, in the presence of acetic acid they found the corresponding acetate esters, for instance EG diacetate. It is not clear whether the presence of acetic acid improved CO conversion compared to having just water in the reaction mixture, or if it promoted the formation of C-C coupled polyols; however, it does not seem to impair formation of C-C coupled products. Notably, the reaction times were very short, ca. 30 minutes. It was found that for optimum yield, the concentration of the products should be low; an ideal situation for continuous processes. In contrast, in a following patent,[17] the workers from DuPont described repeating very similar reactions in alcoholic media like butanol, EG or methanol as solvents; short reaction times yielded the same product quantities of glycol and high boiling fractions. On some of the occasions the total weight increase was quite impressive, up to 35 grams, although the precise composition of the product is unsure. Some of it may well be water, which is a byproduct of longer chain alcohol formation, but which also indicates loss of functionality. After that early work by Gresham there was not a great deal of activity on this subject until the oil embargos in the seventies renewed the interest into finding alternative sources for fuel, and thus the way to utilise coal as a source for chemicals.

1.2 Muetterties

A conceptually logical approach to the homogeneous reduction of triply bonded molecules, such as CO and N_2 was pioneered and developed by Chini[18] and Muetterties[19-21]. Muetterties and his co-workers have done work on the hypothesis that metal clusters could serve as models of metallic surface catalysts,[22] by analysing the organometallic bonding in metal clusters and their relationship to metal surface chemistry and homogeneous chemistry or vice versa. The bulk of this work was published in a series of papers wherein, among other things, the reduction of triple bond molecules was discussed from the point of view that in order to successfully activate these molecules there is a need to maximally reduce the bond order.[23] In other words, the most activated CO moiety is the one with the lowest bond order, or the longest bond length. The effect of bond order in relationship to the bond distance is not a linear one. The difference in changing from bond order from 3 to 2 only effects a small change in C-O bond distance compared to going from 2 to 1 (Figure 1.2).[24] The authors argued that the reduction of carbon monoxide might be easier when the carbon is already electronically in a product-like state (sp vs. sp_2/sp_3).

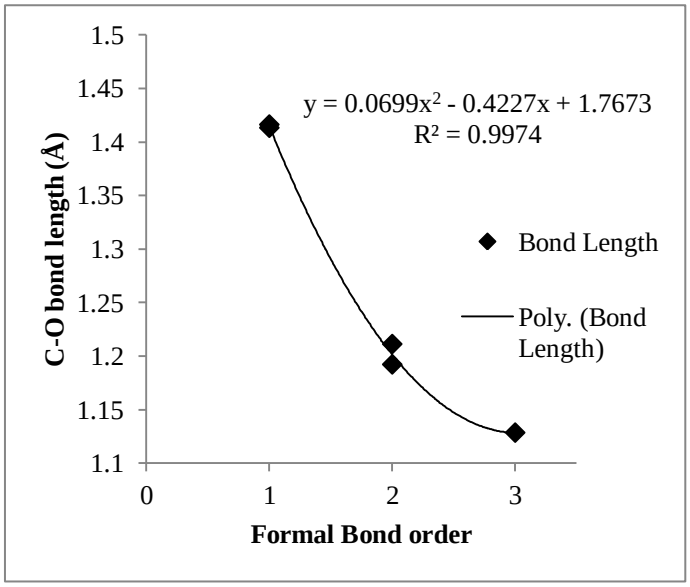

Figure 1.2 the C-O bond length against the formal bond order for methanol, aldehyde, ketone and CO. Data from The Handbook for Chemistry and Physiscs[25], this plot is a re-drawing of a plot (with updated bondlenghts) from Muetterties[23].

The first consideration involves factors that determine metal induced bond order reduction. In mononuclear complexes binding occurs either linearly end-on, bent end-on or side-on to the metal (π-interaction). The effect of bonding modes can be measured from the C=O bond distance in complexes, and in this way a series may be formed that

shows the relative effect of the bonding mode on the bond order. In none of these bonding modes will the bond order of triply bonded molecules be reduced beyond a value of 2. However, binding to multinuclear species can be expected to lower bond orders. In general the bond order in Figure 1.3 decreases going from left to right.

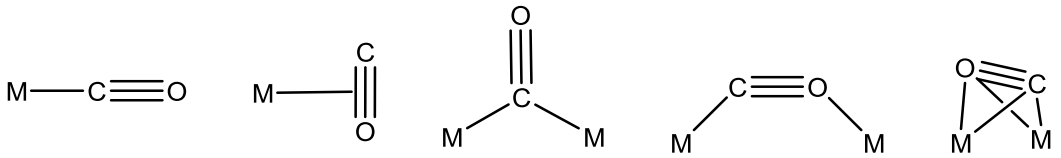

End-on σ-complex | π bonding, η-complex | bridging μ-complexes

Figure 1.3 Bonding modes of M-X=X species. The relative bond order is reduced going from left to right. Figure redrawn from Muetterties[23]

Even lower bond orders are found in species containing 3 or 4 metal sites. Therefore, one can expect complexes such as A, B and C (figure 1.4) to be very good for the activation of molecules containing triple bonds. For some species these complexes have been well characterised. [21, 23, 26] (and references therein). Also for metal surfaces, these higher bonding modes seem quite likely. The large size of most metal atoms compared to the size of for instance carbon means that the substrate can easily sit in positions interacting with three or four metal atoms at a time, thus maximally activating small substrates for F-T chemistry.

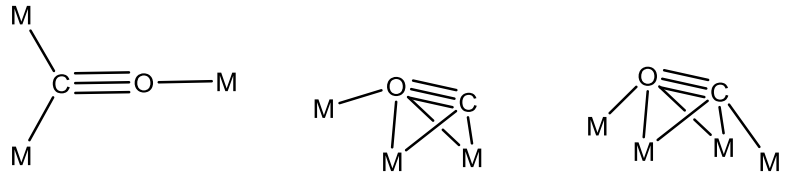

A B C

Figure 1.4. Highly activated bonding modes through multiple site stabilisation. Redrawn from Muetterties[23].

For acetylene complexes with these higher bonding modes the reduction to form ethylenes is quite facile and does not require elevated temperatures, and even N_2 complexes of the form B and C have been found although they are not reactive.[27, 28] For metal clusters with CO the picture is slightly different. The most common bonding mode for CO in homogeneous systems is end-on and only on rare occasions can bonding modes be found wherein CO binds through π-interactions. However, using elevated temperatures, it seems that these activated bonding modes can be established, $[Ru_3(CO)_{12}]$ for instance forms metal carbide species around 140 ^oC at ambient pressures.[29, 30] The carbide carbon was shown to be from CO. And is thus formed via

extended C-O activation to the point of C-O dissociation. However, carbide formation is accompanied by decomposition to metallic Ru at these temperatures thus preventing formation of a stable active species. Metallic surfaces do not experience this instability and common F-T chemistry occurs readily between 200 and 300 ^{o}C. With the right configuration for good bonding with CO this required activation temperature may be lowered considerably. One of the most stable complexes is $[Ir_4(CO)_{12}]$. Between 150 and 180 ^{o}C this complex in toluene slowly reacts with hydrogen to form methane and an insoluble complex.[26, 27]. In search of extra stabilisation of CO the same reaction was performed in NaCl $2AlCl_3$[31] The reaction ran at a slow rate (1 CO every 12 minutes per cluster) yielding methane, ethane, propane, n-butane and i-butane and throughout the reaction no sign of catalyst decomposition was found. When the same solvent was used in the absence of any catalyst, or in the presence of finely dispersed metallic iridium no product formation was observed. The solvent effect is believed to come from additional stabilisation of CO through bonding (M-CO--$AlCl_3$) with the aluminium (Figure 1.4, species A). Carbonyl clusters of chromium, molybdenum, tungsten, iron, osmium, cobalt, nickel and rhenium were also subjected to the same conditions but these proved inactive.[31] $[Rh_6(CO)_{16}]$, $[Rh_4(CO)_{12}]$ and $[Ru_3(CO)_{12}]$ all showed F-T activity. However, the rhodium system was partially solid so questions remain about the nature of the active species. The reactions of the active clusters seemingly established the validity of Muetterties' concept and showed that cluster chemistry might provide a solution to the homogeneous hydrogenation of CO. This and the proven effectiveness from previous cluster related catalysis provided a good starting point for other groups to develop CO hydrogenation catalysts using carbonyl clusters.

1.3 Union Carbide

In the early seventies researchers from Union Carbide actively re-examined Gresham's homogeneous CO reduction by metal carbonyl species.[32, 33] The first example was the development of the reaction of syngas with group VIII complexes and clusters. The bulk of the discoveries are presented in patents, but the volume of examples presented in the patent literature is too large to be presented here so the basic trends will be mentioned along with the most interesting features that were also published in journals. In the preliminary reports a variety of metals was tested for their activity in the synthesis of oxygenated chemicals.[34] Among the tested metals were

rhodium, ruthenium, cobalt, copper, manganese, platinum, zinc, lead, chromium and iridium and the conditions that were used were quite extreme, e.g. up to 3400 atm pressure combined with temperatures up to 250 ^{o}C. Using these conditions the synthesis of oxygenated chemicals was achieved only from rhodium species. The product solution contained methanol, ethylene glycol (EG), ethanol, propylene glycol, glycerol and erythritol. Of these, only methanol, EG and glycerine where formed in significant amounts.[33] Also, the rhodium could be added (not exclusively) in the form of $[Rh(CO)_2(acac)]$, $[Rh_6(CO)_{16}]$ or $[Rh_4(CO)_{12}]$ indicating that the catalyst is formed *in situ* under reaction conditions and that under these conditions mono nuclear species or rhodium clusters all go through the same species before becoming active. Importantly, it was discovered that the addition of Lewis base promoters enabled the conversion of CO at considerably lower pressures. Interestingly, for the synthesis of alkanes Muetterties used Lewis acidic promoters. In order to further reduce the required pressure, additional effects of the solvents and promoters were investigated and described in patents.[35, 36] The solvent was found to have a large influence on the overall activity and selectivity of the system, for instance, Table 1.1 shows that there is a clear difference between using tetraglyme (TG) and glyme. The cause of this difference is unclear, yet the concept demonstrates that the catalysis is sensitive to changes and thus could possibly be improved. In addition, a marked difference was found when the pressure and the catalyst loading were lowered (exp 2 vs. 3) slightly. Even when the reaction was allowed to proceed for an additional hour the product formation seems to be reduced more than we would expect. It shows that the catalyst loading has a significant effect on the overall activity of the system and that most likely there is a high order in H_2 for catalysis. Furthermore, the product distribution also changes to disfavour chain growth. This demonstrates not only that the overall activity can be altered, but also that product distribution can in principle be enhanced using different conditions.

Table 1.1. Some illustrative experiments on the reaction of $Rh(CO)_2(acac)$ with syngas[a]

Solvent	Temperature (^oC)	Pressure (atm)	Time	Products (g)		
				methanol	EG	glycerine
THF	230	1360	3 hr	7.9	18.6	1.7
TG	220	1360	3 hr	3.9	16.1	2.7
TG[b]	220	1224	4 hr	2.6	1.2	0
glyme	220	1360	3 hr	3	9.6	1.9
methanol	220	1360	3 hr	n.d.	8.9	n.d.

[a]Conditions: 3 mmol $[Rh(CO)_2(acac)]$, 75 mL solvent, 1.1 g 2-hydroxypyridine, 1:1 $CO:H_2$. TG= tetraglyme, EG= ethylene glycol n.d.= not determined.[b]$CO:H_2$ 3:2, 2.25 mmol $[Rh(CO)_2(acac)]$. Data from Pruett[33].

The addition of promoters was tested as well;in this case the effect of the addition of alkali metal cations. The results can be found in Table 1.2. In these experiments the pressure was lowered considerably to 544 atm compared to the previous set of experiments. Yet, significant amounts of products were formed.

Table 1.2 The effect of the addition of a number of promoters on CO hydrogenation in the presence of rhOdium based catalysts.[a]

Salt	methanol	EG
-	2.1	1
LiOAc	1.72	1.65
NaOAc	1.34	2.57
KOAc	0.89	2.15
CsOAc	1.58	3.9
Ba(OAc)2	0.7	0.65
$[(P(PPh_3))_2N]OAc$	1.8	3.6

[a]Conditions: 3 mmol Rh 220 ^oC, 544 atm syngas (1:1), 4 hr, 75 mL TG, 10 mmol 2-hydroxypyridine and 0.5 mmol of the salt. [b] Product formation in grams. From Pruett[33].

The use of large cations was found to be beneficial for the formation of EG. Using PPN or caesium acetate increases the formation of EG by a factor of 3.6 and 3.9 respectively. Interestingly, although effects are considerable in EG formation, for the synthesis of methanol there does not seem to be a strong correlation between the size of the cation and its production. The effect of the concentration of the added salt on the product distribution is considerable. Figure 1.5 shows some interesting features. First of all, the selectivity towards each compound can be tuned according to the Cs loading. This indicates that again certain pathways can be tuned for optimal selectivity to the desired compound, in this case EG.

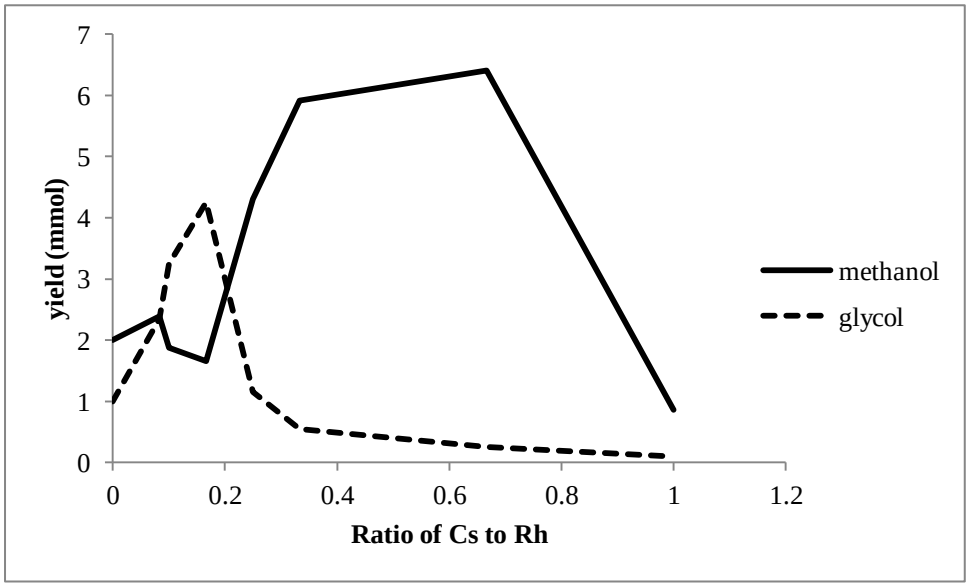

Figure 1.5 The correlation between methanol and EG yield and the addition of Cs promoters in homogeneous Rh catalysed CO hydrogenation. Conditions: 544 atm, 220 ^{o}C, 75 mL TG (tetraglyme), 3 mmol Rh, 10 mmol 2-hydroxypyridine, 4hrs. Data from Pruett[33]

Another interesting feature is that the selectivity towards EG comes at a cost for the synthesis of methanol and this could be an indication that the species leading up to methanol is also a species leading towards EG, e.g. they seem to be coupled. The cation loading experiment was also conducted for the bis(triphenylphosphine)iminium (PPN) cation (not shown), which also proved effective and shows the same maximum selectivity towards EG at a 1:6 ratio of cation: Rh loading. From this ratio it can be reasoned that a 1:6 Cs-Rh species could have a key impact on glycol synthesis and accordingly it was believed that $Cs_2[Rh_{12}(CO)_{34}]$ could have a beneficial effect on EG synthesis. This species was thought to be observed in the infrared spectrum of a solution under elevated pressures and temperature.[37] However, independent analysis by Fumagalli et al. showed that this species is in fact $[Rh_5(CO)_{10}(\mu_2\text{-}CO_5)]^-$.[38] Interest into the rhodium species existing under catalysis conditions prompted further investigation and it was shown that at higher temperatures this $[Rh_5(CO)_{10}(\mu_2\text{-}CO_5)]^-$ species was converted into higher nuclearity rhodium clusters. Since the rate of reduction of CO is increased considerably under these conditions it logically follows that these high nuclearity clusters could play an important role. Scheme 1.2 shows the qualitative changes in the composition of solutions of rhodium carbonyl species upon the application of heat and pressure of syngas. The most effective conditions for catalysis occur at temperatures above 200 ^{o}C in combination of the presence of promoters.

	high pressure conditions (60-1000 atm)	
Ambient conditions	<180 °C	>180 °C
$[Rh(CO)_2acac]$ $[Rh_m(CO)_m]^{x-}$ $[Rh_6(CO)_{15}]^{2-}$ $[Rh_7(CO)_{16}]^{3-}$	$\rightleftharpoons$ $[Rh_5(CO)_{15}]^- + [Rh(CO)_4]^-$	$\longrightarrow$ $[Rh_{13+x}(CO)_mH_y]^{n-} + [Rh(CO)_4]^-$
$[Rh_6(CO)_{15}C]^{2-}$ $[Rh_9(CO)_{21}P]^{2-}$ $[Rh_{17}(CO)_{32}S_2]^{3-}$	$\rightleftharpoons$	$[Rh_6(CO)_{15}C]^{2-} + [Rh(CO)_4]^{-\,a}$ $[Rh_9(CO)_{21}P]^{2-}$ $[Rh_{17}(CO)_{32}S_2]^{3-}$

Scheme 1.2. Overall representation of the behaviour of rhodium carbonyl clusters under syngas. Re-drawn from Vidal and Walker[37] [a]Only observed after longer times

The lower part of scheme 1.2 shows the behaviour of more heat resistant heteroatom encapsulated clusters under the same conditions. It was shown that the species in Scheme 1.2 are the only (spectroscopically detectable) species present under catalytic conditions after 20 minutes at temperature. Interestingly, the appearance of $[Rh(CO)_4]^-$ in the most active systems is striking. It can be assumed that for the P- and S-clusters the formation of this species is considerably slower than for the pure and the carbide centred clusters. The trend for catalytic activity displayed in Table 1.3 broadly shows a similar trend.

Table 1.3 catalytic activity of Rhodium Catalysts based on clusters.

	species probably present under conditions[a]		relative catalytic activity
Added complex	clusters	$[Rh(CO)4]^-$	
$[Rh(CO)_2acac]$	x	x	1
$[Rh_6(CO)_{15}C]^{2-}$	x		0.5
$[Rh_{17}(CO)_{32}S_2]^{3-}$	x		0.3
$[Rh_9(CO)_{21}P]^{2-}$	x		0.1

[a]Detected by IR spectroscopy after 0.5-1 hr under 800-1000 atm of CO and H_2at 240-260 °C in the presence of promoters e.g., R_3N and/or alkali carboxylates. From Vidal et al.[37].

Nonetheless, the merit of this species for catalysis can be questioned; the trend for the formation of this species does not seem to match this trend linearly. Although these species were found to be catalytically less active than pure rhodium clusters, they did display significant product formation. The reduced activity is believed to come from a degree of catalyst poisoning through the heteroatoms, not from the presence of other, more critical species in the non-heteroatom cluster solutions. Also, this observation

seems to confirm Muetterties and Chini's observations that metal carbonyl clusters can be involved in the activation of CO towards hydrogenation due to their likeness to metal surfaces.

1.4 Bradley

Despite the fact that workers from Union Carbide found that ruthenium was not an active homogeneous catalyst for the synthesis of C_{2+} species, others[31, 39] had observed that solubilised ruthenium proved somewhat active for CO hydrogenation. Bradley and co-workers from Exxon also found an active application of ruthenium clusters.[4] They investigated the reaction of CO and hydrogen using clusters, following Muetterties' suggestion that they may have beneficial features in these kinds of syntheses.[5] They chose to use ruthenium as a starting point, as it is known that ruthenium is a good catalyst for the F-T reaction. For their investigations they used different ruthenium complexes $[H_4Ru_4(CO)_{12}]$, $[H_3Ru_4(CO)_{12}]^-$, $[Ru_3(CO)_{12}]$ and $[Ru_6C(CO)_{16}]^{2-}$ in solution at very high pressures (1300 atm) and temperatures (225-300 ^oC).[4] It was observed that all complexes showed similar activities and that all precursors were formed into one observable (by IR) species in solution; $[Ru(CO)_5]$. Thereby, it was established that the cluster-precursors that they used were quite sensitive to dissociation into the single centred ruthenium pentacarbonyl species ($[Ru(CO)_5]$) under these high pressures. To assess the activity of the ruthenium catalyst, solutions were made containing 10 mM of $[Ru(acac)_3]$ in THF and brought to the testing conditions (40:60 $CO:H_2$, 1300 atm, 268 ^oC). Under these conditions periodic sampling of the solution showed no observable decomposition of the catalyst by IR and that there was near exclusive (>99 %) formation of C_1-products; methanol and methylformate. In terms of ruthenium, the rate of CO conversion was found to be constant at 0.86 mol per mol Ru per second, with a steady ratio of methanol to methyl formate of 4.1. See figure 1.6.

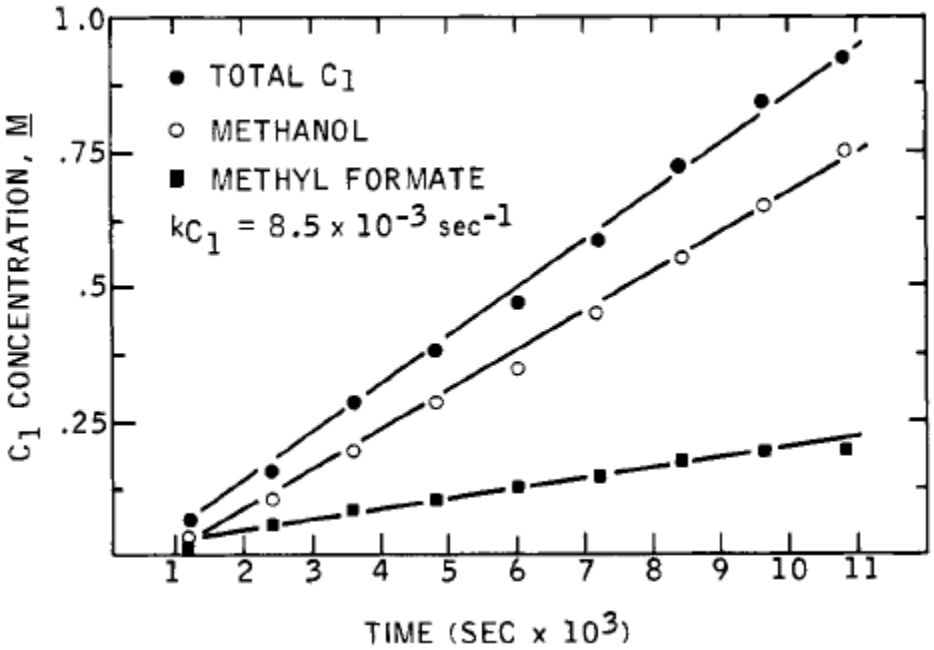

Figure 1.6 Reprinted with permission from J. S. Bradley, *J. Am. Chem. Soc.*, 1979, 101, 7419-7421.[4] Copyright 1979 American Chemical Society, Figure 1.

On surveying the effect of the individual partial pressures of H_2 and CO on the catalysis it was found that a relative increase in the CO partial pressure resulted in an increase in the formate yield, but a decrease in the total hydrogenation of CO. On the other hand, addition of PPh_3 to the solution led to an increase of the selectivity towards methanol. When combined these factors were reported to lead to 95% selectivity towards methanol. Further, it was reported that within the limitations of precision the hydrogenation of CO showed a first order dependence on [Ru]. Interestingly, Masters and van Doorn[39] (Shell) had claimed that, at similar temperatures but at significantly lower pressures (150-200 atm), $[Ru_3(CO)_{12}]$ was found to be active for the synthesis of n-alkanes, while other ruthenium carbonyl species were inactive. This led to worries that maybe $[Ru(CO)_5]$ was indeed inactive and that there may be unexpected activity from multi-metal ruthenium species that may have been overlooked. Therefore, Bradley undertook a series of IR experiments on solutions of $[Ru_3(CO)_{12}]$ in THF under different conditions. They found that at 80 ^oC and 135 atm these solutions contained more or less equimolar amounts of $[Ru_3(CO)_{12}]$ and $[Ru(CO)_5]$. At higher pressures and temperatures (180 ^oC and 265 atm) the only visible compound was $[Ru(CO)_5]$. The conversion of $[Ru_3(CO)_{12}]$ to $[Ru(CO)_5]$ was found to be very rapid under these conditions. The solution was found to be very stable and no decrease in $[Ru(CO)_5]$ was found over a period of 6 hr. However, when the temperature of the solution was

increased to 270 ^{o}C while the pressure was maintained it was found that [$Ru(CO)_5$] decreased significantly due to formation of insoluble metallic ruthenium. See figure 1.7.

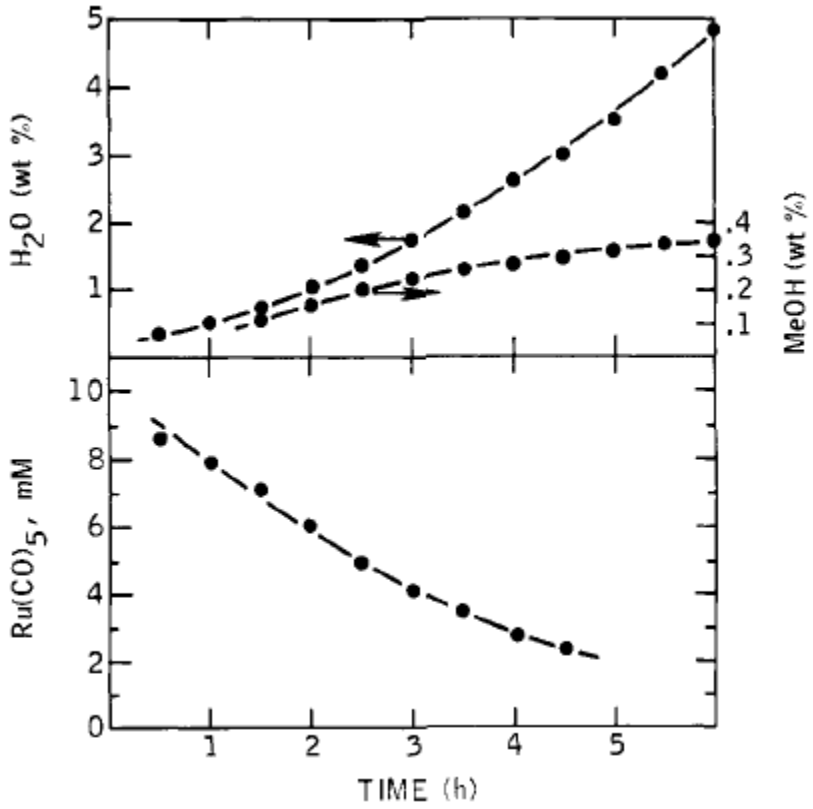

Figure 1.7 Reprinted with permission from J. S. Bradley, *J. Am. Chem. Soc.*, 1979, 101, 7419-7421.[4] Copyright 1979 American Chemical Society, Figure 3.

As the concentration of [$Ru(CO)_5$] decreases the rate of formation of water increases. This coincides with the decrease in methanol formation. This raised the suggestion that, since solid transition metal catalysts were proven to be active in F-T chemistry, the presence of methanation products, water and alkanes could be taken as an indication of catalyst decomposition and that solvated ruthenium carbonyl species were responsible for the more selective hydrogenation towards oxygenates. In fact, a subsequent addition to the literature by the workers from Shell shows that considerable insoluble species are formed during their reaction of [$Ru_3(CO)_{12}$] at 113 atm and 250 ^{o}C.[40] However, the conversion of CO continues even when all spectroscopic evidence of ruthenium in solution was minimal. When the precipitate was collected after the reaction and reused in a following experiment it was found to be active in F-T chemistry, meaning the synthesis of linear alkanes. Interestingly, the decomposition of the catalyst was believed to be induced by impurities introduced during filling. They found that when special care was taken to work under cleaner conditions,

decomposition did not occur at 250 ^{o}C and 99 atm for 26 hrs nor was there any CO conversion observed. However, upon increasing the temperature to 270 ^{o}C the concentration of ruthenium decreased accompanied by formation of linear alkanes, which is in accordance to the observation made by Bradley.

1.5 Keim

Up to the end of the 1970's the performance of mainly Group 6 and rhodium, cobalt and ruthenium metal clusters had been investigated, some due to their relative stability for higher temperature, some because of their activity in F-T-chemistry as heterogeneous catalysts. To expand this field Keim et al. decided to include all group 8 metals in the investigations. As a start their activity as clusters was assessed in both polar and non-polar media, namely N-methyl pyrrolidone (NMP) and toluene.[12] Importantly, the conditions used to test all the compounds were quite extreme, pressures of 2000 bar and temperatures of 230 ^{o}C were used. At the time it was shown by Dombek et al. (discussed later) that ruthenium clusters could be activated to form C_2-products at lower pressures. However, for these "new" metals this optimisation had not taken place yet and, therefore, it was reasoned that the application of high pressure might provide a means to perform F-T chemistry without the use of additional promoters. A selection of the results is shown in Table 1.4.

Table 1.4. The conversion (%) of syngas to products as calculated by Keim et al.[12] sorted by precursor and solvent.[a]

Catalyst	Toluene	NMP
$Fe_3(CO)_{12}$[b]	-	10
$Co_2(CO)_8$[c]	19	4
$Ni(acac)_2$	2	traces
$Ru_3(CO)_{12}$	11	25
$Rh(CO)_2(acac)$	3	25
$Pd(acac)_2$	3	2
$Os_3(CO)_{12}$	-	5
$Ir_4(CO)_{12}$	2	14
H_2PtCl_6*$6H_2O$	7	traces

[a] Conditions: CO:H_2 = 1:1, 2000 bar, 230 ^{o}C, catalyst concentration: 50 mmol (atom) L^{-1}, 25 mL [b] [$Fe_3(CO)_{12}$] 100 mmol (atom) L^{-1} [c] [$Co_2(CO)_8$] 200 mmol (atom) L^{-1}. Adapted from from Keim et al.[12] (Table 2) The time scale can vary and go up to 24 hrs.

The most active species are indeed based upon cobalt, ruthenium, rhodium and iridium. In addition, the effect of the solvent can be considerable; overall, the polar solvent seems to have the most beneficial effect on CO conversion, the exception to the rule being cobalt. It was reasoned that, for cobalt clusters, $[HCo(CO)_4]^-$ from the reaction of H_2 with $[Co_2(CO)_8]$ will act as a Brønsted acid in polar solvents, but as a hydride in non-polar solvents. The following series shows the order of activity for the various clusters[12, 13]:

NMP: Rh > Ru > Ir > Co > Pt > Fe > Ni > Pd ~ Os

Toluene: Co > Ru > Rh > Pt > Ir > Ni > Pd > Fe ~ Os

(with permission from W. Keim, M. Berger, A. Eisenbeis, J. Kadelka and J. Schlupp, *Journal of Molecular Catalysis*, 1981, 13, 95-106.[13])

A range of products was found during the reactions, including C_1, C_2 and even C_3 oxygenates. The cobalt (toluene) and rhodium (NMP) complexes were found to be particularly active towards EG formation, the respective weights % of EG were 25.1 and 44.4. Other products where methanol, methylacetate and methylformate and to a lesser extent glycerine and EG monoformate. To further optimise the chemistry of cobalt, it was decided to investigate the effect of pressure, temperature and catalyst concentration on the yield and product distribution.

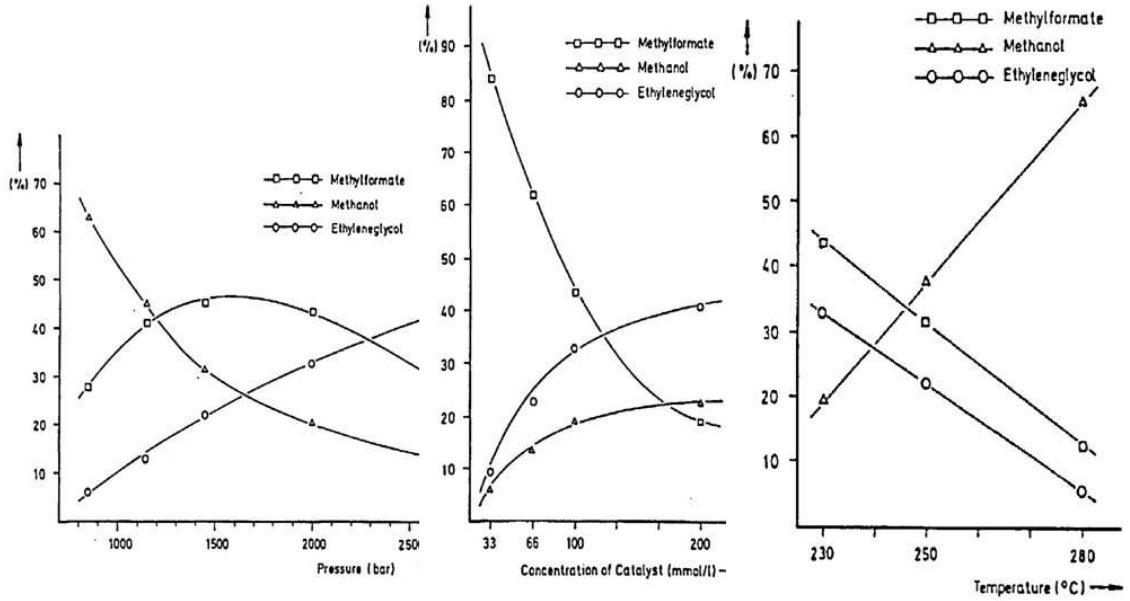

Figure 1.8 The influence of pressure, catalyst loading and temperature on C1 and EG yields in cobalt catalysed CO hydrogenation. Conditions: 2000 bar, 230 ^{o}C, $[Co_2(CO)_8]$: 100 mmol L^{-1}, 05-2 hr, $CO:H_2$ = 1:1, in toluene. Copied with permission from W. Keim, M. Berger, A. Eisenbeis, J. Kadelka and J. Schlupp, *Journal of Molecular Catalysis*, 1981, 13, 95-106.[13] and W. Keim, M. Berger and J. Schlupp, *J. Catal.*, 1980, 61, 359-365.[12]

It can be seen that the effect of pressure is such that with increasing pressure the formation of EG is favoured over methanol. Furthermore, increasing the concentration of Cobalt also leads to increased formation of EG, also for methanol but not for methylformate. The formation of methylformate follows a very different trend from methanol and EG with varying [Co]. Also interesting is that formation of EG and methyl formate both benefit from the use of lower temperatures. IR analysis after reaction showed the presence of only one species, $[HCo(CO)_4]^-$, it was suggested that CO hydrogenation did not occur through cluster chemistry as suggested by Muetterties. A similar observation was made by Rathke and Feder two years prior to Keim's publication.[14] Instead, formation of methanol and EG was thought to occur through the addition of $[HCo(CO)_4]^-$ to a cobalt formyl intermediate yielding a L_4-Co-$\mathbf{CH_2}$-**O**-Co-L_4 (for clarity CO was replaced by L) species. From here CO insertion leads to either methylformate or EG. How this explains the observed product distribution at different catalyst concentrations remains unclear. In fact, in the light of these observations it would be more likely that the formation of methylformate occurs through a mononuclear route, while methanol and EG are formed through higher nuclearity interactions.

1.5.1 Using Iridium

Keim also focussed on the behaviour of iridium complexes.[41] Using ambient pressures, Muetterties had shown iridium clusters to be active in homogeneous FT chemistry forming methane and linear alkanes. These products were later found by Bradley to be indicative of heterogeneous metal catalysis. Even though no catalyst decomposition was observed, it can be questioned now whether the system was fully homogeneous. Nonetheless, in preliminary studies Keim had shown that iridium is effective at higher pressures in the reaction of syngas to C_1 chemicals, and only slightly towards EG. He had also demonstrated that the solvent had a large effect on the overall activity of the system and on the distribution of the products that are formed. This, and promising results by others,[42, 43] led to more extensive investigations on iridium catalysed reduction of CO. Despite previous beliefs, it was found now that the $[Ir_4(CO)_{12}]$ system was in fact not much affected by the polarity of the solvent. The contrasting results obtained using NMP and toluene are thought now to have arisen from the functional groups on NMP rather than the inherent polarity of the solvent, so it acts as a promoter as well as a solvent. Using solvents like NMP, pyridine or n-octylamine the uptake of syngas was considerable (Table 1.5). The selectivity towards EG was very low, in fact only the relatively inactive non-polar solvents induced minor EG formation. Interestingly, analysis of the gas phase for some highly active catalyst systems showed considerable water-gas shift activity, especially in NMP or pyridine, where almost all the syngas was consumed by the WGS reaction.

Table 1.5 Homogeneous hydrogenation of carbon monoxide by iridium catalysts. The effect of different solvents.[a]

Solvent	gas uptake (bar)[a]	Volume % gas phase				wt. % liquid products		
		H_2	CO	CO_2	HC[b]	methylformate	methanol	glycol
n-pentane	120	34.8	64.9	0.4	-	40	46.6	3.6
toluene	180	30.1	67.2	2.6	0.1	19.2	39.6	4.8
THF	150	22.9	76.3	0.6	0.2	6.8	30.8	-
NMP	450	0.5	3.9	92.5	3.1	2.1	25	-
Sulfolane	150	41.6	57.7	0.7	0.1	15.3	78.9	-
n-propanol	160	31.1	68.1	0.7	0.1	22.5[e]	18.5	-
methanol	100	34.2	63.4	2.3	tr	83.5	-	-
Pyridine[c]	1030	0.8	2.2	93.6	3.4			
n-octylamine[d]	600	33.5	39.3	26.3	0.8	variety of unidentified products		

[a]Conditions: $[Ir_4(CO)_{12}]$ (0.125 mmol), solvent (10 mL), 2000 bar syngas 1:1, 250 °C, 4 hrs. [b]hydrocarbons' mainly methane. [c]245 °C, 1 hr. [d]230 °C 2 hrs. [e]n-propylformate. Table reproduced from Keim et al. [41], Table I.

Further, footnote "e" in Table 1.5 shows that, for alcohols, the solvent can be incorporated into the products. It may be clear that for methanol the same applies, one can wonder how the product distribution is formulated in this particular example. A likely place where the solvent can interact with the product is where the metal formyl species is formed. A nucleophillic attack would yield the metalloester. One might expect the same would occur for the nucleophillic amines, thus activating the system, yet complicating product analysis. Because of the good selectivity and the small amount of WSG-reaction it was decided to use n-pentane as a solvent in the further examinations. First, the effect of amine promoters was tested (Table 1.6).

Table 1.6. Homogeneous hydrogenation of carbon monoxide by iridium catalysts. Amines.[a]

amine	Activity[b]	HCO_2CH_3[c]	$HCO_2C_2H_5$[c]	CH_3OH[c]	C_2H_5OH[c]	$HCO_2C_2H_4OH$[c]	Glycol[c]
-	12.5	38.2	0.2	52.9	0.1	0.4	2.6
pyridine	33.8	17.1	1.2	75.4	3.8	0.2	1.1
n-butylamine	32.7	16.5	1.7	71.5	4.8	0.1	1.3
n-octylamine	44.7	11.2	2.3	61.1	9.6	0.2	2.2
di- butylamine	33.8	20.1	0.9	71.2	2.7	0.2	2.4
di-octylamine	44.7	18.4	1.6	61.3	7.5	0.2	2.5

[a]Conditions: Ir (0.5 mmol), amine (0.5 mmol), pentane (10 mL), 2000 bar syngas 1:1, 245 °C, 8 hrs. [b]g of product per g Ir [c]weight percentage liquid products. Table adapted from Keim et al. [41], Table II.

Again, it is clear that the presence of amines promotes the activity. Compared to having no promoter in the system the addition of amine promoter increases the activity

2-3 fold. Of these, the long-chain n-alkyl amines have the highest activity and the main products are C_1 chemicals. In addition, there is considerable WGS activity (not shown) and methanation, there is up to 45% CO_2 and 11% of CH_4 in the gas phase. The increase in activity is not as extensive as in the examples of Table 1.6 and this may be because the concentrations of promoters are far less. To examine the effect of the amount of promoter relative to catalyst, a series of reactions was performed (Table 1.7). As can be expected there is an initial high increase in activity when amines are added. However, the difference between N/Ir= 2 and 4 is not that great. The product distribution does not seem to be affected much by the amine concentration. Only the formation of ethanol is increased linearly with increasing promoter concentrations.

Table 1.7. Homogeneous hydrogenation of carbon monoxide by iridium catalysts. Amine/Iridium ratio.a

N/Ir	Activity[b]	HCO_2CH_3[c]	$HCO_2C_2H_5$[c]	CH_3OH[c]	C_2H_5OH[c]	$HCO_2C_2H_4OH$[c]	Glycol[c]
-	3.6	26.2	0.1	65.7	0.1	0.1	2
1	16.6	15.7	0.1	72.9	1	0.1	4.3
2	20.3	18	0.5	70.7	3.4	0.1	3.2
4	21.3	14.6	0.9	66.1	7	0.1	3.3

[a]Conditions: Ir (0.5 mmol), n-octylamine (0-2 mmol), pentane (10 mL), syngas 1:1(2000 bar), 230 ^oC, 8 hrs. [b]g of product per g Ir. [c]weight percentage liquid products. Data from Keim et al. [41], Table III.

Because of their superior donor properties, it is interesting to see the effect of phosphines on the catalysis. Phosphines are highly tunable in their donor properties, and usually have a larger donor effect than nitrogen ligands. However, in this system the increase in activity upon addition of phosphines is smaller than when amines are used. The overall activity using phosphines (Table 1.8) is larger than using nitrogen donors (Table 1.6) however the *increase* in activity is smaller. Also, the formation of C_2 products is strongly inhibited. This difference can be explained if the promoters are not viewed as acting as donor, but rather as bases. Amines are generally better bases and may therefore show this pattern. If for instance hydride formation from H_2 is a rate limiting step (as thought to be in other systems), the presence of a base could increase hydride formation through assisting in the heterolytic splitting of hydrogen by capture of the second hydrogen through acid base interactions. This way the catalyst does not need to undergo oxidative addition and increase the formal oxidation state by two, but rather keep the low oxidation state and form more potent hydrides. Even if H_2 splitting by the complex is not the rate limiting step, the catalyst may, for instance, not have

enough hydritic character. Removal of H^+ from a complex increases the electron density on the complex, making the remaining hydride more basic or hydridic.

Table 1.8 Homogeneous hydrogenation of carbon monoxide by iridium catalysts. The effect of phosphine promoters.

ligand	activity	HCO_2CH_3	$HCO_2C_2H_5$	CH_3OH	C_2H_5OH	$HCO_2C_2H_4OH$	glycol
-	25	38.2	0.2	52.9	0.1	0.4	2.6
P-t-bu_3	34.4	26.1	2.9	69.4	0.1	-	-
PCy_3	18.8	12.3	-	84.5	-	-	-
P-i-Pr_3	39.1	12.1	0.1	86.8	0.2	-	-
PBu_3	32.9	8.1	0.9	90	-	-	-

Conditions: Ir (0.25 mmol), ligand (0.25 mmol), pentane (10 mL), 2000 bar syngas 1:1, 245 ^oC, 8 hrs. [a]g of product per g Ir. [b]weight percentage liquid products. Data from Keim et al.[41], Table IV.

In terms of chain growth the picture is quite similar, the C-C coupling, migration of a methoxymethyl group onto CO is thought to be a slow step compared to reductive elimination towards free product. Hence, there is a large amount of methanol and other C_1 products compared to C_2 products. Having an increasingly negative charge on the complex will inhibit reductive elimination of a M(H)(CH_2-OH) to a M-Methanol species, thus the lifetime for a methoxymethyl complex species may be prolonged long enough for CO migration to become a significant pathway. In fact, Dombek and co workers from Union Carbide showed that increasing the ionic character of a complex may have a beneficial effect on catalysis. This will be the subject of discussion in the next section.

1.6 Dombek

Despite earlier work by Bradley and co workers, which showed that, in contrast to Rh and Ir (for example), Ru was not effective in the synthesis of C_2 products, Dombek from Union carbide decided to develop more synthesis gas chemistry using ruthenium with the hope of forming ethylene glycol.[7] This work has a significant influence on our studies and will be discussed in detail. Their starting point concerns the hydrogenation of CO using a ruthenium species, [Ru_3CO_{12}] (**1**) at high temperature but relatively moderate syngas pressures (340 bar) promoted by carboxylic acids, particularly acetic acid. Preliminary work had shown that the addition of carboxylic acid might be beneficial to the stabilisation of the metal-hydroxymethyl group M-CH_2-OH, which was believed to be an intermediate species of F-T reactions, especially EG

formation.[44] Despite this belief the isolation of this species proved quite difficult, but not impossible[45] due to its instability. Ironically, but logically, the most likely decomposition pathway is dehydrogenation to CO, possibly via ß-H elimination. The acyloxymethyl group, M-CH_2-O-COR, is inert towards ß-elimination and is readily synthesised and isolated.[46] Reaction of $Mn(CO)_5(CH_2OCOR)$ with hydrogen under moderate pressures (<10 bar) yielded the ester of glycol aldehyde, which is a product from CO insertion into the M-acyloxy methyl[a] group. See Scheme 1.2.

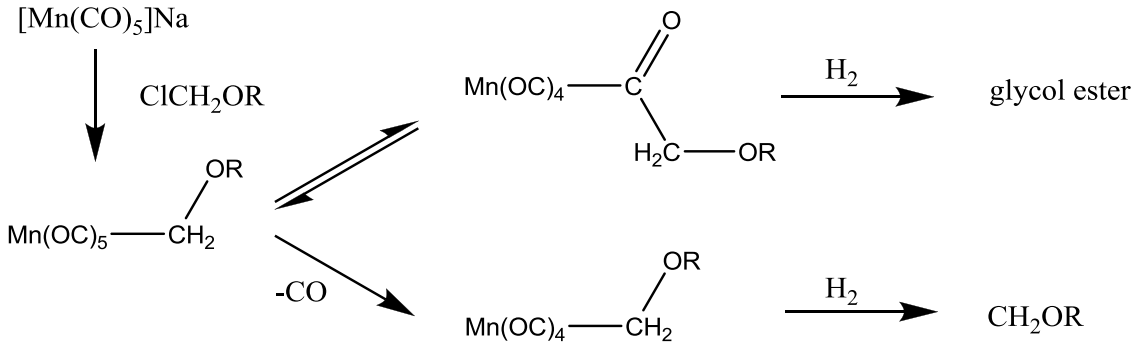

Scheme 1.2 the formation of glycol via CO insertion into a Mn-acyloxy methyl bond. Adapted from Dombek[46] scheme I.

For syngas chemistry, it is thought that in a carboxylic acid or ester rich environment the acyloxy methyl species may be formed *in situ*, and that this, then, provides a more facile route to C-C coupled products, by stabilisation of the hydroxy methyl intermediate and maybe prolonging its lifetime. Indeed, reactions of ruthenium dissolved in acetic acid with syngas at elevated pressures and temperatures yielded the formation of small amounts of glycol. In table 1.9 the reaction of ruthenium and syngas in different media is presented. For these reactions a number of precursors can be used and these will be discussed later.

[a] The hydroxy methyl group is M-**CH_2-OH**, the methoxy methyl group and the acyloxy methyl groups are analogues where the hydrogen has been replaced by a methyl or a acyl group respectively.

Table 1.9. Bronsted acid catalysed CO hydrogenation by soluble ruthenium species[a]

reaction	solvent	amount (mL)	$-CH_3-O-$ (mmol)	$-O-CH_3-CH_3-O-$ (mmol)
1	acetic acid	50	52.2	1.37
2	propionic acid	50	61	1.03
3	acetic acid[b]	50	14.9	0.41
4	acetic acid[c]	50	139	1.58
5	acetic acid	40	66.8	0.75
	water	10		
6	acetic acid	40	39.7	0.82
	cyclohexane	10		
7	acetic acid	40	45.9	1.03
	THF	10		
8	acetic acid	40	48.2	0.21
	H_3PO_4	10 grams		
9	THF	50	19.4	
10	ethyl acetate	50	33.1	
11	ethanol	50	55.6	
12	ethanol[c]	50	109	

[a]All reactions were performed with $[Ru_3(CO)_{12}]$ (2.35 mmol of Ru), 230 ^oC, 340 atm, H_2/CO 1:1, 2 hrs [b]0.7 mmol Ru [c]260 ^oC. Data from Dombek.[7]

Surprisingly, the yields are very high considering the relatively low pressure that is used. The products in the case of a carboxylic acid solvent are in fact not methanol and EG but more likely their acetate esters. It was observed that only carboxylic acids are necessary for the formation of glycol, whilst other moieties; Brønsted acids and esters, ethers, alcohols, hydrocarbons etc. do not promote C-C coupling. The methanol production in this system remains largely unaffected by the solvent, however increasing the temperature by 30 ^oC more than doubles methanol formation. The -COOH dependency works to such an extent that dilution with inert co-solvents decreases total activity (except in the case of dilution by water) and also the rate of C-C coupling (in all cases). The rates of C-C coupling to EG and acetic acid are linearly correlated (Figure 1.9). The increased rate of formation shows that there must already be an interaction of the carboxylic acid with the catalyst before or during the rate determining step. Therefore, it is safe to say that the bulk of acetates that are formed are not due to esterification after product release. Further attempts were made to clarify some aspects of the mechanism. Varying the $CO:H_2$ ratio shows that the EG yield as a function of these partial pressures depends on H_2 pressure with an order of about 1.3. The

dependence on CO partial pressure is different. Up to a syngas ratio of 1:1, glycol formation is affected to a large extent; however as the CO partial pressure increases beyond this point the order in CO seems to approach zero order.

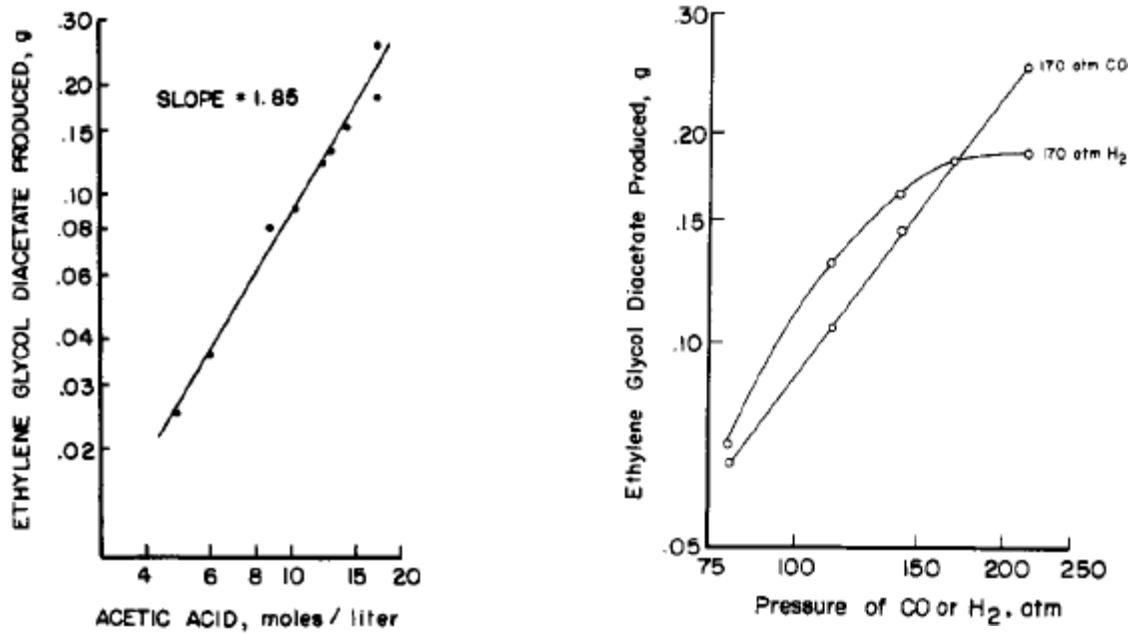

Figure 1.9. The effect of dilution of the solvent, acetic acid, with methyl acetate and water to the EG formation (left). The effect of changing the CO and H_2 partial pressures to EG formation (right). Conditions: All reactions were performed with $[Ru_3(CO)_{12}]$ (2.35 mmol of Ru), 230 ^oC, 340 atm, H_2/CO 1:1, 2 hrs. Reprinted (adapted) with permission from B. D. Dombek, *J. Am. Chem. Soc.*, 1980, 102, 6855-6857. Copyright (1980) American Chemical Society.[7]

The high dependency of the rate on P_{H2} shows a significant order in H_2 for EG formation. The p_{CO} dependency is different, the shape of the curve where p_{H2} is held constant indicates that there is a dependency on p_{CO} until a level of 150 bar of CO is reached and after which there is no effect. This indicates that until 150 bar of CO is used, mass transfer issues occur, but using pressures of over 150 bar solves this. High pressure IR experiments show that under the reaction conditions the main observable species is $[Ru(CO)_5]$ which can be hydrogenated to a mixture of polynuclear clusters.[47] How the dependence on hydrogen comes about is still uncertain and it most likely has to do with the mechanism and reactivity of the catalytic species. A number of precursor can be used to yield the same activity and species under reaction conditions. For instance $[H_4Ru_4(CO)_{12}]$, $[Ru(CO)_2(CH_3CO_2)_2]_n$, $[Ru_6C(CO)_{17}]$, $[H_3Ru_3(CO)_9(CCH_3)]$, $[Ru(acac)_3]$ and $[Ru_3(CO)_{12}]$ are equivalent precursors for this reaction. In fact, the first of these is thought to be a product of the hydrogenation of $[Ru(CO)_5]$ at elevated temperatures and pressures. [47] A mechanism was proposed by Dombek and is depicted in Scheme 1.3.

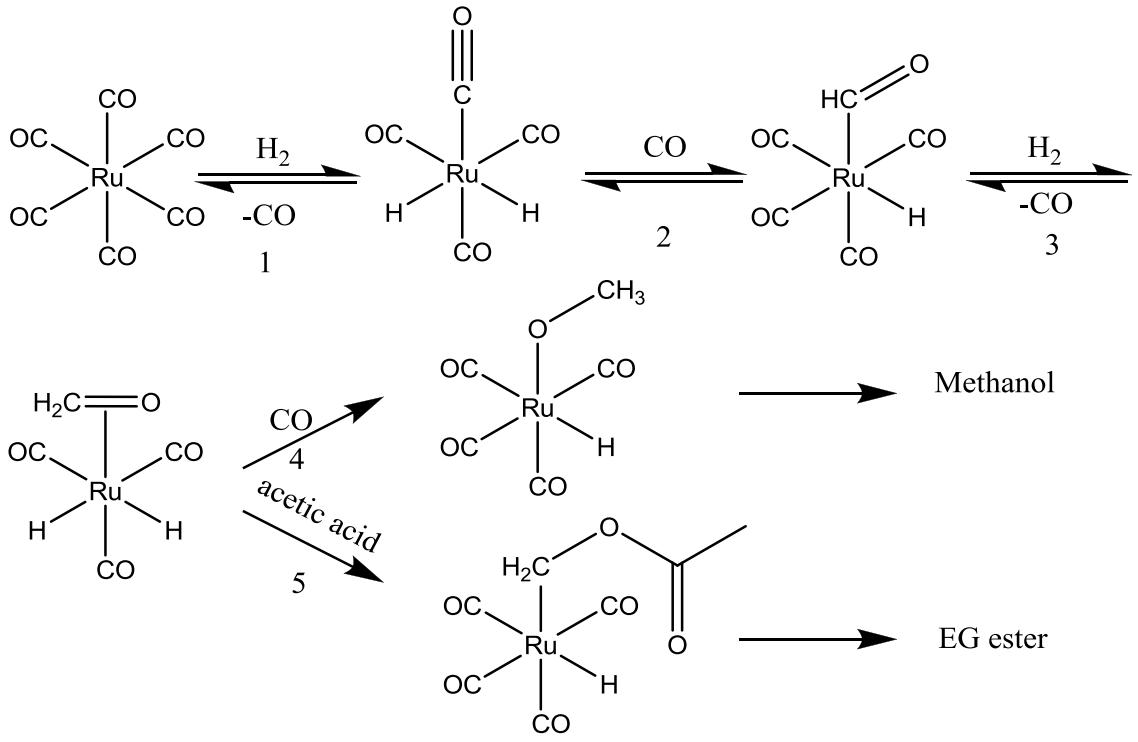

Scheme 1.3 Dombek proposed two distinct pathways that lead to Methanol or EG. With the help of acetic acid pathway 5 to EG can be promoted. This scheme was re-drawn and adapted from Dombek[7].

One important feature of this scheme is that it leads to two distinct species in steps 4 and 5. One leads to the formation of C_1 products, like methanol and methylformate. The other leads to C-C coupled products. The mechanism does not involve the interaction with of carboxylic acids until the hydroxy methyl species has been formed. According to Dombek, this accounts for the improved selectivity towards C-C coupled products with increasing levels of acetic acid, while the formation of methanol should be unaffected. However, in case step 4 and 5 are competing, favouring one mechanism over the other should lead to diminished product formation of the other. Interestingly, the scheme does not really provide an answer to the H_2 dependency of the reaction. Step 1 is thought to be easy and step 2 difficult. However, the rate dependency shows the opposite, and this suggests that step 3 may be rate determining. In any case, the pathway that is shown is a reasonable starting point for investigations and shows some key intermediates that are likely to exist at some point during product formation. It therefore provides a good addition to the current theory of the time. We can make a quick comparison with work done by Knifton and co-workers from Texaco, who published a patent concerning the hydrogenation of CO in acetic acid using various Ru, Os and Rh catalysts at pressures ranging from 90-500 bar.[48] The solvent used in this study is usually acetic acid, and therefore it can be expected that the products will

contain –OAc groups derived from the solvent. Most of the information of the patent is omitted, because of its ambiguous nature. Table 1.10 shows the results of the first set of experiments performed in this study.

Table 1.10 CO hydrogenation in acetic acid. Precursors[a]

	amount (mmol)	promoter	concentration (wt%) in the solvent		
			MeOAc	EtOAc	$(CH_2OAc)_2$
$Ru(acac)_2$	1	-	1.9	0.3	1.4
$Ru_3(CO)_{12}$	2	-	4.2	0.5	0.4
$Ru(CO)_3PPh_3$	1	-	3.4	0.8	0.2
$Ru(6F\text{-}acac)_3$[d]	1	-	5.7	0.2	0.26
$Os_3(CO)_{12}$	0.66	-	present	present	present

[a]Conditions: 186 bar, 18 hr, 220 ^oC, acetic acid(50 mL). [b] 0.40 g. [c]"present" means that the product was detected, but no quantities were stated in the text. [d]Ruthenium tris(hexafluoro-acetylacetonate). Data adapted from Knifton[48]

The use of electron withdrawing groups on the acetylacetonate ruthenium is beneficial to CO hydrogenation, even in catalytic amounts. Also having phosphine donors on the metal is beneficial over unpromoted systems for the formation of C_1 products, unfortunately it seems to inhibit the formation EG-derived products. Phospines, being less good π-acceptors and better σ-donors than CO increase the electron density on the metal, so might be expected to increase the rate of oxidative addition reactions and reduce the rate of reductive elimination. The increased rate of methanol formation when phosphines are employed may mean that hydrogen addition to the ruthenium is rate determining. However, the addition of phosphines seems to inhibit C-C bond forming reactions. In table 1.11 the effect of cesium as a promoter is investigated. There seems to be a maximum in activity at a Ru/Cs ratio of 1/10. However, maybe the beneficial effect is not from the use of caesium itself, but from the addition of a basic counter ion in the solution. In fact, a set of examples using barium propanoate instead of cesium propanoate (both in propanoic acid) show that both systems yield similar product distributions. Indicating that it is in fact the counter(an)ion that promotes the effect.

Table 1.11 CO hydrogenation in acetic acid. Cesium promoter[a]

		product yield (wt%)			
cesium salt[b]	Cs/Ru	H_2O	MeOAc	EtOAc	$(CH_2OAc)_2$
0	0	6.8	19.9	23.1	0.22
4	1	1.1	19.4	15.6	0.18
12	3	0.4	23	3.8	0.86
20	5	0.3	38.9	4.2	2.28
40	10	0.4	42	5.7	3.2
60	15	0.5	33.1	5.6	2.66

[a] Conditions: $RuCl_3.xH_2O$ (4 mmol Ru), 220 ^oC, 275 bar, acetic acid (50 g). [b] Added as CsOAc. Data adapted from Knifton[48]

Further Knifton shows in these examples that an increase in the CO partial pressure leads to a change in the product distribution towards more C-C coupled products. Also Knifton finds that the use of phosphonium salt solvents leads to an increase of activity. We will discuss these observations at a later point.

1.6.1 Ionic promoters

As the rate limiting step is believed to concern the activation of H_2. Adding promoters that increase this H_2 activation by the complexes might provide a way to increase the rate of product formation. The addition of a negative charge to the complexes will promote hydride formation and should therefore increase reactivity. In a subsequent paper,[10] Dombek discusses the use of ionic promoters in the hydrogenation of CO. Table 1.12 looks at the effect of different anions on the product formation rate. Compared to previous experiments the pressure that is applied is much higher, 840 atm opposed to 340 atm, the catalyst loading has also almost tripled compared to previous runs. However, the main focus of this investigation is to increase the selectivity towards C-C coupled products, primarily to EG. Previous studies on unpromoted Ru catalysts by Dombek had shown that very little EG was formed in these systems and the first entry in Table 1.12 reconfirms this observation. Addition of salts improves this and, especially for the iodide anion, the selectivity is increased dramatically. Further, the total activity of the system is also improved more than 14 times. Interestingly, the acetate anion also increases the activity and, as seen before by Knifton, yields moderate amounts of EG.

Table 1.12 Rates to product formation[a]

salt	CH_3OH (mmol h^{-1})	glycol (mmol h^{-1})	ratio
none	13.9	-	-
KI	202	43.5	0.22
KBr	81.3	17.2	0.21
KCl	39.7	6.9	0.17
KF	44.7	1	0.02
K_3PO_4	60	1.9	0.03
KO_2CCH_3	55.8	1.5	0.03

[a]Conditions: sulfolane (75 mL), Ru (6 mmol), salt (18 mmol), 850 atm, 1:1 syngas, 230 ^oC. Data from Dombek.[10]

In Table 1.13 the effect of the cation is shown using iodide as the counter ion. As in the studies of rhodium catalysed CO hydrogenation[33] there is no correlation between the size of the cation and formation of methanol. Unlike in the rhodium study, there also does not appear to be a correlation to EG formation either.

Table 1.13 The effect of the cation on ruthenium catalysis.[a]

Salt	CH_3OH (mmol h^{-1})	$(CH_2OH)_2$ (mmol h^{-1})
LiI	146	24.8
NaI	119	26.3
KI	152	23.3
CsI	120	21
PPNI	143	26.3

[a]Conditions: Sulfonlane (75 mL), salt (18 mmol), Ru ($[Ru_3(CO)_{12}]$, 3 mmol), 1:1 syngas, 861 bar, 230 ^oC. Data from Dombek.[49]

1.6.2 Promoter concentration[10]

The addition of increasing amounts of iodide salts induces an increasing activity of the catalyst, apparently up to the solubility limit of the salts into the solvent. This is not an electrolyte effect; it is not the increase of the general concentration of electrolytes that improves catalysis. Adding to the system another salt will only increase the catalytic activity by the amount that can be expected from that salt alone; there is no progressive effect. Figure 1.10 shows how the rate of formation of methanol and EG is changed upon increasing the iodide concentration. For methanol, the rate of formation shows a straight line on the log-log plot. For EG this is not the case. The figure shows that the slope of the rate of formation of EG vs. $[I^-]$ is steep at low concentrations of

iodide, however when the concentration of iodide reaches approximately half that of ruthenium this trend abruptly changes and a much shallower increase with [I^-] is observed. Below [I^-] of 0.03 mol kg^{-1} the selectivity to EG increases with increasing [I^-]. However, rate dependence of methanol formation for [I^-] has an order of 0.6 and for glycol the order of 0.45 (above 0.03 mol kg^{-1}), so the activity for methanol increases more than the activity for glycol and therefore high concentrations of iodide can increase the overall activity of Ru-halide systems while the product ratio becomes less and less favourable.

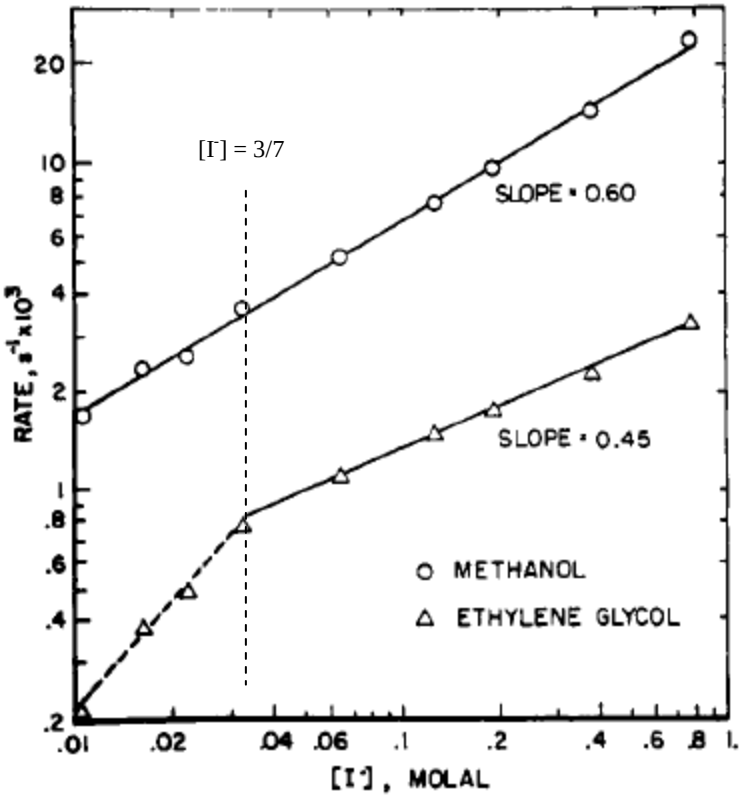

Figure 1.10 The correlations between the reaction rate for methanol or glycol and the iodide concentration. "Reprinted (adapted) with permission from B. D. Dombek, *J. Am. Chem. Soc.*, 1981, 103, 6508-6510. Copyright (1981) American Chemical Society."[10]

It is postulated that the origin of this behaviour can be found in the following equilibrium of species (equation 1.1). Identification of the ruthenium species after catalysis showed that the solutions only contained species **8** and **9**, [$Ru(CO)_5$] was not observed (although it had been in previous unpromoted Ru studies)

$$7/3\ Ru_3(CO)_{12}\ (\mathbf{1}) + H_2 + 3\ I^- \longrightarrow 2\ [HRu_3(CO)_{11}]^-\ (\mathbf{8}) + fac\text{-}[RuI_3(CO)_3]^-\ (\mathbf{9}) + 3\ CO \quad (1.1$$

As can be seen the ideal [I]/[Ru] value for this reaction would be $^{3}/_{7}$, which falls close to the limits of the observation in figure 1.10. Species **8** and **9** have been synthesised and characterised before[50, 51] and additional examination shows that, when both species **8** and **9** are tested for activity individually, only minor amounts of glycol are formed. However, when both species are added together, catalysis to glycol occurs either in the presence or absence of additional promoters. Interestingly, the best results were obtained for a mixture of 2:1 (**8**:**9**), as suggested by Equation 1.1 (Figure 1.11).

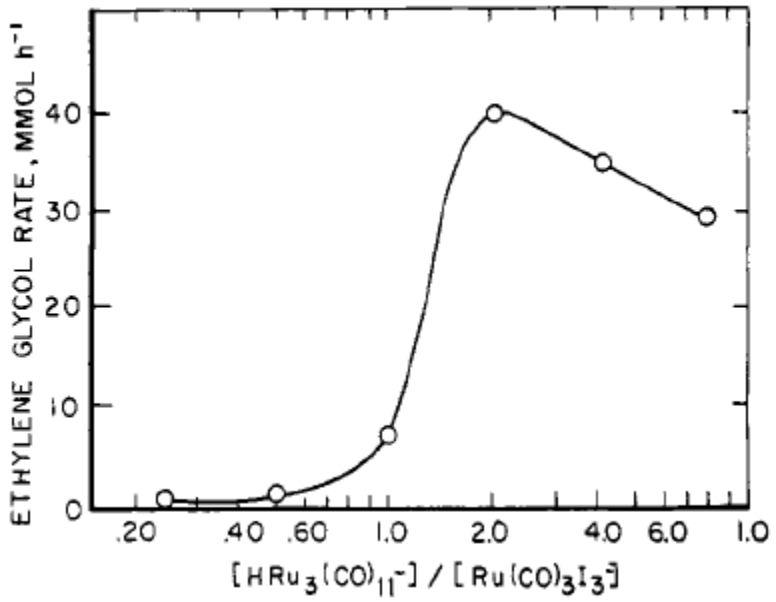

Figure 1.11 The dependence of the catalytic activity of Ru upon the molar ratio of species 8 and 9 [a] "Reprinted (adapted) with permission from B. D. Dombek, *J. Am. Chem. Soc.*, 1981, 103, 6508-6510. Copyright (1981) American Chemical Society."[10]

These findings prompted deeper investigations into the exact nature of the active species. Before we address the possible active species in this system we will consider some other factors. A rather extensive paper[49] by Dombek was published in 1983 and it presents a more in depth discussion of factors influencing catalytic activity including pressure, temperature, product distribution and catalyst loading. This will be reviewed briefly before returning to the mechanistic implications.

1.6.3 Product formation[49]

The general activity of the Ru catalysts fall between 1.5-4.0 x 10^{-2} s^{1} Ru^{-1}, based on the combined formation of MeOH and glycol. This is comparable to the activity of other metal catalysts. Without halide promoter this falls to less than 0.5 x 10^{-2} s^{-1}. In

figure 1.12 the rate of formation is examined throughout 4 hours. It should be noted that, for this reaction, very large amounts of ruthenium are used.

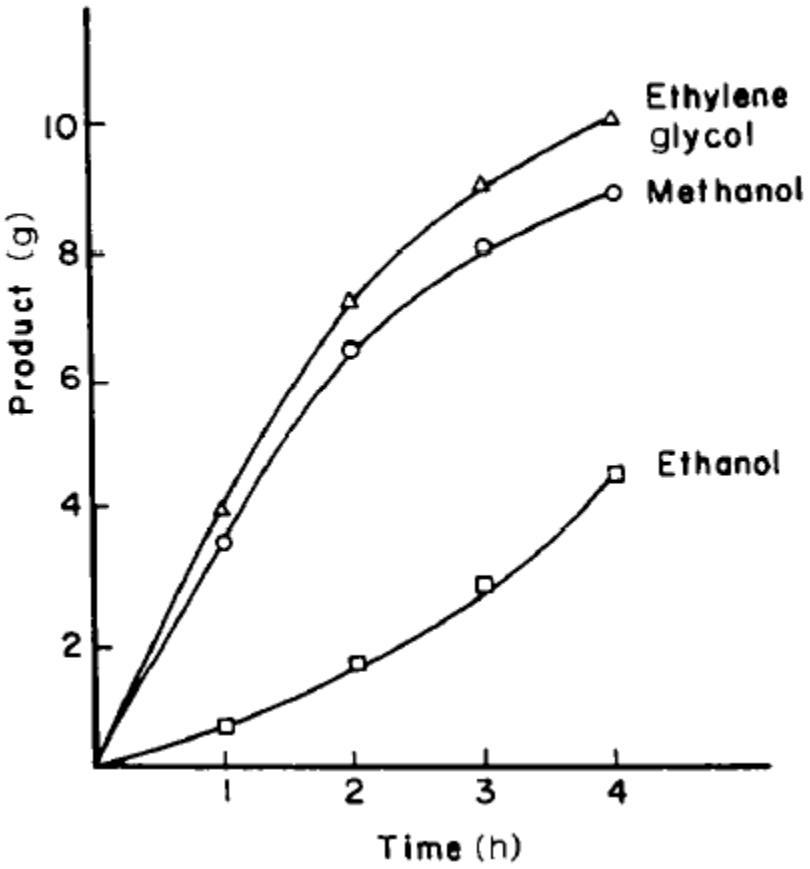

Figure 1.12 Product formation of methanol, ethanol and EG over time, Conditions: NMP (75 mL), Ru (30 mmol), KI (120 mmol), 850 atm, 200 ^{o}C. "Reprinted from J. of Organomet. Chem., 250 (1), B.Duane Dombek, Hydrogenation of carbon monoxide by ruthenium complexes with iodide promoters: catalytic and mechanistic investigations, 467-483, Copyright (1983), with permission from Elsevier." [49]

Next to methanol, ethanol and ethylene glycol, a variety of other products is produced; these are shown in Table 1.14. It can be expected that most of the higher products are probably from sequential-reactions. As time progresses the rate of formation of these compounds should increase while the rate of formation of methanol and EG should appear to decrease. Dioxolanes are the glycol acetals of aldehydes, so they are likely to come from secondary reactions. Table 1.14 shows some of the products and their typical weight percentages.

Table 1.14. Product distribution of iodide promoted ruthenium catalysed carbon monoxide hydrogenation[a]

product	weight percent
Methanol	30-80
Ethylene glycol	5-60
ethanol	2-30
glycerol	0.2-3
2-methyl-1,3-dioxolane	0.2-4
2-hydroxymethyl-1,3-dioxolane	0.2-3

Data from Dombek[49]. No conditions mentioned.

1.6.4 Solvent effect

The nature of the solvent seems to have an enormous effect on the activity of the ruthenium halide system. As will be discussed later it is very clear that the phosphorus containing solvent is the most active one. The higher activity of the crown ether vs. tetraglyme may arise from the higher solubility of the salt in the crown ether, which increases the iodide concentration in solution. Also, as discussed later but notable now, ion pairing is shown to have a large effect on catalysis and might explain the difference in reactivity between using tetraglyme (TG) and the crown ether. However, if solubility of the salt is considered, all the effects observed here could arise from the increased solubility of KI into the solvent. In contrast, for water, the solubility of the catalyst (though thought to be ionic) might pose an initial problem, see table 1.15.

Table 1.15 The effect of the solvent on iodide promoted ruthenium catalysed carbon monoxide hydrogenation[a]

solvent	CH_3OH (mmol h^{-1})	$(CH_2OH)_2$ (mmol h^{-1})
sulfolane	270	44
NMP	398	48
Pr_3PO	435	50
18-C-6	380	45
Tetraglyme	75	5.2
n-Butanol	16	trace
Water	23	trace

[a]Conditions: solvent (75 mL), Ru (6 mmol) ([$Ru_3(CO)_{12}$] source), KI (18 mmol), 861 bar, 1:1 syngas, 230 ^{o}C. From J. of Organomet. Chem., 250 (1), B.Duane Dombek, Hydrogenation of carbon monoxide by ruthenium complexes with iodide promoters: catalytic and mechanistic investigations, 467-483, Copyright (1983), with permission from Elsevier.

1.6.5 Catalyst concentration[49]

The influence of the catalyst concentration on the reaction rate ((mol product) (mol cat)$^{-1}$ (unit time)$^{-1}$) provides information on the species involved up to the slowest step in a cycle. In the case of the Ru-KI system there is a glycol formation rate dependence on ruthenium in the order of 1.3. The fractional nature of the order indicates that a number of equilibria may be involved before arriving at the active catalytic species from the precursor. Interestingly the order in ruthenium for methanol formation is lower: ca. 1 (Sulfolane) or less (NMP), depending on the solvent. This means that increasing the catalyst concentration will increase the selectivity towards ethylene glycol.

1.6.6 Temperature and pressure[49]

A rise in temperature increases the overall activity for CO hydrogenation; however, the selectivity towards methanol increases more than that towards ethylene glycol. Temperature dependent measurements show that the energy of activation towards methanol is about 18 kcal mol^{-1}. The energy of activation for EG is lower, 9 kcal mol^{-1}. This behaviour is reversible up to temperature ranges between 230 and 270 ^{o}C depending on the pressure. Beyond this temperature irreversible decomposition of the catalyst occurs and overall activity drops. This maximum temperature of stability is dependent on pressure; at ambient pressure decomposition occurs at around 140 ^{o}C. Masters and van Doorn had shown that, in their reactions at 99 atm, the decomposition occurs at 270 ^{o}C.

1.6.7 Pressure

An interesting effect of the pressure on the catalytic activity is shown in Table 1.16. It shows that the total pressure of the system influences the reaction rate even if the partial pressures of CO and H_2 are the same. This is interesting, because, if thermodynamic equilibrium is reached, such an effect would not be observed. Therefore, the effect must be kinetic, and thus the pressure influences the energy of activation for product formation, it can be doubted that at these pressures substrate diffusion would be a rate limiting step. However, it would be wise to investigate this.

Table 1.16 The effect of pressure on performance[a]

$p(H_2)$ (Mpa)	$p(CO)$ (Mpa)	$p(N_2)$ (Mpa)	Methanol (mmol h^{-1})	Glycol (mmol h^{-1})
43	43	-	426	44
43	43	86	961	137

[a]The conditions: 18-crown-6 (75 mL), Ru (6 mmol), KI (18 mmol), 230 °C. According to Dombek[49], the additional effect of pressure by an inert gas shows that there is a substantial volume of activation. Data From J. of Organomet. Chem., 250 (1), B.Duane Dombek, Hydrogenation of carbon monoxide by ruthenium complexes with iodide promoters: catalytic and mechanistic investigations, 467-483, Copyright (1983), with permission from Elsevier.[49]

1.7 On the mechanism and species present under reaction conditions

Earlier, the behaviour of clusters under elevated temperatures and pressures was discussed. Now, we shall discuss the behaviour of ruthenium clusters in halide rich environments. Above we have described some of the factors that influence catalytic reactivity of these clusters, but the mechanisms and the active species remain unclear.

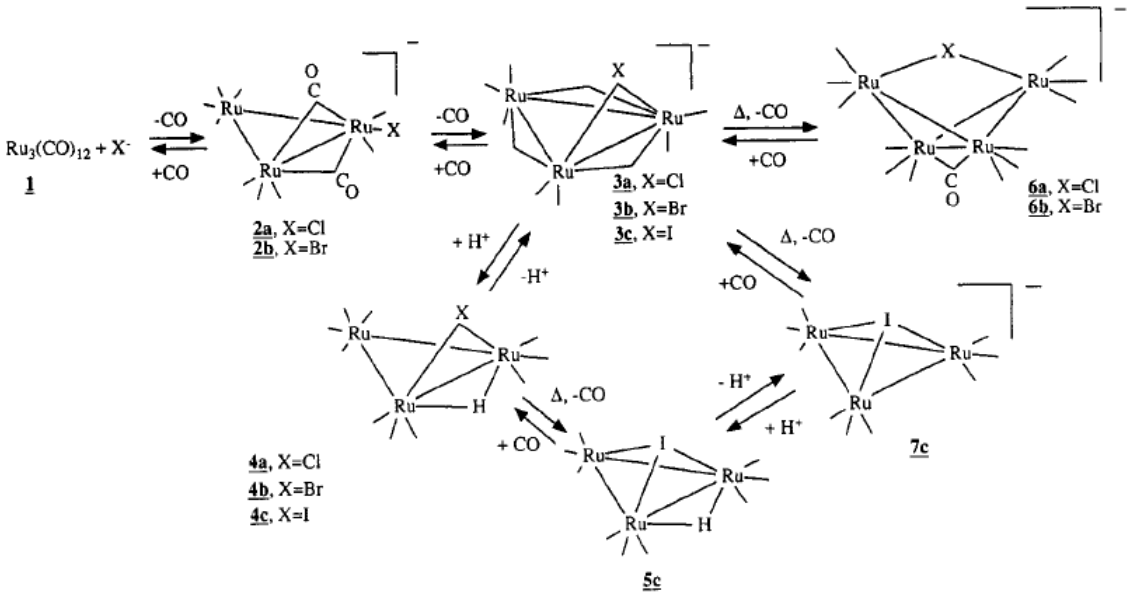

Scheme 1.4 The ruthenium species that are formed upon reaction with halide ions under low N_2, CO and H_2 pressures. For the sake of clarity most CO ligands have been omitted from the scheme. "Reprinted with permission from S. H. Han, G. L. Geoffroy, B. D. Dombek and A. L. Rheingold, *Inorg. Chem.*, 1988, 27, 4355-4361. Copyright 1988 American Chemical Society." [52]

Due to the particular reactivity of ruthenium halides in syngas conversion, it was decided to look more in depth at the species that ruthenium forms.[52-55]. Especially the ionic halide and hydride species are of interest. We will review some of the reactions following Han's work[52] which describes the behaviour of Ru-halide systems in aprotic

solvents for a temperature range of 20-150 ^{o}C at low pressures of CO, N_2 and H_2 and can be summarized in Scheme 1.4. Species **1** can be obtained commercially. Species **2**, **3**, **4** and **5** are formed from **1** by addition of halide ions to the solution (usually THF). The halide ions are added to the system as [PPN]X, with X being a halide ion. Here the halide nucleophile substitutes CO rapidly. It is observed that, many nucleophiles will perform these reactions.[55] The position of the equilibria is mostly dependent on the CO pressure and the halide used. For X= Cl and Br species **2** is formed readily from **1** in a closed vessel under N_2. The partial pressure of the released CO from this step is sufficient to prevent further conversion to **3**. However, upon removal of this CO, **3** can be formed at room temperature. Complete conversion to **4**, a tetranuclear species, takes days at ambient conditions, but is accelerated by heating. This species is only accessible to the Cl^- and Br^- complexes. For the iodide promoter the same treatment results in the formation of **5**, a μ_3-trinuclear complex. This complex can be protonated to form the hydride **6**, with the hydride bridging two Ru-atoms, and still only accessible to the iodide complex. However, the final species discussed in Scheme 1.4, **7**, can be formed by further addition of CO to the hydride complex. It might be important to stress that **7** can be observed for all of these halide complexes, leaving species **5** and **6** only accessible to iodide complexes.

1.7.1 Reactions of $[Ru_3(CO)_{12}]$ with Iodide in the presence of H_2:

In the presence of H_2 or CO/H_2 the solutions of **1** ($[Ru_3(CO)_{12}]$) and [PPN]I form different species than in the system with CO and N_2 only. The hydrogen is activated and the complex disproportionates in the following reaction:

$$3/7\ [Ru_3(CO)_{12}]\ (\mathbf{1}) + H_2 + 3\ I^- \xrightarrow[3\ atm\ H_2/CO]{THF,\ 65\ ^oC} 2\ [HRu_3(CO)_{11}]^-\ (\mathbf{8}) + fac\text{-}[RuI_3(CO)_3]^-\ (\mathbf{9}) + 3\ CO \qquad \text{(eq. 1.2}$$

The mechanism is not yet fully understood, but from the experiments described above it is obvious that the bound CO is quite labile and the complexes quite fluxional. Therefore, it is not inconceivable to imagine the dissociation of one CO ligand and a subsequent addition of H_2 to form a species similar to **2**. The addition of a base such as triethylamine results in deprotonation, and hydride **8** formation. In addition, the experiments correlating the iodide concentration to the rate of EG formation showed a

sudden break at a value similar to $[I^-]/[Ru]= 3/7$ (Figure 1.10). The origin of this behaviour may come from the halide assisted $[Ru_3(CO)_{12}]$ disproportionation (eq. 1). Up until $[I^-]/[Ru]= 3/7$ the solution does not contain enough iodide to shift the equilibrium all the way to disproportionation. However, above this level the $[I^-]$ may have a promoter effect as free iodide. The mechanism of formation of **9** from **1** is less straightforward, however it is thought to go through species **6**, the μ_3-bridged complex, since species **8** and **9** can be formed starting from **6**:

3 $[Ru_3(\mu_3\text{-}I)(CO)_9]^-$ **(6)** $+H_2$ +12 CO

$$2\ [HRu_3(CO)_{11}]^-\ \textbf{(8)} + [RuI_3(CO)_3]^-\ \textbf{(9)} + 2/3\ [Ru_3(CO)_{12}]\ \textbf{(1)} \qquad \text{(eq. 1.3.}$$

Note, that no additional halides are present for this reaction. Furthermore, it is thought that deprotonation of the intermediate hydrogen complex $[H_2Ru_3(CO)_{11}]$ from **1** could occur by bases as weak as halide anions.[52] Additionally, $[RuI_3(CO)_3]^-$ (**9**) can be formed from **1** by addition of HI at room temperature with the formation of H_2 and CO. At higher temperatures the $[Ru_3(CO)_{12}]$ halide solutions undergo reactions to form $[Ru_6(CO)_{18}]^{2-}$ (**10**) (100 ^oC) and the carbide $[Ru_6C(CO)_{16}]^{-2}$ (>140 ^oC) (**11**)[6, 30]. In the solutions that are of true interest the conditions are much more severe in terms of temperature and pressure. Therefore, we still cannot predict what species are present under the reaction conditions; however, it is apparent that the Ru-complexes are highly interchangeable even at low temperatures. This indicates that the species capable of CO hydrogenation will probably be formed in equilibrium concentrations.

Improving catalysis can be tackled in two ways; one is to identify the species that performs the catalysis and alter the conditions in order to improve their concentrations, whilst another is to make completely new species that are based on the make-up of the active catalyst in the current system. Both require knowledge of the active species. Therefore, the synthesis of ruthenium species under catalytic conditions was studied.[49]

1.7.2 Catalytic conditions: The Ru-I system

At elevated temperatures and pressures, the only observable species by IR are species **8** and **9** which are made from **1**.[49] In addition to this, it was found that neither species was active on its own: a solution of both species is needed to obtain catalytic

activity. Additionally, it was shown that there is an additional promoting effect of NaI salt, i.e. if NaI is omitted from the solution of **8** and **9**, activity is reduced by half (no. 8 and 9, Table 1.17).

Table 1.17 Active species in the Ru-halide system[a]

No	complex	Amount (mmol)	NaI	MeOH (mmol h^{-1})	Glycol (mmol h^{-1})
1	$[Ru_3(CO)_{12}]$	2	18	171	35
2	$(PPN)_2[Ru_6C(CO)_{16}]$	1	18	89	8
3	$(PPN)_2[Ru_6C(CO)_{16}]$	0.86	18	12	trace
	$PPN[Ru(CO)_3I_3]$	0.86			
4	$PPN[Ru(CO)_3I_3]$	6	0	0	0
5	$PPN[Ru(CO)_3I_3]$	6	18	0	0
6	$PPN[HRu_3(CO)_{11}]$	2	0	33	trace
7	$PPN[HRu_3(CO)_{11}]$	2	18	123	8
8	$PPN[HRu_3(CO)_{11}]$	1.72	18	188	34
	$PPN[Ru(CO)_3I_3]$	0.86			
9	$PPN[HRu_3(CO)_{11}]$	1.72	0	80	15
	$PPN[Ru(CO)_3I_3]$	0.86			

[a] Conditions: Sulfolane (75 mL), 841 atm, 1:1 syngas, 230 °C. From J. of Organomet. Chem., 250 (1), B.Duane Dombek, Hydrogenation of carbon monoxide by ruthenium complexes with iodide promoters: catalytic and mechanistic investigations, 467-483, Copyright (1983), with permission from Elsevier.[49]

Testing the activity of solutions **8** and **9** at different concentrations compared to one another shows that for glycol production the maximum activity is achieved for solutions composed of 2/1= $[HRu_3(CO)_{11}]^-/[RuI_3(CO)_3]$, the same ratio in which they are formed from $[Ru_3(CO)_{12}]$. See eq. 2. A part of Figure 1.13 was shown before but now the EG formation dependency for **9** is shown as well. It shows that at low concentrations of **8** there is no EG formation at all. The skewed symmetry between the two curves point to a difference in dependency on EG formation between the compounds **8** and **9**.

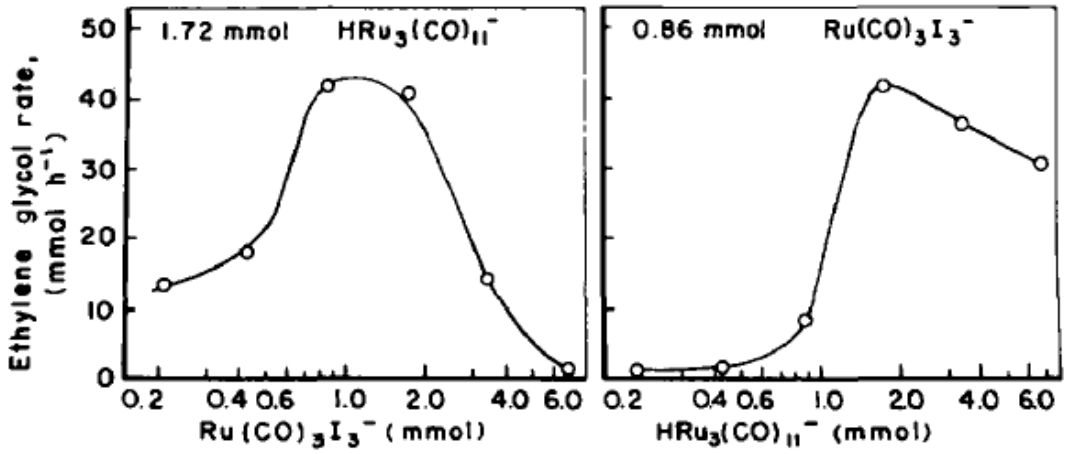

Figure 1.13. The EG formation rate at different ratios of species 8 and 9. "Reprinted from J. of Organomet. Chem., 250 (1), B.Duane Dombek, Hydrogenation of carbon monoxide by ruthenium complexes with iodide promoters: catalytic and mechanistic investigations, 467-483, Copyright (1983), with permission from Elsevier."[49]

So far it has been shown that species **8**, **9** and [I^-] all show concentration dependencies towards the product. Hence, an equation is considered. In this scenario the order of the [I^-] dependency comes close to that of the one observed (0.43). However, the observed order in Ru does not correspond to this equation:

$$2/7\ [HRu_3(CO)_{11}]^-\ \mathbf{(8)} + 1/7\ [RuI_3(CO)_3]^-\ \mathbf{(9)} + 4/7\ I^- + 3/7\ CO \longleftrightarrow$$

$$1/7\ H_2 + Ru(CO)_4I\ \mathbf{(10)} \longrightarrow \text{product}$$

Another scenario is postulated wherein species **8** transfers a hydride to species **9**, or a species more susceptible to hydride attack in equilibrium with **9**, for instance:

$$[Ru(CO)_3I_3]^- + CO \longleftrightarrow [Ru(CO)_4I_2]\ (\mathbf{11}) + I^-$$

However, this scenario is unlikely, since the order in I^- would be inversed, and the ratio of **8**/**9** would not give maximum conversion at 2. In this system the CO dependency is stated to be large, even though this has not been quantified[7]; it seems that the system is more *pressure* dependent than *CO-pressure* dependent. High CO pressures may result in cluster breakdown that may not be directly observed:

$$[HRu_3(CO)_{11}]^-\ (\mathbf{8}) + 3\ CO \longleftrightarrow [HRu(CO)_4]^-\ (\mathbf{12}) + 2\ [Ru(CO)_5]$$

Even though $[Ru(CO)_5]$ is a species that is very stable from **1** under acidic conditions, and under high CO pressures[7], Dombek postulates that this species will react immediately with H_2 and I^- to produce **8** and **9**. However, taken together species **12**

(better hydride donor than **8**) and **11** (more susceptible to hydride attack than **9**) could be active species in the formation of a formyl complex, which would be a precursor to the formation of glycol. The rate determining step could be this formyl formation or the formation of species **12** or **11**. For this mechanism to hold, the found rate dependencies and orders in the Ru-I system should fit into these postulates. Since no kinetic data can yet be presented, the qualitative comparisons of the rates will only be rough estimates. However, this mechanism does agree with the observation that **9** does not catalyse the reaction on its own, and that **8** can be converted to promote limited catalysis in the presence of I^-. Further, it can be noted that since both **12** and **8** are sensitive to water and alcohols, their presences should inhibit the conversion to glycol or other products.

1.8 On the synthesis and stability of the metal formyl species

Earlier we discussed the presence of methoxy methyl species and how we can stabilise them to our advantage using carboxylic acids. In terms of the catalysts and the "active species" we have focussed primarily on the equilibria within the metal clusters. However, we should also discuss the chemistry of the first species that is formed in CO reduction. We have described how the clusters are believed to form a hydride donor and an activated carbonyl complex set. Further, it is believed that the first step should be hydride transfer to the activated carbonyl, yielding a complexed metal formyl species. Studies on **10** and **11** show that they will react with one and another quite readily even at -60 ^oC. However, no presence of formyl complexes could be detected, probably because of the rapid decomposition of Ru-formyl complexes. A rhenium-model complex of **11** which forms more stable formyl complexes, and of which the IR CO absorptions show that the CO should have a comparable bond order to **11**, shows that it readily reacts with **10** to form a more or less stable formyl complex.[49] This indicates that the reaction between **10** and **11** is at least plausible and that a formyl product may be formed before it quickly decomposes. Furthermore, the remaining metal complex from that reaction, $[Ru(CO)_4]$ seems to react with **10** to form $[HRu_2(CO)_8]^-$ which could be involved in further hydride transfer. In a reaction to the proposal that the hydrogenation of CO might occur via the hydride transfer of $[HRu_3(CO)11]^-$ (**8**) to $[RuI_3(CO)_3]^-$ (**9**) or related complexes (like $[Ru(CO)_4I_2]$) the ability of **8** to transfer hydrides to model ruthenium compounds with activated carbonyls was investigated.[56] Further attention was given to the role of ion pairing by the involved ions in the solvent

and its effect to the nearby carbonyl. It was found that the reaction of **8** (paired with either K^+ or PPN^+) with *trans*-$[Ru(CO)_2(dppe)_2][SbF_6]_2$ or *trans*-$[Ru(CO)_2(dp)_2][SbF_6]_2$ (dppe= 1,2-ethylenebisdiphenylphosphine and dp = *o*-$(Ph_2P)_2C_6H_4$) yields unknown products, but not the formyls, or the decomposition products thereof. However, reaction of $K[HRu(CO)_9(dppe)]$ (a more electron rich variation to **8**) with *trans*-$[Ru(CO)_2(dppe)_2][SbF_6]_2$ and *trans*-$[Ru(CO)_2(dp)_2][SbF_6]_2$ *does* yield the formyl product, *trans*-$[Ru(CHO)CO(dppe)^2]^+$ at -30 ^oC in DCM under CO atmosphere. To investigate the effect of the hydride complex ion pair the same reaction was performed with the $Na[HRu(CO)_9(dppe)]$ salt (instead of the K-salt). This time no product was found. However, when dibenzo-18-crown-6 was added to the same solution the formyl-complex was indeed formed. Likewise, the addition of $NaClO_4$ to the potassium hydride complex prevented all formyl formation. See table 1.18.

Table 1.18. Ion pairing effect in the formyl formation of Ruthenium carbonyl complexes[a]

Hydride donor	additive	formyl yield
$Na[HRu(CO)_9(dppe)]$	-	0
$Na[HRu(CO)_9(dppe)]$	18-C-6	100
$K[HRu(CO)_9(dppe)]$	-	100
$K[HRu(CO)_9(dppe)]$	$NaClO_4$	0

[a]Conditions: in DCM, under CO, -30 ^oC. Data from Barrat et al.[56]

That ion pairing has a substantial effect on anionic complex carbonyl chemistry was investigated earlier. It was found by Collman et al.[57] that ion pairing in an anionic alkyl-carbonyl complex activated the complex for migratory insertion. In media where the ion pair was broken up the insertion was inhibited. It was shown earlier[58] that ion pairing does occur in anionic carbonyl complexes, but also importantly this complexation can occur from a unique carbonyl, distinguishable from the remaining carbonyls. It was therefore suggested that, in this case, the cation complexed to a CO-oxygen activating it for the insertion. In the hydride transfer described above, activation of the hydride may be impaired by the presence of the cation. A strong interaction of the cation with the carbonyls of the hydride complex may reduce the electron density on the complex to such extent that hydride transfer does not occur anymore. For cluster carbonyls the effect of ion pairing is less strong than for mononuclear species,[59] probably due to the reduced locality of the charge. Nonetheless, Collman and Barrat have demonstrated that ion pairing can affect the reactivity of metal carbonyls in two

distinct ways; by affecting the hydridic nature of the hydride and by activation of the receptive carbonyl. The examples above have also shown that, in principle, the reduction of CO can occur via intermolecular hydride donation, it may be good to discuss now the nature and stability of this species.

1.8.1 The stability of the formyl species

The decomposition of a metal formyl species usually occurs quite readily.[60, 61] The hydrogen is transferred to the metal and a CO ligand is formed. Finding and making stable formyl complexes is difficult and they usually decompose if a free site is available anywhere on the complex. The decomposition does not require any formal charge movement from ligand to metal centre and can therefore not be stabilised by influencing the charge on the complex. The availability of a free site, the stability of the formyl complex and the kinetics towards more stable products are therefore the only factors that can be influenced. So far this has been done by using large pressures and by finding metals that form stable formyls. The work by Barratt *et al.*[61] considers the stability of ruthenium formyl species (which are not stable at room temperature). They discovered earlier[62] that *trans*-[Ru(CHO)CO(dppe)$_2$][SbF_6] decomposes via a mechanism which involves the dissociation of one of the P-atoms from the metal, followed by migration of the hydride from the formyl to the free site, dissociation of CO and re-coordination of the phosphorus, now forming a cis-complex. (Scheme 1.5)

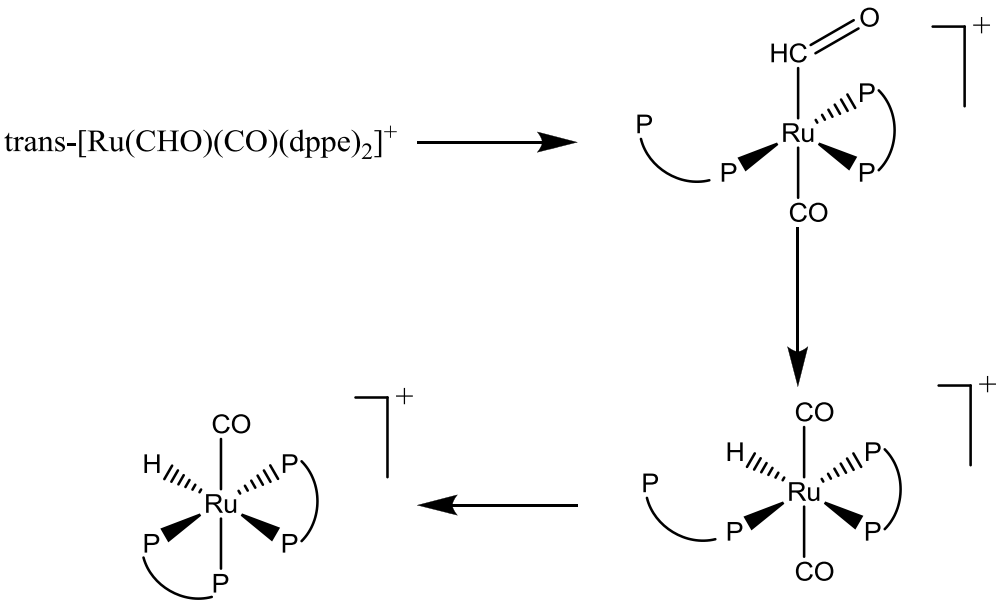

Scheme 1.5 The decomposition of *trans*-[Ru(CHO)(CO)(dppe)2]$^{+}$. Redrawn from Smith et al. [63].

In order to block this decomposition pathway, a more rigid bidentate phosphine was used, thus preventing P atom dissociation by preventing formation of a free site. The ligand of choice is dp (*o*-$(Ph_2P)_2C_6H_4$) to form the complex *trans*-[Ru(CHO)(CO)$(dp)_2$][SbF_6] from *trans*-[Ru$(CO)_2(dp)_2$][SbF_6] and K[BH(O-i-Pr)$_3$]. The new complex has a $t_{1/2}$ of ca. 30 minutes at 30 ^{o}C which a significant improvement compared with the first complex ($t_{1/2}$= 9 min). Furthermore, it was found that the decomposition product is not the *cis*- but the *trans*- complex. The decomposition pathway had changed, and no longer involved migration of the formyl hydride to a free site on the complex. Instead, the decomposition seemed to occur via the homolytic cleavage of the Ru-CHO bond, followed by abstraction of the H atom. Addition of a radical sensitive monomer to the reaction yielded the polymer whilst in the first reaction no polymer was found. From this, we can estimate that the ruthenium formyl species will be very short-lived under catalytic conditions. Even at room temperature the complex will decompose via a homolytic cleavage route, indicating highly unfavourable electronic configurations. For this reason it makes sense that the hydrogenation of CO requires such forcing conditions, even to form methanol. If the formation of C_2 species occurs via the reaction of formyl species it seems that it will be necessary to find a ligand or species that will stabilise the Ru-CHO bond significantly or conditions which favour coupling of two formyl radicals. For the anionic species $[(HCO)Fe(CO)_4]^-$ the IR and NMR spectra are highly dependent on the nature of the counterion, and on the tightness of the solvation cage.[64] Collman et al. had found that there is a close

resemblance to the acyl derivatives and that they have resonances that are characteristic of carbene complexes (Scheme 1.6).

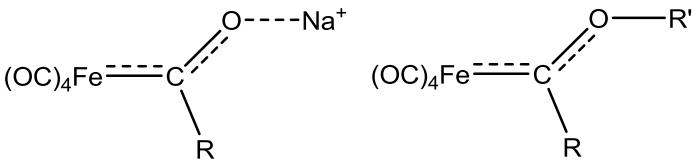

Scheme 1.6. The formyl and acyl carbene complexes of $Na[(CHO)Fe(CO)_4]$ and $[(RCOR)Fe(CO)_4]^-$. Structures redrawn from Collman et al.[64]

Additionally, the formyl carbene species show CO stretching frequencies that are usually in the aldehyde range. Protonation of the formyl complex yielded the formaldehyde. Similarly, others have synthesised formyl species for Ru and Os metals and also found that the metal formyl species generally react with electrophiles such as (CF_3SO_2Me and CF_3SO_2H) to form the methoxy and hydroxy carbene complexes.[65] In this study the formyl complexes were created by intermolecular hydride attack on carbonyls yielding $[M(CHO)(CO)(P\text{-}P)_2]^+$ species. Despite the cationic nature of these formyl complexes, further hydridic attack was not observed. It was suggested that this mechanism provides a route to alcohols which is free of aldehyde intermediates and uses two hydrides and two protons to form methanol from CO. In this mechanism the hydride transfer makes the formyl while three subsequent proton (two) and hydride (one) additions form the methanol (also see scheme 1.7). Casey et al. have shown that the hydrogenation of formyl carbenes to the hydroxy methyl group is indeed possible.[66] However, further investigations[45] show primarily the formation of the methyl-formyl ester. Additionally, it was found that the activation of metal CO not only occurs through hydride attack but that they are susceptible to attack by nucleophiles in general.[67] These investigations show how the formation of esters can occur during typical catalytic runs and therefore provide good background knowledge for this type of chemistry.

Returning to the actual catalytic system, The formation of $[HRu_3(CO)_{11}]^-$ from $[Ru_3(CO)_{12}]$ and H_2 produces a proton, so makes the solution acidic. Even though, a formyl formed by intermolecular hydride transfer from $[HRu_3(CO)_{11}]^-$ to $[RuI_3(CO)_3]^-$ or some species derived from it may be quite unstable, it would be trapped by the available protons to give a bound hydroxycarbene, which is much more stable. A second transfer of hydride would lead to the hydroxymethyl intermediate which could then proceed *via* protonation to methanol or *via* migration onto CO to EG, as in Scheme 1.7

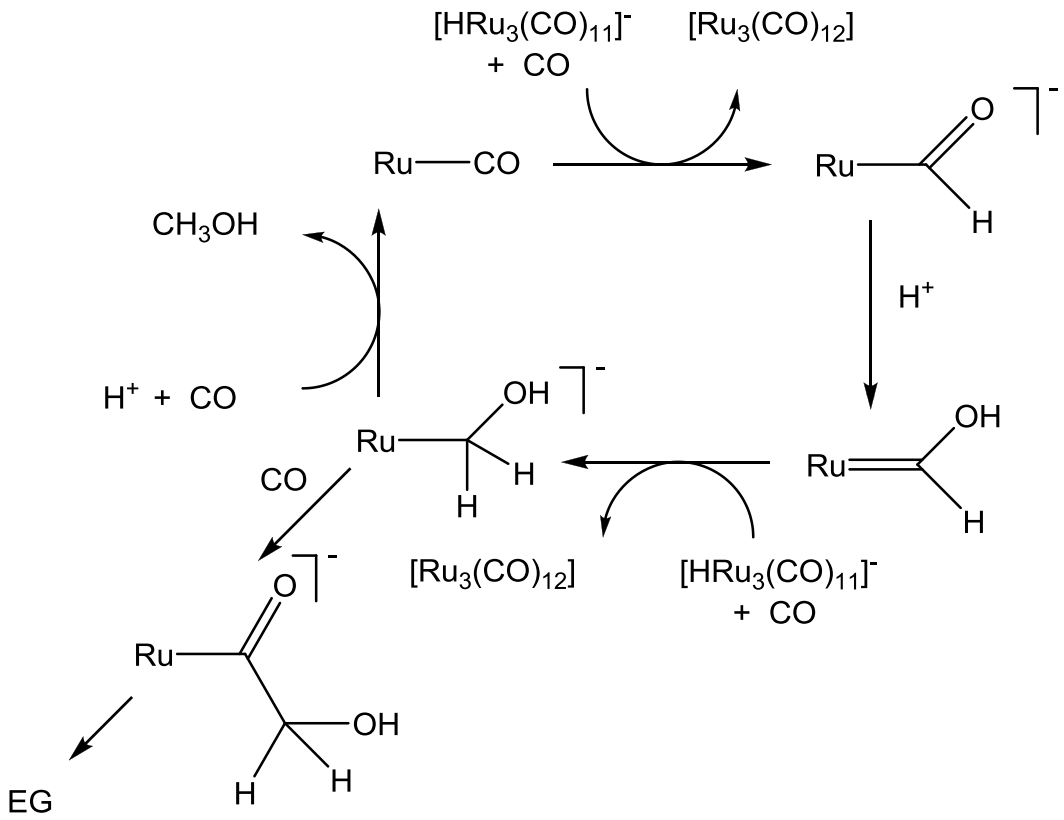

Scheme 1.7 Possible route to the formation of methanol and EG from CO and hydrogen involving the formation of a hydroxymethyl intermediate by sequential addition of H^- and H^+

1.9 Melt Chemistry

Knifton and co-workers from Texaco performed very similar work on ruthenium halide chemistry. Instead of using customary organic solvents as used by Dombek, Knifton used ionic liquids. An advantage of these solvents is that the formation of ionic ruthenium species should be promoted. Further, in the previous systems, the concentration of iodide in solution limited by the solubility of the iodide salt in the chosen solvent. Here this is not the case and the concentration of iodide is maximised. Because most of the work was reported in the form of patents it is sometimes less straightforward to comprehend the reasoning behind the chosen systems, apart from their high activity. Therefore, it may be more useful to discuss first some papers authored by Knifton and only then move towards the patents. In principle, the underlying mechanisms and species uncovered by Dombek can be extended to this new chemistry and can provide additional insights into its reactivity.

The first work to be discussed concerns the preparation of ethylene glycol from syngas using ruthenium and phosphonium salts.[11] It provides a good preliminary survey into the effects of precursor and solvent on catalysis as well as the influence of pressure,

catalyst loading and syngas ratio. The ruthenium source is usually dispersed into tetrabutylphosphonium bromide. The melting point of this salt is around 100 ^{o}C so it is, therefore, fully liquid during catalysis. Importantly, the phosphonium salts are usually very stable at higher temperatures and do not decompose, unlike some ammonium salts. After reaction (batch wise) the product can be distilled from the solution leaving the catalyst in the ionic phase which could be recycled. Table 1.19 shows some results:

Table 1.19 The performance of Ru-melt catalysis[a]

			product yield				
Ru-source	salt	promotor	EG	$HOCH_2$-CH_2OR[b]	MeOH	EtOH	Total yield, wt %[c]
RuO_2	Bu_4PBr		56	64	242	120	166
$Ru(acac)_2$	Bu_4PBr		48	66	253	225	186
$Ru_3(CO)_{12}$	Bu_4PBr		25	45	251	181	160
$[Bu_4P][HRu_3(CO)_{11}]$	Bu_4PBr		39	37	237	183	162
$[Bu_4P][Ru_6(CO)_{18}]$	Bu_4PBr		8	4	139	11	113
$RuO_2.xH_2O$	Bu_4PBr		34	53	250	204	193
$RuO_2.xH_2O$	Bu_4PCl		11	58	224	127	184
$RuO_2.xH_2O$	Bu_4PI		6	8	275	211	154
$RuO_2.xH_2O$	Bu_4POAc		10	14[d]	118[e]	9	59
$RuO_2.xH_2O$	Bu_4POH		8	9	206	36	83
$RuO_2.xH_2O$	$(C_{16}H_{33})Bu_3PBr$		14	23	456	252	217
$RuO_2.xH_2O$	$(C_{12}H_{25})Me_3NBr$		3	5	228	32	76
$RuO_2.xH_2O$	Bu_4PBr	PPh_3	30	31	168	185	133
$RuO_2.xH_2O$	Bu_4PBr	Ph_3PO	37	45	246	178	201
$RuO_2.xH_2O$	Bu_4PBr	TDPME[f]	17	21	138	140	78
$RuO_2.xH_2O$	Bu_4PBr		13	9	158	45	87[h]

[a]Charge: Ru (4.0 mmol); R_4PX (15 g); run conditions: 220 °C, 430 atm, constant pressure, CO/H_2 1:1, 6-18 h. [b]R=Me, Et, Pr. [c]liquid yield wt% calculated based on total charge. [d]total ethylene glycol acetate esters. [e]plus significant quantity of methyl acetate. [f]TDPME, 1,1,1-tris[(diphenylphosphino)methyl]ethane; P/Ru mole ratio = 1. [h]runtime 2 hr. [11]

Because the exact reaction times are not given, the comparison of the yields cannot provide useful insights. However, the product distributions are valuable characteristics and these can be compared. The use of different precursors shows significant effects in composition of the product liquid, although only C_1 to C_2 ratio's should be compared. In this case the reactions with the promoters and the phosphonium halide solvent gave the best results. The best EG to methanol ratio was accomplished using dry [RuO_2] and PBu_4Br. The difference in activity for the halides is surprising Dombek had found iodide to be the best promoter for his systems. Here, however, the bromide phosphonium salt seems to yield the best activity and selectivity. Also interesting are the different results obtained from using different precursors. In Dombek's work it was found that most precursors yield the same species under the catalytic conditions; therefore one can expect the same outcome. This is not the case in Knifton's study, so the addition of different precursors may yield the same species, but the equilibriums may be shifted. From these preliminary findings it was decided to use [RuO_2].xH_2O and PBu_4Br as the standards for further research (x is most likely 3). This combination does not provide the best selectivity, but perhaps the rates were good. In Figure 1.14 the product yield changes are compared at different catalyst loading, syngas ratios and pressures. First, it shows that the best ratio of Ru to phosphonium is 1:10. The solubility of the catalyst in the phosphonium salt might be the origin of this phenomenon. Secondly, the effect of different H_2/CO ratios on the activity was measured. The total synthesis decreases significantly at high and low ratios. In previous systems this seemed much less the case and especially EG showed a low (0^{th} order) dependency in CO partial pressure. Third, the effect of pressure is measured; in this system too it shows that the higher the pressure that is used, the higher will be the yield. This is in agreement with what Dombek observed.[49]

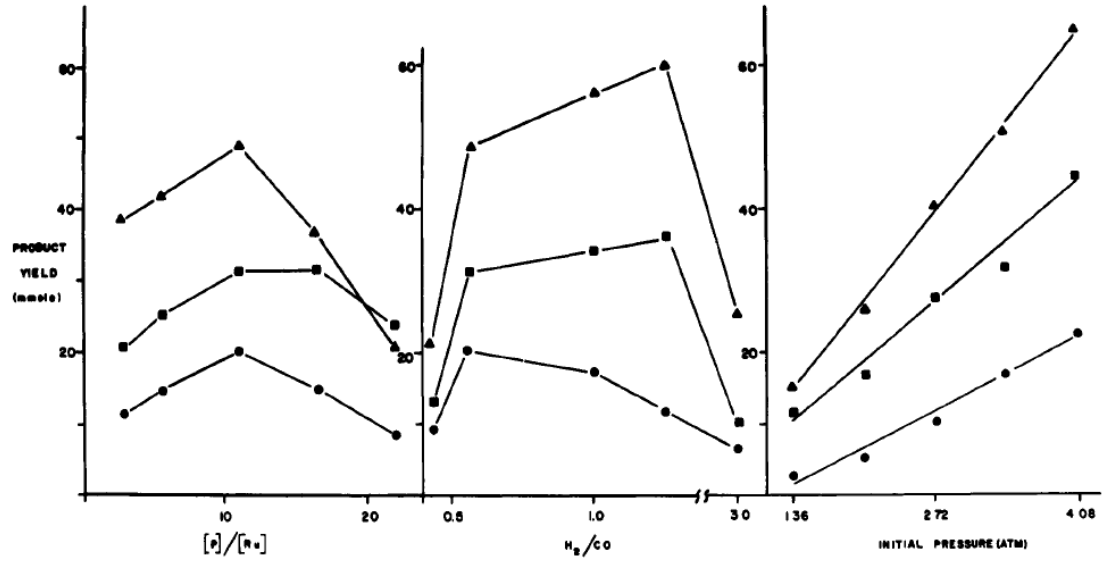

Figure 1. Ethylene glycol from synthesis gas. Total ethylene glycol (glycol plus glycol monoalkyl ether), ●; total methanol, ▲; ethanol, ■. Effect of [P]/[Ru] ratio (typical operating conditions: $RuO_2 \cdot xH_2O$, 2.67 mmol; CO/H_2 = 3:2; 220 °C; 6 h; 340 atm initial pressure), H_2/CO ratio (typical operating conditions: $RuO_2 \cdot xH_2O$, 2.67 mmol; Bu_4PBr, 10 g; 220 °C; 6 h; 340 atm initial pressure), and initial pressure (typical operating conditions: $RuO_2 \cdot xH_2O$; 2.67 mmol; Bu_4PBr, 10 g; CO/H_2 = 3:2; 220 °C; 6 h.

Figure 1.14 The product yield upon changing the gas composition, pressure and catalyst ($RuO_2.xH_2O$ loading for Knifton's system. Typical conditions: [RuO_2] xH_2O (2.67 mmol), H_2:CO = 2:3, 340 atm initial pressure, [PBu_4]Br (10 gr), 6 hr. "Reprinted with permission from J. F. Knifton, *J. Am. Chem. Soc.*, 1981, 103, 3959-3961. Copyright 1981 American Chemical Society.[11]

More extensive are the results published in patents, one of the first patents filed by Knifton concerns a RuO_2 catalyst in [PBu_4]Br and 430 atm pressure in a batch autoclave.[68] Table 1.20 shows how different precursors affect the product distributions. Here we can see that, indeed, the hydrated ruthenium oxide precursor gives the highest yield and good selectivity towards EG. It seems that the best selectivity is found for the ruthenium chloride precursor, however the yield is low and large amounts of water are formed.

Table 1.20 Performance of the Ru melt catalysis[a]

				product yield (wt.%)					
expt.	cat	Amount (mmol)	solvent	EG	glycol ethers	MeOH	EtOH	total (g)	yield
1	RuO_2	4	Bu_4PBr	13.4	20.2	30.1	21.4	41.3	
2	$RuO_2.xH_2O$	8	Bu_4PBr	17.1	10	27.8	28.7	62.1	
3	$RuO_2.xH_2O$	5	Bu_4POAc	17[a]		30.7[b]	-	33.3	
4	$RuO_2.xH_2O$	8	Bu_4PBr	9.4	11.9	31.4	30.6	38.1	
5	$Ru(acac)_3$	8	Bu_4PBr	5.6	16.2	26.1	33.4	55.8	
6	$RuCl_3.xH_2O$	8	Bu_4PBr	1.1	0.9	-	0.4	7.2	
7	$Ru(acac)_3$	4	Bu_4PBr	9.5	12.6	35.3	22.8	17.4	
8	$Ru_3(CO)_{12}$	8	Bu_4PBr	6	14.2	31.5	32.7	48	
9[c]	4, recycled	8	Bu_4PBr	9.6	13.1	31.5	29.5	30.6	

[a]Usual conditions, 430 atm syngas 1:1 constant pressure 220 ^oC. 18 hr. [a] combined yield of EG + glycol ethers. [b] plus 11.7% methyl acetate. [c]475 atm, 12 hrs. Data abstracted from Knifton[68].

The total yield in Table 1.20 depends on the initial loading of the autoclave. We will show an example of Table 1.21 which can be treated the same way; if for expt. 10 the total loading was 10 g of solvent and 1 g of catalyst. The total yield would be 11 g x 41%= 4.51 g of product. For sake of clarity, some products were not incorporated into the table, namely water and propanol. The glycol ethers were added together to form one column, consisting of Methyl-, Ethyl- and Propyl-monoethers. A remarkable effect is seen with the iodide salt; with a total yield of 312 %. The selectivity of this catalyst is unfortunately not so good, only 8.5 % of the total weight consists of C-C coupled products. A better selectivity was obtained using heptyl-triphenylphosphonium bromide (exp 10 (Table 1.21)). It seems that almost all products are 2-carbon compounds. Unfortunately, like the experiment with ruthenium chloride, the activity of this system is not so great. The relatively large formation of glycol ethers indicates that the formation of alcohols occurred but they rapidly reacted to form the ethers. One can wonder whether the selectivity is due to the phenyl-groups of the phosphonium salt or perhaps a very dense or dilute catalyst loading. The patent is not clear on this.

Table 1.21 Ruthenium melt catalysis, anion effect[a]

expt.	cat	solvent	product distribution, wt%				liquid yield (wt.%)
			EG	MeOH	EtOH	EG ethers	
10	$RuO_2.xH_2O$	$[HpPPh_3P]Br$[b]	1.4	-	1.4	17.5	41
11	$RuO_2.xH_2O$	$[Bu_4P]Cl$	6.4	5.5	20.4	9.7	82
12	$RuO_2.xH_2O$	$[Bu_4P]I$	1.7	40.6	31.8	6.8	312
13	$RuO_2.xH_2O$	$[Bu_4P]NO_3$	0.1	50.5	13.7	-	59
14	$RuO_2.xH_2O$	$[Bu_4P]OH$	3.7	52.9	13.3	5.8	83
15	$RuO_2.xH_2O$	$[Bu_4P]F$	0.1	59.9	4.3	0.1	62
16	$RuO_2.xH_2O$	$[Bu_4P]CrO_4$	7.4	8.2	16.5	8.6	54
17	$RuO_2.xH_2O$	$[Bu_4P]BF_4$	0.4	44.9	3	1.9	11
18	$RuO_2.xH_2O$	$[Bu_4P]Br$	1.2	0.5	-	0.9	29
19	$RuO_2.xH_2O$	$[Me_3RN]Br$[c]	1.9	57.8	11.6	3.3	76
20	$RuO_2.xH_2O$	$[Me_4N]OH$	1.9	36.3	-	0.2	<5

[a]General conditions: 440 bar syngas (1:1), 220 °C, 18 Hr, 10-30 g phosphonium, 2-8 mmol Ru. [b]Hp = heptyl. [c]R = dodecyl. Abstracted from Knifton[68].

An additional result in the patent is that the product composition is highly affected by the amounts of solvent used. Particularly, there are two examples that use 2.7 mmol of Ru and 5 or 20 g of PBu_4Br under similar pressures of syngas ($CO:H_2$ = 3:2), 550 and 520 bar, respectively. It shows that the diluted example has only 18% yield, compared to 65% in the concentrated sample. The product distribution shows that it contains 2.6 % and 17.6 % EG for the diluted and the concentrated example respectively. This behaviour shows that the C-C coupling probably follows a higher order in [Ru] than methanol synthesis and agrees with the observations by Dombek.

1.9.1 Group IV promoted Cobalt catalysis

The use of cobalt catalysts has also been examined for CO hydrogenation; the highest yields are obtained when tin or germanium promoters are used additionally, and especially if formaldehyde is added.[69] These reactions do not employ the use of ionic liquids, but are attractive because of the low pressures used, while still getting relatively good yields. The product compositions are given in terms of the liquid yield by mass. If the solvent interacts with the products (as in the case of alcohols) the numbers can give slightly skewed impressions. The weight difference between EG and the mono- or diether is considerable depending on the weight of the solvent chain. This results in

relatively high numbers for the ethers. To prevent any confusion the results of these experiments are not added to this discussion.

Table 1.22 Ethylene glycol from syngas and formaldehyde[a]

Catalyst	Promoter	EG	EGME	MeOH	Water	Dioxane	Methylformate
$Co_2(CO)_8$	Ph_3GeH	3.1	1.5	1.9	5.5	80	0.7
$Co_2(CO)_8$	Et_3GeCl	2.2	1	2	5.8	80.9	0.7
$Co_2(CO)_8$	PPh_3GeBr	2.1	0.7	2	5.5	82.3	0.6
$Co_2(CO)_8$	Me_3GeBr	3	1.2	1.7	6.3	80.7	0.6
$Co_2(CO)_8$	Ph_4Ge	2.7	1.3	1.5	5.9	81.5	0.4
$Co_2(CO)_8$	Et_4Ge	2.3	1.6	2.3	4.9	79.8	0.6
$Co_2(CO)_8$	Bu_3SnH	2.8	1.6	2.2	5	80.1	0.7
$Co_2(CO)_8$	Bu_3SnCl	1.4	0.7	2.9	5.2	84.6	0.8
$Co_2(CO)_8$	Ph_3SnH	trace	0.1	4	4.9	86	1.4
$Co_2(CO)_8$	Ph_4Sn	1.1	0.4	2.9	5.6	83.3	0.7

[a] Liquid product compositions in weight percentages. Conditions: Co, 3.0 mmol; Ge/Sn 1.5 mmol; HCHO 0.1 mmol; Solvent: 1-4-dioxane; 187.2 atm initial pressure, 160 ^oC 4 hrs. Data abstracted from Knifton.[69]

The real reasoning behind the use of these promoters is unclear, except that they are larger analogues of phosphonium salts, though not ionic per se. Previous limitations of using quaternary compounds of group 15 and 16 included that they should have a low melting point. Aside from that, Germanium and Tin are known one electron donors. Perhaps Knifton tried to assess their effect in catalysis because one electron donor metals can lead to formation of C-C coupling of aldehydes (often using samarium stoichiometrically). If such a coupling reaction can be turned into a catalytic system then it could be quite valuable. It was shown earlier that for ruthenium the use of these promoters was not beneficial. Solubilising the Ge and Sn compounds may have provided a new route into investigating their activity for other metals, as shown here. The system shows the most selective performance yet discussed at such low pressures and temperatures. The product yield composition can show selectivity towards ethylene glycol over methanol of 1.6:1. When this is converted to molar ratios it becomes 0.8:1. Furthermore, the conditions used in this system are relatively mild, only 160 ^oC. The autoclave is pressured up to 187 bar, and only then heated to the desired temperature causing the increase of pressure. Therefore, the pressure is not exactly known but it should lead to pressures of around 275 bar using basic gas law equations. Table 1.22 is

concerned mostly with the influence of the promoter type on the catalysis. [Ph_4Ge] and [Me_3GeBr] give the best selectivity for EG over methanol. Interestingly, [Me_3GeBr] contains a halide, but this does not seem to be the cause of the increased selectivity. Other halides have good selectivity, but not more than the protonated or hydritic compounds. In fact, the dataset is too small to correlate structure and selectivity. Factors like size, electronics and ligand lability would be interesting yet remain to be discussed. We can only assume that the electronic state of the Ge or Sn must be so that it can easily undergo catalytic one electron redox reactions. In Table 1.23 it can be seen that the selectivity is the highest using 2[$Co_2(CO)_8$]-2[Ph_4Ge] and 4[$Co_2(CO)_8$]-[Et_4Ge] as promoters. We can examine the data provided to see how some factors influence the results. First, the catalyst loading has a large effect on selectivity. Looking at exps 11, 12 and 13 the catalyst loading is doubled sequentially. *If we do not take into account the influence of the promoters*, we can see that the selectivity increases dramatically at higher Co loadings. In the ruthenium chemistry by Dombek and Knifton high concentrations of catalyst yielded good selectivity too. The dataset is too small to determine an order, however it seems higher than 1. The addition of more formaldehyde increases the total activity considerably; however, the selectivity decreases correspondingly. This indicates that formaldehyde is a substrate towards the formation of methanol and not to EG, or that the order in formaldehyde is much higher for the conversion to methanol than to EG. The pressure effect on the selectivity is very large. In going from a 113 atm to 337 atm the selectivity for EG over methanol increases linearly. Keim et al obtained a similar result for Co catalysts.[12, 13] However, the activity does not share this behaviour; between 113 atm and 206 atm the activity increases significantly based on the amount of solvent in the product, but from 216 to 337 atm there is hardly a noticeable difference (exp 1, 19 and 20). This indicates that after 216 bar the kinetics are not gas dependent anymore with this catalyst loading.

Table 1.23 Chemicals from syngas plus formaldehyde II[a]

			Product composition (Wt. %)						
No.	Catalyst	Solvent	EG	EGMME	MeOH	H_2O	solvent	MeOOCH	HCHO
11	$Co_2(CO)_8$-$2Ph_3GeH$	1,4-dioxane	2.7	2	3.1	4.6	80	-	-
12	$2Co_2(CO)_8$-$2Ph_4Ge$	1,4-dioxane	4.1	1.8	1.1	6.7	77.7	0.3	none
13	$4Co_2(CO)_8$-Et_4Ge	1,4-dioxane	4.6	1.9	1.1	7.2	70.7	0.2	none
14	$Co_2(CO)_8$-Ph_4Ge	1,4-dioxane/ 2x HCHO	4.3	2.1	3	10.6	69.7	0.6	0.04
15	$Co_2(CO)_8$-Ph_4Ge	1,4-dioxane/ 3x HCHO	3.5	2.4	8.3	9.7	66.2	3.2	0.06
16	$Co_2(CO)_8$-$2Ph_3GeH$[b]	1,4-dioxane	1.5	1.6	5.3	3.6	82.2	-	-
17	$Co_2(CO)_8$-Ph_3GeH[b]	1,4-dioxane	2.2	1.9	3.8	3.7	81.9	1.2	0.03
18	$Co_2(CO)_8$-Ph_3GeH[c]	1,4-dioxane	2	0.8	1.2	6.6	84.6	0.3	-
19	$Co_2(CO)_8$-Ph_3GeH[d]	1,4-dioxane	3.3	0.7	1.2	6.1	79.8	0.4	-
20	$Co_2(CO)_8$-Ph_3GeH[e]	1,4-dioxane	1.2	2	3.7	4.1	85.5	0.5	0.05
21	$Co_2(CO)_8$-Ph_3GeH[f]	1,4-dioxane	2.3	1.5	2.2	5.2	79.3	0.7	0.5
22	$Co_2(CO)_8$-Ph_3GeH[g]	1,4-dioxane	2.5	1.4	1.3	6	79.2	0.3	-
23	$Co_2(CO)_8$-Ph_3GeH	1,4-dioxane	1.2	-	2	18.8	60.5	-	-
24	$Co_2(CO)_8$-Bu_3SnH	Ph_2O	-	-	0.8	0.1	94.7	2	none
25	$Co_2(CO)_8$-Et_4Ge	Ph_2O	1.2	1.1	4	3.7	81.4	2.8	-
26	$Co_2(CO)_8$-Et_4Ge	THF	3.3	1.9	2	10.3	53.4	0.1	none
27	$Co_2(CO)_8$-Et_4Ge	Pr_2O	0.2	-	2	1	86.3	1.4	-
28	$Co_2(CO)_8$-Ph_3GeH	1,4-dioxane	13.2	-	13.3	58.3	-	0.5	-
29	$Co_2(CO)_8$-Ph_3GeH	1,4-dioxane/ EG	-	-	0.1	0.5	88.4	-	9.7

[a]reaction conditions: Co, 3.0 mmol; Gn/Sn, 1.5 mmol; HCHO, 0.1 mmol; solvent 15 g.; temperature 160 ^oC; initial pressure 185 bar; solvent 1,4-dioxane; 4 hrs. [b] 190 ^oC [c] 130 ^oC [d] 306 atm [e]103 atm [f]1 hr [g]18 hr. Data from Knifton.[69]

The effect of temperature is very interesting; at 190 and 130 ^{o}C the overall activity is less than at 160 ^{o}C. It should be expected though, that the differences in temperature would lead to a difference in pressure. Higher pressures usually lead to higher selectivity towards EG, this is also visible from Tables 1.22 and 1.23 (exp 1, 19 and 20). And this trend is also seen in going from 130 ^{o}C to 160 ^{o}C, we think that at 190 ^{o}C this trend halts because the catalyst may be subject to degradation. These temperature effects can be compared from exp. 1, 17 and 18. A very interesting effect is found when the product yield is compared for samples with differing reaction times. The total liquid yield does not change much between reacting for 1 hr or 18 hrs. This suggests that the system reaches equilibrium yields very quickly or that the catalyst decomposes. The selectivity towards EG remains constant, however the contribution of methanol to the total weight is decreased with time, additional reactions like ester formation or maybe even homologation reactions may be occurring, explaining reduced methanol levels. Unfortunately, the further composition of the product mixture is not disclosed. Analysis of the gas phase, however, shows very little WGS products. Some systems using ruthenium showed the contrary, with almost full conversion to CO_2 depending on the solvent used. It is not clear yet whether there is WGS activity in the ruthenium melt systems. For more detailed insight into the system's activity and the actual amounts of product formed we have decided to expand on the next example: an example using the pre-formed $[GePPh_3][Co(CO)_4]$ was also active for catalysis; reaction of this catalyst (3.0 mmol), 0.1 mmol formaldehyde in 1-4-dioxane with 2:1 (H_2:CO) syngas at 160 ^{o}C. It also yielded high conversion, see Table 1.24. In this example some of the numbers have been converted so that the relation between weight percentage distribution, weight and amount can be viewed.

Table 1.24 Process for preparing ethylene glycol[a]

product distribution	EG	EGMEE[b]	MeOH	Methyl formate	Water	1,4-dioxane
wt. %	3.2	2.4	2.4	1.5	5	79.9
total weight (g)	0.7	0.5	0.5	0.3	1.1	17.0
mmol	11	6	16	5	59	193

[a]Conditions: 3.0 mmol Co, 0.1 mmol formaldehyde, solvent: 1,4-dioxane(15 g), 160 ^{o}C, initial pressure 187.2 bar, 4 hrs. [b]EGMEE= ethylene glycol monoethyl ether. Data from Knifton.[69]

In contrast to non-pre-formed catalysts the reactions using pre-formed catalysts do not yield high cobalt recovery after synthesis. This is a common observation in all examples by Knifton (not shown) using pre-formed catalysts. This strongly indicates that the catalysts, pre-formed and formed *in situ*, even though they show the same activity, are different or have different decomposition pathways. All together, the cobalt catalysis seems a very effective means for preparing ethylene glycol from syngas under relatively mild conditions. Spectroscopic information about the species present under catalytic conditions and how these change with varying promoters will be of particular interest next to more elaborate quantitative data into the kinetics and product distributions of different catalyst promoter systems.

1.10 Bimetallic synthesis

Another approach to finding a good catalyst might be through the use of bimetallic systems. Numerous studies have been performed whereby presumably one metal hydride reduces another metal carbonyl. Making use of the beneficial properties of either metal, a very reactive system could in theory be prepared. One of these systems is the rhodium-ruthenium system described by Knifton;[70] $Ru(acac)_3$ and $Rh(acac)_3$ are used in combination with phosphonium salts. This system shows higher activity under similar conditions and better selectivity towards glycol then just ruthenium. Also in this system it appears that the use of iodide salts is better for the total activity than the bromide. However, the selectivity towards EG products is better using tributylphosphonium bromide (see Table 1.25).

Table 1.25 Product yield from the bimetallic system[a]

metal source	solvent	product yield mmol^{-1}				total liquid yield, wt %
		EG	$HOCH_2CH_2OR$[b]	MeOH	EtOH	
$Ru(acac)_3$-$Rh(acac)_3$	Bu_4PBr	77.2	62.6	250	168	189
$Ru(acac)_3$-$Rh(acac)_3$	Bu_4PI	80.4	41.6	312	237	214
$Ru(acac)_3$-$Rh(acac)_3$	$(C_{16}H_{33})(Bu)_3PBr$	11.4	42.8	295	228	176
$Ru(acac)_3$-$Rh(acac)_3$	$(C_7H_{15})(Ph_3)PBr$	0.5	0.4	0.1	0.7	<3
$Ru(acac)_3$-$Rh(acac)_3$	None	0.2	-	8.9	0.9	T[c]
$Ru(acac)_3$-$Rh(acac)_3$	Bu_4PBr[d]	30.3	14.3	96	23	57

[a]Charge: Ru (4.0 mmol); Rh (2.0 mmol); solvent (15 g); run conditions: 220 ^oC, 430 atm. CO/H_2 (1:1), 6-18 hr. [b]R=Me, Et. [c] total yield >90% water. [d]run time 2 hr. Data taken from Knifton[70].

It is interesting to see that using larger cations increases the selectivity towards EG. However the total activity also decreases. Perhaps the decreased polarity of the solvent causes less catalyst to be dissolved or changes the rate of formation of active species. To resolve this issue spectroscopic information would be quite valuable. The most effective ratio at which the catalysis should be performed was examined by running the catalysis with different catalyst loadings. Increasing amounts of ruthenium when using a constant amount of rhodium has a beneficial effect to the selectivity. However, when the level of ruthenium is held constant, there is a maximum selectivity towards EG when the level rhodium is changed. This non-symmetrical behaviour indicates that the selectivity is also affected by the absolute concentration of the metals in the solvent, as was seen before in previously described concentration experiments. Chromatographic analysis of the reaction media *after* catalysis show the formation of a Rh-Ru mixed metal cluster $[RhRu_2(CO)_{12}]$ and $[Ru_3(CO)_{12}]$, no monometallic rhodium compound was observed. In terms of reactivity this suggests special selective C-C coupling effects of this mixed metal cluster. Higher levels of rhodium might cause the synthesis of metal clusters with higher rhodium to ruthenium ratios which might be unsuccessful in EG formation. Dombek also investigated a bimetallic Rh-Ru halide system, but then without ionic liquid solvents.[71] In fact, his findings about the ideal Rh:Ru ratio where very similar to those of Knifton, and he also performed high pressure

spectroscopic measurements on the system in NMP. He found the existence of ruthenium species **8** and **9** but also $[Rh(CO)_2I_2]^-$ but no evidence was found for mixed metal clusters during catalysis. In contrast to the phosphonium melt chemistry of Knifton the halide concentration in Dombek's system is very low, and an experiment to measure the dependency on halide concentration was performed. For this they used a Rh:Ru of 1:6 and increasing amounts of halide.

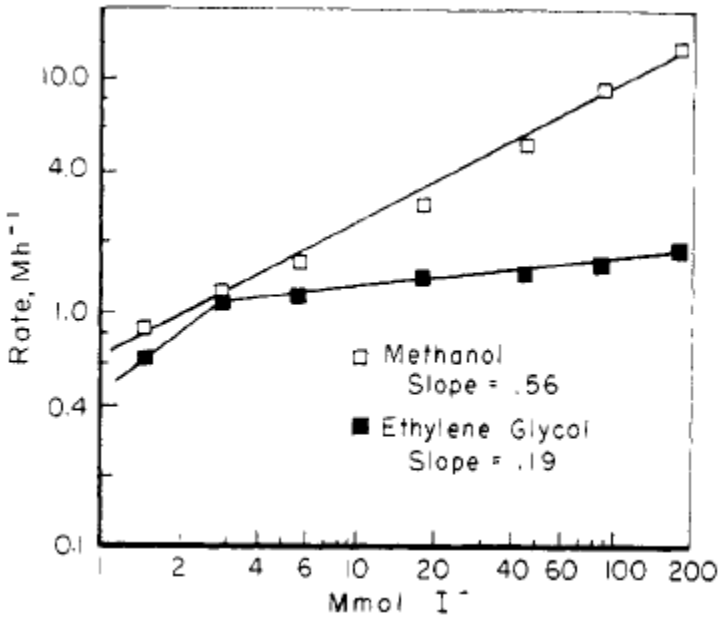

Figure 1.15 rates to product formation of the mixed metal vs. iodide concentration. Conditions: NMP (75 mL), Ru (6 mmol), Rh (1 mmol), 230 oC, 850 atm syngas 1:1. Reprinted (adapted) with permission from B. D. Dombek, Organometallics, 1985, 4, 1707-1712.. Copyright (1985) American Chemical Society.

The shapes of the curves are very similar to those obtained for ruthenium alone. However, the rate of formation of EG is much higher than previously reported, Figure 1.15. It is postulated that the hydride donor $[HRu(CO)_4]^-$ (**12**) is generated and that this attack on either Ru-CO or Rh-CO with the ruthenium carbonyl yielding primarily C_1 products and the rhodium yielding primarily C_2 products (Scheme 1.7).

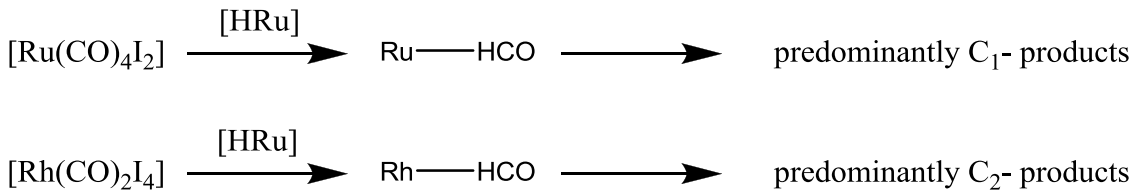

Scheme 1.7 The hydridic attack on different metal carbonyls could lead to the observed higher selectivity towards C_2 products. Redrawn and adapted from Dombek[71]

1.11 Warren, Dombek and the Japanese C1 project

Some of the latest publications on homogeneous conversion of syngas were produced by Warren and Dombek and by a group of researchers from Japan. They contain very valuable knowledge on promoter activity. We will start with the work from Warren and Dombek. In her paper[72], Warren discussed the use of HX acids as promoters in the ruthenium system. She found that the addition of HI or I_2 (they both have the same effect in a suitable solvent) leads to a change in both catalyst composition and product selectivity. The HI or I_2 reacts with Ru(0) to form Ru(II), to be specific $[RuI_3(CO)_3]^-$ is formed, which was confirmed by IR analysis of the samples after catalysis. In effect, the addition of HI leads to a change in the catalyst composition by converting the $[HRu_3(CO)_{11}]^-$ into $[RuI_3(CO)_3]^-$. However, this change also leads to generation of higher levels of ethanol during catalysis. With the use of up to one equivalent of HI (to Ru) the selectivity changes from predominantly methanol to predominantly ethanol. At this point it was unclear how the ethanol was formed and it was speculated that the ethanol was formed in a single sequence of reactions on the metal centre. To test this hypothesis labelling experiments were performed where ^{13}C-labelled methanol was added at the start of the reaction. If methanol is an intermediate in the formation of ethanol, and free methanol is homologated to ethanol by the catalysts then labelled ethanol could be found after the reaction. Otherwise, it was more likely that the ethanol is formed directly from syngas. They found that indeed significant amounts of ^{13}C were found in the ethanol after reaction, confirming the homologation pathway to higher alcohols. Label was also found in propanol and methane, but not in ethylene glycol, suggesting the latter is formed independently of methanol formation. This labelling study was later also performed by Ono et al.[73], who found similar results. Ono working for the Japanese "C_1 project", which looked at the conversion of syngas into higher products,also used ruthenium and conventional solvents, as in Dombek's work. However, instead of using KI salts as promoters Ono used primarily PPN salts. With this, he tested the system activity using different halides and also testing the addition of HX salts. In contrast to Dombek's findings, using the chloride halide salts yielded the highest activity towards both methanol and ethanol, followed by bromide. Also the selectivity towards ethanol is higher using iodide than when using bromide. Addition of HX leads to even higher activities using bromide and

iodide, but slightly lower activity using chloride.[74] The effect of using HX is always improved selectivity to ethanol relative to methanol, but in general it also led to very high levels of methane. This may suggest that ethanol and methane formation are promoted by the presence of the same ruthenium species. Possibly, they have the same intermediate species formed from methanol, namely a ruthenium methyl species formed from the addition of methylhalide to ruthenium. The presence of acid increases the chance of protonation towards methane, while alternatively the methyl group could migrate onto CO leading towards ethanol. More of this will be discussed in Chapter 5. Additionally Ono tested the effect of alternative acids on the ruthenium system. Phosphorus containing acids (notably phosphoric acid, and phosphorous acid) led to increased selectivity towards ethanol. Ono also tested the use of several solvents in combination with the use of HBr and phosphoric acid. With that he reported that solvents containing accessible O or N groups where beneficial with respect to methane formation, relatively inert solvents like toluene yielded the highest levels of methane while using dibenzyl ether led to the lowest relative levels of methane. To examine how phosphoric acid improves catalysis Ono also tried trimethyl phosphate as a promoter instead of phosphoric acid. Interestingly he found that methyl phosphate leads to even higher product yields. Ono also noted that this may be due to a reduced intitiation time. IR analysis of the product liquids showed that the addition of HX leads to a change in the ratio of the species $[HRu_3(CO)_{11}]^-$ and $[RuX_3(CO)_3]^-$. However the spectrum after using only $[Ru_3(CO)_{12}]$ and H_3PO_4 shows that the presence of H_3PO_4 suppresses the formation of $[RuX_3(CO)_3]^-$. Ono suggests that the use of phosphoric acid enhances catalysis by the release of the proton, and that the proton increases the rate of catalysis. Where HX has a counterion that coordinates to ruthenium, an inactive species $[RuX_3(CO)_3]^-$ is formed, but phosphate does not coordinate and thus the amount of free protons and $[HRu_3(CO)_{11}]^-$ is optimised. However, the observion of an induction time when phosphoric acid is used and the lack of induction time with methyl phosphate, may suggest that it is not the amount of free protons that is decisive in catalysis but rather that another mode of action occurs with the use of the phosphate group. Perhaps the phosphate does coordinate to the catalyst, or maybe it acts a good leaving group in the formation of the Ru-Me species by nucleophilic attack of a ruthenium centre by MX. In the case of trimethylphosphate, the methyl group is already attached to the

anion so that it may participate directly in ethanol formation without an induction period, which might be required if the trimethylphosphate has to be formed from phosphoric acid.

With this we conclude the review of the literature and move on to our own findings and developments. With this project we aim to develop better the routes to C_{2+} oxygenates, like EG and ethanol from syngas. In our approach we aim to react syngas with known and new catalysts dissolved in various media. Our starting point will be to increase the halide ion concentration by making use of ionic liquids as solvents. For these solvents the nature of the cation as well as the anion can be adjusted relatively easily, and thus provides a good basis for study. In addition, we will determine the effect of adding various promoters to the solvent system in order to improve selectivity and activity. For instance we would like to expand on Knifton's melt chemistry with the use of acids. By making use of spectroscopy techniques such as IR and NMR we hope to find out what species is most active in CO hydrogenation and from there use rational design to develop interesting catalytic centres that we can subject to further mechanistic studies. We use high pressure setups for the testing of catalysts, solvents, promoters and conditions, completed by in depth analysis of their effects on the system, such as kinetics, gas uptake, product formation and product distribution and gas phase composition. On the other hand we will make use of high pressure IR and other analysis tools to develop insights into the mechanism and active species. We can then reproduce and, if possible, improve these systems towards commercially interesting rates and selectivities.

Chapter 2
Benchmark reaction analysis and product formation routes of the Ru/[PBu4]Br system

Reproducibility and assessment of benchmark reactions in product formation through homogeneous CO hydrogenation followed by identification of basic product formation routes.

In starting the practical part of the investigation the choice of starting point was a decision between Dombek's[49] and Knifton's[75] system. Both types of chemistry are similar in activity and operation and have plenty of room for additional discovery. However, of the two systems Knifton's system has had the least amount of published spectroscopic analysis. Additionally, Dombek's work points to the use of halide promoters with increasing activity with increasing concentration of halide in the solvent *up to the solubility limits of the promoter in the solvent*.[49] In Knifton's system there is the inherent advantage that the halide concentration is maximal as it is an inherent part of the solvent. Furthermore, the use of Ionic Liquids (IL's) is well-established in the Cole-Hamilton[76-79] and Eastman[80] laboratories and this is valuable experience we could draw upon in developing our system. An additional feature of IL's is that they display a very low vapour pressure and this feature makes IL's an attractive choice for continuous flow systems.[81] If the catalyst can be contained in the reactor, e.g. it is not volatile, and the solvent is not volatile either, then the only mobile compounds in the reactions are the substrates and the products, besides the carrier gas. Theoretically, this should reduce catalyst recovery and product purification while minimising operation costs and time. For these reasons we chose to use Knifton's system as a starting point in our studies. The first task was to produce a good setup for our measurements and then to test it.

2.1 Rig design and setup

After some preliminary studies using existing equipment we decided to build a setup containing a gas booster, a large ballast vessel, a flow meter, a high pressure internally stirred Hastelloy reactor and a backpressure regulator, in that order, upstream

to downstream. The ballast vessel was a large tube of a 0.5 L internal volume, capable of withstanding pressures of up to 330 bar. Before and/or during operation, this vessel would be filled with any reducing gas to pressures higher than 250 bar, the autoclave operating pressure. The ballast vessel pressure was logged in 10 second intervals using a computerised Picolog logging system and the results stored on the computer for analysis. From the ballast vessel gas would flow through the Bronkhorst Mass Flow Controller (MFC), set in an open position letting in a small flow of gas. The gas would enter the autoclave where it would mix with the IL and react to form products. Downstream of the autoclave there would be a Jasco Back Pressure Regulator (BPR) which is equipment to determine the upstream pressure and which opens a valve if that pressure is higher than the set point pressure. The gas coming through the valve could be reduced in flow, and led through a cold trap to collect volatiles and to let the permanent gases vent to atmosphere (in a fume cupboard). During the very first measurements we noticed that this setup was not adequate in assessing the reaction yield. Gas coming from the pressure vessel would come in pulses/bursts which were of sufficient strength to sweep all volatiles through the coldtrap(s). Furthermore, we could notice the build-up of an orange coloured compound in the tube lining which meant that the catalyst was volatile enough to be transported in the gas phase. It was therefore decided to cancel continuous flow measurements and to focus on batch wise experimentation for assessing the activity of the system. For this a forward pressure controller was added between the ballast vessel and the MFC and the BPR was removed (Scheme 2.1). Thus, batch reactions could be carried out while keeping the pressure in the system constant (at 250 bar). Whenever the reaction would take up gas to form less volatile products, the pressure would drop below the threshold and the pressure controller would open to let in more gas from the ballast vessel. Now we could assess the kinetics by plotting the ballast vessel pressure over the reaction and furthermore the products could be contained in the reactor until the end of the reaction. Cooling down the reactor allowed the volatiles to condense and they could then be distilled from the IL (not volatile) and analysed by GC. In the mean time, the reactor could be cleaned by refluxing hot solvent to remove remaining products and other contaminants.

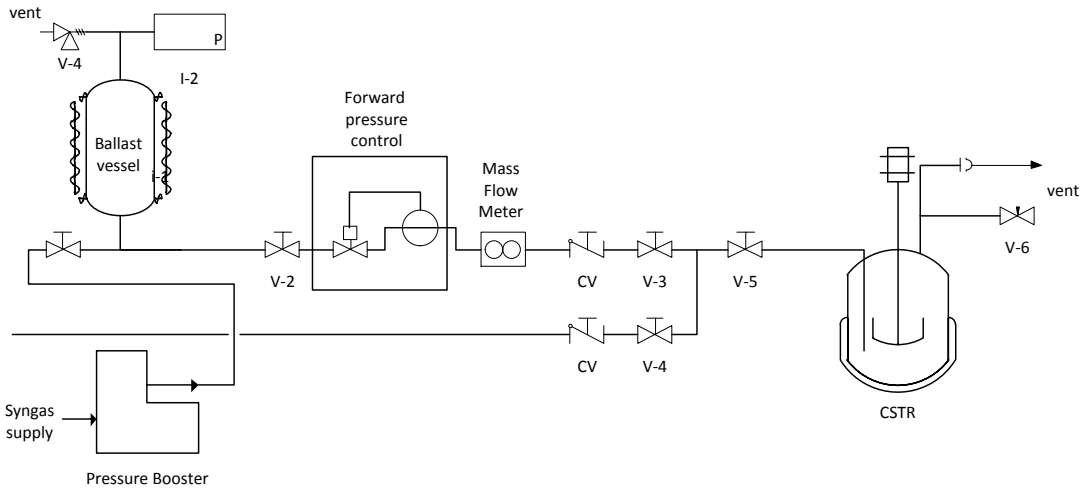

Scheme 2.1 A schematic overview of the rig. cv = check valve, v-x = valve, v-4 = pressure relief valve, I-2 = heat trace, P = pressure transducer

2.2 Introductory remarks and testing the system

After assembly of the testing equipment, it was extensively tested for leaks, and leak testing and equipment troubleshooting was a daily task in operating the rig. In the first set of experiments there was poor reproducibility. A range of promoters were tested, so we expected differences in activity. However, when four benchmark reactions in a row were performed, it was discovered that the reproducibility was poor. Furthermore, the catalyst solution at the end of the reactor varied in colour. This indicated that there was an impurity reacting with the catalyst and that therefore the activity was different for each reaction. Figure 2.1 shows the recovered product yield for 4 consecutive reactions using the same conditions.

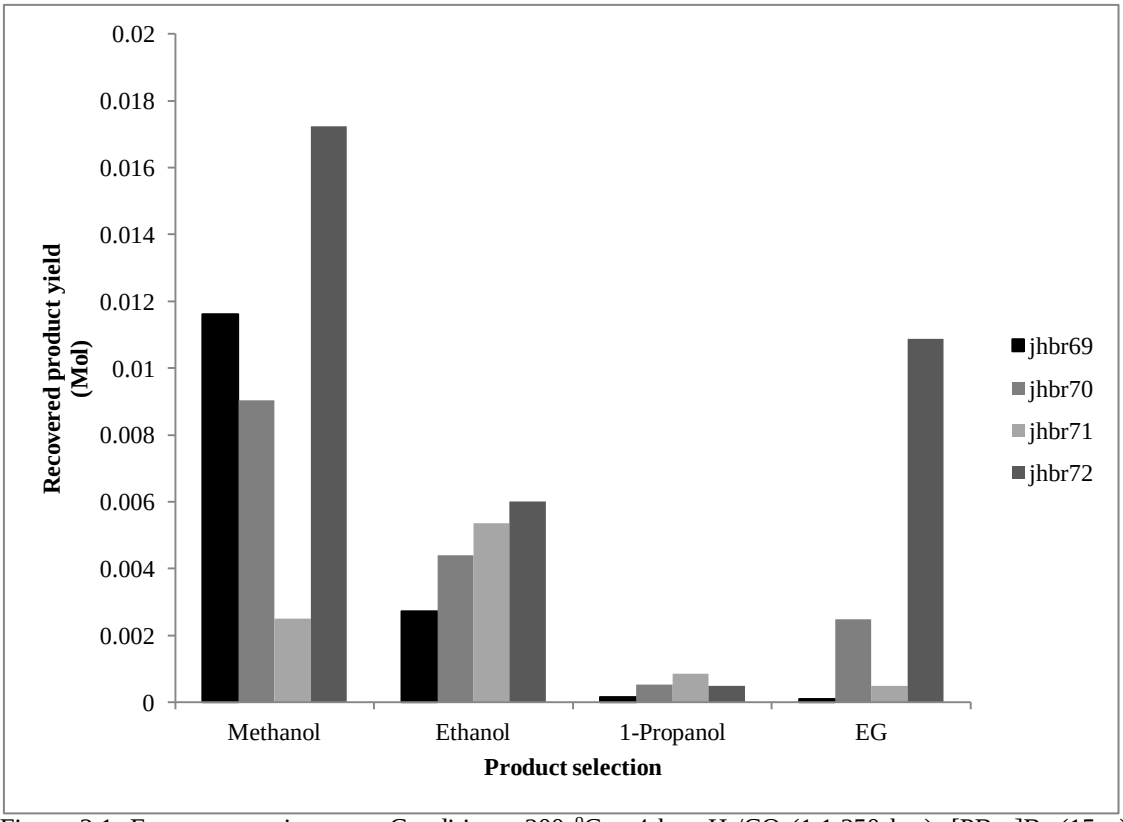

Figure 2.1. Four consecutive runs. Conditions: 200 ^{o}C, , 4 hrs, H_2/CO (1:1,250 bar), [PBu_4]Br (15 g), [$Ru_3(CO)_{12}$] (0.5 g); Cleaning autoclave with DCM. The reproducibility is very poor.

The reproducibility in this system is obviously very poor. Comparison of the IR analysis on the product liquid after reactions jhbr71 and jhbr72 shows that they contain different (or different ratios of) metal carbonyl species (figure 2.2):

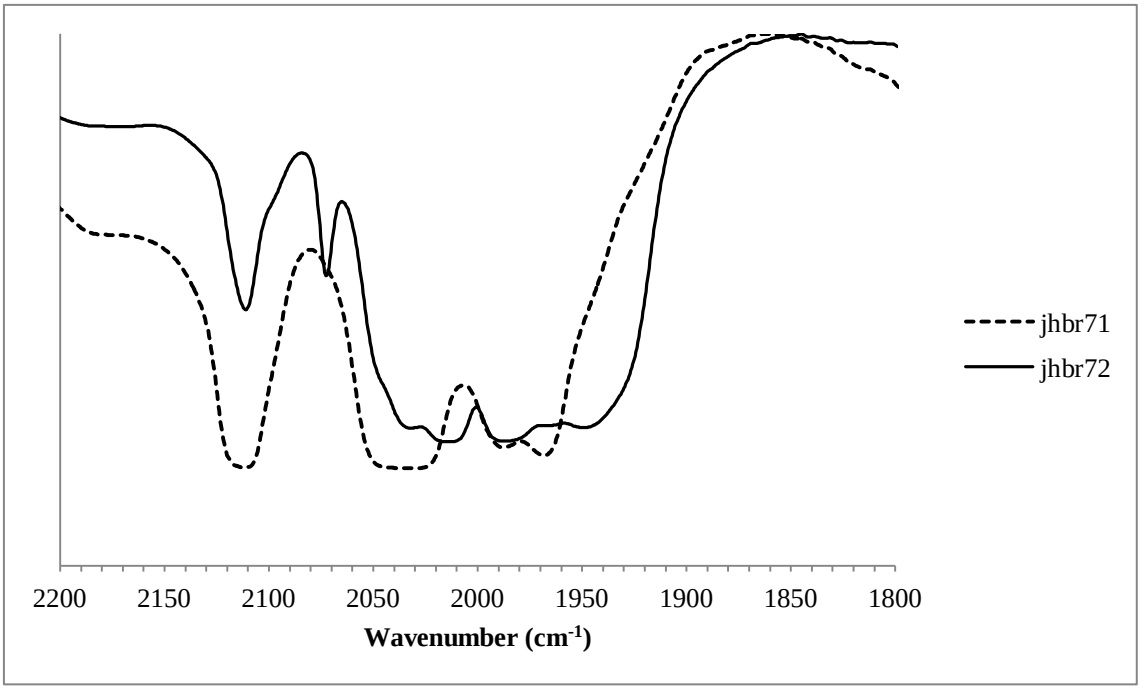

Figure 2.2 Overlapping IR spectra of jhbr71 and jhbr72. Although both samples may contain some of the same species, they are present in different ratios. For the sake of clarity, both spectra have been resized and shifted along the intensity axis for easier comparison.

In a later section, a more in-depth analysis of the species that are present will be presented. Because the amount of product formed during the reaction was so little, sample jhbr71 was a thick slush. Samples were prepared by pressing the product liquid between two plates. Because the sample was very thick and concentrated in terms of catalyst, sample jhbr71 has 100% absorption in the strongest peak, however it shows a clear difference in the species present.[b]

2.3 Improving on reproducibility

Even though the reactor was cleaned, disassembled and dried carefully after each run it was suspected that not all solvent would be removed during the drying process, and that the solvent may not be innocent during the reaction. Dichloromethane was used at the time. Switching to a procedure where the autoclave was washed with methanol yielded much better reproducibility (figure 2.3 A and B)

[b] This method yields different amounts of catalyst per sample to pass the path of the beam, resulting in inconsistency in intensity in going from one sample to another. This renders an absolute comparison of peak intensity between different samples meaningless. However, relative peak sizes within one sample can be compared and a further advantage is that the different spectra can be resized and shifted along the y-axis so they do not overlap which increases clarity.

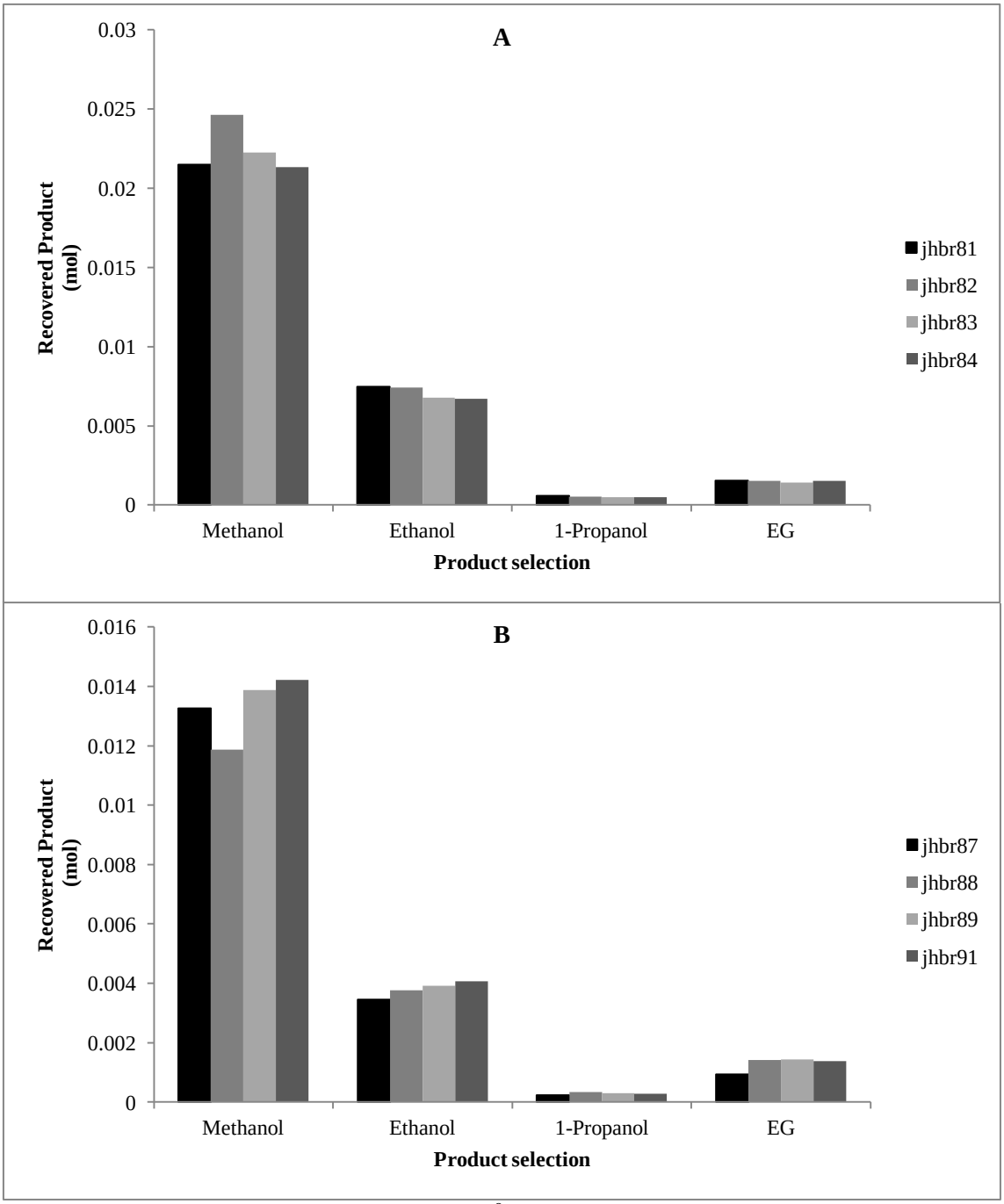

Fig. 2.3 A) four consecutive runs. Conditions: 200 ^{o}C, 250 bar, 4 hrs, H_2/CO 1:1, 15 g $[PBu_4]Br$, 0.5 g $[Ru_3(CO)_{12}]$. Cleaning autoclave with methanol B) four consecutive runs. Conditions: 200 ^{o}C, 250 bar, 4 hrs, H_2/CO 1:1, 15 g $[PBu_4]Br$, 0.308 g RuO_2. Also cleaning the autoclave using methanol. The reproducibility is much better.

These new results open the way to start systematically testing the catalytic system. First, the outcomes of these reproducibility reactions will be discussed in more detail, so they can be used for comparison and benchmarking. The set of experiments using RuO_2 as a precursor shows different behaviour from the set using $[Ru_3(CO)_{12}]$. The precise cause for this is not fully known.

2.3.1 Using $[Ru_3(CO)_{12}]$

Reacting a mixture of of $[PBu_4]Br$ (15 g) and of $[Ru_3(CO)_{12}]$ (0.5 g) at 200 ^oC at 250 bar syngas (H_2:CO 1:1, constant pressure) for 4 hours yields a dark-red liquid which can be distilled to yield products which by analysis of GC-MS shows a spectrum (figure 2.4) containing more than 40 different products.

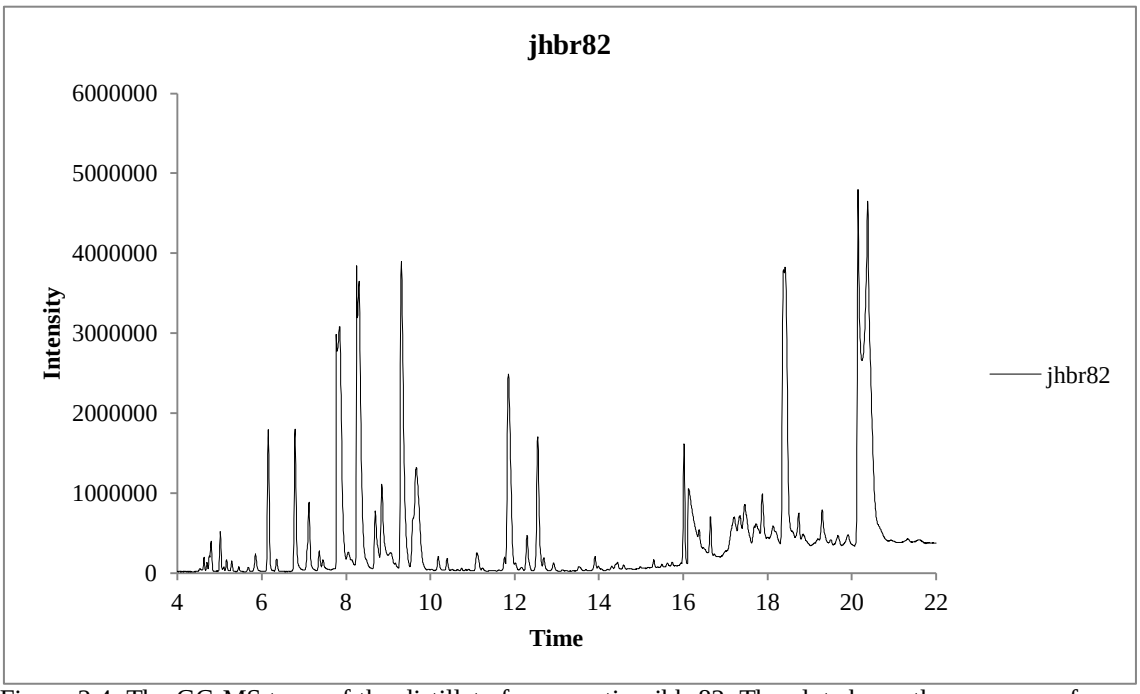

Figure 2.4. The GC-MS trace of the distillate from reaction jhbr82. The plot shows the presence of over 40 products, some of which were identified. Conditions: 200 ^oC, 250 bar, 4 hrs, H_2/CO 1:1, $[PBu_4]Br$ (15 g), $[Ru_3(CO)_{12}]$ (0.5 g).

The products can be grouped into aldehydes, alcohols, ethers, carboxylic acids, esters and compounds that remain unidentified. A full list of the identified compounds can be found in Table 2.1:

Table 2.1. identified compounds from reaction jhbr82. The GC-MS trace shows the presence of other compounds, but identification was often not possible due to their small peak size

dimethylether	1-butanol	ethylene glycol
methylethylether	1-pentanol	2-methyl-1,3-dioxolane
diethyl ether	2-methyl-1-propanol	1,3-dioxolane
methylpropyl ether	acetaldehyde	2-ethyl-1,3,-dioxolane
dimethoxy methane	1,1-methoxyethoxyethane	2-methoxy ethanol
diethoxymethane	1,1-dimethoxypropane	2-ethoxyethanol
methanol	acetic acid	2-propoxy ethanol
ethanol	methyl formate	2-methoxy-1-propanol
propanol	methyl acetate	1-methoxy-2-(methoxymethoxy)-ethane

Of these compounds the most abundant are methanol, ethanol, 1-propanol and EG and their analysis was daily routine. However, a plethora of additional compounds were formed during catalysis for which analysis is more difficult because of the absolute quantities compared to the main compounds.[c] For now, most of the discussion will be limited to the formation of the four main compounds. Only in special cases will I draw on the formation of other compounds, e.g. if it gives clues about mechanistic pathways or when formation of the particular compound shows some other insight. For instance, the presence of ethers are most likely to arise from the alcohols, their chain distribution resembles that of the alcohols, e.g. there is dimethylether, diethylether but also cross products like methylethylether. The quantification of ethers is rendered very difficult as a result of their high volatility The presence of minor amounts of acetaldehyde indicates that alcohols could pass through an aldehyde intermediate. It is likely that dimethoxymethane originates from the reaction of formaldehyde with methanol, whilst dioxolanes are formed from formaldehyde and ethylene glycol. The presence of methyl acetate and methylformate most likely arise from the formation of carboxylic acids which react with the alcohols. Overall, the presence of most identified products *could* be derived from the synthesis of methanol, ethylene glycol, carboxylic acids and aldehydes.

[c] For routine analysis the quantitative analysis was performed for many of these products, using calibrated stock solutions. However for assessment of the total reaction yield knowing exact amounts is of limited value. They constitute only minor side reactions that take place. It should be recognised that they may point to interesting mechanistic pathways.

1.1.1.1 IR analysis

All samples have a similar IR profile, which show the presence of metal carbonyl species. Both Dombek's system and Knifton's system have similar reactivity and use the same precursor/promoter mixture although using different solvents (Dombek)[10] or conditions (Knifton)[11], which makes it very likely that we will find related ruthenium containing species during the reactions. In addition to this, Dombek has been able to identify many species that form from reacting $[Ru_3(CO)_{12}]$ with high pressure syngas in the presence of iodide, and found that in his system the predominant species are $[HRu_3(CO)_{11}]^-$ and $[RuI_3(CO)_3]$-.[52] Using a bromide salt we may expect formation of the bromide analogue of the latter. Figure 2.5 shows the IR spectrum of the product liquid of reaction jhbr82.

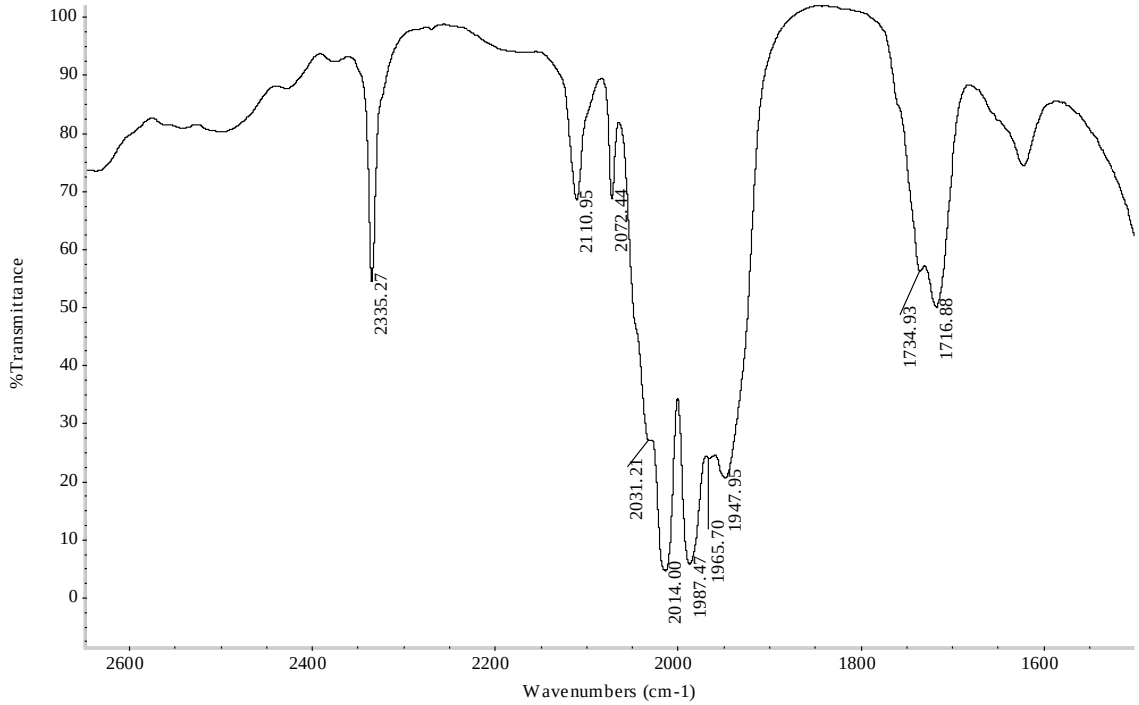

Figure 2.5. IR spectrum of the product liquid of reaction jhbr82. Conditions: 200 °C, 250 bar, 4 hrs, H2/CO 1:1, $[PBu_4]Br$ (15 g), $[Ru_3(CO)_{12}]$ (0.5 g). Spectrum taken after the reaction at ambient conditions.

Absorptions occur at 2111.0, 2072.4, 2031.2, 2014.0, 1987.5, 1965.7 and 1948.0 cm^{-1}. Peaks at 2335.8 cm^{-1} (absorbed/free CO_2) and 1735 cm^{-1} (water/alcohols overtones) most likely do not belong to any metal complexes in this case. Cleare and Griffith have made several ruthenium carbonyl halide complexes and published the IR spectra.[51] Comparisons of this spectrum with the work of Ono, Dombek and Cleare and Griffith indicates the presence of the two species $[HRu_3(CO)_{11}]^-$ (major component,

2072.4, 2014.0, 1987.5, 1948.0 and perhaps a contribution in 1716.9 cm^{-1}) and $[RuBr_3(CO)_3]^-$ (minor component, 2111.0 and 2031.2 cm^{-1}).[51, 52, 74]

1.1.1.2 NMR analysis

Later investigations on samples derived from the exact same conditions and reagent mixtures, for which the IR spectrum was nearly identical, also included NMR analysis and showed the existence of a peak in the hydride region consistent with the presence of $[HRu_3(CO)_{11}]^-$.[d] One complete such spectrum is shown below in figure 2.6.

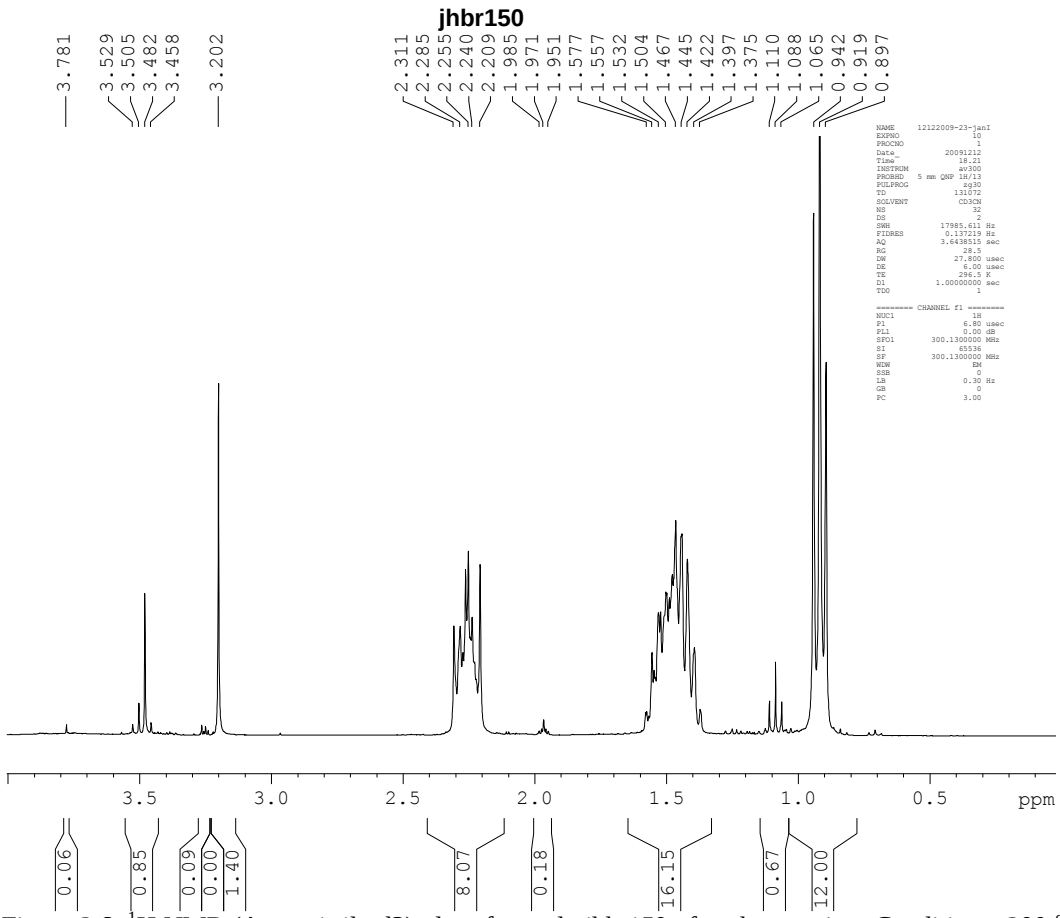

Figure 2.6. ^1H NMR (Acetonitrile-d3) plot of sample jhbr150 after the reaction. Conditions: 200 ^oC, 250 bar, 4 hrs, H_2/CO 1:1, $[PBu_4]Br$ (15 g), $[Ru_3(CO)_{12}]$ (0.5 g).

This spectrum shows presence of the phosphonium salt, at δ (ppm): 0.919, 1.445, 1.504, 1.50 and 2.25. The second most abundant species is methanol at δ 3.20

[d] Product samples were stored throughout the period of the work. However catalytic species are prone to decomposing (for instance Dombek reported the reaction of $[HRu_3(CO)_{11}]^-$ reacting with methanol) making it difficult to take old samples and obtain meaningful NMR spectra on them.

ppm followed by ethanol and ethylene glycol (δ 1.08, 3.49 ppm and δ 3.48 ppm respectively). Expansion reveals many more peaks, but their assignment becomes difficult as they overlap and there exists ambiguity over which is which. Of more interest however, in terms of catalytic species are some relatively prominent peaks in the hydride region shown in figure 2.7:

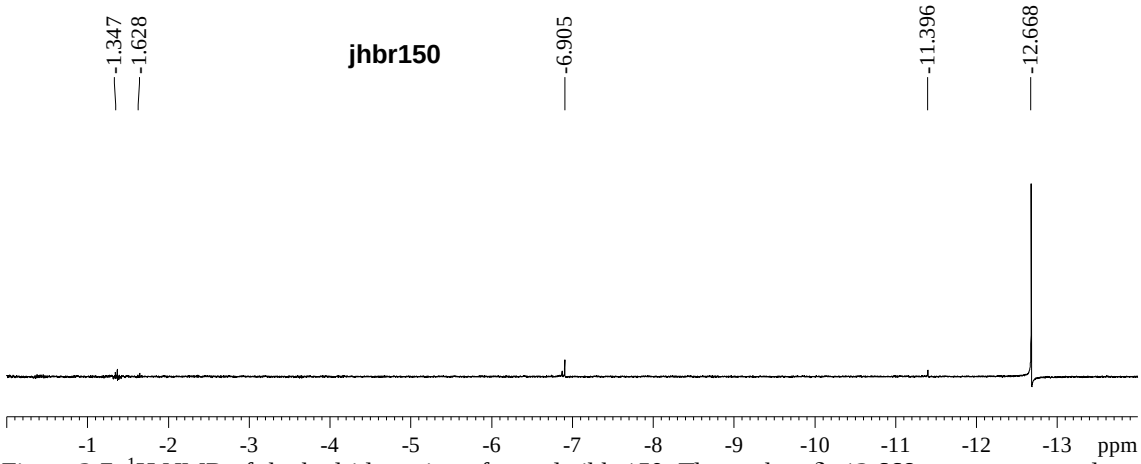

Figure 2.7. ^{1}H NMR of the hydride region of sample jhbr150. The peak at δ -12.668 ppm corresponds to the $[HRu_3(CO)_{11}]^-$ species. Other peaks remain unidentified.

The peak at δ -12.668 ppm corresponds to $[HRu_3(CO)_{11}]^{-}$[82-84] which from IR looks like the most abundant metal species. The assignment of the hydrides at δ -11.396 and -6.905 ppm has not been achieved yet.

2.3.2 Using RuO_2

Reacting a mixture of $[PBu_4]Br$ (15 g) and RuO_2 (0.308 g) at 200 ^{o}C at 250 bar syngas (H_2:CO 1:1, constant pressure) for 4 hours yields a black liquid. This can also be distilled to yield liquid products, which by analysis of GC-MS shows a similar product spectrum as to the reactions carried out with $[Ru_3(CO)_{12}]$ (figure 2.8).

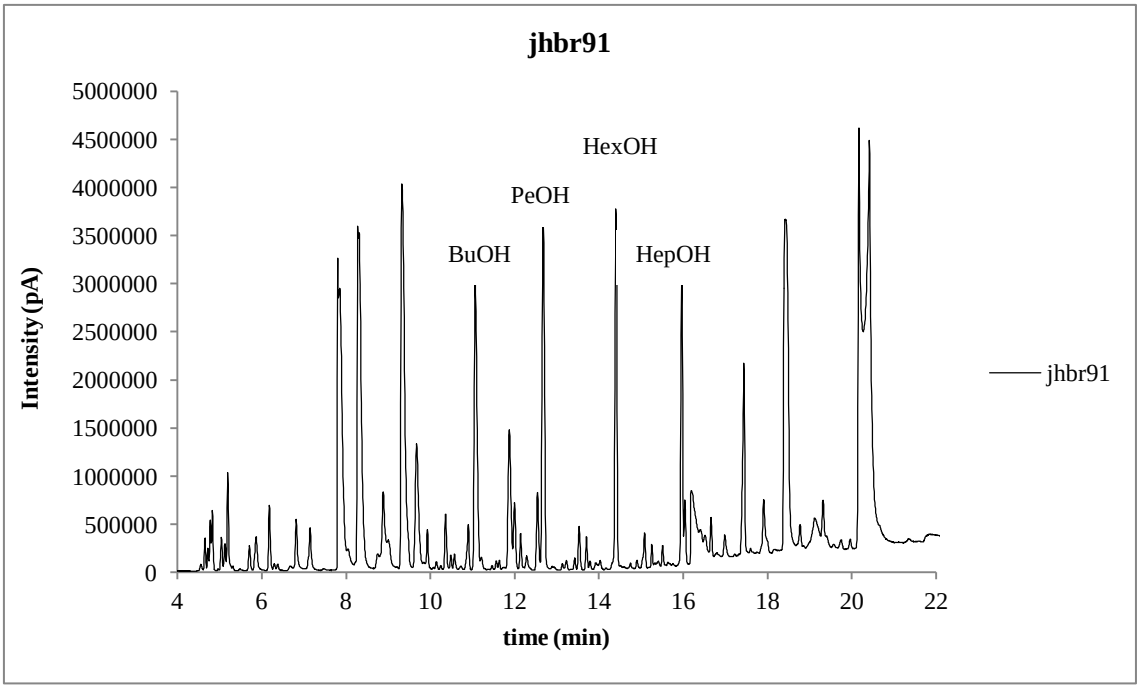

Figure 2.8. The GC-MS trace of the distillate from reaction jhbr91. The plot shows the presence of over 50 compounds. Conditions: 200 ^{o}C, 250 bar, 4 hrs, H_2/CO 1:1, [PBu_4]Br (15 g), g [RuO_2] (0.308).

Again, the products can be grouped as aldehydes, alcohols, carboxylic acids, ethers, esters and unidentifiable compounds. What is striking in this case is the presence of the higher alcohols. There is much more butanol, pentanol, hexanol and heptanol. Most of these compounds were present in the reaction using [$Ru_3(CO)_{12}$], however much less prominent. Also interesting is the discovery of minor amounts of alkanes. A full list of identified compounds is given in Table 2.2.

Table 2.2. Identified compounds from reaction jhb91.[a]

methylethylether	methyl acetate	ethylene glycol
methylpropyl ether	acetic acid	2-methyl-1,3-dioxolane
dimethoxy methane	butylacetate	1,3-dioxolane
butene	methanol	2-methoxy ethanol
butane	ethanol	2-ethoxyethanol
hexane	propanol	2-butoxyethanol
methyl cyclopentane	1-butanol	propylene glycol
3-methylpentane	1-pentanol	2-methyl-1-propanol
decane	1-hexanol	2-methylbutanol
undecane	1-hexanol	2-methylpentanol
dodecane	1-heptanol	2-ethylpentanol
acetaldehyde		

[a]Conditions: 200 ^{o}C, 250 bar, 4 hrs, H_2/CO 1:1, $[PBu_4]Br$ (15 g), $[RuO_2]$ (0.308 g).

In reality, there are more compounds, but only those in Table 2.2 where found in enough quantities or with enough separation for identification. Most likely the unidentified compounds are from the same "families" of compounds that where identified. Even though the presence of alkanes is reported here, their quantities remain low as assessed from the GC-FID by peak area.

1.1.1.3 IR analysis

Even though the product mixture is black, indicating the presence of some unreacted ruthenium oxide or other ruthenium species, the IR spectrum shows great similarity to that of the reaction with $[Ru_3(CO)_{12}]$:

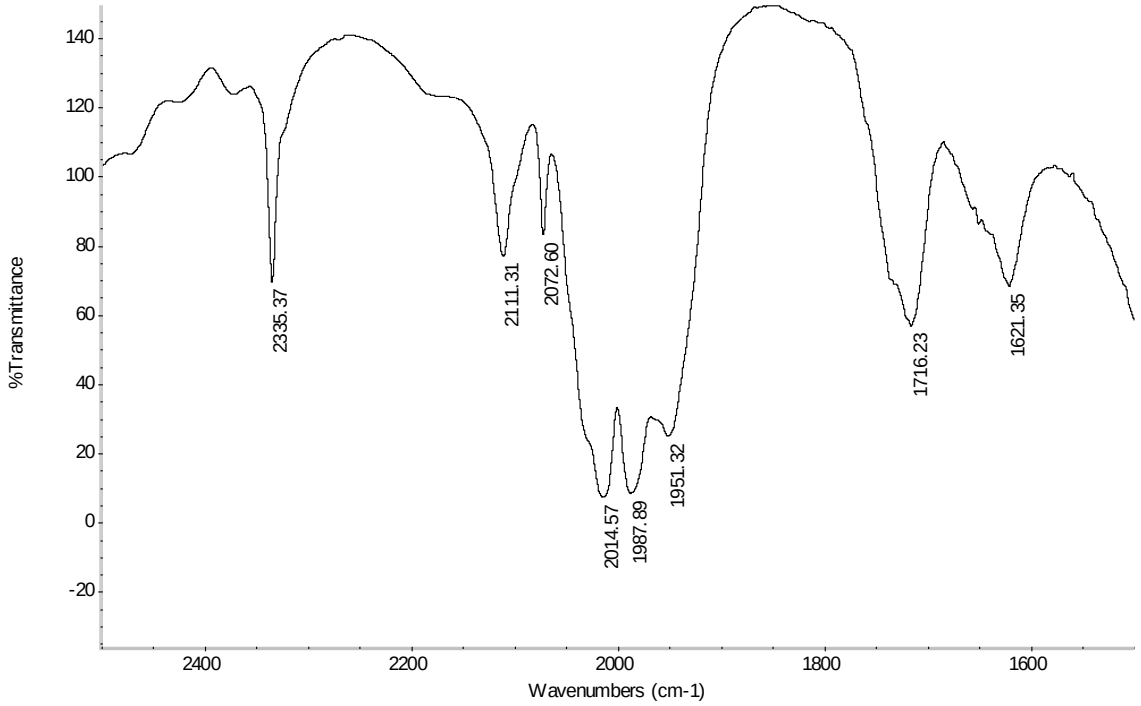

Figure 2.9. IR spectrum of the liquid product after reaction catalysed by RuO_2. Conditions: 200 ^oC, 250 bar, 4 hrs, H_2/CO 1:1, $[PBu_4]Br$ (15 g), $[RuO_2]$ (0.308 g). Spectrum taken after the reaction.

The spectrum is nearly identical to the one using $[Ru_3(CO)_{12}]$ (see Figure 2.10). This indicates that the active species are most likely the same. Together with the observation that the product liquid is black instead of the dark-red from $[HRu_3(CO)_{11}]^-$ and that the product yield for methanol and ethanol is much lower this also indicates that not all ruthenium is converted into the catalytically active species.

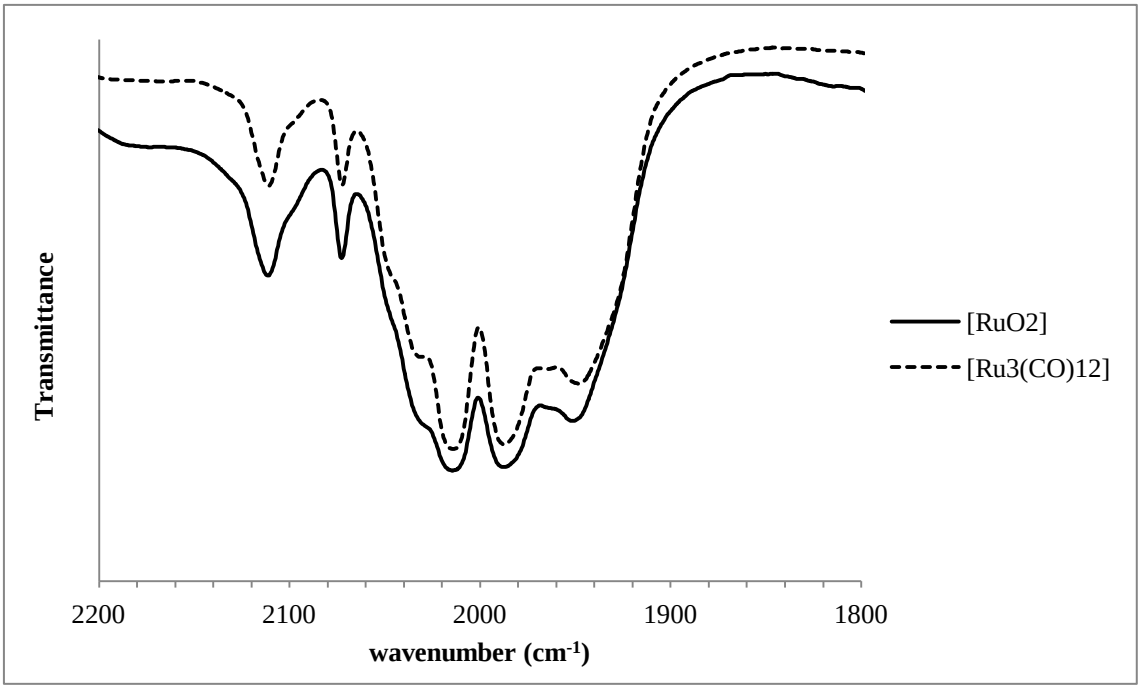

Figure 2.10. The normalised overlap IR spectra of the product solutions using either RuO_2 or $[Ru_3(CO)_{12}]$ as a catalyst precursor.

Unfortunately, a useful NMR spectrum of this reaction was not obtained. Spectra taken later on in the investigations using additional ^{13}C labelled methanol also showed bad resolution and inspection of the induction signal showed rapid relaxation of the signal. This indicates that there may be some paramagnetic species in the solution which is not present in the $[Ru_3(CO)_{12}]$ reaction. Possibly this comes from ruthenia particles that have not been converted during the reaction. In that case the ruthenia does not seem to aid in CO conversion. It has been shown by others that ruthenium oxide can consist of different phases, some of which may not be as reactive as the others.[85] In fact, it may well be that much of the ruthenium is not dissolved, but instead dispersed.

2.4 Balllast vessel uptake and mass balance

As can be seen in Scheme 2.1 the equipment set-up contains a ballast vessel to determine gas uptake over the course of the reaction. However, because the pressure is very high, small changes in ambient temperature result in similar pressure changes. For this reason and because of differences between the reproducibility reactions the uptakes vary slightly.

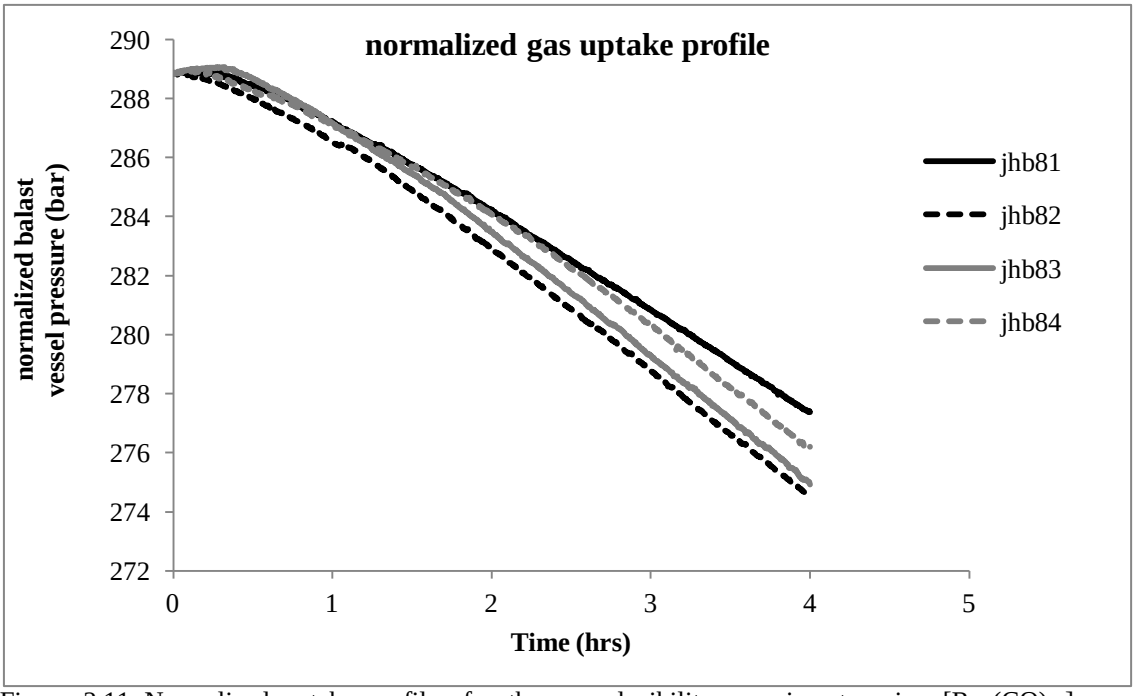

Figure 2.11 Normalized uptake profiles for the reproducibility experiments using $[Ru_3(CO)_{12}]$ as a catalyst precursor.

The uptake curves show that the rate of gas uptake is fairly constant throughout the reaction period.

2.5 The mass balance

This indicates that overall activity of the catalyst remains consistent with time. The volume of the ballast vessel is 0.5 L and therefore the average total CO consumption over 4 hours of time is on average 0.130 mol. However, from the GC analysis of all known compounds that have been calibrated the total calculated CO consumption is only 0.071 mol on average. It is reasonable to assume that the uncalibrated and calibrated compounds are similar in nature and therefore each average carbon gives rise to the same average response factor per incorporated CO. By extension, the total amount of CO captured in the liquid product can be estimated. In table 2.3 the mass balance is calculated for each reproducibility reaction from the $[Ru_3(CO)_{12}]$ series.

Table 2.3 CO consumption as calculated by gas uptake compared to the recovered amount through GC analysis.

	jhb81	jhb82	jhb83	jhb84	average
peak area of known compounds	0.072	0.077	0.068	0.067	0.071
peak area of all compounds	0.085	0.087	0.076	0.076	0.081
gas uptake	0.114	0.141	0.140	0.126	0.130

Extensive investigations on the liquid analysis show that it is accurate. As a result of these calculations and investigations it can be concluded that the analysis does not capture the complete set of products that is made during the reaction. As will be shown in chapter 3 the catalyst mixture will also produce a significant amount of gaseous products that are difficult to capture. For instance, there is significant methane formation, as well as ether formation. Both reactions consume liquid products, to produce gaseous ones. It was proposed that the catalytic system may also produce significant amounts of waxes which might escape detection. However, regular inspection of the ^{1}H NMR of the liquid product mixture should reveal sharp wax signals in case any significant amount is generated. These signals have never been observed. Because we find no wax, gaseous products must be formed in significant amounts. The formation of gaseous products will be discussed in chapter 3. For the moment, we will consider the liquid product formation mostly.

2.6 Differences between using RuO_2 and $[Ru_3(CO)_{12}]$

So far we have demonstrated many similarities between the use of RuO_2 and $[Ru_3(CO)_{12}]$ as metal precursors in the homogeneous hydrogenation of CO, however there are also some important differences. The most remarkable is the lower activity of the RuO_2 precursor compared with the $[Ru_3(CO)_{12}]$ in the synthesis of methanol, ethanol, propanol and ethylene glycol. As explained above this may be a result of incomplete conversion of the RuO_2 precursor into catalytically active species, while $[Ru_3(CO)_{12}]$ does not display this property. There is a constant reduced formation of methanol, ethanol and propanol (on average between 54 and 59% product formation compared to $[Ru_3(CO)_{12}]$) but not for ethylene glycol, of which there is a relatively high yield (86% compared to $[Ru_3(CO)_{12}]$). On the other hand, RuO_2 shows a small, but significant effect in higher alcohol synthesis. Where $[Ru_3(CO)_{12}]$ seems to form only

methanol, ethanol, propanol and butanol in continuously decreasing amounts, RuO_2 shows a marked rise in activity for the synthesis of butanol, pentanol, hexanol and heptanol. The GC-FID trace shows this behaviour quite well. However, it must be said that the response factor of the GC detector also increases with increasing carbon number. In other words, the peaks are relatively prominent, but in practise, the actual amount is not very high.

At this point, there exists no real explanation for this behaviour, however finding a catalyst that selectively promotes the formation of C_4-C_6 alcohols is interesting. However, realisation that there may be different processes going on at the same time leads to more questions in how their formation comes about. So far, it seems that there are three independent processes occurring in our system:

A. Formation of the C_1-C_4 alcohols
B. Formation of higher alcohols
C. Formation of ethylene glycol

The formation of the lower alcohols (A) seem to follow their own set of rules, the product distribution of methanol, ethanol and propanol may suggest that methanol may be reincorporated into ethanol through a methanol carbonylation reaction. Furthermore, the productivity towards each of these compounds is similarly affected on going from RuO_2 to $[Ru_3(CO)_{12}]$. Likewise, there exists a mechanism for formation of higher alcohols (B) in using RuO_2 that does not exists in using $[Ru_3(CO)_{12}]$. Finally, the formation of ethylene glycol (C) does not follow the same trend as the lower alcohol formation, and as such, the mechanisms are likely to be independent from one and another.

2.7 Identification of the different pathways

These interesting observations and questions led to the use of ^{13}C-labelled CO and methanol in order to differentiate between the possible mechanisms and pathways available to C-C coupled products. We start with assuming that the reaction of CO with H_2 using a homogeneous mixture of ruthenium and phosphonium salt can be summarised by scheme 2.2.

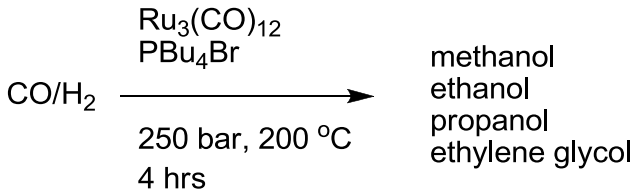

Scheme 2.2. The homogeneous hydrogenation of CO in $[PBu_4]Br$ using $[Ru_3(CO)_{12}]$ as the catalyst precursor

Others have shown[72, 73, 86] that in similar systems adding ^{13}C labelled methanol yields labelled ethanol in all cases. More explicitly: Warren and Dombek[72] find that when $^{13}CH_3OH$ was added to a system using Pr_3PO (75 mL), of Ru (5 mmol), I_2 (7.5 mmol) at 230 °C and 861 bar of syngas, labelled ethanol, propanol and methane are formed during the reaction. Ono[73] found the same and also reported formation of labelled acetic acid and acetaldehyde (most likely formed in the Warren and Dombek system too, but not reported) using Ru (0.2 mg from $[Ru_3(CO)_{12}]$), PPNCl (2 mmol), Ph_2O (19 mL) at 240 °C and 333 bar syngas.[73] Finally, Knifton[86] using ruthenium and cobalt (4 mmol each), $[PBu_4]Br$ (10 g) at 220 °C and 276 bar syngas reported labelled methanol, ethanol, and acetates but interestingly, he reported that labelling took place at the terminal methyl. However similar the systems used by the others, they are not the same: Knifton used a secondary catalyst Co (seemingly to promote ethanol formation), Dombek and Ono used traditional solvents with different salts or iodine and all of them used harsher conditions. It is fair to say that most likely we will find very similar results, but we cannot be certain. Additionally, we are interested in the additional pathway to C_4-C_6 alcohols that exists when using RuO_2, but was not reported before. It might be possible that the large amounts tetrabutylphosphonium bromide present could act as a C_4 source for higher alcohol formation if some phosphonium degradation were taking place. It is suspicious that the synthesis of exactly the C_4-and higher alcohols seemed to be promoted. In total, we are interested in how the C-C coupling reactions take place and in more detail, we consider four main mechanistic routes towards C-C coupled products:

1 Chain growth at the metal centre with irreversible release of the product alcohol
2 Chain growth through methanol carbonylation
3 C-C coupling via aldol condensation from free aldehyde intermediates
4 Alcohol synthesis via solvent degradation

2.8 Labelling studies

The pathways can be differentiated using butanol as the key compound. It is formed through both mechanisms of alcohol formation and we will use this to see if there are different outcomes if we apply labelled CO or methanol to the reaction. Expectations can be summarised in the following table 2.4, where there are three columns, one citing the mechanism and the other two columns citing our expectation in applying either ^{13}CO or ^{13}C methanol to the system.

Table 2.4 Possible pathways to butanol, predicted labelling patterns and outcomes from CO hydrogenation using partially ^{13}C labelled CO or $^{13}CH_3OH$.

Mechanism	**Expected labelling pattern for butanol**	
	Using ^{13}CO	Adding $^{13}MeOH$
All C entirely from Gas $CO + H_2 \rightarrow BuOH$	Up to 4 ^{13}C in butanol	No label in butanol
Methanol reincorporation $MeOH + CO + H_2 \rightarrow$ $\rightarrow BuOH$	Up to 4 ^{13}C in butanol	labelling in butanol
Acetaldehyde and aldol $MeOH + CO \rightarrow CH_3CHO$ $\rightarrow \rightarrow BuOH$	Up to 4 ^{13}C in butanol	Odd or even labelling pattern: eg. $^{13}CH_3CH_2{}^{13}CH_2CH_2OH$
Solvent degradation $[Bu_4P]Br \rightarrow BuOH$	No label in butanol	No label in butanol

Using ^{13}C enriched syngas and no added methanol we would expect that ^{13}C incorporation should take place uniformly throughout the products, regardless of the mechanism except when product formation occurs through degradation of the solvent. The mass spectrum (MS) of, for instance butanol, should therefore display an isotopic abundance pattern consistent with the abundance of ^{13}C CO in the gasphase. More specifically, all products should display a pattern consistent with a single gas phase ^{13}CO abundance. So back calculation of the abundance of ^{13}C in the products from an MS pattern should give rise to a single abundance value regardless of the compound that is subjected to this assessment. For example, a pattern that shows say 10% ^{13}C abundance in butanol means that we have to find a pattern that is consistent with also 10% ^{13}C abundance in ethanol too. Then, if for instance the C_{4+}-alcohols display a significantly lower ^{13}C abundance than the C_{1-3} alcohols, this would indicate that the higher alcohols were made from another source containing no additional ^{13}C, most

likely the solvent. Our equipment is not suited for accurate reading of low pressures (i. e. the pressures of ^{13}CO that are added), and as a result it is impossible to determine more than a rough estimate of enrichment of the syngas. However, from the GC-MS analysis of our products we were able to determine accurately what was the abundance of ^{13}CO in the gas phase, obtained by a simulation based on the labelling of the individual products.

2.9 Labelling theory and assessment

Two sets of experiments were performed using either $[Ru_3(CO)_{12}]$ or RuO_2 as a catalyst precursor. In one set we enriched the gas phase CO with additional ^{13}CO to form a mixture of ^{13}CO, ^{12}CO and H_2. Where

$$Abundance(\%) = \frac{^{13}CO}{(^{12}CO + ^{13}CO)}\ x\ 100.$$

In any natural source of carbon the abundance is 1.1% ^{13}C. How ^{13}C is distributed through molecules depends on how they are formed, but usually this is random. The appropriate way of doing calculations with abundances is by using statistics and probability calculations. Let us focus on butanol, a C4-straight chain alcohol that has a direction, so each carbon is distinguishable from the others by their location with respect to the alcohol group. When butanol was formed from naturally abundant ^{13}CO, there was a 1.1 % chance for each carbon that was incorporated to be a ^{13}C. Therefore, there is a good chance that the molecule has no ^{13}C's incorporated in it, in fact it is $(98.9\%)^4$ =95.7%. The chance of having exactly 1 ^{13}C is equivalent to 4 times 0.989^3 x 0.011^1 = 4.26 % etc.etc. The equation for deriving these numbers is given by

$$P(n,r) = \left(\frac{(n+r)!}{n!\,r!}\right) {P_{12C}}^{n} {P_{13C}}^{r}$$

Where $P(n,r)$ is the chance of finding n ^{12}C's and r ^{13}C 's in any molecule, n is the number of ^{12}C's, r is the number of ^{13}C's, P_{13C} is the abundance of ^{13}C and P_{12C} is the abundance of ^{12}C (=1-P_{13C}). Basically, the first part of the equation exists to correct for the number of times 1 (or any number of) label can be distributed throughout the

molecule, and the P's give the chance for a label to occur. Applying this equation to any molecule one can assess the extent of labelling in that species as a function of the abundance of that label. Importantly it tells something about the mass pattern one can expect in a mass selective detector. Two examples: when butanol is formed in an environment where there is 10% or 30% of ^{13}C we would expect the molecular ion (or any other C_4 fragment) in the MS to have the mass patterns shown in figure 2.12.

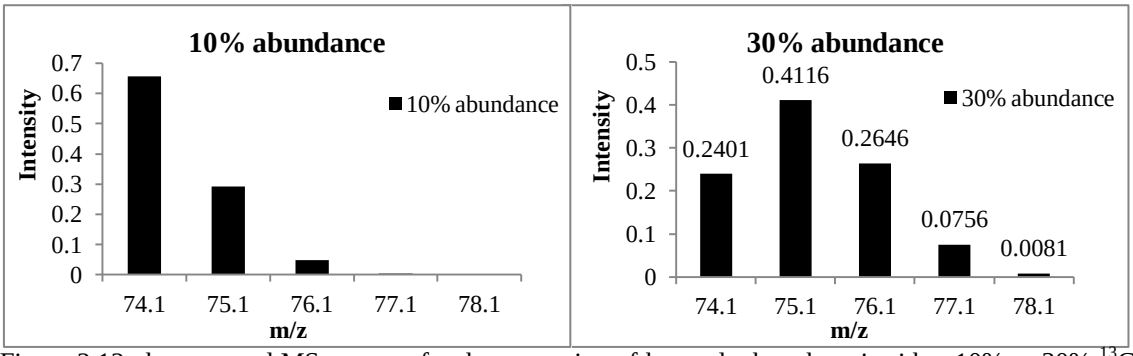

Figure 2.12. the expected MS patterns for the parent ion of butanol when there is either 10% or 30% ^{13}C labelling in the fragment.

As can be seen the patterns change significantly with the extent of labelling. The butanol containing 30% labelling now has a higher chance of finding a label in it than of not finding a label in it at all, while the example containing 10% label does not. Thus, if you know the abundance then you know the pattern you can expect in the MS. We used this argument in reverse to derive the gas phase abundance of ^{13}CO from a measured labelling pattern. We took the observed labelling pattern taken from a reaction and compared it to simulated samples, initially adjusting the percentage in the gas phase of ^{13}CO manually until a good fit between the simulation and the observed spectrum was observed. In reality the fragmentation pattern of any compound is subject to impurities, column bleed and side reactions taking place in the ionisation chamber of the GC-MS. To deal with this we decided to take a "natural pattern" from an unlabelled source, namely the reaction where we did not add any label and use this to construct a pattern with labelling. A constructed pattern would be a pattern that is the sum of the natural patterns where we added mass +1 to act for each label. If you name the natural pattern N_1 then the natural pattern shifted one mass up would be N_2, the pattern you would get if there is exactly 1 label, N_3: 2 labels, N_4: 3 labels, etc. They are shown in figure 2.13.

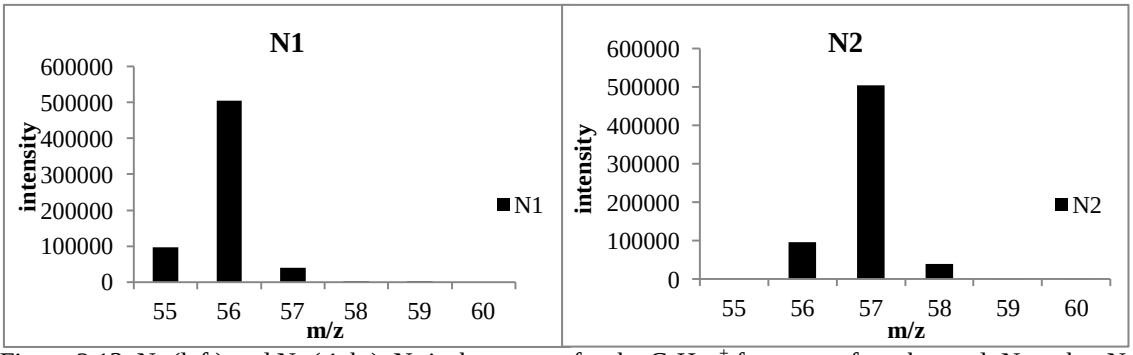

Figure 2.13. N_1 (left) and N_2 (right). N_1 is the pattern for the $C_4H_{7\text{-}9}^+$ fragments from butanol. Note that N_1 and N_2 look exactly the same but are in fact shifted by m/z = 1.

Then a constructed pattern is C = k1 N_1 + k2 N_2 +k3 N_3 … k_n N_n, with n goes up to the number of carbon atoms in the compound + 1. The constants, k, have to fit the patterns derived above in Figure 2.12 and must sum up to 1. So the sample with abundance 30% could be constructed using N_1 which is a pattern for butanol without label, N_2, which is N_1 but every mass shifted 1 up, etc. and the constants follow the pattern seen above in Figure 2.12, k1= 0.2401, k2= 0.4116, k3 = 0.2646, k4 = 0.0756 and k5= 0.0081. As follows then the constructed pattern is: C = 0.2401 N_1 + 0.4116 N_2 + 0.2646 N_3 + 0.0756 N_4 + 0.0081 N_5. A construct can be easily made for all values of abundance (going from 0% abundance and up) and can then be compared to the real labelled pattern that was obtained. A good fit should match the real signal exactly in relative intensity, therefore the construct with a good fit correlates to the correct abundance. An example below shows the natural pattern and the pattern of the labelled compound after spiking the reaction with ^{13}CO (Figure 2.14 a) on the left hand side, and the constructed pattern that matches the labelled pattern on the right handside and bottom left hand side (Figure 2.14 b and c). The final plot shows the corresponding abundance pattern for a C_4 species that has 7.4 % ^{13}C abundance. The constants in 2.13d where used to build 2.13 b and c.

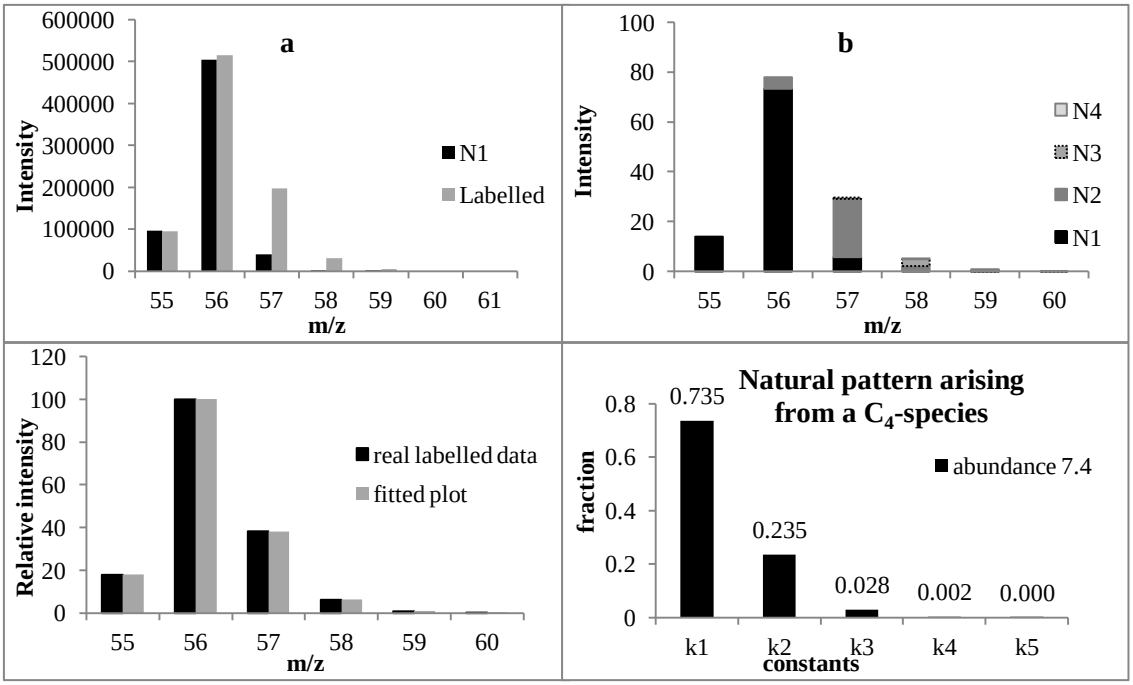

Figure 2.14 a) the spectra of butanol from natural abundance and from partially labelled CO (this is the $C_4H_9^+$ -fragment) b) a constructed pattern to match the labelled pattern in a c) A comparison of the constructed pattern (fit) with the labelled pattern, it shows a very good, but not perfect fit d) the constants used for constructing b and c, they themselves form a pattern equal to a theoretical C_4-species that contains 7.4% ^{13}C abundance.

At this point it is good to mention that it is imperative to apply the correct number of permutations to the calculations. For instance, in the case where labelled methanol is carbonylated to acetaldehyde, where ^{13}C ends up in the β-position and subsequently undergoes aldol condensation the possible outcome can only be as follows:

$$CH_3\text{-}C{=}O + CH_3\text{-}C{=}O \rightarrow CH_3\text{-}CH_2\text{-}CH_2\text{-}CHOH + H_2O$$

The label can only end up in two different locations, β or δ. And therefore the number of permutations changes from dealing with a compound that has 4 possible locations for ^{13}C to a species that has 2 different locations. This is especially significant if the extent of labelling is low, and the number of ^{13}C's in the molecule is low. In practice, this means that the fitted spectra do not match the real labelled data if this is not taken into account. The constructed pattern will never match the real pattern, making a bad fit. In practice, this is could be used to differentiate between mechanisms!

2.10 Applying the fit

We automated the fitting process to fit the MS spectra of the alcohols and EG against the range of constructed patterns from 0% abundance to 40% abundance in steps of 1% and assigned a fitness value to each fit. When we plot the fit against abundance we find a minimum where the fit is the closest. In this case the fitness was calculated by summing the squared difference between the fit and the real value for each mass and then dividing it by the number of masses included in the fit and taking the root of that number:

$$fitness = \frac{\sqrt{\sum_N (Yreal - Yfit)^2}}{N}$$

In other words, the average distance between the real value and the fitted value. In this way, a perfect match would have a fitness of 0 (average difference between fit and real is 0 per mass), and a bad fit would be higher than 5 (the average distance of the fit against the real plot would be more than 5 points off). Then the fit was re-iterated around the minimum fit for refinement to the decimal point. The best fit was used to mark the abundance of that compound. For this to work it is important that the fitness value of a comparison show a significant convergence approaching a good match. In other words, when the constructed plot is different from the real plot the fitness value has to be significantly higher than when a construct matches very well. The following figure shows that it does:

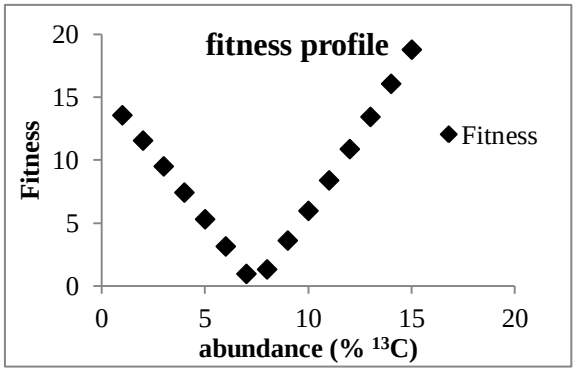

synthesised abundance (% ^{13}C)	found abundance (% ^{13}C)
10	9.7
20	18.2
30	30.2
40	40.5
50	49.6

Figure 2.15 Left: a fitness profile over a range of tried abundances. The values change significantly when the tried abundance does not correspond to the real abundance present. Right: the applied versus the found abundances for calibration of the fitting method.

Visual inspection of the matches also shows that bad fits really are different from the real plots. Only around the very minimum some ambiguity can occur and that is why we used the fitness value to determine the minimum. This way we get a result that is repeatable and better justified and not subject to our hopes or expectations. Furthermore, we decided to test the quality of the fitting by making mixtures of labelled and unlabelled methanol in different ratios and to subject them to the fitting procedure. Ideally the calibration curve should be a line y=ax+b where a is unity and b is zero. This is not the case, but very close; y=1.021x-0.99, most likely an error is introduced because we use natural patterns as a basis and they contain 1.1 % labelling as this occurs in nature. Therefore, we adjusted the values obtained using the calibration curve, and this should give us an accurate value for the gas phase abundance of ^{13}CO.

2.11 Results

Now we could fit any ^{13}C abundance to each compound and obtain the ^{13}C abundance of the carbon source for each compound that we subjected to this procedure and for each reaction that we did. Figure 2.16 shows the abundance found per alcohol after a 4 hour reaction of using ^{13}C enriched syngas (H_2:CO 1:1) with either [$Ru_3(CO)_{12}$] or RuO_2 in tetrabutylphosphonium bromide at 200 ^{o}C and at a starting pressure of 260 bar in a closed batch system.

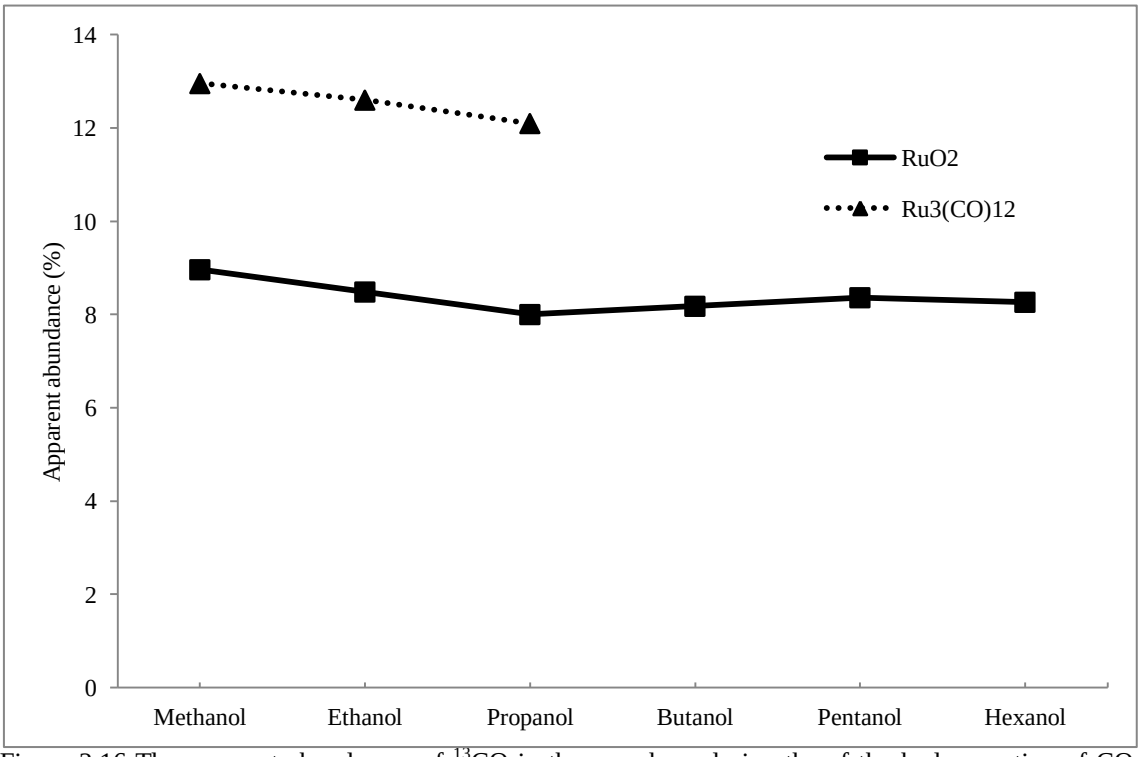

Figure 2.16 The apparent abundances of ^{13}CO in the gas phase during the of the hydrogenation of CO based, based on the isotope pattern found in the GC-MS analysis for each product. The values given $^{13}C/^{12}C$ x 100 are the average values when fitting using 4 different starting natural peaks from the 4 benchmark reactions.

2.12 Discussion of the results

Figure 2.16 clearly shows that a reaction using RuO_2 in ^{13}C enriched syngas yields isotopically enriched products. The average apparent abundance of gas phase ^{13}CO found for this reaction was 8.4 % ($^{13}C/^{12}C+^{13}C$). More interesting is that the apparent abundances calculated for all compounds are of the same order, indicating that all products come from the same carbon source and that solvent degradation does not contribute significantly to the formation of the longer chain alcohols. For the reaction using $[Ru_3(CO)_{12}]$ the average level of ^{13}C in the samples was higher because the initial pressure of ^{13}CO in the cylinder used for the $^{13}CO/^{12}CO$ mixture was higher. Again, the GC-MS of the product methanol, ethanol and propanol show patterns consistent with extensive and even labelling in the products. The found abundances for the first three alcohols are more or less the same.

2.13 Using ^{13}C labelled methanol

Before concluding on butanol formation, we will address the reactions where we added ^{13}C-labelled methanol. After excluding mechanism 4 as a mechanism to higher alcohols we decided to add ^{13}C labelled methanol to the reaction mixture in order to differentiate between mechanisms 1-3 for butanol formation. If methanol were reincorporated into ethanol in a carbonylation reaction we would expect to see increased labelling at the β-position of ethanol but not in the α-position. Likewise, if propanol is synthesised in a similar fashion from ethanol we would expect the label to remain exclusively on C_3 of the propanol. This should be visible in both the ^{1}H NMR spectrum of the product (^{13}C satellites) and from analysis of the GC-MS. Alternatively, if ethanol and propanol are not made from methanol then we expect no labelling to occur in the higher alcohols. With this in mind we added 99% ^{13}C enriched methanol to reactions using either $[Ru_3(CO)_{12}]$ or RuO_2 as catalyst precursors. The ^{1}H NMR spectrum (figure 2.17) of the product mixtures showed large ^{13}C coupled satellites for the ethanol β-protons. Interestingly, the protons from the α-position did not show increased ^{13}C labelling in either case. The NMR for RuO_2 (not shown) showed the same features.

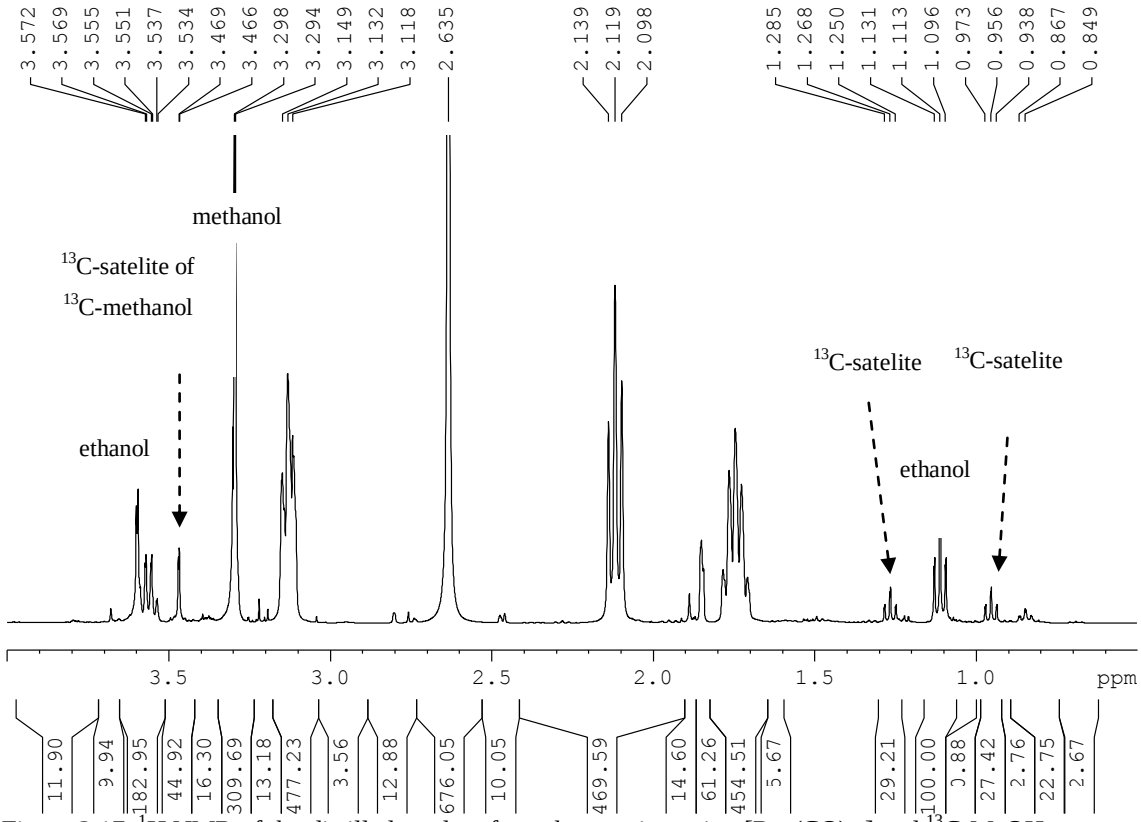

Figure 2.17. ^{1}H NMR of the distilled product from the reaction using [$Ru_3(CO)_{12}$] and ^{13}C-MeOH.

The ^{1}H NMR of the products distilled from the reaction using [$Ru_3(CO)_{12}$] and ^{13}C-Methanol show the presence of methanol, (δ 3.298 ppm) and the ^{13}C satellite at δ 3.469 ppm (the other satellite is hidden under peaks of NMP that where added for GC purposes. It also shows the two main peaks of ethanol (β-protons at δ 1.114 and α-protons at δ 3.562 ppm), important here is that the β-protons are accompanied by significant satellites at δ 1.268 and δ 0.956 ppm while the protons of the α-carbon are not. This shows that in going from methanol to ethanol the methanol ends up exclusively in the methyl group of the ethanol, as is usual in carbonylation reactions. Propanol is also present, but mostly overlaps with other peaks, the protons on C_3 are visible at δ 0.849 ppm and there is even a tiny satellite visible at δ 0.691, however the signal is very small, and therefore too uncertain to be used for quantitative purposes. Other visible peaks are from EG (δ 3.572 ppm, s, *no significant satellites*), NMP (GC solvent, δ 1.764 ppm CH2-C**H2**-CH2, m; δ 2.119 t -C**H2**-C=O; δ 2.635 ,s, N-C**H3**; δ 3.132; C**H2**-N, t), acetic acid (δ 1.889 ppm) and acetonitrile (internal standard, δ 1.851).

2.14 The extent of labelling in using ^{13}C-methanol

Due to the crowded nature of the ^{1}H NMR spectra only rough estimates of the isotopic abundances for some compounds found in the products can be made. The GC-MS data analysis showed that ethanol contained 40% and 34% of the ^{13}C isotope for the reactions using RuO_2 and $[Ru_3(CO)_{12}]$ respectively. The GC-MS pattern was consistent with the observation of labelling having occurred at a single position in the product, not only in assessment of the individual fragments, but also by determining the abundance. For ethanol the GC-MS analysis once again indicated exclusive labelling at the C_2-position. Thus, in combination with the evidence from NMR studies we conclude that methanol carbonylation is the major pathway to ethanol. Table 2.5 shows the determined labelling in the products (and their fragments) of both reactions.

Table 2.5. The isotopic enrichment of the products. The isotopic enrichment is calculated as $^{13}C/(^{12}C+^{13}C)$ x 100% based on GC-MS isotopic patterns of the relevant peak groups.

Precursor	Methanol	Ethanol	Propanol	Butanol	Pentanol
RuO_2	22	41	34	3	1
$[Ru_3(CO)_{12}]$	15	35	34	22	8

The high yield of ^{13}C labelling of the ethanol and propanol products indicates that in fact carbonylation of alcohols is the primary route to ethanol and propanol for both reactions. Interestingly, we found that in the case of propanol formation, the isotopic enrichment does not occur exclusively at the C_3-position. Instead, the label is also found with almost equal abundance at the C_2-position but not in the C_1-position (see Scheme 2.3). In each case, there can only be 1 label in the product propanol. The Figures 2.18-20 show how this information was derived.

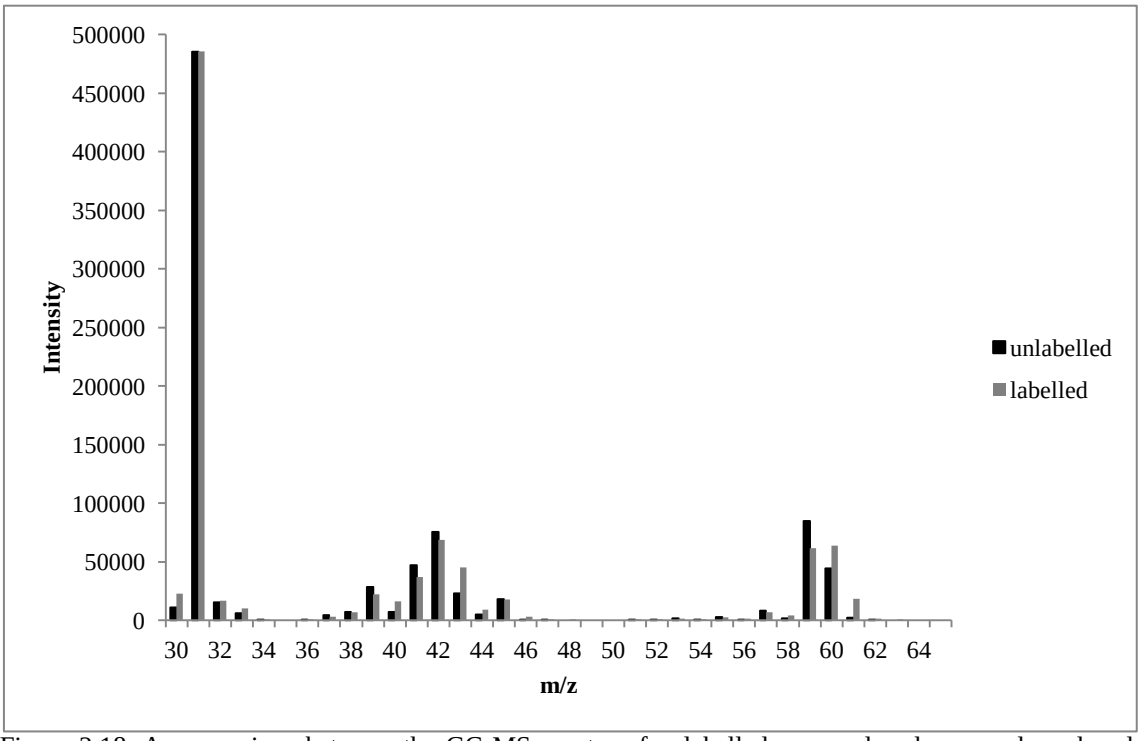

Figure 2.18. A comparison between the GC-MS spectra of unlabelled propanol and propanol produced when adding ^{13}C-methanol to a reaction using $[Ru_3(CO)_{12}]$. The latter spectra has been multiplied by a normalisation constant to obtain a spectrum where the intensity of the peak with m/z =31 are equal.

From the spectrum in Figure 2.18 it can be seen that there is a clear difference between the unlabelled propanol and propanol formed in the reaction with added^{13}C-methanol when using $[Ru_3(CO)_{12}]$. A few observations are very important. First, we cannot see doubly labelled fragments, as is shown in Figure 2.19a, which shows the molecular ion fragments for both labelled and unlabelled propanol. This means that, for all propanol that have been labelled, only one label was incorporated. Further inspection of the fragmentation patterns provides more information on the exact site of the label in the singly labelled products.

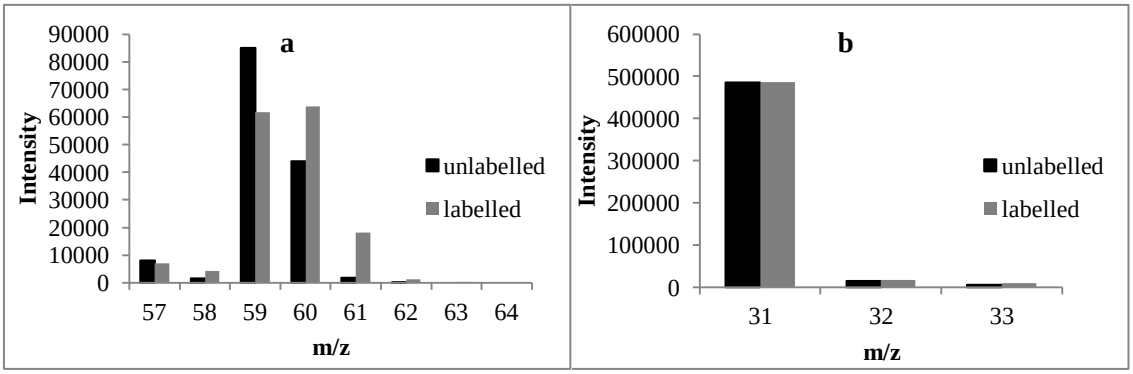

Figure 2.19 a) a close up of the molecular ion pattern it can clearly be seen that there is incoorporation of a label, but only 1 label. b) a close up of the fragment arising from the α-carbon and the alcohol group. It can be seen that there is no additional labelling in this position.

The fragment arising from C_1-C_2 bond scission, that is the fragment containing the hydroxyl group and the α-carbon, shows no label. This is shown in Figure 2.19 b). If we draw the structure of propanol as such: CH_3-CH_2-CH_2OH. The labelled species must come from either $^{13}\mathbf{CH_3}$-CH_2-CH_2OH or CH_3-$^{13}\mathbf{CH_2}$-CH_2OH. There are other fragments formed during the GC ionisation, however most of them form overlapping masses. However, the peak at m/z 45 comes from a species where C_2-C_3 bond scission occurred. It is the $^{+}CH_2$-CH_2OH species so contains both the original C_1 and C_2 carbon atoms from propanol.

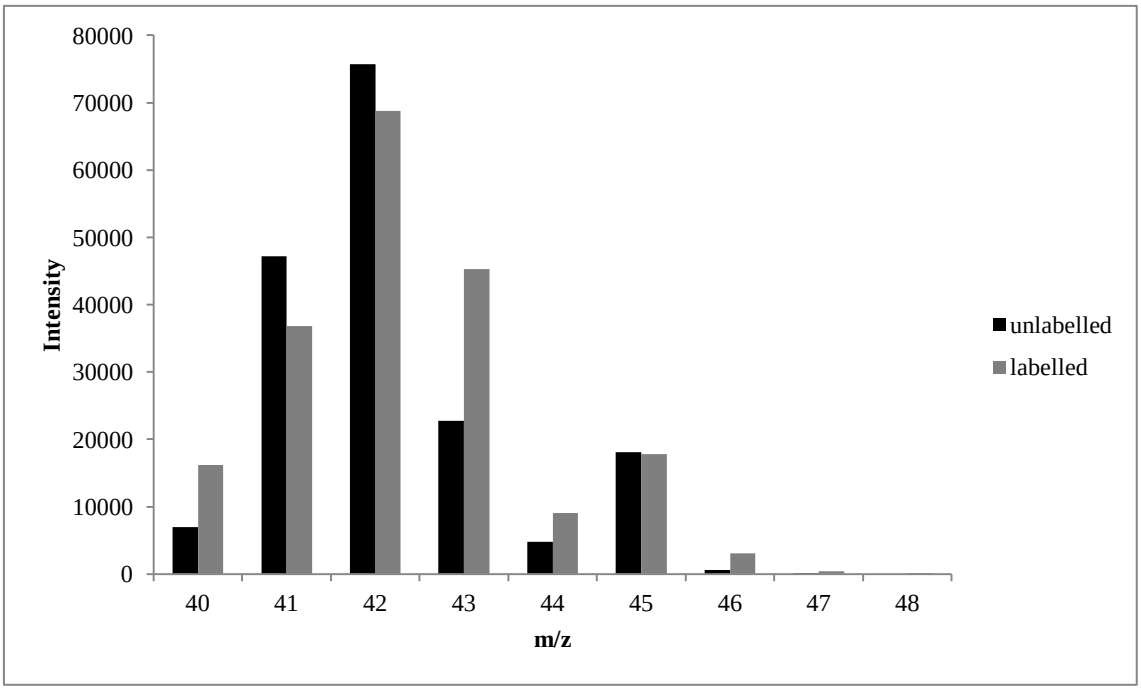

Figure 2.20. The GC-MS pattern of a group of species fragmented from propanol. One species is the CH_2-CH_2OH^+ fragment at m/z 45. At m/z 46 we can see the singularly labelled fragment of $^{13}CH_2$-CH_2OH^+.

Figure 2.20 shows that this species is labelled and contains about 17.3% ^{13}C, which must all be at position 2, this is visible at m/z 46. However, the total amount of labelling in the propanol from this reaction is 34 % ^{13}C, as shown in Figure 2.19a and Table 2.5. Therefore, the remaining 17% must be at the C_3 position. In other words, in this reaction isotopic scrambling occurs in going from labelled ethanol to propanol, so that the label is equally distributed between C_3 and C_2. A likely mechanism responsible for such chemistry would involve ethanol first being converted into ethyl bromide, which can then oxidatively add to the ruthenium centre forming a metal alkyl species, which can undergo insertion of CO and subsequent hydrogenation to form propanol. The fact that scrambling occurs points to a slow CO insertion step and a kinetically competitive reversible β-hydride abstraction. The formed metal hydrido alkene species can undergo rotation about the Ru-ethene bond.

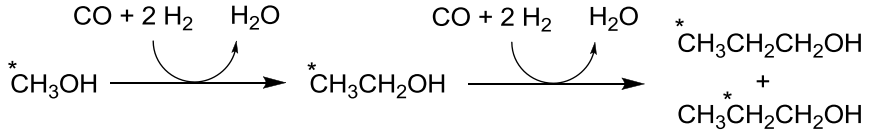

Scheme 2.3. Higher alcohols synthesis via alcohol carbonylation. The * indicates the position of ^{13}C when starting with $^{13}CH_3OH$

GC-MS analysis of the higher alcohols produced when using RuO_2 as the catalyst and adding ^{13}C labelled methanol showed that no label is present in the final products. All the C atoms come from the gas phase and hence the mechanism of formation of these longer chain products is different from that of the formation of ethanol and propanol and probably concerns chain growth on the metal centre with irreversible release of the product.

2.15 Other compounds

We can now look at the other compounds formed during the reaction. Some of them may be intermediates in side reactions or can give us clues about the reactivity of the catalyst and about how compounds are formed.

2.15.1 Dimethoxymethane

One compound of interest is dimethoxymethane. The most likely route to this compound is by formation of formaldehyde which can be methanolised to

dimethoxymethane in a methanol rich environment. It would be interesting to see for instance whether the central carbon is labelled when we add ^{13}C methanol at the start of the reaction as this would indicate that the methanol is oxidised to formaldehyde in the system, if this were the case we can expect full oxidation towards CO too. Inspection of a fragment of $CH_3OCH_2^+$ containing one "formaldehyde" carbon and one "methanol" carbon one can see the presence of a singly labelled compound, but there is no significant increase in intensity at m/z +2. See figure 2.21. This suggests that the formaldehyde C atom is not labelled and that significant dehydrogenation of methanol does not occur in this system.

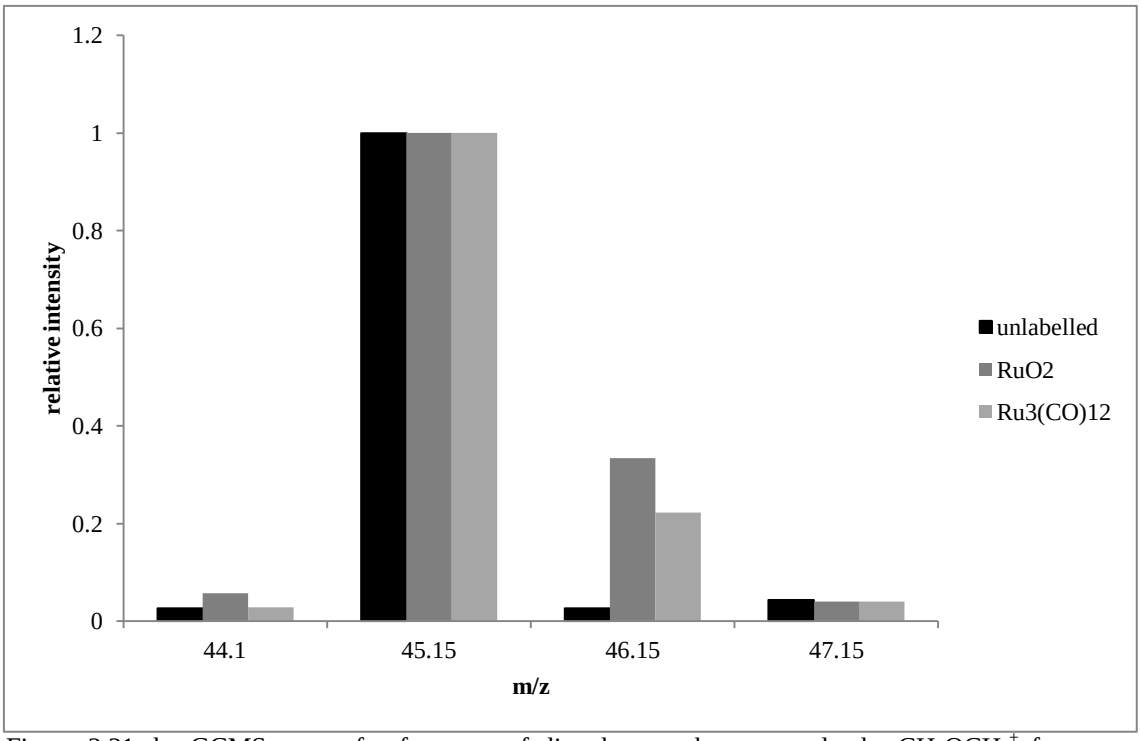

Figure 2.21 the GCMS trace of a fragment of dimethoxymethane, namely the $CH_3OCH_2^+$ fragment. There clearly is a single label, likely arising from the addition of labelled methanol to formaldehyde formed from the gasphase.

2.15.2 EG formation

The alcohols are not the only compounds formed, and identifying if and how the label is incorporated into other products may give some clues about other reactions taking place in our system. We already suspected that the formation of ethylene glycol occurs independently of methanol. And when we look at the GC MS and NMR signals arising from the EG peaks we can confirm that there is no label to be found. This means that the formation of ethylene glycol does not seem to involve the prior formation of

free methanol. Adding ^{13}C CO however, does lead to labelled EG. From this we can conclude that ethylene glycol is probably formed on the metal centre in its entirety or as an aldehyde (followed by hydrogenation) before it undergoes release into the solution. So, even though they may still share a common intermediate like coordinated formaldehyde or formyl groups, EG formation is on a path that diverges from methanol and ethanol formation before either of them is formed.

2.15.3 Acetic acid formation

It is also of interest to find out if acetic acid is formed from methanol in the ruthenium $[PBu_4]Br$ system. Knifton reported formation of labelled acetic acid when he used cobalt as a promoter. Most likely the acetic acid is formed in a similar fashion to the alcohols. We suspect first the conversion of methanol to methyl bromide, oxidative addition to ruthenium followed by CO insertion. However, where ethanol is formed by subsequent hydrogenation, acetic acid could be formed by reductive elimination of acylbromide followed by hydration or alternatively direct attack of water onto the acyl intermediate. We cannot really differentiate between these routes, but the first step is to identify whether methanol is indeed an intermediate in the ruthenium/$[PBu_4]Br$ system. Inspection of the GC-MS trace shows the presence of a single label, positioned almost exclusively on C_2. For these compounds we found 12.25% and 7.45% labelling for the reactions using $[RuO_2]$ and $[Ru_3(CO)_{12}]$ respectively.

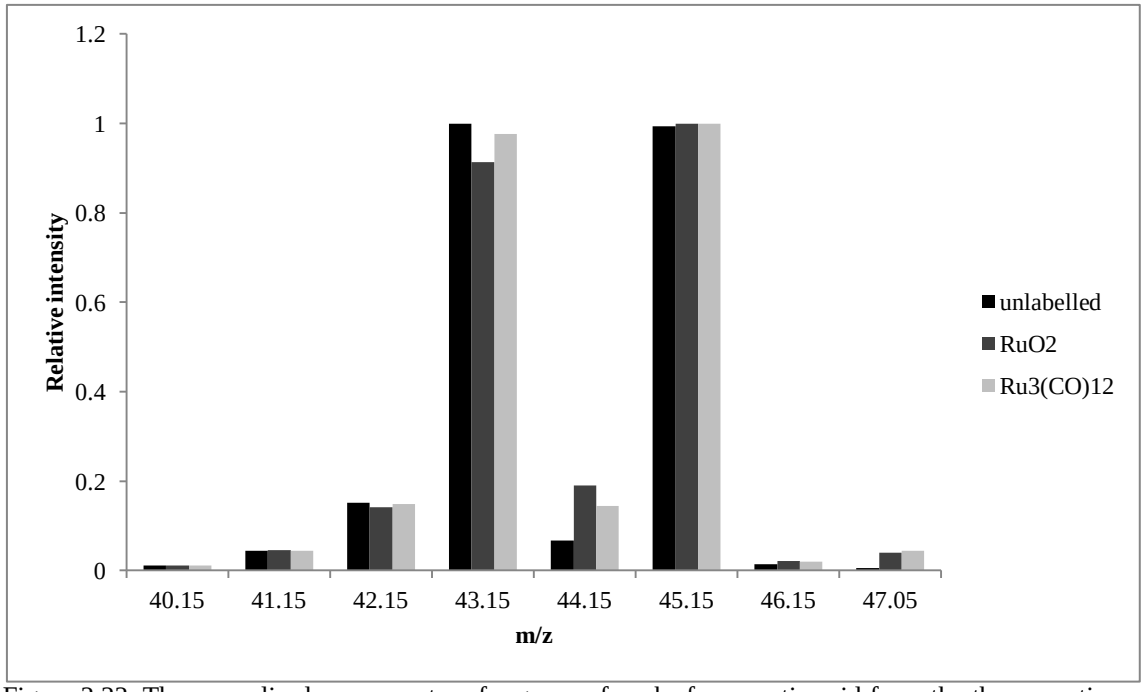

Figure 2.22. The normalised mass spectra of a group of peaks from acetic acid from the three reactions, one unlabelled, and two using ^{13}C-Methanol using [$Ru_3(CO)_{12}$] or RuO_2. There are two fragments, one belonging to the CH_3-CO^+ at m/z 43 accompanied with significant labelled fragments at m/z 45 and the other belonging to a CO_2H^+ fragment at m/z 45.

2.15.4 Acetaldehyde formation

Acetaldehyde is an interesting compound because it could be an intermediate towards ethanol formation. In case it is, the levels of acetaldehyde would never rise very high before it was reduced to ethanol. Thus, the extent of labelling should be close to that of methanol as it should have a relatively small lifetime in the reactor. If its lifetime is long however, the levels should be relatively high (we don't see large peaks in the GC trace) and the extent of labelling should be in between of ethanol and methanol. In addition, we expect only a single label, in the C_2 position. The GC-MS trace (figure 2.23) shows that there is in fact a single label. However, we cannot ascertain with certainty that the label is positioned in the C_2-position because of a mass cut-off applied in the mass selective detector to shield it from high intensity signals. However, we are able to apply the fit and this leads to a good fit. Using [$Ru_3(CO)_{12}$] and ^{13}C methanol we find that the acetaldehyde formed has 18% labelling (for methanol we found 15% and for ethanol we found 35% labelling) which fits the scenario where acetaldehyde is a short-lived intermediate towards ethanol from methanol. Using RuO_2 we find a similar result. (Labelling: acetaldehyde 22%, methanol 22%, ethanol 41%).

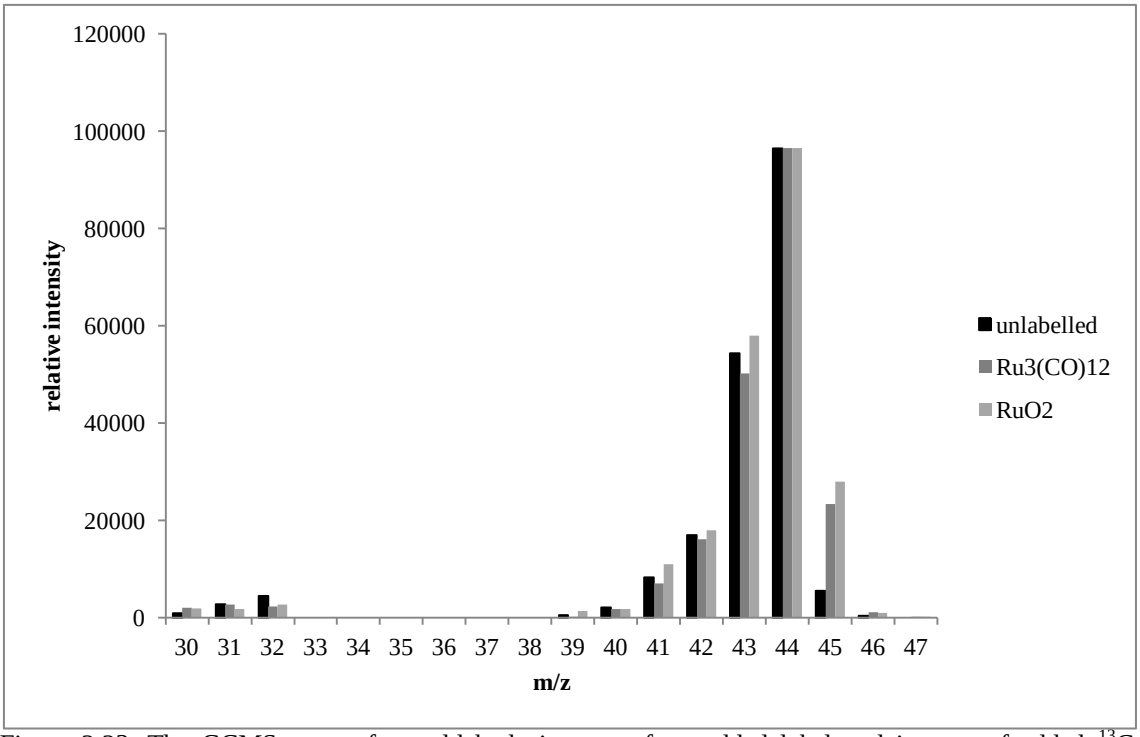

Figure 2.23. The GCMS trace of acetaldehyde in case of no added label and in case of added ^{13}C methanol using either $[Ru_3(CO)_{12}]$ or RuO_2. There is only one label to be found.

2.16 Experimental

2.16.1 General notes

Unless stated otherwise, all chemicals where obtained from Sigma Aldrich and used as received. Air-sensitive compounds where handled under N_2 using standard Schlenk techniques. NMR spectra where recorded on a Varian 300 NMR or on Bruker AM 300/400 NMR spectrometers. The chemical shifts where referenced to the solvent, which were in turn referenced to a TMS standard. ^{31}P NMR Spectra where referenced to external 85% H_3PO_4. IR spectra were recorded by pressing a sample of the liquid product between two KBr plates in a holder. The samples were recorded on a Thermo Nicolet Avatar FTIR spectrometer with a nitrogen cooled MCT detector. For quantitation Gas Chromatography analysis was performed using a Supelcowax-10 Capillary Column (60 m x 0.32mm x 1.0 µm film thickness) using an Agilent 6890N Network GC system equipped with a Flame Ionisation Detector. For identification a HP 6890 series GC system equipped with a HP 5973 Mass Selective Detector was used. Both machines used the same column using 1 ml min^{-1} Helium carrier gas flow and 250 ^oC injector and detector temperatures. The temperature programmes was as follows: 50 ^oC, hold 3 minutes, ramp 20 ^oC min^{-1}, 150 ^oC, hold 5 min, ramp 20 ^oC min-1, 220 ^oC, hold 13 minutes. Split ratio: 1:100.

2.16.2 Catalytic runs:

Reactions jhbr69-72, jhbr81-84, jhbr87-89, jhbr91: (Reproducibility experiments) Materials were purchased from Sigma Aldrich and used without further purification. In a typical reaction the autoclave was loaded with the reagents and then purged 6-7 times using syngas, to remove all air. The autoclave was then pressurised to 170 bar and checked for leaks overnight. The following morning the heater was switched on and when the reactor had reached a temperature of 200 ^oC the pressure was adjusted to 250 bar. After 4 hours of stirring the heating was switched off and the autoclave was allowed to cool to below 30 ^oC before venting. If gas samples were collected they would be collected during venting. After venting the autoclave was opened and the product mixture was transferred into a flask for analysis and product isolation. We regularly sampled for IR and NMR, and the distillate was analysed by

GC-FID and/or GC-MS. The autoclave was washed with solvent 3 times and the tubing was flushed until no colouring could be detected. After drying the autoclave was ready for use. For instance, jhbr70: $[Ru_3(CO)_{12}]$ (0.4997 g, 2.345 mmol Ru) and $[PBu_4]Br$ (15.0002 g, 44.205 mmol) were added to the autoclave. The autoclave was screwed onto the holder and purged by pressuring to 11 bar and venting to ambient 6 times using CO/H_2 1:1 v/v before pressuring to over 170 bar. A leak test was performed and no pressure drop was observed overnight other than that resulting from cooling the autoclave. The following morning the heating jacket was mounted, and switched on, the stirrer was switched on, and when the temperature reached 200 ^oC the pressure was adjusted to 250 bar and the stirrer was set to a fixed power input. The temperature and pressure was held constant until the heating and stirring switched off after 4 hrs. Taps to the autoclave were closed to prevent gas flowing into the reactor because of the cooling. When the autoclave temperature reached below 30 ^oC the autoclave was vented and opened up. The product mixture was usually a red liquid of which a small sample was stored and was often analysis using NMR or IR. The remainder of the liquid was transferred to a flask and stripped of volatiles by vacuum distillation using temperatures up to 250 ^oC and a liquid N_2 cold trap. The volatiles that where collected where diluted using acetonitrile/NMP stock solution (2 mL of 5% (v/v)) and analysed using GC. The total product amounts where calculated using the NMP and acetonitrile peaks as internal references. The yields are given in Table 2.7. The autoclave was cleaned by refluxing DCM through the system three times until the solvent remained colourless. Then the warm autoclave was dried and disassembled to replace o-rings.

All other reactions used the same conditions and received the same treatment and procedure unless specifically stated. Reactions jhbr69-72 were washed with DCM 3 times after reaction. For all other reactions this was done using methanol. Table 2.6 shows the reagents and conditions used in each reaction.

Table 2.6 used material in for reactions in Chapter 2[a]

reaction	solvent	Amount (g)	mmol	Catalyst precursor	Amount (g)	mmol Ru
jhbr69	$[PBu_4Br]$	15.0140	44.25	$[Ru_3(CO)_{12}]$	0.4993	2.343
jhbr70	$[PBu_4Br]$	15.0002	44.20	$[Ru_3(CO)_{12}]$	0.4997	2.345
jhbr71	$[PBu_4Br]$	14.9988	44.20	$[Ru_3(CO)_{12}]$	0.5009	2.350
jhbr72	$[PBu_4Br]$	14.9997	44.20	$[Ru_3(CO)_{12}]$	0.4997	2.345
jhbr81	$[PBu_4Br]$	15.0028	44.21	$[Ru_3(CO)_{12}]$	0.4994	2.343
jhbr82	$[PBu_4Br]$	15.0023	44.21	$[Ru_3(CO)_{12}]$	0.4997	2.345
jhbr83	$[PBu_4Br]$	14.9982	44.20	$[Ru_3(CO)_{12}]$	0.4989	2.341
jhbr84	$[PBu_4Br]$	15.0033	44.21	$[Ru_3(CO)_{12}]$	0.5011	2.351
jhbr87	$[PBu_4Br]$	15.0019	44.21	RuO_2	0.3042	2.338
jhbr88	$[PBu_4Br]$	15.0005	44.21	RuO_2	0.3054	2.348
jhbr89	$[PBu_4Br]$	14.9992	44.20	RuO_2	0.3049	2.344
jhbr91	$[PBu_4Br]$	15.0006	44.21	RuO_2	0.3058	2.351

[a]The reaction conditions where 200 ^oC, 250 bar syngas 1:1 v/v, 4 hrs.

The following table shows the product yield for each reaction. The values presented are those from what was recovered during the reaction work up. This will always be an underestimate of the real product yield as some of it may be lost upon venting and when some of it has condensed on the reactor tubing.

Table 2.7. The recovered product after distillation by analysis with GC using an internal standard (amounts in mmol).

name	Methanol	Ethanol	1-Propanol	1-Butanol	1-pentanol	n-hexanol	Acetic Acid	EG	2-Methoxyethanol	2-Ethoxyethanol
jhbr69	11.61	2.72	0.15	0.00	0.01	0.05	0.28	0.09	0.12	tr
jhbr70	9.05	4.40	0.54	0.00	0.19	0.36	0.93	2.48	tr	tr
jhbr71	2.51	5.37	0.86	0.00	0.08	0.12	6.51	0.49	tr	tr
jhbr72	17.24	6.01	0.49	0.00	0.13	0.20	1.09	10.87	0.67	tr
jhbr81	21.48	7.47	0.59	0.03	0.08	0.01	0.38	1.53	0.44	0.03
jhbr82	24.62	7.43	0.53	0.02	0.06	0.01	0.52	1.53	0.46	0.03
jhbr83	22.27	6.77	0.48	0.02	0.06	0.01	0.31	1.43	0.42	0.03
jhbr84	21.33	6.72	0.50	0.02	0.06	0.01	0.35	1.51	0.43	0.03
jhbr87	13.26	3.45	0.23	0.38	0.21	0.11	0.33	0.93	0.20	0.01
jhbr88	11.86	3.76	0.33	0.42	0.26	0.13	0.48	1.42	0.35	0.08
jhbr89	13.87	3.93	0.29	0.44	0.24	0.14	0.69	1.44	0.28	0.02
jhbr91	14.22	4.07	0.29	0.40	0.22	0.13	0.53	1.37	0.26	0.01

2.16.3 Labelling experiments:

The procedure for the reactions with enriched ^{13}C was slightly different from the reactions described above:

Jhbr102: Reaction using RuO_2 and ^{13}C-labelled CO

$[PBu_4]Br$ (15.0007 g, 44.21 mmol)) and RuO_2 (0.3060 g, 2.35 mmol Ru) were added to the autoclave. The system was purged using 1:1 syngas and brought to 185 bar to test for leaks. When the system did not leak the autoclave was vented to ambient pressure. Then the pressure was raised to approximately 13 bar using ^{13}C labelled CO and H_2 was added to approximately 24 bar total pressure. Then the pressure was increased to 180 bar using regular 1:1 syngas. These pressures were measured using the Back Pressure Regulator (BPR) which is accurate at higher pressures but not very accurate at low pressures. The autoclave was closed and subsequently heated to 200 ^oC under constant stirring. The reaction was allowed to proceed for 4 more hours and the reactor was cooled to below 30 ^oC. The autoclave was vented and the product liquid was sampled for analysis and further treated as described above. In this case, the distillate was analysed by GC-MS to assess the compound individual masses and fragmentation patterns.

Jhbr103: Reaction using RuO_2 and ^{13}C-labelled methanol

$[PBu_4]Br$ (15.0003 g (44.21 mmol))and RuO_2 (0.3058 g (2.35 mmol)) and 99% ^{13}C and 12% ^{18}O-methanol (0.5 ml, 12.35 mmol) were added to the autoclave. The system was purged using 1:1 syngas and then pressurised to 180 bar. The autoclave was closed and heated to 200 ^oC and stirred for 4 hrs. The autoclave was cooled to 30 ^oC and treated as for sample jhb102

Jhbr105: Reaction using $[Ru_3(CO)_{12}]$ and ^{13}C-labelled CO

$[PBu_4]Br$ (15.0005 g, 44.21 mmol) and $[Ru_3(CO)_{12}]$ (0.4995 g, 2.34 mmol) were added to the autoclave. The system was purged using 1:1 syngas and then vented to ambient pressure. ^{13}C CO was added to bring the pressure to 17 bar and H_2 was added to bring the pressure to 33 bar and balance syngas was added to bring the pressure to 180 bar.

The reactor was heated to 200 ^{o}C and stirred for 4 hrs. The reactor was cooled and the procedure followed was as for sample jhbr102

Jhbr107: Reaction using $[Ru_3(CO)_{12}]$ and ^{13}C-labelled methanol

As jhbr103, only in this case $[PBu_4]Br$ (15.0007 g, 44.21 mmol), $[Ru_3(CO)_{12}]$ (0.4994 g, 2.34 mmol) and 99% ^{13}C and 12% ^{18}O-methanol (0.5 ml) was added to the reactor.

2.16.4 Calibration for the labelling studies

The procedure for finding the abundance was described in above, for the calibration a series of labelled solutions of methanol was prepared and then used: the results are summarised in the following table and plot:

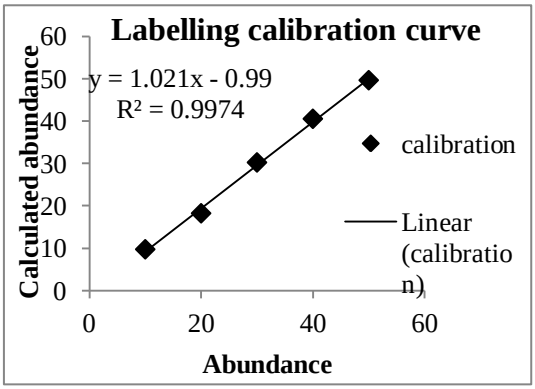

Synthesised abundance (%)	found abundance (%)
10	9.7
20	18.2
30	30.2
40	40.5
50	49.6

Figure 2.23 the calibration curve for quantification of the label.

2.17 Conclusion

On the basis of ^{13}C labelling studies, we conclude that methanol reincorporation is the primary route to higher alcohol synthesis in the homogeneous hydrogenation of CO using $[Ru_3(CO)_{12}]$. For the same reaction, using RuO_2 we find the same process, except that there exists an additional pathway to the C_{4+} alcohols, where the carbon source is gas phase CO and free methanol is not an intermediate. The position of the label in propanol suggests that migration of the ethyl group onto CO is slow compared with reversible β-H abstraction. An interesting implication of having a system where ethanol is made from methanol is that this turns methanol into an intermediate. So the rate of ethanol formation should be dependent on the methanol concentration. It is then possible to draw a scheme where one can express the formation of methanol and ethanol in terms of a rate constant and [MeOH] and [EtOH], carry out kinetic analysis on them and perform a form of modelling on the product formation. In addition, one can imagine a process where one goes directly from CO and H_2 to ethanol in one pot by recycling methanol.

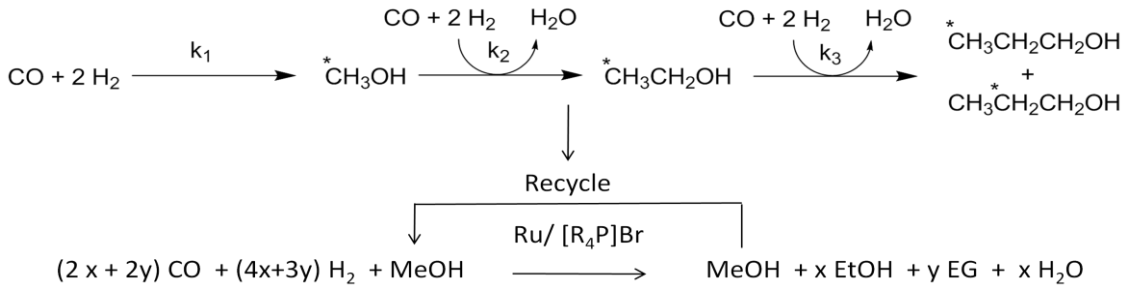

If the level of methanol is high enough to increase the ethanol formation to the same rate as the methanol formation then a truly continuous system providing ethanol from CO and H_2 could be designed. To find out whether this is feasible one needs to find out the rate of ethanol formation and compare it to the rate of methanol formation. Preferably, one would also find a way to adjust the individual reactions to increase control and for that, one needs to find out which factors play a role in their synthesis. This will be the subject of the next few chapters.

Chapter 3
Gas phase behaviour of the system

Analysis of the headspace components and Water-Gas Shift activity

3.1 Introduction

The poor mass balance described in Chapter 2 indicates that there must be significant gas phase behaviour in the $[Ru_3(CO)_{12}]$-phosphonium halide system that is not fully understood. From GC it is apparent that very light compounds are present after reaction which elute very early into the detector, often as part of overlapping peaks. GC-MS analysis shows us that we form ethers and minor amounts of hydrocarbon products. Work from Ono[73, 74], Warren[72] and Knifton[87] has shown that formation of methane can be a large part of the product formation. As part of our investigations the first step is to identify which compounds are in the gas phase and the second step is an attempt to quantify them. This is not trivial. We do not have specialised gas detection equipment for gas analysis. Furthermore, during catalysis the pressure is usually higher than 250 bar and after cool down to ambient temperature the pressure is reduced to 170 bar. Most gas analysis equipment can only handle ambient pressures or pressures of two orders of magnitude smaller. Furthermore, the dilution of products in this large amount of gas does not make for high detection levels. Not all equipment can reproducibly detect small levels of methane, and these levels are small because they are diluted by the high pressure of syngas. Therefore, significant effort has gone into finding a good method for analysing the gaseous compounds. For instance, storing gas samples for injection into a GC is not easy. Using specialised gas trap bags for analysis has proven unfruitful because it turns out to be permeable to hydrogen. Most (micro)GC equipment is able to accept gas at ambient pressures and in our reactor gas is stored at 170 bar at ambient temperature. So either gas has to be stored in cylinders close to ambient pressure, where there is only enough low pressure gas stored for one or two analyses (little room for error), or the outcoming gas must be sampled directly into a syringe for quick analysis. We expect that, because of these difficulties, gas analysis has been largely ignored in most studies that were published so far. Only Ono has published quantitive data on

methane production in one article.[74] Because the methods were continuously improved upon, there are some differences between the methods and quality for measurements between early and later samples.

3.2 The effect of pressure

We were intrigued by a finding in Dombek's published results, that there was a net effect of overall pressure.[49] He performed two experiments; in both experiments the partial pressure of H_2 and CO were both 430 bar, but in one experiment he added an additional amount of 860 bar of N_2. The increase in catalytic activity was profound:

Table 3.1 The effect of total pressure on the reaction rates.[a]

pressure used			rates found	
$p(H_2)$[b]	$p(CO)$[b]	$p(N_2)$[b]	Methanol[c]	Ethanol[c]
43	43	-	426	44
43	43	86	961	137

[a]Conditions: 18-cromwn-6 (75 mL), Ru (6 mmol), KI (18 mmol), 230 [o]C. [b]pressure in MPa. [c]rates of formation (mmol hr^{-1}). Adapted from [[49]], table 4.

The increase in the rates of formations of different products were attributed to a negative volume of activation, which suggests that, during the rate determining step, the volume of the species that makes up the transition point is smaller than the volume of the starting species of the reaction. We decided to perform similar reactions to find out if the ruthenium melt system displayed similar properties. Because we saw a significant mass transfer effect we also were interested in increasing gas diffusion into the liquid phase. CO_2 is considered to be a good transport vector in ionic liquid catalysis[88, 89] and we decided to extend the measurements with an additional reaction containing CO_2. Table 3.2 shows the starting conditions of the reactions and Figure 3.1 shows the results of the experiments.

Table 3.2 Experiments to measure the effect of total pressure and the addition of CO_2.

experiment	pressure used[d]				
	$p(H_2)$[b]	$p(CO)$[b]	$p(N_2)$[b]	$p(CO_2)$	total
1	125	125	-	-	250
2	75	75	-	100	250
3	75	75	100	-	250
4	75	75	-	-	150

Conditions: $[Ru_3(CO)_{12}]$ (0.5 g), $[PBu_4]Br$ (14.503 g), $[HPBu_3]Br$ (0.4145 g), 200 ^oC, 4 hrs. [d]Pressure in bar.

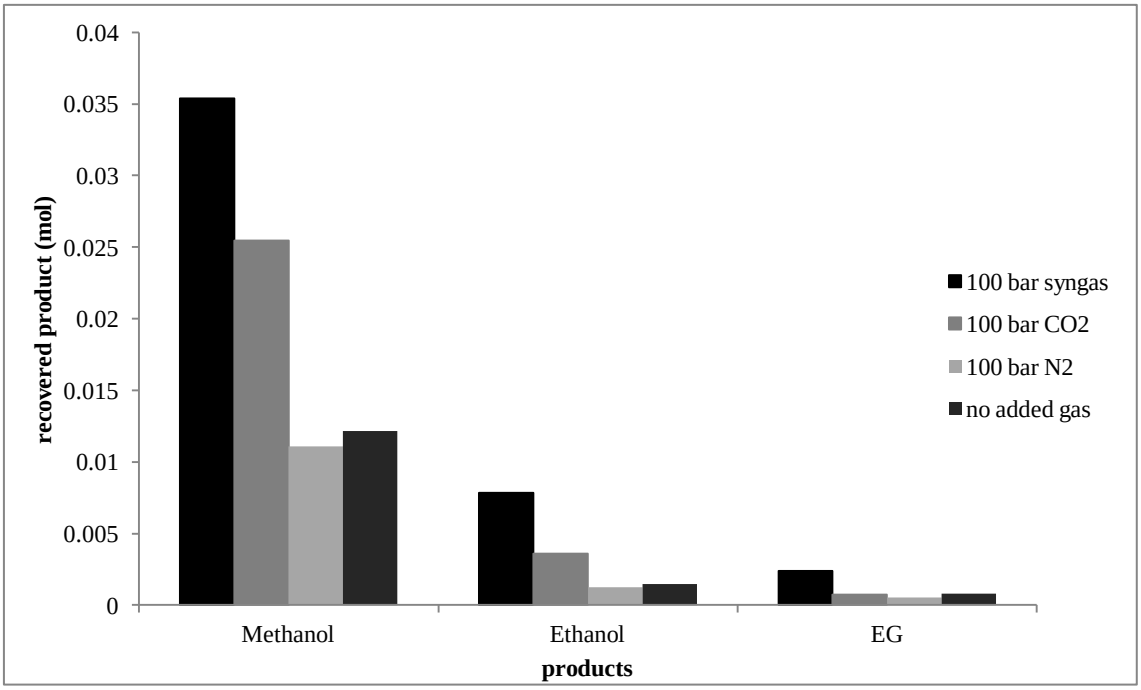

Figure 3.1. Product formation from the set of experiments described in Table 3.2. The legend states the amount of added gas in addition to 150 bar of 50:50 syngas.

The effect found by Dombek was not reproduced in this pressure range (difference between no added gas and 100 bar added N_2). There is a chance that this effect becomes more apparent only at very high pressure differences. The difference in pressure in Dombek's system is very high; 430 bar. The second interesting finding is that the addition of CO_2 is beneficial to catalysis, compared to added N_2. This is a strange find, because the net partial pressure of both CO and H_2 is not changed, and we believe that only CO and H_2 are involved in CO hydrogenation. We could interpret this in two ways. One, there occurs a net "carbon" pressure effect, where the rate of catalysis is affected by the partial pressure of both CO and CO_2. Two, CO_2 increases the rate of catalysis because of more effective transport of CO and H_2 to the catalyst phase.

Ultimately, we can also see that the total partial pressure of syngas is very relevant to the rate of catalysis. High syngas pressures led to higher product formation. To estimate how the partial pressures of CO and H_2 affect catalysis we decided to perform a set of experiments with varying starting pressures of CO and H_2. Another objective was to estimate the activity for the Water-Gas Shift reaction, or alternatively how the presence of CO_2 affects the rate of reaction.

3.3 The water-gas shift (WGS) reaction

CO, H_2, CO_2 and CH_4 could be relatively easily separated and detected using micro GC equipment operated and maintained by another group in the department. We could sample some of the gas from reactions by purging them into flasks. We then took 3 mL samples of this gas and diluted them using N_2 (17 mL) and capping the plastic syringe. We then connected the syringes to the micro GC equipment with TCD detectors using a custom-built connector. We then slowly vented the gas through the GC insertion line while the machine sampled. Because this method does not provide precise control of the amount of gas injected into the machine, we can only compare relative peak sizes. We assumed that the CO, H_2, CO_2 and methane constituted 100% of the gas phase. This is because we did not detect other products in the micro GC. Although, compounds such as dimethyl ether will not usually not elute rapidly from these columns. Because the volume, temperature and pressure in the reactor are known, the quantity of each compound can be determined if their relative response factor is known. To assess this relative response mixtures of gases with known partial pressures were prepared. Using this, the gas phase composition after a number of reactions was assessed. In five separate reactions the starting conditions in our system were varied, and the gas phase composition after 4 hours of reacting was checked. Because we did not want to influence the gas phase composition during catalysis by letting in additional syngas, we performed closed batch reactions. The starting conditions in the reactors can be represented by the following table 3.3.

Table 3.3 the starting conditions for closed batch experiments.[a] The experiments were pressured to the following pressures at 50 °C, and the reactor was then heated to 200 °C for 4 hrs for the reaction.

Exp. No.	CO	H_2O[b]	<--->	CO_2	H_2
5	-	-		63	126
6	63	-		-	63
7	126	63		-	-
8	63	63		-	63
9	-	63		63	63

[a]Conditions: 0.5 g $[Ru_3(CO)_{12}]$ 14.5 g $[PBu_4]Br$, 0.4145 g $[HPBu_3]Br$, 200 °C, 4 hrs. Closed batch experiments.[b] Added as liquid water (4.3 mL).

The top line in table 3.3 represents the water gas shift reaction. The experiments were performed starting from different positions of this equation, so as to observe the positions are at the end of the reactions. The quantities of the materials are given in bar of pressure at 50 °C assuming that all materials behave as ideal gases and are in the gas state. For water this means we added 4.3 mL to make up 63 bar when fully in the gas phase and at a temperature of 50 °C.

$$CO + H_2O \underset{K_{473K} = 222.7}{\overset{\Delta H^o = -41 \text{ kJ mol}^{-1}}{\rightleftharpoons}} CO_2 + H_2$$

Scheme 3.1 The water gas shift reaction. The equilibrium position at 200 °C lies far to the side of CO_2 and H_2.

If the WGS reaction is fast we would expect to see equilibrium positions, and primarily this constitutes a shift towards the right hand side of the equilibrium. For instance, experiment 5 starts out very close to the equilibrium position so we would not expect much change however, this reaction also does not contain any CO. Therefore, if we find formation of methanol this indicates that a process is available, directly from CO_2 and H_2 to liquid products (probably via the generation of free CO from the WGS reverse reaction). In order to know what to expect we have calculated the equilibrium position of the WGS reaction using the starting points for each reaction. This is shown in Figure 3.2 (right hand side). For better comparison we have made a visual version of Table 3.3 where the starting levels are displayed.

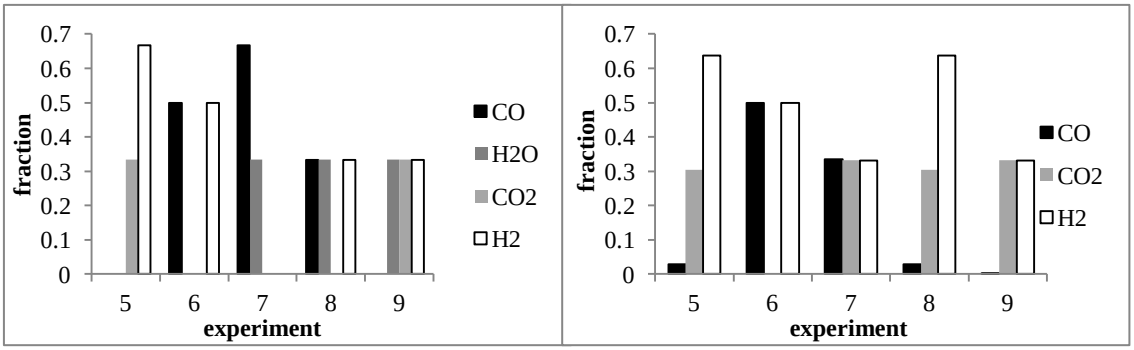

Figure 3.2 A (left), the starting levels of WGS compounds in the experiments from Table 3.3. B (right), the calculated equilibrium positions of the WGS reaction of the experiments described in Table 3.3.

As can be seen we would not expect major changes in the gas phase composition for reactions 5, 6 and 9 because they are near the equilibrium position (5 and 9) or because they only have one gas from each side of the WGSR equilibrium (6). However, reaction 7 and 8 are away from the equilibrium position so if the catalyst is active for WGS reactions we would expect a large shift. The found gas phase compositions after reaction are shown in figure 3.3. At first sight, the found gas phase compositions are not like the equilibrium positions that were calculated in figure 3.2 (B, right). For all reactions the CO_2 peaks is much larger than expected based on the WGS reaction. However, we did not take into account formation of products, which should lower both H_2 and CO and also form water, which turns into CO_2 in this system. Although exact quantification is difficult at this point, because these figures show the relative gas content in the autoclave. However, in a following section we can see how the gas profile evolves over time. These figures show that the ruthenium melt system is very active for WGS reactions.

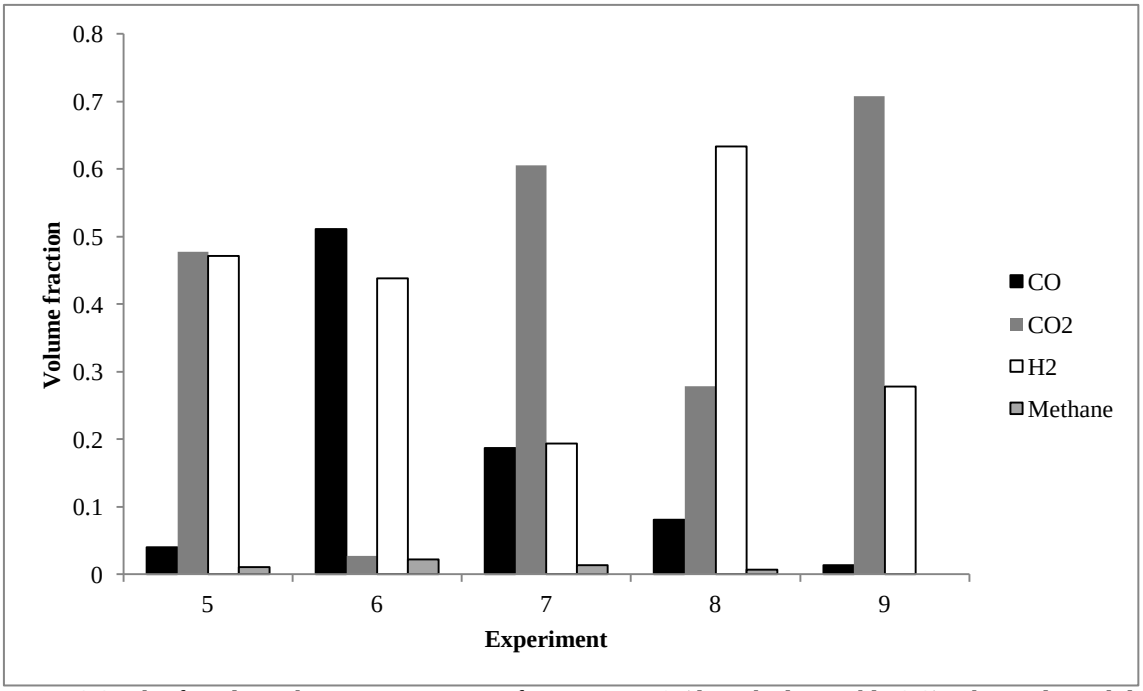

Figure 3.3. The found gasphase compositions of reactions 5-9 (described in Table 3.3). The analysis did not include water.

We also detected small amounts of methane in the gas phase. The levels never exceeded 2.3 % of the gas phase compounds by volume, however, because the pressure is relatively high there is considerable dilution, and the actual number of methane molecules formed are significant. In figure 3.4 the liquid product formation and methane formation are shown.

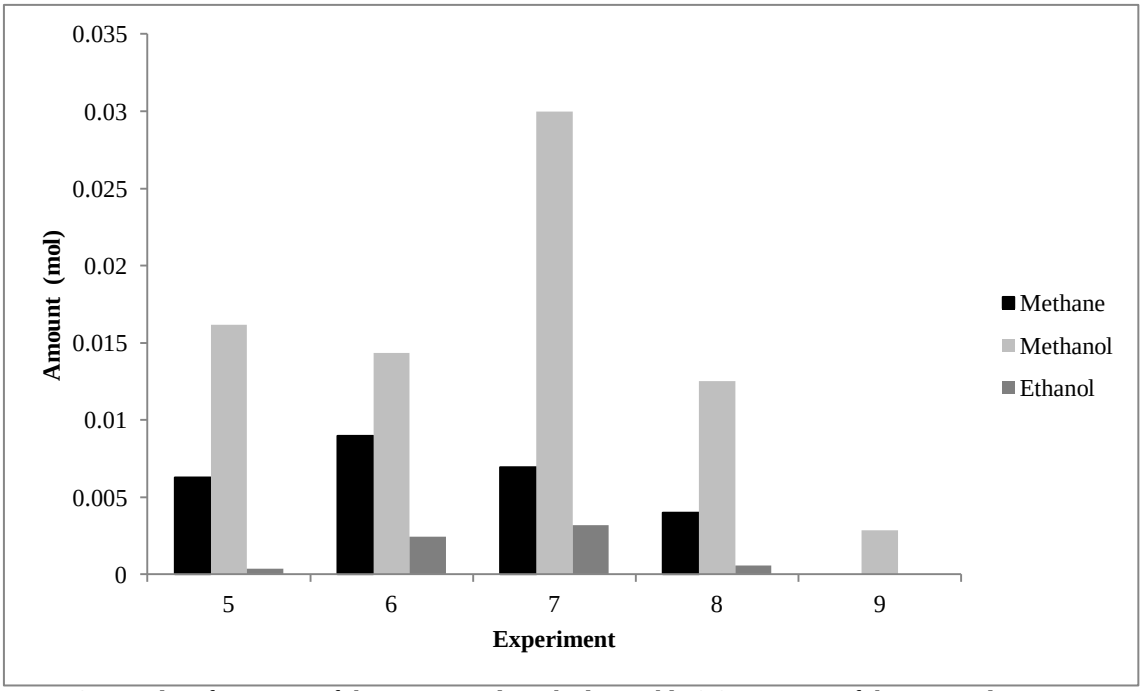

Figure 3.4 product formation of the reactions described in Table 3.3. Because of the gas analysis we were able to calculate and add the methane production.

The amount of methane that is formed is considerable compared to the methanol, between 21 and 53% of the methanol formation. This is comparable to the amounts reported by Ono in his system.[73] Formation of methane is counterproductive, especially if first methanol has to be formed in order to make it.

Further notable is the fact that in almost all reactions methanol is formed in significant quantities, except for reaction 9, where the starting conditions were set-up to deliberately drive the reaction conditions away from CO. Excitingly, in reaction 5 the only gases present are CO_2 and H_2 and methanol is the major product. Thus this system proofs to be relevant for the conversion of CO_2 and H_2 to methanol.

To further the insight into the speed at which the gaseous product are formed, we performed a repetition of reaction 7 and sampled the gas phase regularly. This is a batch reaction where instead of H_2 and CO we added only water and CO. The starting point is far from the equilibrium position of the WGS reaction, but nonetheless the gas phase composition went to near equilibrium in the course of 1 h. The results are shown below in figure 3.5.

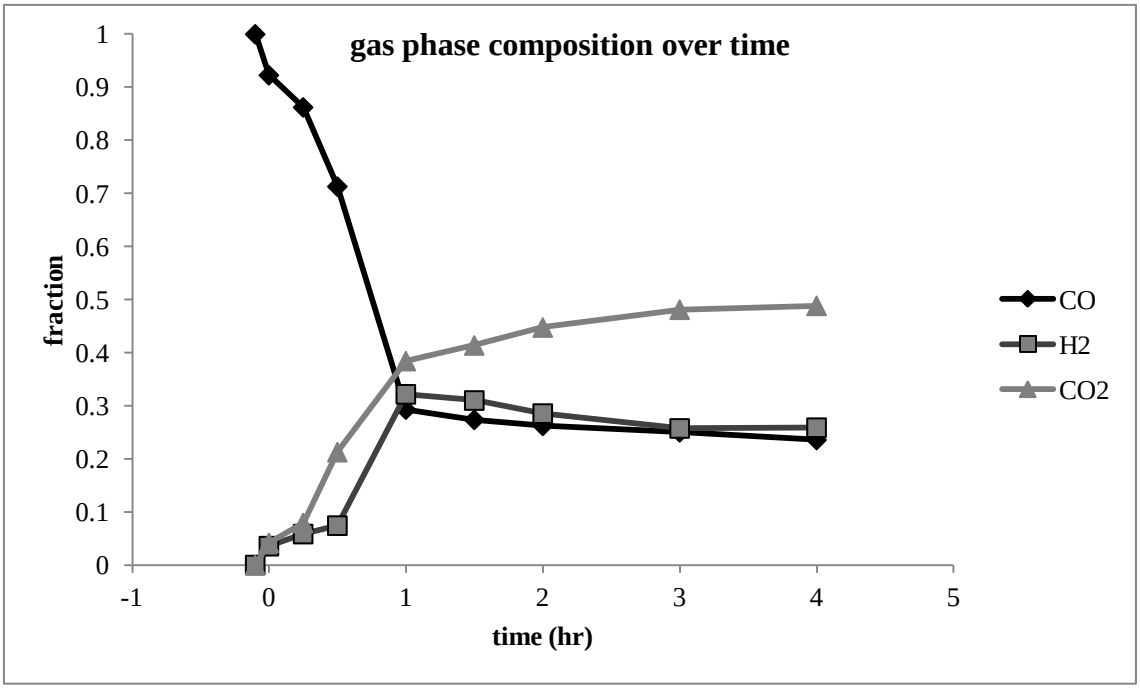

Figure 3.5 the gas phase composition throughout the course of one reaction. The conditions are described in Table 3.3. This was a repeat of reaction 15, starting with only water and 126 bar of CO. The WGS reactions start taking place during the heat-up, and reaches equilibrium in 1 hr after starting reaching 200 ^{o}C.

Figure 3.5 clearly shows that the system is a good WGS catalyst. The WGS reaction starts before the reactor is at temperature (the sample at -10 minutes was taken at around 150 ^{o}C). Within 1 hour after the reactor reaches 200 ^{o}C the WGSR conversion is complete. Interestingly, the gas phase composition at 1 hr reaction time is close to what was predicted in figure 3.4 (right) based on the WGS equilibrium. After this time, any changes seem to be due to the formation of products. A literature search shows that Wasserscheid has developed a very effective WGS catalyst using very similar species as can be found in our system, namely the dimer $[Ru_2Cl_4(CO)_6]$.[90] Our conclusion is that the WGS reaction occurs very fast compared to the methanol and ethanol production.

Additional to CO, H_2 and CO_2 we also detected formation of small levels of methane during the reaction. The levels of methane over time are shown in Figure 3.6.

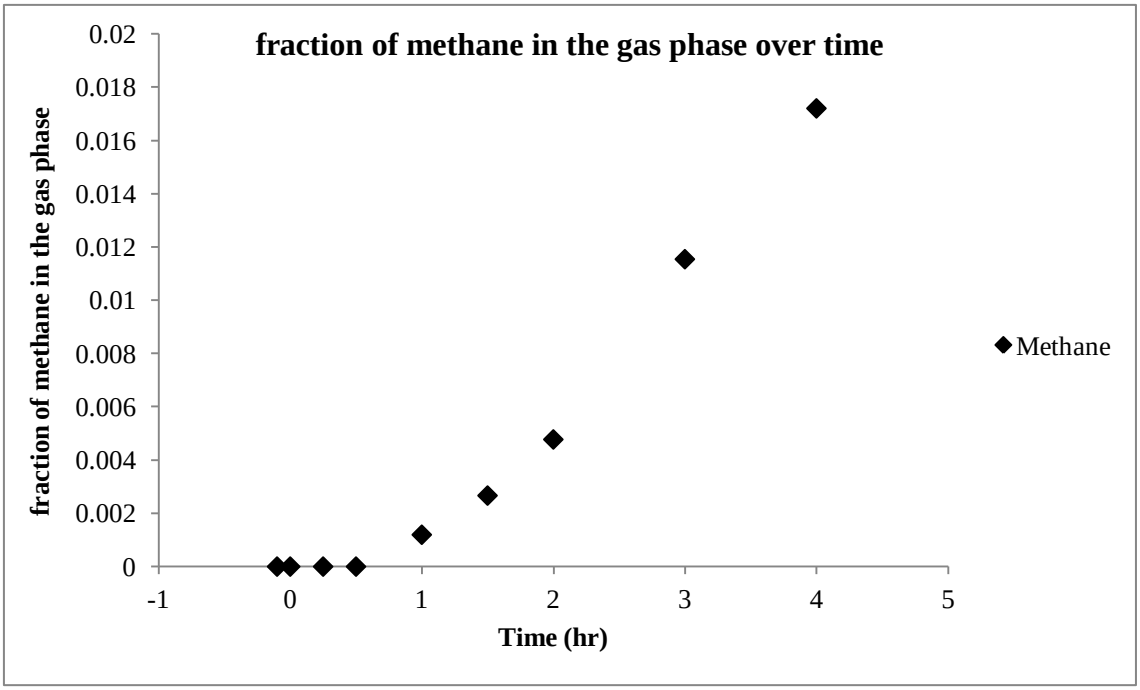

Figure 3.6 the fraction of methane in the gas phase over time. The peak level corresponds to approximately 1.8 % (v/v) methane in the gas phase. The total pressure at 50 ^{o}C was 125 bar, which is 10 bar lower than after experiment 15, because of the sampling.

Because there was continuous sampling the end pressure was quite low and it makes it difficult to estimate the number of moles of methane that were generated, but it should be close to the value presented in figure 3.4. The fraction of methane in the gas phase is undetectable in the first hour of the reaction but it then increases almost exponentially with time. One of the questions that remains is how the methane is produced in our system. Bradley[5] suggested that the formation of alkanes is the result of decomposition of the catalyst resulting in F-T chemistry, however, Ono[73] and Warren[72] had reported that the methane is formed from free methanol. To confirm this for the melt catalysis we conducted our own labelling experiment using ^{13}C-labelled methanol.

3.4 The origin of methane

For the labelling studies three experiments were performed. Two reactions with added ^{13}C-methanol, using either [PBu_4]Br or [PBu_4]Cl, and one reaction without added methanol (for reference of the MS signal). This is similar to the previous labelling studies that were performed. However, this time we performed analysis on gas phase components. Because, in the setup, the CO and methane peak co-elute; there are no pure peaks for them, however using the MS signals we can still detect the fragments (and

labelled fragments) of each individual product. The normalised MS signals were plotted side by side to compare the signal of the fragments arising from the presence of methane in figure 3.7:

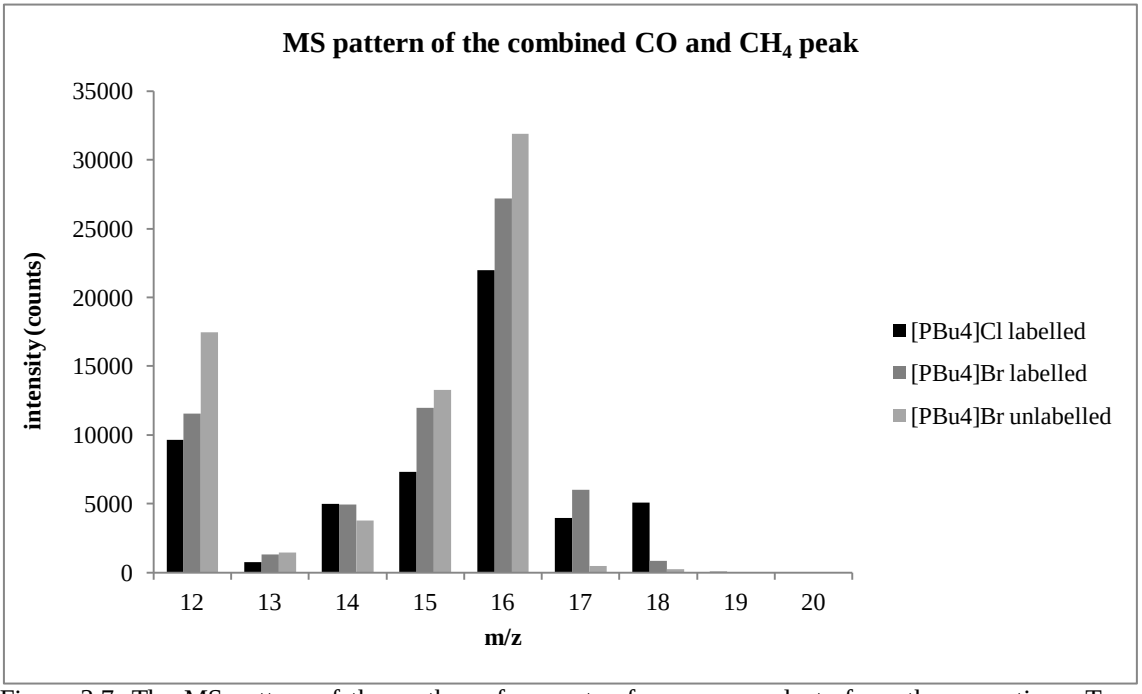

Figure 3.7. The MS pattern of the methane fragments of gaseous products from three reactions. Two reactions with $[PBu_4]Cl$ and $[PBu_4]Br$, with 0.5 mL of added ^{13}C-methanol at the start of the reaction and one reaction without added methanol.

The pattern clearly shows that at m/z =17 there is clear difference between the labelled and unlabelled experiments. The fragment with m/z 16 arises from CH_4^+, the fragment at m/z = 17 is the same fragment but for ^{13}C-labelled CH_4^+. This shows that indeed the labelled methanol is incorporated into methane. Comparison of the intensity between fragment 16 and 17 indicates that 15.3 % of the methane is labelled in the reaction using $[PBu_4]Cl$ and 18.1 % of the methane is labelled in the reaction using $[PBu_4]Br$, while the control without labelled methanol shows only 1.5 % labelling. Notably, in a duplicate of the labelling experiment described in chapter 2 it shows that methanol is labelled up to 15 % after the reaction (see table 2.5). This could suggest that the bulk of methanol that is formed, is formed very late during the reaction, further evidence of this can be seen in the shape of the methane evolution profile in figure 3.6, which is exponential. Alternatively, additional methane formation could occur via an unkown secondary pathway directly from CO or another carbon source. A less likely alternative is the suggestion that the methane and methanol carbons are rapidly

interchangeable. The CO peak in this sample shows no isotopic enrichment at the CO-carbon. This suggests that the reverse reaction of methanol to CO does not occur under these conditions.

3.5 Experimental

This experimental concerns reactions used in chapter 3. The experimental sections are grouped by the type of reactions that was performed and their respective experimental procedures are described separately. The same general notes concerning equipment and general procedures apply to this section as described in the experimental section of chapter 2.

Reactions 1-4 the neat effect of pressure

Exp. 1

The clean and dry autoclave was assembled and $[PBu_4]Br$ (14.5024 g, 42.736 mmol), $[Ru_3(CO)_{12}]$ (0.4991 g, 2.334 mmol Ru) and $[HPBu_3]Br$ (0.4144 g, 1.469 mmol) were added to the autoclave. The autoclave was sealed and purged 6 times using CO/H_2 (1:1). The system was pressured to 170 bar of CO/H_2 (1:1). The system was tested for leaks: no leaks were found. The system was left under pressure overnight. The following morning the heater and stirrer were switched on. When the temperature reached 200 ^oC the time was noted and the pressure adjusted to 250 bar. Then the picolog datapoint was noted and the Mass Flow Controller (MFC) datalogger was started. After 4 hours the heater was switched off, the stirring was reduced and the taps were closed. The picolog datapoin was noted and the MFC datalogging switched off. During the reaction the pressure was kept constant at 250 bar via the MFC and pressure controller. Gas feed (CO/H_2, 1:1) was from the ballast vessel fitted with a pressure transducer. The picolog recorded the pressure of the ballast vessel every 10 seconds. When the temperature was below 30 ^oC the autoclave was vented. After venting, the autoclave was opened and inspected. The product mixture was a red liquid which was analysed by IR and ^1H NMR spectroscopy and a small sample was stored. The remainder of the liquid was transferred to a flask and stripped of volatiles by vacuum distillation using temperatures up to 250 ^oC and a liquid N_2 cold trap. The volatiles that were collected were diluted using acetonitrile/NMP stock solution (5 mL of 2% (v/v)) and analysed using GC. The total product amounts were calculated using the NMP and acetonitrile peaks as internal references. Table 3.5 contains the found product yields for all reactions. The autoclave was then cleaned and dried for future use.

Exp. 2

The clean and dry autoclave was assembled and [PBu_4]Br (14.5031 g, 42.738 mmol), [$Ru_3(CO)_{12}$] (0.4996 g, 2.336 mmol Ru) and [$HPBu_3$]Br (0.4146 g, 1.470 mmol) were added to the autoclave. The system was sealed and then purged using CO/H_2 (1:1) 6 times and then charged to 93 bar of pressure and left overnight. The following morning the system was checked for leaks and the heater and stirrer were switched on. When the temperature had reached 200 ^oC the pressure inside the autoclave was reduced to 140 bar. CO_2 was added until the pressure was 240 bar. Further CO/H_2 (1:1) was added again until the pressure was 250 bar. The remainder of the experiment was performed as in exp 1.

Exp 3

The clean and dry autoclave was assembled and [PBu_4]Br (14.5020 g, 42.735 mmol), [$Ru_3(CO)_{12}$] (0.4999 g, 2.337 mmol Ru) and [$HPBu_3$]Br (0.4147 g, 1.470 mmol) were added to the autoclave. The system was sealed, purged using CO/H_2 (1:1) 6 times and then charged to 140 bar of pressure, checked for leaks and left overnight. The following morning no pressure drop was observed. The heater and the stirrer were switched on. When the temperature reached 199 ^oC pressure was removed until the autoclave contained 50 bar of CO/H_2 (1:1). Next N_2 was added until the pressure was 150 bar, followed by the addition of CO/H_2 (1:1) until the pressure was 250 bar. The temperature was 200 ^oC, the stirrer was switched to setting 9 and the time was noted. The remainder of the reaction was as exp 1.

Exp 4

The clean and dry autoclave was assembled and [PBu_4]Br (14.5020 g, 42.738 mmol), [$Ru_3(CO)_{12}$] (0.4999 g, 2.336 mmol Ru) and [$HPBu_3$]Br (0.4147 g, 1.471 mmol) were added to the autoclave. The system was sealed and then purged using CO/H_2 (1:1) 6 times and then charged to 150 bar of pressure, checked for leaks and left overnight. The following morning there was no pressure drop, and the heater and stirrer were switched on. When the temperature reached 199 ^oC pressure was removed until the

autoclave contained 150 bar of CO/H_2 (1:1). The remainder of the reaction was as exp 1.

Experiments 5-9 and 18: Experiments to test for the WGS activity of the system

Exp 5:

The clean and dry autoclave was assembled and $[PBu_4]Br$ (14.5017 g, 42.734 mmol), $[Ru_3(CO)_{12}]$ (0.4995 g, 2.335 mmol Ru) and $[HPBu_3]Br$ (0.4149 g, 1.471 mmol) were added to the autoclave. The autoclave was sealed and purged 3 times using CO/H_2 (1:2). Next the system was purged with H_2 4 times to ensure complete removal of air. The system was then pressured to 120 bar of H_2. The autoclave was warmed to 50 ^oC. The pressure was adjusted to 126 bar of H_2 before adding CO_2 until the pressure was 189 bar. The system was closed and tested for leaks: no leaks were found. The heater was switched off and the system was left under pressure overnight. The following day the setup was tested for leaks once more: no leaks were found. The heater and stirrer were switched on. When the temperature was 200 ^oC the time was noted and the reaction was allowed to proceed for 4 hours after which cool-down began. When the temperature reached 50 ^oC the pressure was recorded to be 155 bar. When the temperature was below 30 ^oC the autoclave was vented and a gas sample was taken to be analysed by GC the results of all gas sample analyses are displayed in figure 3.4 and 3.5. After venting, the autoclave was opened and inspected. The product mixture was a red liquid which was analysed by IR and ^1H NMR spectroscopy and a small sample was stored. The remainder of the liquid was transferred to a flask and stripped of volatiles by vacuum distillation using temperatures up to 250 ^oC and a liquid N_2 cold trap. The volatiles that were collected were diluted using acetonitrile/NMP stock solution (5 mL of 2% (v/v)) and analysed using GC. The total product amounts were calculated using the NMP and acetonitrile peaks as internal references. Table 3.5 contains the found product yields for all reactions. The autoclave was then cleaned and dried for future use.

Exp. 6

The clean and dry autoclave was assembled and $[PBu_4]Br$ (14.5028 g, 42.737 mmol), $[Ru_3(CO)_{12}]$ (0.4994 g, 2.335 mmol Ru) and $[HPBu_3]Br$ (0.4150 g, 1.471 mmol)

were added to the autoclave. The autoclave was sealed and purged 3 times using CO/H_2 (1:2). Next the system was purged with CO 4 times to ensure complete removal of air. The system was then pressured to with CO (33 bar). The autoclave was warmed to 50 ^oC. Next the pressure was adjusted to 32 bar of CO before adding CO/H_2 (1:2) until the pressure was 126 bar. The system was closed and tested for leaks: no leaks were found. The heater was switched off and the system was left under pressure overnight. The remainder of the procedure was as for exp. 5, except that the pressure after cool-down to 50 ^oC read 105 bar. The product mixture was a red moist paste.

Exp. 7

The clean and dry autoclave was assembled and $[PBu_4]Br$ (14.5017 g, 42.734 mmol), $[Ru_3(CO)_{12}]$ (0.5000 g, 2.338 mmol Ru) and $[HPBu_3]Br$ (0.4151 g, 1.471 mmol) were added to the autoclave. The autoclave was sealed and purged 3 times using CO/H_2 (1:2). 4.3 mL of water was added through a syringe under a positive CO/H_2 flow. Next the system was purged with CO 4 times. The autoclave was warmed to 50 ^oC and the pressure was adjusted to 126 bar of CO. The system was closed and tested for leaks: no leaks were found. The heater was switched off and the system was left under pressure overnight. The remainder of the procedure was as for exp 5, except that the pressure after cool-down to 50 ^oC read 135 bar. The product mixture was a red liquid containing a slush.

Exp. 8

The clean and dry autoclave was assembled and $[PBu_4]Br$ (14.5018 g, 42.734 mmol), $[Ru_3(CO)_{12}]$ (0.5000 g, 2.338 mmol Ru) and $[HPBu_3]Br$ (0.4154 g, 1.472 mmol) and water (4.3 mL) were added to the autoclave. The autoclave was sealed and purged 3 times using CO/H_2 (1:2). Next the system was purged with CO 4 times. The autoclave was warmed to 50 ^oC, the pressure was adjusted to 32 bar of CO before adding CO/H_2 (1:2) until the pressure was 126 bar. The system was closed and tested for leaks: no leaks were found. The heater was switched off and the system was left under pressure overnight. The remainder of the procedure was as for exp. 5, except that the pressure after cool-down to 50 ^oC read 148 bar. The product mixture was a red liquid.

Exp 9

The clean and dry autoclave was assembled and [PBu_4]Br (14.5028 g, 42.737 mmol), [$Ru_3(CO)_{12}$] (0.4994 g, 2.335 mmol Ru) and [$HPBu_3$]Br (0.4161 g, 1.475 mmol) and water (4.3 mL) were added to the autoclave. The autoclave was sealed and purged 7 times using H_2. Next the system was pressured to 80 bar and checked for leaks: no leaks. It was left under pressure overnight. The following morning I warmed the autoclave was warmed to 50 ^oC and the pressure reduced to 63 bar. CO_2 was added until the pressure read 126 bar. After a leak check, the reaction was started. The remainder of the procedure was as for exp 5, except that the pressure after cool-down to 50 ^oC read 138 bar. The product mixture was a light red liquid.

Exp 18 (WGS reaction, with regular sampling)

This reaction was a repeat of exp 7, however with gas sampling at regular intervals

The clean and dry autoclave was assembled and [PBu_4]Br (14.5025 g, 42.736 mmol), [$Ru_3(CO)_{12}$] (0.4997 g, 2.336 mmol Ru), [$HPBu_3$]Br (0.4149 g, 1.471 mmol) and water (4.3 mL) were added to the autoclave. The autoclave was sealed and purged 7 times using CO. Next the system was pressured to 130 bar and checked for leaks: a small leak was found, which was fixed; after that no leaks were discovered and the system was left under pressure overnight. The following morning the autoclave was warmed to 50 ^oC and checked for leaks, none were found. The pressure was reduced to 126 bar. The heater and stirrer were switched on. During heat-up a sample of gas was taken, the temperature was approximately 150 ^oC. Then when the temperature reached 200 ^oC the time was noted and another gas sample was taken. Gas samples were taken at 15, 30, 60, 90, 120, 180 and 240 minutes after the start of the reaction. After 4 hours the heater was switched off and the reactor was cooled to 30 ^oC. When the temperature was 50 ^oC the pressure was measured: 125 bar. The remainder of the procedure was as for exp 5. The product mixture was a red liquid slush.

Exp 23-25, Labelling experiments to establish the source for methane

These labelling studies were performed in the same way as the labelling studies described in chapter 2, particularly like reaction jhb107. However, at the end of the reaction a sample of the gas was collected in a gas syringe and this was injected into the GC-MS machine with the same column, at 40 ^{o}C. The materials used are described in table 3.4. The liquid product yield is given in table 3.5.

Table 3.4. The used materials for the reactions used in this chapter.Conditions: 200 ^{o}C, syngas (250 bar 1:2 CO: H_2), 4 hrs

	$[PBu_4]X$	mass $[PBu_4]Br$			amount of promoter		mass $[Ru_3(CO)_{12}]$		
Exp.	X=	grams	mmol	Promoter	grams/mL	mmol	grams	mmol Ru	Promoter/Ru
1	Br	14.5024	42.7377	$[HPBu_3]Br$	0.414	1.4631	0.4991	2.342	0.625
2	Br	14.5031	42.7398	$[HPBu_3]Br$	0.415	1.4638	0.4996	2.344	0.624
3	Br	14.5020	42.7366	$[HPBu_3]Br$	0.415	1.4642	0.4999	2.346	0.624
4	Br	14.5030	42.7395	$[HPBu_3]Br$	0.415	1.4656	0.4996	2.344	0.625
5	Br	14.5017	42.7357	$[HPBu_3]Br$	0.415	1.4649	0.4995	2.344	0.625
6	Br	14.5028	42.7389	$[HPBu_3]Br$	0.415	1.4652	0.4994	2.343	0.625
7	Br	14.5017	42.7357	$[HPBu_3]Br$	0.415	1.4656	0.5	2.346	0.625
8	Br	14.5018	42.7360	$[HPBu_3]Br$	0.415	1.4667	0.5	2.346	0.625
9	Br	14.5028	42.7389	$[HPBu_3]Br$	0.416	1.4691	0.4994	2.343	0.627
18	Br	14.5025	42.736	$[HPBu_3]Br$	0.415	1.471	0.4997	2.336	0.630
23	Cl	13.0353	44.2049	-	-	-	0.1247	0.585	-
24	Br	14.7011	43.3233	HBr 48% aq	0.099	0.8810	0.25	1.173	0.751
25	Br	14.7018	43.3254	HBr 48% aq	0.099	0.8810	0.2499	1.173	0.751

Table 3.5. The recovered liquid products for the reactions used in this chapter.

Exp.	Methanol	Ethanol	Propanol	Butanol	EG	2-methoxy ethanol
1	35.3923	7.8242	0.3225	0.0194	2.3814	0.3394
2	25.4747	3.6116	0.0576	0.0109	0.7534	0.0282
3	11.0835	1.2597	0.0511	0.0115	0.5398	0.0391
4	12.1440	1.4782	0.0635	0.0128	0.8071	0.0539
5	16.1775	0.3659	0.0186	0.0458	0.0771	0.0152
6	14.3642	2.4581	0.0933	0.0289	0.8160	0.0700
7	29.9938	3.1717	0.0432	0.0269	0.4254	0.0343
8	12.5034	0.5846	-	0.0323	-	0.0105
9	2.8724	-	-	0.0018	0.1825	0.0089
18	24.7267	2.9603	-	0.0315	0.6369	0.0000
23	37.1224	10.3273	0.5857	0.2049	0.8094	1.0566
24	18.9564	13.4920	0.7531	0.1856	0.4849	0.2534
25	21.2241	12.3660	0.7127	0.1794	0.9973	0.3210

3.6 Conclusions

In this chapter, some aspects of the gas phase behaviour in Knifton's melt system were examined. Firstly, the effect of neat pressure was examined. Unlike Dombek's findings, we could not find a net effect of pressure. Increasing the pressure by addition of N_2 did not increase the rate of catalysis. Strangely, addition of CO_2 did lead to an increase of the rate of catalysis, although the reason for this remains uncertain. Following this, the activity of the system for the Water Gas Shift reaction was explored. The $[Ru_3(CO)_{12}]/[PBu_4]Br$ system is very active and reached equilibrium values within an hour, and the activity for WGS started at temperatures well below 200 ^oC. Literature suggests that this is mainly due to the presence of $[RuBr_3(CO)_3]^-$ or $[RuBr_2(CO)_3]_2$.[91] Because the system is active for the WGS reaction, and water is produced during catalysis, there will be a reduction of the partial pressure of CO other than through the production of methanol or ethanol. Furthermore, it leads to a relative increase in the partial pressure of H_2. In addition to syngas and CO_2, the generation of methane was detected. Subsequent labelling studies showed that free methanol is converted to methane and that at least a large fraction (>15% of the existing methane) must have come from methanol.

Chapter 4
The order in H_2 and CO on product formation and the development of a kinetic tool

4.1 Introduction

Our previous results show that, during the hydrogenation of CO in $[PBu_4]Br$ in the presence of ruthenium based catalyst precursors, we make higher alcohols and many other products *via* methanol. The direct conversion of methanol to ethanol is a particularly interesting reaction, since it is not a widely established reaction. Most of published work on methanol conversion focuses instead on the synthesis of acetic acid and this chemistry is well investigated and employed by industry. Using cobalt (BASF), rhodium (Monsanto[92], Acetica$^{(TM)}$, Eastman[80]) or iridium (Cativa(r)[93]) catalysts the processes follow essentially the same catalytic cycle, but with different conditions, metal centres or starting materials most competitors have avoided patent issues.[94] In the general scheme, methyl iodide, which is generated from a source of methanol and HI (or methyl acetate and iodide, Eastman), oxidatively adds to the catalyst, $[MI_2(CO)_2]^-$, to form the octahedral $[MI_3(CO)_2\mathbf{CH_3}]^-$ species which undergoes CO insertion followed by reductive elimination of the acyl iodide regenerating the catalyst. The acylhalide is then hydrolysed to form acetic acid and HI.[93, 95] Nearly all processes employ this overall cycle, using oxidative addition of MeI, CO insertion, followed by acyl iodide release. The source of MeI and metal centre can change between processes.

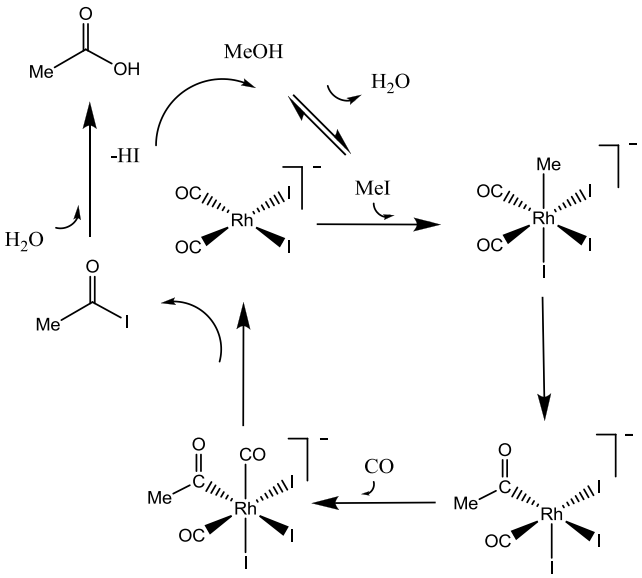

Scheme 4.1. The Monsanto Acetic acid synthesis.

The acetic acid processes are widely used and the product is employed amongst other things as a feedstock for the production of vinyl acetate based polymers. In contrast, the homologation of methanol to ethanol is commercially less successful.[2, 96] Some possibilities for making ethanol from syngas include direct methanol homologation[97-99], or one pot synthesis from syngas (e.g. HAS[100], Ru/I system[72, 74, 97]).[2, 101, 102]

From the labelling studies we know that it is likely for all homogeneous systems that the ethanol synthesis goes through intermediate formation of methanol and therefore looking at the homologation step is very interesting to our process. When we focus on homogeneous conversion of methanol the metals of choice are often cobalt[98, 103-105], ruthenium[72, 74] or rhodium[106]. Presumably, cobalt was used as a secondary catalyst in Knifton's work to effect ethanol formation from the methanol that was generated *in situ:* particularly, Knifton[75, 107] Vidal[99] and Bradley[97] and others[108, 109] employ ruthenium-cobalt chemistry with good results. The ethanol formation step may be the result of a tandem reaction where methanol is formed first and then converted by the cobalt component, or a truly bimetallic[105] catalysts may be present which is active for direct methanol homologation.[86, 103] Ono et al.[73, 74] and Warren et al.[72] are to our knowledge the only groups who published results where high selectivity towards ethanol is achieved using only ruthenium in the presence of a halide source. Nevertheless, these processes have not reached the stage for commercial application and

remain relatively underdeveloped, partly because it is easy to obtain ethanol from different routes. Both in ethanol and in acetic acid synthesis the common intermediate is presumed to be a metal-methyl species, which undergoes carbonyl insertion followed by either reductive elimination with halide or hydride to yield either product (scheme 4.2).

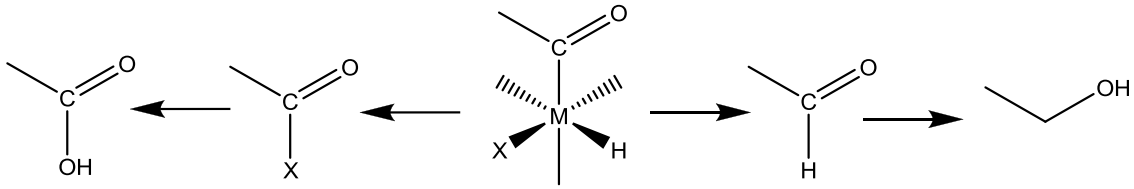

Scheme 4.2. The same intermediate could lead to either ethanol or acetic acid

Considering that both the acetic acid synthesis and ethanol synthesis systems employ high halide concentrations, similar conditions, and similar species it is still unknown what causes a catalyst to display selectivity to one product over the other. The fact that catalytic systems using ruthenium have a "natural" tendency towards ethanol is worthy of a separate investigation.[106] In chapter 2, it was demonstrated that the used system was reproducible and might be suitable for continuous flow experimentation and synthesis if an effective recycle system is developed for the catalyst. It was found that the primary synthesis in the $[Ru_3(CO)_{12}]$/$[PBu_4]Br$ system is the formation of methanol and from that, a variety of other compounds is made when using this $[Ru_3(CO)_{12}]$ catalyst. Especially the higher alcohols, ethanol and propanol, are of interest and in this system they are the most abundant next to methanol.

The major components of the products are methanol, ethanol, propanol and ethylene glycol. A good place to start the investigation into higher alcohol formation is by assessing reaction rates and product distributions. Scheme 2.3 in chapter 2 shows that a kinetic model can be made to assess reactivity. It would be useful to be able to measure the rates of each individual reaction and to see how they are affected by altering conditions. In the following section we try to derive a model for the reactions and furthermore we try to assess how the model functions compared to real data, how and if it can predict outcomes for reactions and if or when the model can be used as a tool to make data comparative.

The WGS reaction influences the partial pressures of CO and H_2. Therefore, the rate of reaction should be influenced accordingly. To estimate the order of the reaction

rate in p_{H2} and p_{CO} a theoretical framework needs to be developed and the rate of reaction should be determined at various pressures. In a series of experiments the starting pressures and gas phase composition were varied. We assumed a 1:2 feed of CO and H_2 would keep the p_{CO} and p_{H2} constant as this stoichiometry is needed for methanol synthesis. In the first set of experiments the CO partial pressure was held constant at 75 bar (at 50 ^oC) with increasing pressures of H_2 (25 bar, 50 bar, 75 bar and 100 bar). The same set was repeated, but now holding p_{H2} constant. Table 4.1 shows the list of experiments.

Table 4.1. A list of the conditions used for assessing the effect of p_{CO} and p_{H2}.

	Pressure at rt			Pressure under reaction conditions	
Experiment No.	p_{CO}[a]	p_{H2}[a]	Total pressure at 200 ^oC (bar)	p_{CO}[a]	p_{H2}[a]
10	75	25	150	112.5	37.5
11	75	50	177.2	106.3	70.9
12	75	75	217	108.5	108.5
13	75	100	262	112.3	149.7
14	25	75	150	37.5	112.5
15	50	75	183	73.2	109.8
16	100	75	262.4	149.9	112.5
17	75	50	188	112.8	75.2

[a]pressures in bar at room temperature. Conditions: $[Ru_3(CO)_{12}]$ (0.5 g), $[PBu_4]Br$ (14.5 g), $[HPBu_3]Br$ (0.4145 g), 200 ^oC, 4 hrs, 1:2 ($CO:H_2$) feed after assessing the pressure at 200 ^oC.

Because experiment 11 gave results that indicated that some error had occurred during the workup, catalysis or analysis we repeated that reaction in experiment 17. Because we cannot pinpoint the cause of error, we will take both reactions in consideration. Product yields are shown in figure 4.1.

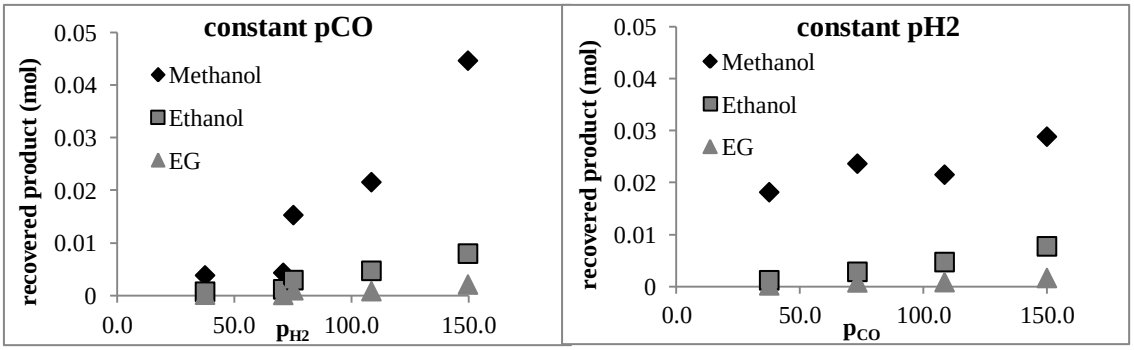

Figure 4.1. The product formation with varying H_2 (left) and CO (right) partial pressure. The balance pressure is around 112 bar at 200 °C. Conditions described in Table 4.1.

Both an increase in p_{H2} and in p_{CO} increases the rate of product formation, However, the increase in the H_2 partial pressure leads to a much greater increase in methanol production than the increase in p_{CO} does. Furthermore, it is observed that even though the methanol levels are much higher in the variable p_{H2} series this does not result in a higher ethanol production than in the variable p_{CO} series, they are more or less the same. This suggests that the rate of homologation benefits especially from a higher p_{CO}. To find the orders in H_2 and CO the rates of each reaction needs to be estimated. For this, the underlying theoretical framework needs to be developed first.

4.2 Rate expressions

In Chapter 2 it was found that the product formation occurs sequentially, there are two basic reactions taking place; A) methanol synthesis from syngas, B) methanol conversion to higher products. The events can be summarized in the following scheme (4.3):

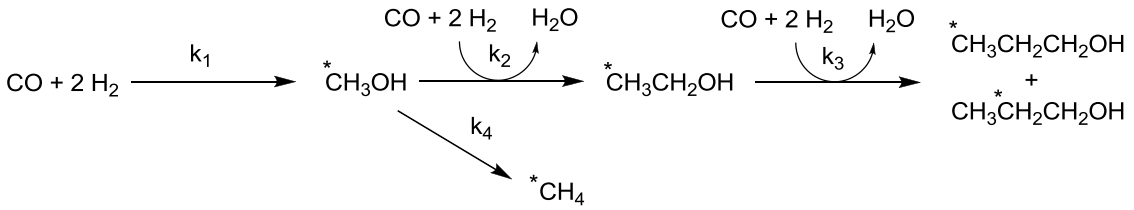

Scheme 4.3. Alcohol formation in the Ru/[PBu_4]Br system. The overall reaction scheme can be split up into three different reactions, each with their own rates and preferred conditions.

In addition to this, labelling studies have shown that from methanol methane is formed too. Moreover, from the alcohols ethers are formed in condensation reactions. Overall this leads to a very complicated system of reactions. For this reason we chose to simplify the description of the system in order to get to useful conclusions. To start, we

will ignore the ether formation reactions, because they the ethers are in equilibrium with the alcohols and we assume that they are affected equally. If this is the case, measuring the yield of the alcohols provides an accurate reflection of relative reaction rates, although the absolute reaction rates are underestimated. In general, the ether formation is also affected to some extent by the WGS reaction because of the generation of water, yet still the alcohols still reflect the relative conversions. Two cases will be discussed, in case one the kinetic expressions for the complete set of equations will be derived. In case two we will constrain ourselves to only the liquid products to come at a working model to predict the levels of liquid products at the end of a reaction and to estimates the relative rates of individual reactions.

4.2.1 Case one

The expressions to be solved simultaneously in scheme 4.3 are as follows:

$$\frac{\partial[MeOH]}{\partial t} = k_1\, p_{H_2}^m p_{CO}^n - (k_2 p_{H_2}^s p_{CO}^t + k_4 p_{H_2}^o p_{CO}^p)[MeOH] \quad \text{(eq. 4.1}$$

$$\frac{\partial[EtOH]}{\partial t} = k_2 p_{H_2}^o p_{CO}^p [MeOH] - k_3 p_{H_2}^q p_{CO}^r [EtOH] \quad \text{(eq. 4.2}$$

$$\frac{\partial[PrOH]}{\partial t} = k_3 p_{H_2}^q p_{CO}^r [EtOH] \quad \text{(eq. 4.3}$$

$$\frac{\partial[CH_4]}{\partial t} = k_4 p_{H_2}^s p_{CO}^t [MeOH] \quad \text{(eq. 4.4}$$

Where p_{H2} and p_{CO} are the partial pressures of H_2 and CO respectively, k_1, k_2, k_3 and k_4 are the rate constants for methanol, ethanol, propanol and methane formation reactions respectively, m, o, q, s are the orders in p_{H2} for the methanol, ethanol, propanol and methane formation reactions respectively, n, p, r and t are the orders in p_{CO} for the methanol, ethanol, propanol and methane formation reactions respectively. [MeOH], [EtOH], [PrOH] and [CH_4] are the levels of methanol, ethanol, propanol and methane at time t (hrs). In this analysis it is assumed that the homologation reactions are first order in the starting alcohol. If we assume that the partial pressures remain constant throughout the reaction the set can be simplified by replacing $k_x\, p_{H_2}^y p_{CO}^z$ by k_x'. This is an approximation that works quite well if the composition of the gas phase does not change significantly, this be addressed in a later section. The resulting equations follow:

$$\frac{\partial[MeOH]}{\partial t} = k_1' - [MeOH](k_2' + k_4') \quad \text{(eq. 4.5}$$

$$\frac{\partial[EtOH]}{\partial t} = k_2'[MeOH] - k_3'[EtOH] \quad \text{(eq. 4.6}$$

$$\frac{\partial[PrOH]}{\partial t} = k_3'[EtOH] \quad \text{(eq. 4.7}$$

$$\frac{\partial[CH_4]}{\partial t} = k_4'[MeOH] \quad \text{(eq. 4.8}$$

Now, all the rate constants k_x' contain within them the actual rate constant and the effect of the gas phase composition. Because of this, the simplified model is less accurate, but requires much less effort to solve it and, as will be shown later can be used to solve more accurately. The Mathematica software package can be used to solve this set of equations analytically, and the resulting expressions for methanol, ethanol, propanol and methane exist:

$$[\mathrm{MeOH}]_t = \frac{e^{-\left(k_2'+k_4'\right)t}\left(-k_1+e^{\left(k_2'+k_4'\right)t}k_1'+k_2'[\mathrm{MeOH}]_0+k_4'[\mathrm{MeOH}]_0\right)}{k_2'+k_4'} \quad \text{(eq. 4.9}$$

$$[\mathrm{EtOH}]_t = \frac{e^{-\left(k_2'+k_4'\right)t}k_2'\left(e^{\left(k_2'+k_4'\right)t}k_1'1(k_2'2-k_3'3+k_4'ch4)-e^{\left(k_2'-k_3'+k_4'\right)t}(k_2'+k_4')(k_1'-k_3'[\mathrm{MeOH}]_0)+k_3'(k_1'-(k_2'+k_4')[\mathrm{MeOH}]_0)\right)}{k_3'(k_2'+k_4')(k_2'-k_3'+k_4')}$$

(eq. 4.10

$$[\mathrm{PrOH}]_t = \frac{k_2'\left(\frac{e^{-k_3't}\left(k_2'+k_4'\right)\left(k_1'-k_3'[\mathrm{MeOH}]_0\right)}{k_3'}+\frac{\left(k_2'+k_4'\right)\left(-k_1'+k_3'[\mathrm{MeOH}]_0\right)}{k_3'}+\frac{k_3'\left(k_1'-\left(k_2'+k_4'\right)[\mathrm{MeOH}]_0\right)}{k_2'+k_4'}\right)}{(k_2'+k_4')(k_2'-k_3'+k_4')} +$$

$$\frac{k_2'\left(\frac{e^{-\left(k_2'+k_4'\right)t}k_3'\left(-k_1'+(k_2'+k_4')[\mathrm{MeOH}]_0\right)}{k_2'+k_4'}+k_1'(k_2'-k_3'+k_4')t\right)}{(k_2'+k_4')(k_2'-k_3'+k_4')} \quad \text{(eq. 4.11}$$

$$[\mathrm{CH_4}]_t = \frac{e^{-\left(k_2'+k_4'\right)t}k_4'\left((-1+e^{\left(k_2'+k_4'\right)t})(k_2'+k_4')[\mathrm{MeOH}]_0+k_1'\left(1+e^{(k_2'+k_4')t}(-1+k_2't+k_4't)\right)\right)}{(k_2'+k_4')^2} \quad \text{(eq. 4.12}$$

Where $[\mathrm{MeOH}]_o$ is the level of methanol at t=0. With the values of these compounds determined at the end of the reaction (at t=4) all the parameters, k_x' can be determined by solving the set of equations simultaneously. As a result, information is obtained about the relative rate of each reaction independent of the concentration of the reagents. For instance if the methanol formation is relatively slow, but the ethanol formation is not, then total product formation may be low, including that of ethanol. This may be misleading, as it is impaired by the relatively slow formation of methanol. By calculating the apparent rate constants, this problem is circumvented and it becomes

useful to determine the relative rate constants within a series of experiments as will be shown in the following chapter.

4.2.2 Case two

Since the determination of gaseous products is not always possible it was decided to develop a similar system, for the liquid products exclusively by excluding the formation of methane. Because this presents a severe limitation on how the model describes reality care must be take to fully understand the limitations of this framework, which will be discussed in a following section. The development of the simplified case two equations follows the same rules as equations 4.1-12:

$$\frac{\partial[MeOH]}{\partial t} = k_1\, p_{H_2}^{m} p_{CO}^{n} - k_2 p_{H_2}^{o} p_{CO}^{p}[MeOH] \qquad \text{(eq. 4.13}$$

$$\frac{\partial[EtOH]}{\partial t} = k_2 p_{H_2}^{o} p_{CO}^{p}[MeOH] - k_3 p_{H_2}^{q} p_{CO}^{r}[EtOH] \qquad \text{(eq. 4.14}$$

$$\frac{\partial[PrOH]}{\partial t} = k_3 p_{H_2}^{q} p_{CO}^{r}[EtOH] \qquad \text{(eq. 4.15}$$

Where the parameters and suffixes are the same as for equations 4.1-12. Replacing $k_{\mathrm{x}}\, p_{H_2}^{y} p_{CO}^{z}$ by k'_{x}.leads to equations 4.16-18

$$\frac{\partial[MeOH]}{\partial t} = k_1{}' - k_2{}'[MeOH] \qquad \text{(eq. 4.16}$$

$$\frac{\partial[EtOH]}{\partial t} = k_2{}'[MeOH] - k_3{}'[EtOH] \qquad \text{(eq. 4.17}$$

$$\frac{\partial[PrOH]}{\partial t} = k_3{}'[EtOH] \qquad \text{(eq. 4.18}$$

These equations can be solved to find the analytical solutions 4.19-21:

$$[\mathrm{MeOH}]_{\mathrm{t}} = \frac{e^{-\mathrm{k_2}'t}(-\mathrm{k_1}'+e^{\mathrm{k_2}'t}\mathrm{k_1}'+\mathrm{k_2}'[\mathrm{MeOH}]_0)}{\mathrm{k_2}'} \qquad \text{(eq. 4.19}$$

$$[\mathrm{EtOH}]_{\mathrm{t}} = \frac{\mathrm{k_1}'(\mathrm{k_2}'-e^{-\mathrm{k_3}'t}\mathrm{k_2}'+(-1+e^{-\mathrm{k_2}'t})\mathrm{k_3}')+(-e^{-\mathrm{k_2}'t}+e^{-\mathrm{k_3}'t})\mathrm{k_2}'\mathrm{k_3}'[\mathrm{MeOH}]_0}{(\mathrm{k_2}'-\mathrm{k_3}')\mathrm{k_3}'} \qquad \text{(eq. 4.20}$$

$$[\mathrm{PrOH}]_{\mathrm{t}} = \frac{\mathrm{k_2}'\mathrm{k_3}'(\mathrm{k_2}'-e^{-\mathrm{k_3}'t}\mathrm{k_2}'+(-1+e^{-\mathrm{k_2}'t})\mathrm{k_3}')[\mathrm{MeOH}]_0+\mathrm{k_1}'((1-e^{-\mathrm{k_2}'t})\mathrm{k_3}'^2-\mathrm{k_2}'\mathrm{k_3}'^2t+\mathrm{k_2}'^2(-1+e^{-\mathrm{k_3}'t}+\mathrm{k_3}'t))}{\mathrm{k_2}'(\mathrm{k_2}'-\mathrm{k_3}')\mathrm{k_3}'}$$

(eq. 4.21

Here too, solving for the rate constants can be done when the final liquid product levels have been determined from the GC analysis. The value of k'_1 is the number of

moles of methanol that have been produced per time unit. Since methane and all other major products except for EG have been formed from methanol this number is strictly dependent on the accuracy of the analysis. Furthermore, as in case two the methane formation is neglected, the numbers of k_1' in case two are artificially low, while the values for k_2' should be equal. In some series the effect of adding incremental amounts of promoters or inhibitors is investigated. In this case, the catalyst composition may change, or single reactions may be promoted over other reactions. For instance, if throughout the series the total amount of liquid product continuously declines yet the uptake remains constant, this is a good indication that the promoter selectively promotes the methane synthesis over ethanol synthesis. Therefore, it is necessary to carefully inspect the conditions for which the model is applied before any conclusions can be used. Because the routes to product formation have been established this model will give the relative rates of each reaction, as long as the mechanism itself does not change between reactions. Equally important is to inspect product mixture for independently promoted or inhibited side reactions, giving rise to skewed methanol conversions. Because the reactions described in Table 4.1 all use the same conditions (e.g. catalyst, promoter, temperature, solvent) it is fair to assume that the only cause for changes in activity is because of the changes in partial pressure of the CO and H_2. Additionally, as the WGS shift reaction is important in this system, it is important to validate the assumption that the WGS reaction does not *significantly* influence the total activity of the system. Experiment 6 in chapter 3 shows this. The starting compositions of reactions 10-17 are close to the composition of 6, and the result show that the gas phase composition changes, but not enough (figure 3.3) to significantly skew the rates of the reaction. Furthermore, to determine the order in CO and H_2 what matters is the rate of change in the rate constants with varying pressure. Since all of the measurements are subjected to the same procedure, any bias in our measurements, (for instance using case one or case two) will carry forward, and should not change the slope of the reaction rates but rather the absolute values. In the following section the orders in H_2 and CO will be determined through this method.

4.3 The orders in p_{CO} and p_{H2}

The substitution expression for the conversion from equations 4.13-15 to 4.16-18, namely 4.22 can be used.

$$k_x \, p_{H_2}^{y} p_{CO}^{z} = \; k'_x \qquad \text{(eq. 4.22}$$

A direct relationship between the found and determined rate constant k'_x and the orders in H_2 and CO is found by rewriting 4.22 as follows:

$$Log \; k'_1 = Log \; k_1 + m \; Log \; p_{H_2} + \; n \; Log \; p_{CO} \qquad \text{(eq. 4.23}$$

For the variable p_{H2} series and p_{CO} series respectively this leads to eqs. 4.24 and 4.25:

$$Log \; k'_1 = m \; Log p_{H_2} + \; C_1 \qquad \text{(eq. 4.24}$$

$$Log \; k'_1 = n \; Log \; p_{CO} + C_2 \qquad \text{(eq. 4.25}$$

Where $C_1 = \; n \; Log \; p_{CO} + Log \; k_1$. And $C_2 = \; m \; Log \; p_{H_2} + Log \; k_1$ and these should be constant throughout the series of experiments. Equations 4.24 and 4.25 represent straight lines in a plot of Log $p_{CO/H2}$ against Log k'_1, Where m and n are the orders in H_2 and CO respectively. Similarly, the same equations can be used to estimate the orders for the methanol homologation reaction, for which the rate constant is k_2 or k'_2. In figures 4.2 the rate constants for each individual reaction (methanol formation (k'_1) or methanol homologation (k'_2) are plotted against the partial pressure of CO of H_2.

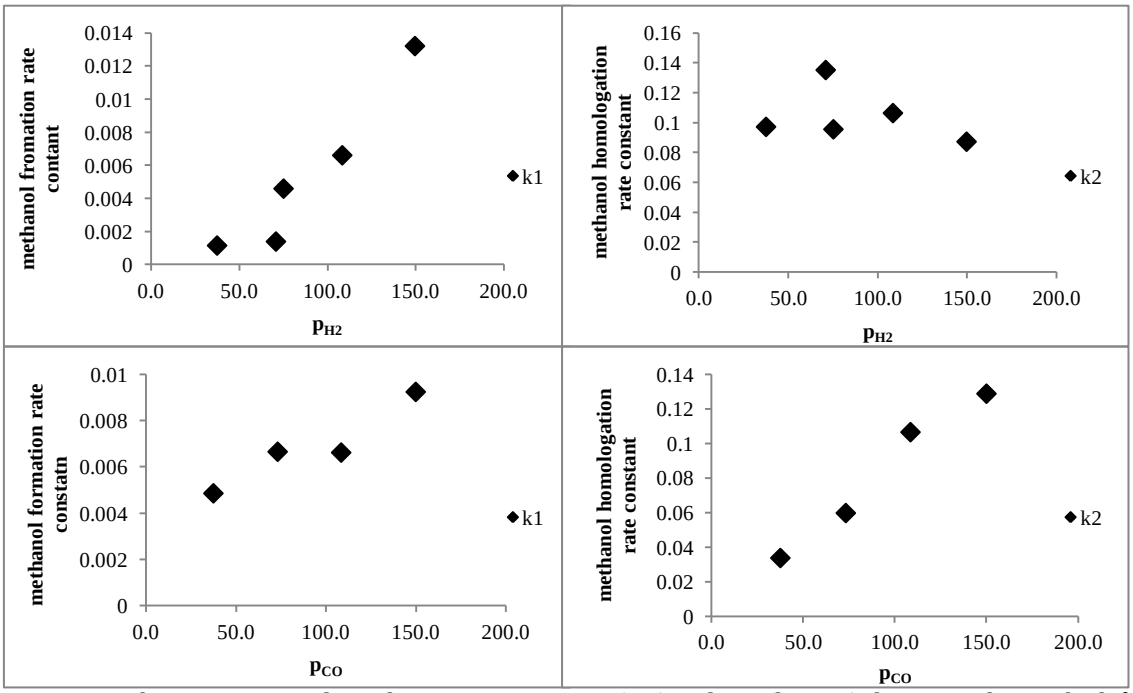

Figure 4.2. The rate constant dependency on varying p_{H2} (top) and p_{CO} (bottom) during catalysis. The left hand figures display the methanol formation and the right hand figures show the methanol homologation rate constants.

The rates show well that increasing the hydrogen partial pressure leads to a higher rate of methanol formation, but it does not lead to improved methanol homologation. They also show that increasing the CO partial pressure leads to both higher methanol formation and methanol homologation. The effect on methanol formation is more profound when increasing the hydrogen partial pressure than when increasing the CO partial pressure. However, the methanol homologation benefits greatly by increasing the CO partial pressure. Effectively this means that for a methanol formation reaction we would try to achieve very high H_2 partial pressures, but for methanol homologation reactions we would try to achieve very high CO partial pressures. The orders in p_{H2} and p_{CO} for the methanol formation can be found by fitting a regression line through the slopes of the Log (p_{H2}) vs. Log k_1' and the Log (p_{CO}) vs. Log k_1' plots (Figures 4.3).

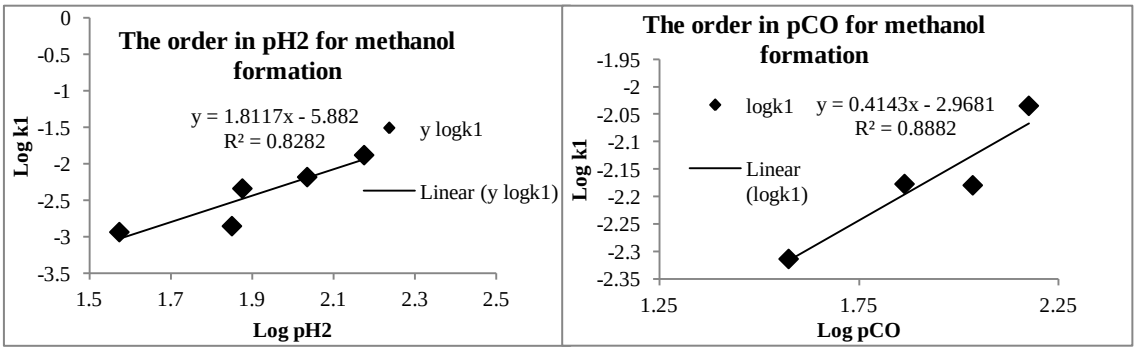

Figure 4.3 A Log-Log plot of the rate of formation of methanol against the partial pressure of H_2 (left) or p_{CO} (right). The slope of the fitted line indicates the order of the reaction with respect to p_{H2} or p_{CO} (right).

We find that for methanol formation the order in H_2 is 1.8 (the R^2 on the fitted line is 0.83, leaving out the outlying data point leads to an order of 1.7 with $R^2 = 0.98$). Likewise, the order in p_{CO} is 0.4 ($R^2 = 0.88$). This results in a refined kinetic expression for the forward reaction in the methanol formation:

$$\frac{\partial[MeOH]}{\partial t} = k_1 \, p_{H_2}^{1.8} p_{CO}^{0.4} \qquad \text{(eq. 4.26}$$

Furthermore, the Log-Log plots could be used to establish the value for k_1 (not k_1'). The place where both plots intersect with the Log k_1-axis determines the values of C_1 and C_2 in eq.3.24 and 3.25. Where $C_1 = n \, Log \, p_{CO} + Log \, k_1$ and

$C_2 = m \, Log \, p_{H_2} + Log \, k_1$. And all except for Log k_1 seem to be known, and thus the value could be calculated. However, to do this would lead to data that could provide false conclusions. The absolute height of the data in figure 4.3 is determined by the rates as calculated by case 2 equations, which do not take into account the methane formation and as such the value of k_1' is too low. Because of this, the absolute values are incorrect. Thus, the absolute height of the graph is incorrect, even though the slope remains valid. For this reason the orders in p_{CO} and p_{H2} are a good estimate, but extrapolation of the graph to the y-axis would lead to incomplete data. The methanol formation rate is after all much faster than calculated using case 2 methodology.

However, as long as this is known and considered, it is still possible to use case two methodology to obtain useful information. For instance, if we are only interested in finding out how much *liquid* product we will find at the end of a reaction, case two

could be used without considering the total gas consumption. For this reason we have still calculated the values for later use and validation of the accuracy of the model.

Because we have two lines it is possible to obtain two values for k_1, they should both be the same. For the line where the p_{H2} was varied the following is obtained:

$$C_1 = n\ Log\ p_{CO} + Log\ k_1\ .$$

Filling in the known values produces:

$$-5.882 = 0.4143\ Log\ 110.5 + Log\ k_1$$

which results in $k_1 = 1.87 \times 10^{-7}$.

The other constant, from the variable p_{CO} measurements leads to:

$$C_2 = m\ Log\ p_{H_2} + Log\ k_1$$

which becomes:

$$-2.9681 = 1.8117\ Log\ 110.8 + Log\ k_1$$

and this results in $k_1 = 2.13 \times 10^{-7}$, these two values for k_1 are very close to each other.

4.4 The order with respect to homologation

For the homologation reaction the substitution is also straightforward. Even though the rate equation contains a term for methanol, k_2' can still be replaced by $k_2\ p_{H_2}^x p_{CO}^y$, because the model tries to find a rate constant k_2' that is independent of the levels of methanol present. To clarify: the general rate equation looks like eq. 3.5: $\frac{\partial[EtOH]}{\partial t} = k_2'[MeOH] - k_3'[EtOH]$. The model finds a k_2' which should be equal to $k_2\ p_{H_2}^x p_{CO}^y$. This leads to $k_2' = k_2\ p_{H_2}^x p_{CO}^y$ and we can generate a Log-Log plot for the two series, figure 4.4

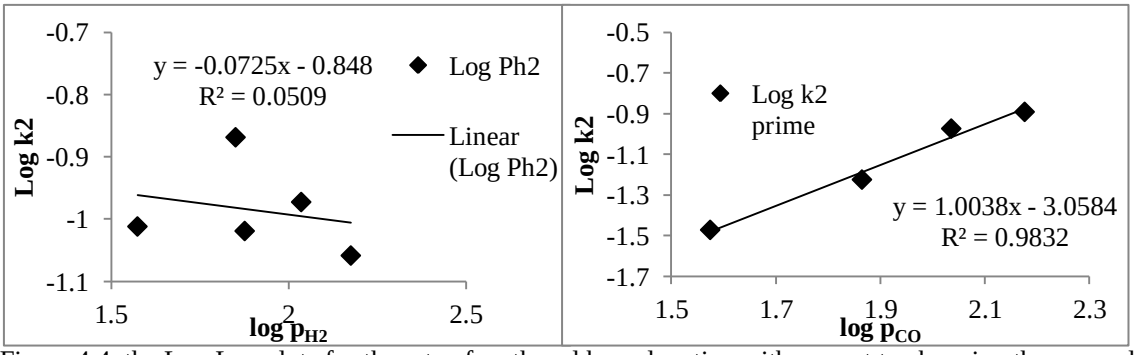

Figure 4.4. the Log-Log plots for the rate of methanol homologation with respect to changing the p_{H2} and p_{CO}.

Interestingly, the plot for the order in H_2 shows almost no correlation. The R^2 is very close to zero and the formal value that was found for the order in p_{H2} in H_2 is -0.0725. Thus, in the pressure range of between P_{H2} = 37.5 and P_{H2} 150 bar, varying hydrogen pressure does not play a role in the rate of methanol homologation. For CO we can see a correlation and the order in P_{CO} is positive and near unity, 1.0038. This means that the higher the CO pressure, the faster the homologation step will proceed. Because there is almost no correlation between the rate in homologation and the pressure of H_2, determining the value of k_2 should not be done using the variable P_{H2} data, because it is meaningless. Therefore, we can only calculate the data using the variable CO pressure data. Because the R^2 is quite good, we expect this to lead to a good estimate. Doing this we get $C_3 = x\,Log\,p_{H_2} + Log\,k_2$ or, $Log\,k_2 = C_3 - x\,Log\,p_{H_2}$ and because the order (x) in H_2 is near zero the last term cancels, resulting in $Log\,k_2 = -3.0584$, $k_2 = 8.74$ x 10^{-4}. The near zero order in H_2 and first order dependence on CO suggest that CO is involved in the rate determining step and that hydrogenation of acetaldehyde is fast compared with the formation of the acetaldehyde. This would also explain why very little acetaldehyde or its hemiacetals and acetals are detected in the products.

4.4.1 Notes on the used methodology

In contrast to the value of k_1, the value of k_2 should be more accurate, unless ethane can be formed from free ethanol, a scenario that is not unlikely; either by dehydration or by the same mechanism of methane formation. Unfortunately, the microGC equipment is not capable of detecting ethane, and its levels (if formed) should be very low because of the dilution in syngas. Thus, ethane formation has not been

included into the calculations, but care should be taken when using the value of k_2 in further calculations.

An additional treatment of the data can be performed to find the orders in p_{CO} and p_{H2} for the ethanol homologation. However, the data becomes more inaccurate as the levels of the product becomes much lower. Because the "trueness" of the data heavily relies on the accuracy of the measurements, we decided not to include the treatment of this data in this section.

Importantly, the established rate constants are intrinsic to this particular reactor, because for our convenience the absolute amount of product collected after the reaction is measured and used directly as a measure for concentration. Because the reactor has a fixed volume the number of moles found at the end of the reaction is linearly related to the concentration (concentration = number of moles / volume reactor (103 mL)).

Moreover, the values that were calculated do not incorporate effects from the ruthenium concentration, catalyst composition, bromide concentration and temperature on the system. Therefore, for now, the values that were calculated only reflect the behaviour under one set of conditions, but these data could be readily expanded by further investigations. Even if the catalyst composition changes by the addition of promoter, we do not expect this to change the order with respect to p_{CO} and p_{H2} as long as the catalytic species themselves do not change.

The meaning of k_1 is different from k_1'. If a more realistic rate constant is desired a rate expression should be obtained that contains a pure rate constant and terms with ruthenium species, the orders with respect to these species, and perhaps the bromide levels, CO_2 and promoters. For example:

$$\frac{\partial[MeOH]}{\partial t} = k_1(T)p_{H_2}^{1.8}p_{CO}^{0.4}[HRu_3(CO)_{11}]^x[RuBr_3(CO)_3]^y[Br^-]^z \text{etc.} \qquad \text{(eq. 4.27}$$

Where k_1 is a function of the temperature, and x, y and z are the orders in $[HRu_3(CO)_{11}]^-$, $[RuBr_3(CO)_3]^-$ and bromide respectively. The greyscale terms are factors that are currently held in the measured rate constants so far. Therefore, changing any of these leads to a change in the rate constants. This means it is difficult to establish

a universal rate constant, because we have shown that the promoters we apply lead to different concentrations of the ruthenium species.

4.4.2 Validation of the used kinetic expressions

The reproducibility experiments can be used to establish the rate constants for each reaction. Using a set of rate constants derived from these reactions a product distribution profile can be made over time. This can then be checked by performing a set of experiments where the reaction time is varied. The first attempt was unsuccessful. As will be discussed in the following section, it was established that there was an impurity in the solvent of the reproducibility experiments that was not present in some of the later experiments. The impurity $[HPBu_3]Br$ causes an increase in activity when present in small amounts. For this reason, kinetics comparison between two sets of experiments that have different rates is not useful here. After establishing the affect of the impurity/promoter, a new set of experiments was performed where the promoter was present, and with similar activity as the reproducibility reactions. Figure 4.5 shows the predicted product formation over time.

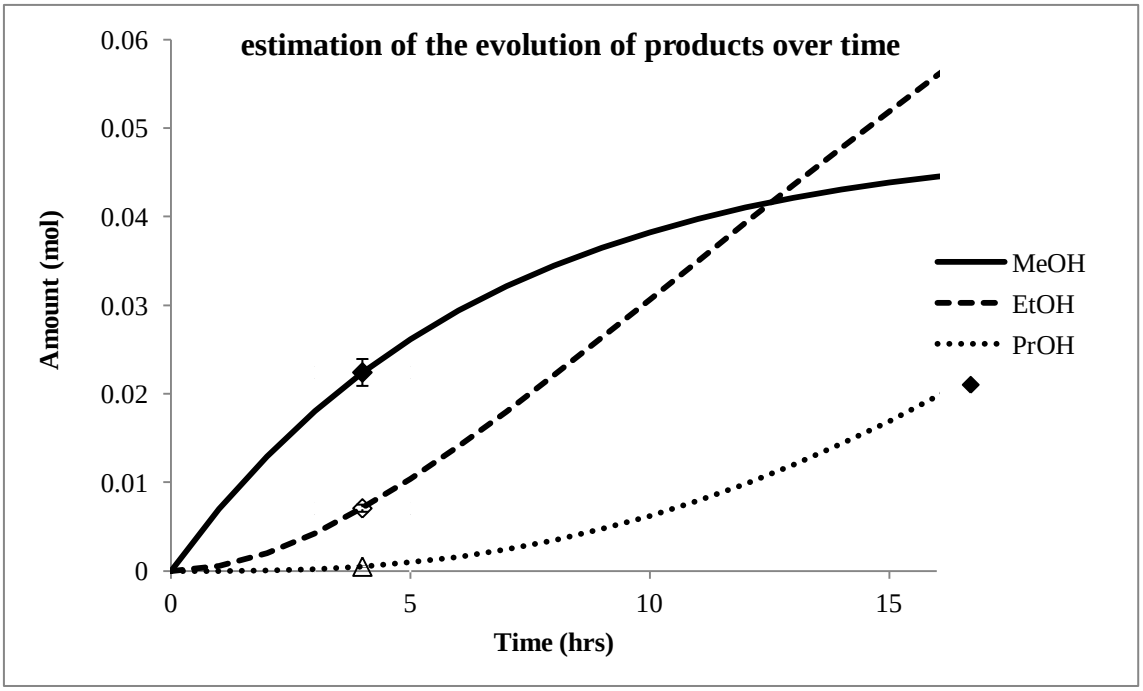

Figure 4.5 the prediction of the evolution of products over time based on the kinetics established using the case two model and input data (square data points: black square = methanol, blank square = ethanol, triangle = propanol) from the averaged reproducibility data (shown in Chapter 2).

It can be seen that it is expected that after a certain amount of time the selectivity towards ethanol is increased. In fact, the case two model expects an equilibrium value of methanol at $\frac{k_1'}{k_2'}$. However, in reality this profile is not observed (figure 4.6):

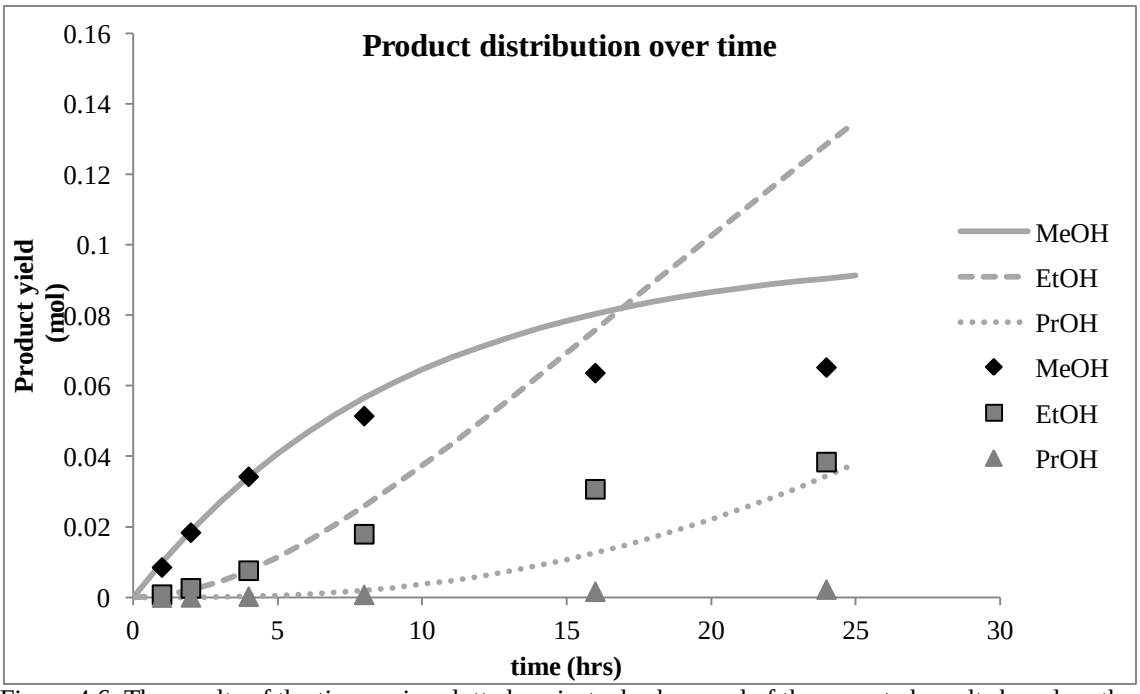

Figure 4.6: The results of the time series plotted against a background of the expected results based on the model. The real data are the discrete values. Conditions: $[Ru_3(CO)_{12}]$ 0.5 g, $[PBu_4]Br$ 15 g, $[HPBu_3]Br$ 0.415 g (0.62 eq to Ru), 250 bar CO/ H_2 1:1, 200 ^oC.

As can be seen the model behaves quite well through the first data points, however after 8 hrs the real values and the predictions do not correspond. Methanol synthesis trails off and seems to slow down relatively quickly compared to the expectations. The ethanol formation behaves much worse and does not reach higher than 60% compared to methanol even though the model predicts higher levels of ethanol compared to methanol. Figure 4.6 shows that both methanol formation and ethanol formation reduce over time and that overall the reaction rates slow considerably. Using the case two model, this can be quantified by determining the rate constants for each separate reaction. This calculated rate constant will be one that is an average over the period of time of the reaction, and not a rate constant *at* that time. See figure 4.7 below. The rate constants show a remarkable effect: it appears that the methanol formations undergoes a kind of induction before it reaches a maximum activity and then dwindles down to a lower activity. This suggests that the promoter takes some time to activate the catalyst for methanol production.

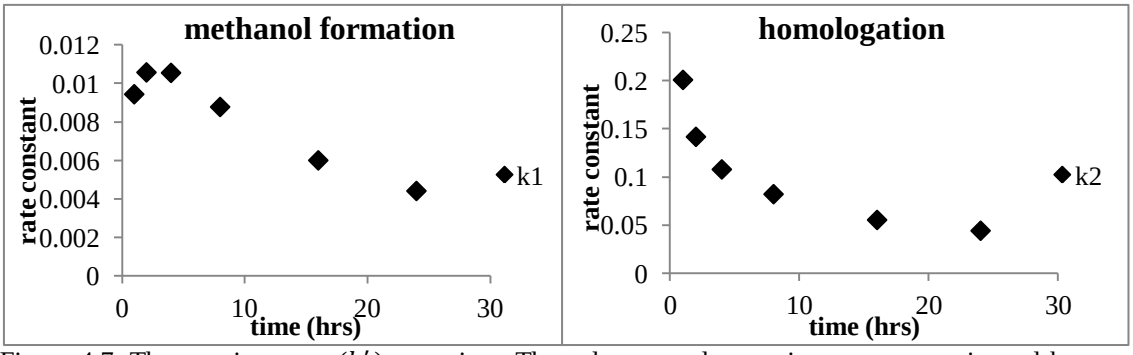

Figure 4.7. The reaction rates (k'_x) over time. The values near longer times are overestimated because they do not take into account the higher rates at the start of the reaction.

Additionally, it can be seen that the overall activity, for which the total methanol formation (k'_1) is a measure, declines over time. The total decrease in activity is quite significant: after 24 hrs the total activity is a factor 0.42 of the peak activity. There is another measure for total activity, which is the gas uptake curve. From this curve it can be seen that the decrease in the rate of uptake is similar: a factor of 0.46. This value is obtained by dividing the slope of the graph at the start of the reaction (-1.03 x 10^{-3} bar s^{-1}) by that at the end (-0.47 x 10^{-3} bar s^{-1}). The uptake plot is shown in figure 4.8.

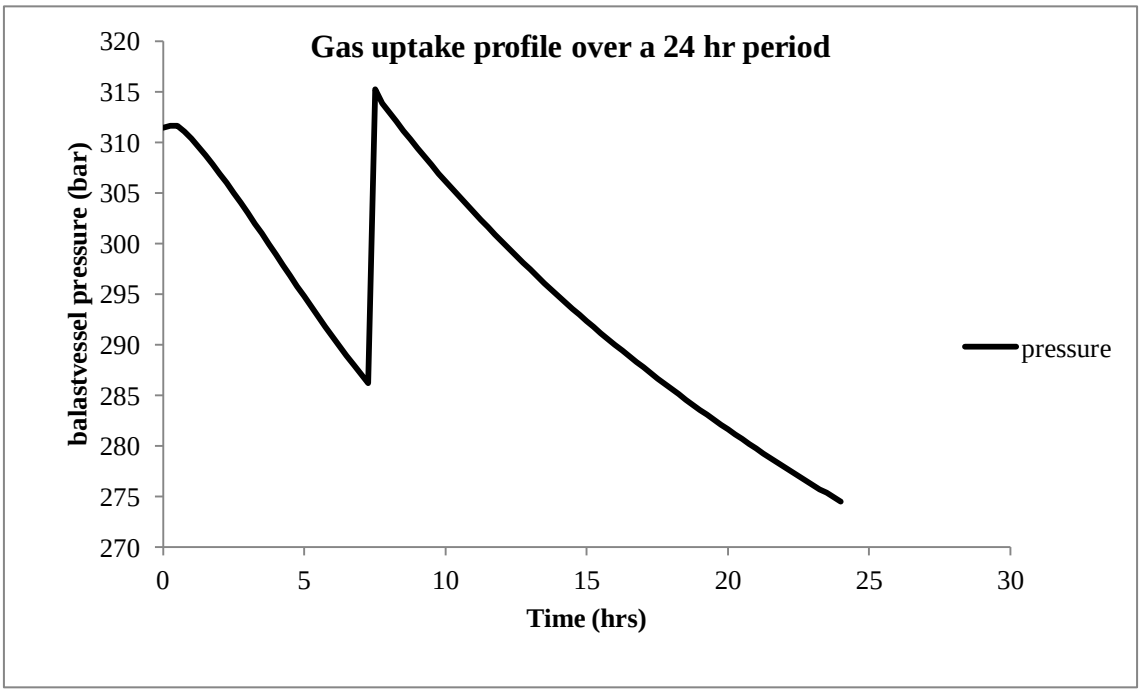

Figure 4.8 the ballast pressure during a 24 hr reaction period. After 8 hours the pressure was replenished to ensure there remains enough pressure until the end of the reaction. Conditions: $[Ru_3(CO)_{12}]$ 0.5 g, $[PBu_4]Br$ 15 g, $[HPBu_3]Br$ 0.415 g (0.62 eq to Ru), 250 bar CO/ H_2 1:1, 200 ^oC.

The fact that both the calculated rate and the measured rate decline a similar amount over time instils confidence in the consistency of the reaction. If for instance,

the calculated rate had decreased while the measured rate had remained constant, this would have been indicative that the gaseous product formation is increasing with time. This is a likely scenario if the catalyst had degraded and formed metallic aggregates.

Because this is not the case, it is likely that the reaction decreases in activity because of secondary effects or "batch effects" where the product formation starts to suffocate the catalyst. In this case, it is likely that the partial pressure of CO and H_2 are decreasing while CO_2 and methane are formed. In addition, the volatile liquid products that are formed must, by the end of the reaction, contribute significantly to the vapour phase components. Fortunately, with the measured orders and known rates this effect can be estimated and corrected for. If however, this calculation does not yield reasonable results, it must be assumed that the catalyst itself is affected over time.

4.5 Accounting for the WGS reaction

The fact that the WGS reaction takes place at a fast rate during catalysis can be used for the modelling of the reaction. Because water is created during the synthesis of ethanol, propanol, methane and ethers, the levels of CO in the system continuously decrease. Additionally, the level of H_2 increases. None of the discussed models so far have incorporated this effect, and therefore cannot yield perfect results. When the results of a regular run are fitted with the model to find the rate constants, this yields an average rate constant that takes into account the decreased p_{CO} and p_{H2} over the first 4 hours. This is why it is difficult to simulate the product formation over time with these rate constants, because they are in reality higher than what we measure. We have tried two approaches to simulate the changing gas phase behaviour. In the first attempt, it was assumed that the rate constants found are correct and the product formation was iterated over time, while for every step we corrected the p_{CO} and p_{H2} in the reactor, by assuming that the WGS reaction occurs instantly. The resulting reaction profile consistently underestimates the product formation for methanol, but not for ethanol. See figure 4.9. The levels of methanol are underestimated because the change in the gas phase composition was already accounted for in the rate constant, and does not need additional correction in the first 4 hours.

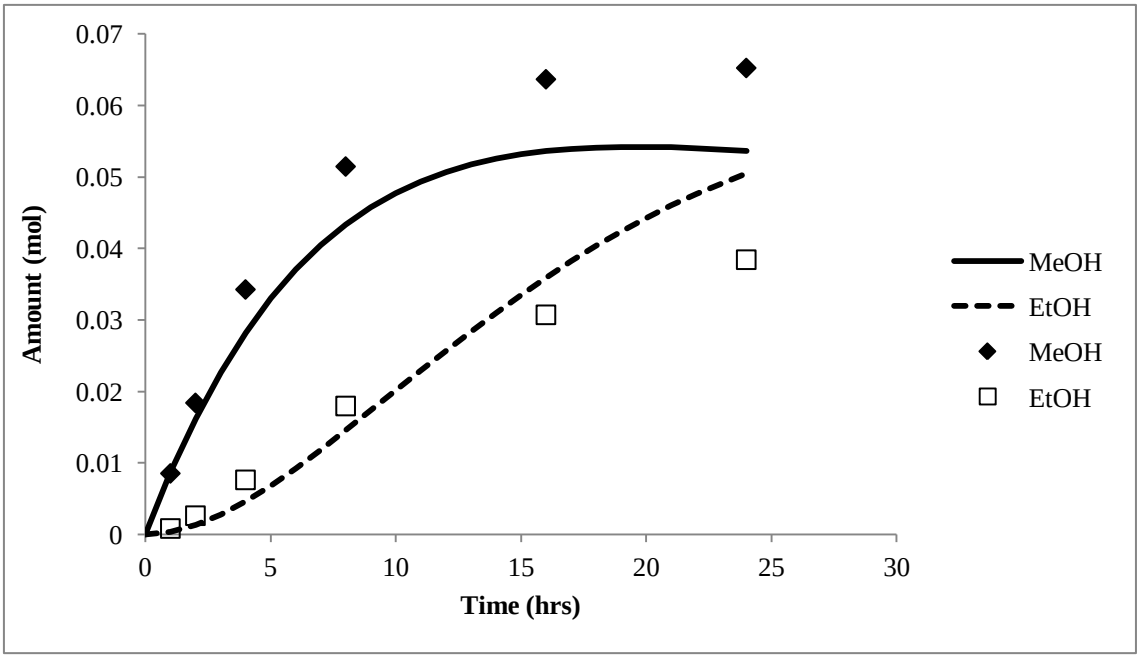

Figure 4.9 applying a correction for the change in the gasphase composition. This iterative process used the rate constants and orders determined in the variable p_{CO} and p_{H2} reactions. k_3 was taken from a regular run over 4 hours. After every iteration the gas phase composition was calculated and adjusted for towards the WGS equilibrium. Conditions: $[Ru_3(CO)_{12}]$ 0.5 g, $[PBu_4]Br$ 15 g, $[HPBu_3]Br$ 0.415 g (0.62 eq to Ru), 250 bar CO/ H_2 1:1, 200 ^oC.

To see if this is true the model was rerun, now starting from t = 4 hrs using starting values of the products that were found after 4 hours in a regular run.

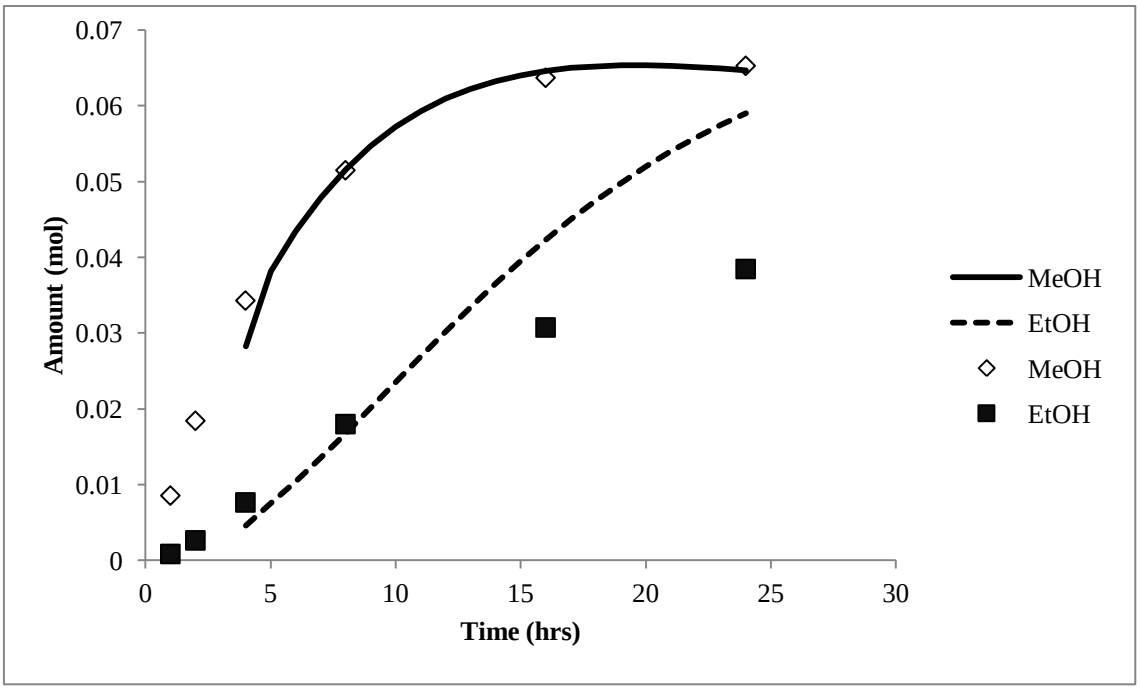

Figure 4.10 the corrected modelling where we take into account the gas phase behaviour in the system. The product formation of methanol is consistent with the observation that the gasphase composition changes over time. For ethanol formation this does not explain the reduction in the rates.

This leads to a near perfect fit for methanol (Figure 4.10). Therefore, the main decrease in activity in the system over time must be due to the changes in the gas phase composition in the reactor. However, there is still a large inconsistency between the real ethanol production and how it was modelled. It was expected to see that the reduction in p_{CO} would also affect the ethanol production rate significantly. However, even though the model also predicts that the level of ethanol increases more slowly, it is not consistent with what was measured. The plot generated here is based on a numerical solution using the rate constants determined from the order determinations, we expect the orders to hold true in the following ranges of pressure: p_{CO} 40-150 bar and p_{H2} 40-150 bar). Therefore we assume that the problem does not lie in the lowering of the p_{CO} or p_{H2} as the reaction proceeds. Likely, the value of the established k_3' is not very precise because it is more difficult to exactly quantify the amount of propanol after the reaction. Additionally, it is very likely that the order in methanol for homologation is not 1, especially considering that the order in CO for this reaction is 1. It is unlikely that both methanol and CO play an important role in the same rate determining step. However, we have repeated all the above procedures assuming the order in methanol is zero. However, this way the observed product formation over time is not reproduced. A final possibility is that the order in methanol is 1 at lower concentrations, but becomes zero as more methanol is available. Further studies are needed to determine this. Use of the model has pointed out that there must be an additional underlying cause for the decrease in the rate of homologation which has not been investigated properly yet.

4.6 Further discussion

It is important to discuss how the above plots were generated. In the first step data was obtained from a series of reactions at various gas phase compositions and pressures. Then a mathematical description was developed of the product formation taking into account a) light alcohol and methane formation or b) only light alcohol formation. In the next step this methodology was used to estimate relative kinetic parameters of each independent reaction; e.g. k_1' represents the total product formation and is indicative of the rate of methanol formation, k_2' represents the rate of methanol homologation to ethanol and k_3' represents the relative rate of ethanol conversion to propanol. The following assumptions were made during the development of this model:

i. Methanol is the primary product from which all other products are eventually formed
ii. The alcohols, methanol, ethanol and propanol are the main products, all other products can be ignored. In case one, also methane formation is considered.
iii. The activity over time remains constant.
iv. Ethanol is made solely from free methanol
v. Propanol is made solely from ethanol
vi. Because the amount of propanol formed is so low, the formation of butanol can be ignored.
vii. in case one, methane is also made solely from free methanol
viii. there are no vapour-liquid equilibrium (VLE) effects, and the products behave as ideal homogeneously spread components
ix. The gas phase composition remains the same over time, and the side reactions are ignored
x. All reactions are first order in alcohols

These are many assumptions, some of which were not verified or tested, and others known to be false. Assumption i and ii we have shown in Chapter 2 and 3 to be reasonable. Assumption iii is very important, however. If for two comparative reactions the same reaction time is used any effects from this assumption should cancel. Assumptions iv, v and vii have not been fully proven, yet the labelling data does indicate that at least a large part of higher alcohol formation occurs through the free lower alcohol intermediate. Assumption vi may be an important reason why the ethanol formation in figure 4.10 does not fit the data correctly, and may result in an under estimation of k_3'. For this reason, we will not use the value of k_3' unless it shows significant insight. Assumption viii is a working assumption in order to simplify the calculations. Under the operating pressures each vapour and permanent gas will most likely behave non-ideally. We have shown that assumption ix is false, and that if corrected for the model seems to behave significantly better. However, if the same reaction times and gas uptakes are applied during the reaction most of the effects from this assumption will cancel out between comparative experiments. Assumption x is based on simple kinetics that the methanol should be activated by reaction with the halide (S_n2) in the solvent. Since the halide concentration is constant the order should be 1 in methanol. It is expected that ethanol conversion will occur in a similar way.

Therefore, if conditions between two reactions are held constant, most effects of the false assumptions will cancel out. For instance, the change in gas phase composition is not going to be *much* different between two reactions, even if the reaction rate of one reaction is 25% faster than the other. The (VLE) effects will be apparent to the same extent in each reaction, and if the ballast vessel pressure does not show very big differences, it can be assumed that the rate constant k_1' does not contain any latent methane formation differences. The main reason why these models have low predictive value is because they do not take into account the decreasing reaction rates for methanol formation because of the WGS reaction, or the fact that the homologation reaction decreases in rate over time (shown in the following chapter). The reason for the latter effect is unknown, and thus cannot be corrected for yet.

Thus even while these rate constants are only relative values. They can be used to compare relative rates within a set of reactions where most conditions (most importantly reaction time) are kept equal. For instance, to assess how a promoter affects catalysis. The change of the relative rates within such a series of experiments shows which particular reactions are enhanced by the promoter. Further, between two series comparisons can be made if the quantities of catalyst and the pressures are kept similar. The usefulness of this model will be shown particularly in the following chapter.

Moving forward, the kinetic parameters derived and estimated using the models were then used to determine relative rate changes with changing partial pressures of the reagents. This yielded the orders in p_{H2} and p_{CO} for each reaction (methanol formation and methanol homologation to ethanol). Additionally the orders were used to independently determine the rate constant specific to this system, reactor and conditions. Thus both the rate constants and the orders in H_2 and CO were measured in reactions were the conditions (see table 4.1) were different from the reproducibility experiments or the time series (see figure 4.6). Yet, using this rate constant and these orders an accurate prediction of the evolution of methanol over time was made. Interestingly, the orders in p_{H2} and p_{CO} are measured by determining the *relative* rate changes upon changing partial pressures while the orders are measured by relative changes. This, in combination with the high precision of predicting the methanol levels over time brings confidence in the accuracy estimated orders.

4.7 Experimental

General notes on the equipment/methodology and materials used are described in the experimental section of the previous chapter.

4.7.1 General catalytic procedure

In a typical reaction the solids were weighed into the clean and dry autoclave, which was screwed onto the holder and sealed, filled with CO/H_2 (50:50 v/v, approx 11 bar) and then vented. This purging sequence was repeated at least 6 times but usually 7 times, to ensure adequate removal of air. Next, the system was filled with syngas to approximately 170 bar and tested for leaks. The heater was attached and set to 200 ^oC. The heater was switched on under continuous stirring. When the reactor had reached the desired temperature of 200 ^oC the reactor pressure was adjusted to 250 bar. During the reaction the pressure was held continuously at 250 bar by the addition of new syngas from an attached ballast vessel through a pressure controller. The pressure of the ballast vessel was monitored throughout the reaction by the use of computerised logging equipment. The reaction was allowed to run for 4 hrs after which the heater was switched off and decoupled to ensure swift cooling. When the temperature of the autoclave was below 30 ^oC the excess pressure was vented from the autoclave and the product mixture was inspected. The usual colour was red, orange or yellow depending on how much promoter was added. Further, the liquid was poured into a glass flask and subsequently weighed. The product mixture was distilled under reduced pressure using temperatures up to 250 ^oC. The condensed vapours were collected in a liquid N_2 cold trap. The products were diluted using a stock solution (5 mL , acetonitrile (2% v/v) internal standard in N-methylpyrrolidone (NMP)). This mixture was then analysed using GC-FID. The retention times of the products were previously determined using GC-MS.

4.7.1 Experiments 10-17: rate dependencies on p_{H2} and p_{CO}

Exp 10.

To the clean and dry autoclave the reagents were added in the amounts described in table 4.3. The system was purged and checked for leaks. The autoclave was warmed

to 50 ^{o}C and 75 bar of CO followed by 25 bar of H_2 were added to the vented autoclave. The autoclave was closed and heated under stirring to 200 ^{o}C. When the reactor temperature had reached 200 ^{o}C the pressure was measured to be 150 bar. The reaction was allowed to proceed for 4 more hours at a constant pressure by adding small amounts of syngas (CO/H_2 1:2). This ratio was chosen as it closely reflects the stoichiometry of the CO hydrogenation reaction so should keep the relative levels of CO and H_2 constant. After 4 hours the heating was switched off and the work-up of the reaction was the same as the other reactions described above.

Exp 11-17

The procedure for these reactions was the same as exp. 10, except that the starting levels of CO and H_2 at 50 ^{o}C were different. These are described in Table 4.2.

Table 4.2 the starting pressures of reaction exp 10-17 in bar.

experiment	P_{CO}	P_{H2}	Total P at 200 ^{o}C
10	75	25	150
11	75	50	177
12	75	75	217
13	75	100	262
14	25	75	150
15	50	75	183
16	100	75	262
17	75	50	188

Table 4.3 describes the amounts of reagents used in these reactions. Table 4.4 describes the liquid product yields where appropriate.

Table 4.3. The used materials for the reactions used in chapter 4.Conditions: 200 ^{o}C, syngas (250 bar 1:2 CO: H_2), 4 hrs

	$[PBu_4]X$	mass $[PBu_4]Br$			amount of promoter		mass $[Ru_3(CO)_{12}]$		
Exp.	X=	grams	mmol	Promoter	grams/mL	mmol	grams	mmol Ru	Promoter/Ru
10	Br	14.5030	42.7395	HPBu3Br	0.415	1.4638	0.4993	2.343	0.625
11	Br	14.5028	42.7389	HPBu3Br	0.415	1.4642	0.4997	2.345	0.624
12	Br	14.5029	42.7392	HPBu3Br	0.415	1.4635	0.4994	2.343	0.625
13	Br	14.5024	42.7377	HPBu3Br	0.414	1.4624	0.4994	2.343	0.624
14	Br	14.5026	42.7383	HPBu3Br	0.415	1.4660	0.4995	2.344	0.625
15	Br	14.5030	42.7395	HPBu3Br	0.415	1.4652	0.4991	2.342	0.626
16	Br	14.5022	42.7371	HPBu3Br	0.415	1.4642	0.4994	2.343	0.625
17	Br	14.5026	42.7383	HPBu3Br	0.4147	1.4642	0.4993	2.343	0.625

Table 4.4. The recovered liquid products for the reactions used in this chapter.

Exp.	Methanol	Ethanol	Propanol	Butanol	EG	2-methoxy ethanol
10	3.8659	0.7612	0.0405	0.0094	0.2007	0.0215
11	4.3526	1.2166	0.0682	0.0135	0.1619	0.0363
12	21.5677	4.7329	0.1910	0.0221	0.8746	0.1463
13	44.6477	7.9988	0.2653	-	2.1345	0.3296
14	18.1910	1.2228	0.0380	0.0215	0.2456	0.0355
15	23.6865	2.8544	0.0946	0.0213	0.8164	0.0824
16	28.8914	7.7628	0.3178	0.0252	1.6704	0.2958
17	15.3173	2.9632	0.1573	0.0193	1.0482	0.1368

4.7.2 Series varying time

In this series the reaction time was varied while all other factors were held constant. In this series purified $[PBu_4]Br$ was used as well as $[HPBu_3]Br$. The use of this promoter will be discussed in chapter 5, as well as the procedures for preparation, and purification of $[PBu_4]Br$. Table 4.6 shows the reagents and conditions used.

Table 4.6. Used reagents and experimental conditions[a] for the series of experiments where the reaction time was varied.

		mass $[PBu_4]Br$		mass $[HPBu_3]Br$		mass $[Ru_3(CO)_{12}]$	
Exp. No.	time (hrs)	grams	mmol	grams	mmol	grams	mmol Ru
30	1	14.5024	42.7377	0.4162	1.4695	0.4999	2.3457
31	2	14.5020	42.7366	0.4158	1.4681	0.4996	2.3443
32	4	14.5024	42.7377	0.4152	1.4660	0.5001	2.3467
33	8	14.5025	42.7380	0.4150	1.4652	0.5001	2.3467
34	16	14.5028	42.7389	0.4150	1.4652	0.4994	2.3434
35	24	14.5021	42.7368	0.4152	1.4660	0.4993	2.3429

[a]Conditions: 200 ^oC, 250 bar syngas (1:1 v/v).

The product yields are given in table 4.7

Table 4.7 the recovered amounts of product for the first time series.[a]

Exp. No	Methanol	Ethanol	1-Propanol	EG
30	8.5581	0.8522	0.0361	0.4855
31	18.4286	2.6428	0.0938	0.8142
32	34.2927	7.6533	0.2830	1.9944
33	51.4931	17.9900	0.8018	2.3578
34	63.6997	30.7439	1.6977	3.1406
35	65.2784	38.4573	2.3055	3.1572

[a]Amounts in mmol.

IR and NMR spectra of the product mixtures may be found in the appendix.

4.8 Conclusion

In this chapter the orders of the reaction rates with respect to the H_2 and CO partial pressures were estimated. In order to achieve this, it was necessary to develop a measure for the reaction rates at various H_2 and CO partial pressures. The change in reaction rate with changing partial pressure determines the orders. Two main reactions were considered: 1) methanol formation from syngas, 2) methanol conversion to ethanol. By assuming a simple reaction profile the relative rates of each reaction can be determined by solving a set of rate expressions. The kinetic parameters present a measure for all global phenomena that influence the reaction rate, but were not specifically recognized. Because the only variable in the set of experiments was the CO or H_2 partial pressure, the variation in kinetic constant is proportional only to the changing partial pressures.

Within the range of pressures and temperatures that were used in this set of experiments, the following was found: for methanol formation the order with respect to the H_2 partial pressure is 1.8, with respect to CO the order is 0.4. The fractional nature of the orders point to the existence of complex chemical and/or physical equilibria, which affect the reaction rate. For methanol conversion to ethanol, the order with respect to H_2 is 0, and the order with respect to CO is 1.

The kinetic framework that was developed was tested and its limitations were defined. The primary failure of the framework is that it does not take into account side reaction that take place in the reactor. As a result, the use of the models should be constrained to the point where the products of side reactions do not significantly inhibit the reaction rates. In our case, that is when the reaction times are smaller than 6 hours. It was demonstrated that when one of the main side reactions, the WGS reaction, is taken into account, the model become quite accurate for describing the methanol formation, but is lacking accuracy with respect to the ethanol formation for yet unknown reasons. For the above reasons the kinetic expressions can be used as a useful tool for assessing the relative reaction rates between similar reactions.

Chapter 5
Improved rates by the presence of impurities in the solvent

Detection of an impurity and subsequent analysis of the action of this impurity.

5.1 Introduction

As briefly mentioned in Chapter 4, during the validation and testing of the mathematical description of the product formation an anomaly was found in the rates of the reactions. In this test, a series of experiments were performed where all conditions remained equal to the reproducibility series except for the reaction time, which was increased incrementally with each experiment (from 1,2,4,8, to 16 hrs). When the observed amounts of products at the end of the reaction were plotted a curve was obtained that reflects the product formation over time. When performing this first time series it was found that the kinetics used in the model and the results from the series did not match. After tracking the cause of this effect a second series of experiments was performed to validate the performance of the model. These results were described in the previous chapter. However, comparing the rates of the first time series with the reproducibility experiments showed that the time series consistently showed much lower activity. This is clearly visible in figures 5.1 and 5.3. The greyscale continuous lines are the predicted product formation over time based on the kinetics of the reproducibility data. This data should at least match at t = 4 hours.

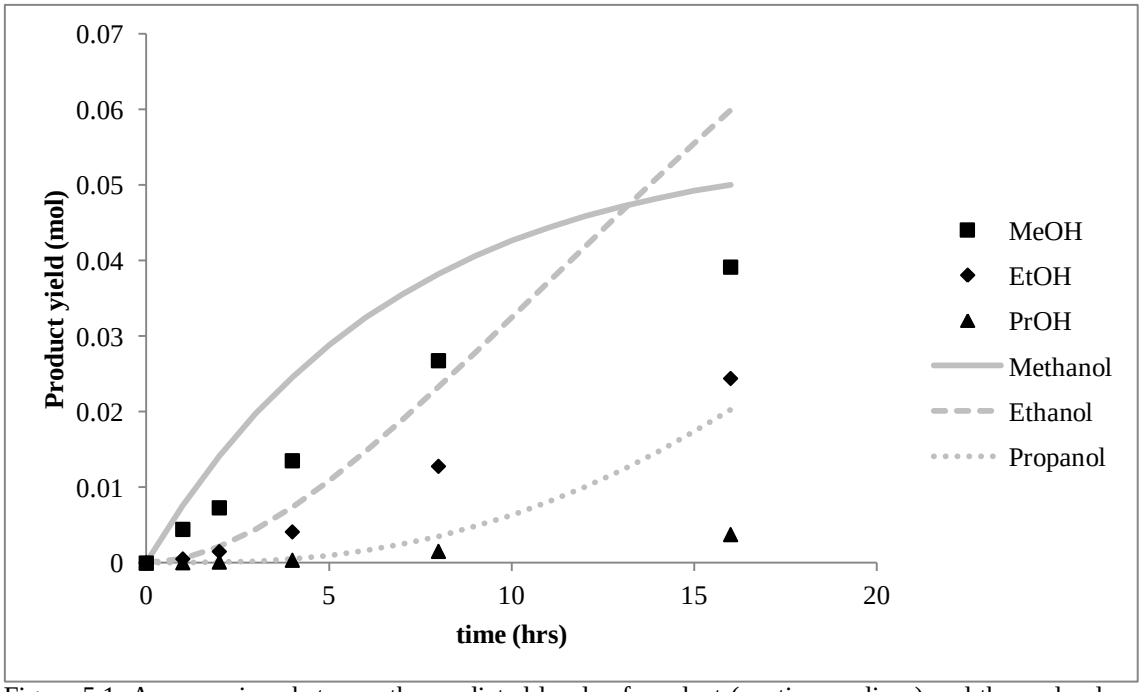

Figure 5.1. A comparison between the predicted levels of product (continuous lines) and the real values obtained (discrete datapoints) over time. Conditions used: 0.5 g $[Ru_3(CO)_{12}]$, 15 g $[PBu_4]Br$, 200 ^oC, 250 bar, CO/ H_2 1:1, 4 hrs.

However, the real data does not resemble the values from the model. In this series, only half the amount of product that was expected was found. Clearly, the rates of the series are lower than the rates in the reproducibility experiments. Out of curiosity, to see if the case two model still gives a reasonable curve the product formation was calculated using the kinetics established from the 16 hour experiment, which has the highest product yield. See figure 5.2 below. This leads to a relatively good fit, which validates the observation that when the total activity is low, there are very little changes in the system's composition, and as a result the model works relatively well. Additionally, it helps validating the use of the models.

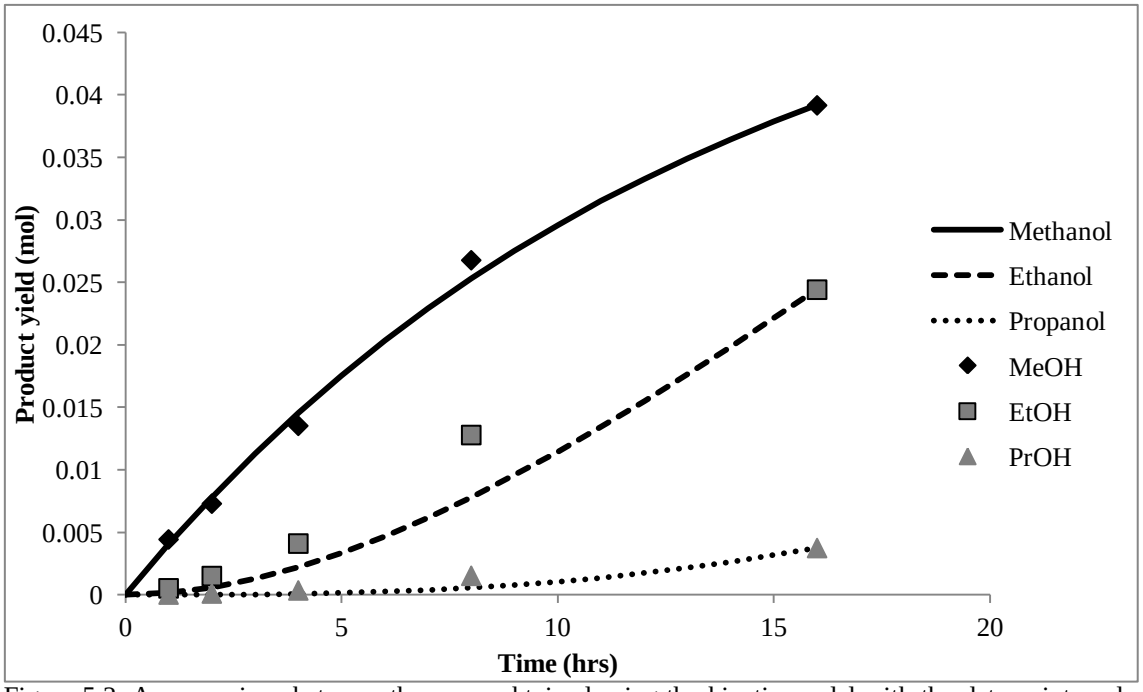

Figure 5.2. A comparison between the curve obtained using the kinetic model with the data points only from the 16 h reaction and the observed amounts of product obtained after different times. Conditions used: $[Ru_3(CO)_{12}]$ (0.5 g), $[PBu_4]Br$ (15 g), 200 ^oC, 250 bar, CO/ H_2 1:1, variable time.

To investigate the underlying cause of the sudden change in reactivity it was decided to start with comparing the relative rates with those of the benchmark reactions. Thus, the case two model was used to establish all kinetic parameters of each reaction. It was found that the rate constants for k_1 (total methanol formation) were affected uniformly, giving a constant value near 50% lower than that of the benchmark reaction. (figure 5.3) This is in contrast to the rate profile shown in figure 4.7 in the previous chapter. Additionally, the rate constants k_2 (homologation) also varied with reaction time, yet, both the benchmark and the time series intersect after 4 hours.

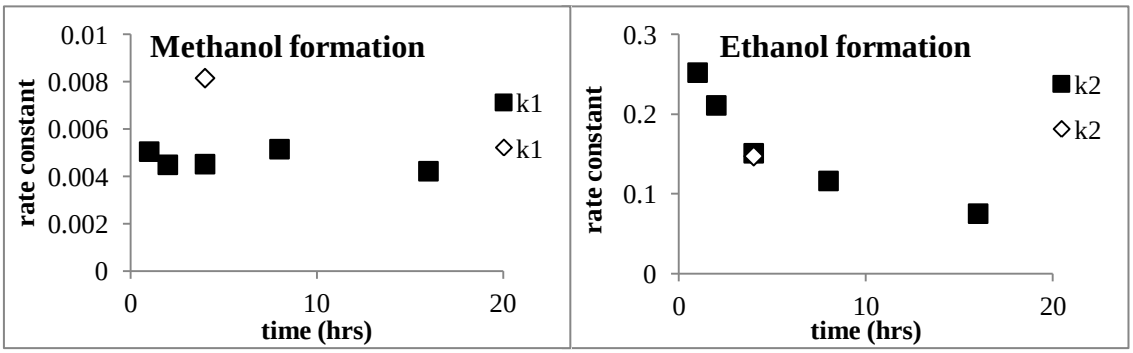

Figure 5.3. The rate constants as determined by the model, throughout the series. The rotated square is from the benchmark reaction of 4 hours. Left, the rate constants for methanol formation. Right, the rate constants for ethanol formation. Conditions used: 0.5 g $[Ru_3(CO)_{12}]$, 15 g $[PBu_4]Br$, 200 ^oC, 250 bar, CO/ H_2 1:1, variable time.

This suggests that only the methanol formation is affected and that the ethanol synthesis remains largely undisturbed by it, but decreases over time by some other cause. The ethanol formation could be affected by a number of factors. For instance, the homologation catalyst decomposes over time, or the catalyst is increasingly involved with competing side reactions, or the levels of CO and H_2 change over time and affect homologation more than methanol formation.

5.2 Identifying the impurity

The sudden change in activity coincided with a change in the batch of $[PBu_4]Br$ that was used. This lead to the conclusion that one of the used batches contained an impurity that either promoted or inhibited activity (mainly methanol formation). Identification of the impurity was carried out by analysis of the NMR spectra of the different batches of tetrabutylphosphonium bromide. It was found that the tetrabutylphosphonium bromide had several impurities, some of which could be identified. Scrutiny of concentrated samples of the different batches of $[PBu_4]Br$ by ^{31}P-NMR spectroscopy revealed three peaks (Figure 5.4). The strongest signal (δ 33.56 ppm) is from tetrabutylphosphonium bromide. In most batches another peak is present at δ 37.49 ppm which is from tri-n-butyl(sec-butyl)phosphonium bromide, formed by Markovnikoff addition of the P-H bond across 1-butene during the synthesis of PBu_3 from PH_3 and 1-butene. This peak was more intense in the less active batch of $[PBu_4]Br$, than in the active batch. The ^{31}P NMR spectrum of the active batch revealed a further peak at δ 11.55 ppm which splits into a doublet (J_{HP} = 487.26 Hz). in the proton coupled ^{31}P-NMR spectrum. Likewise, careful scrutiny of the ^{1}H NMR spectrum of the same sample revealed, in addition to the signals from the butyl groups, a low intensity doublet (δ 6.83, $J_{H\text{-}P}$ = 487.43 Hz).

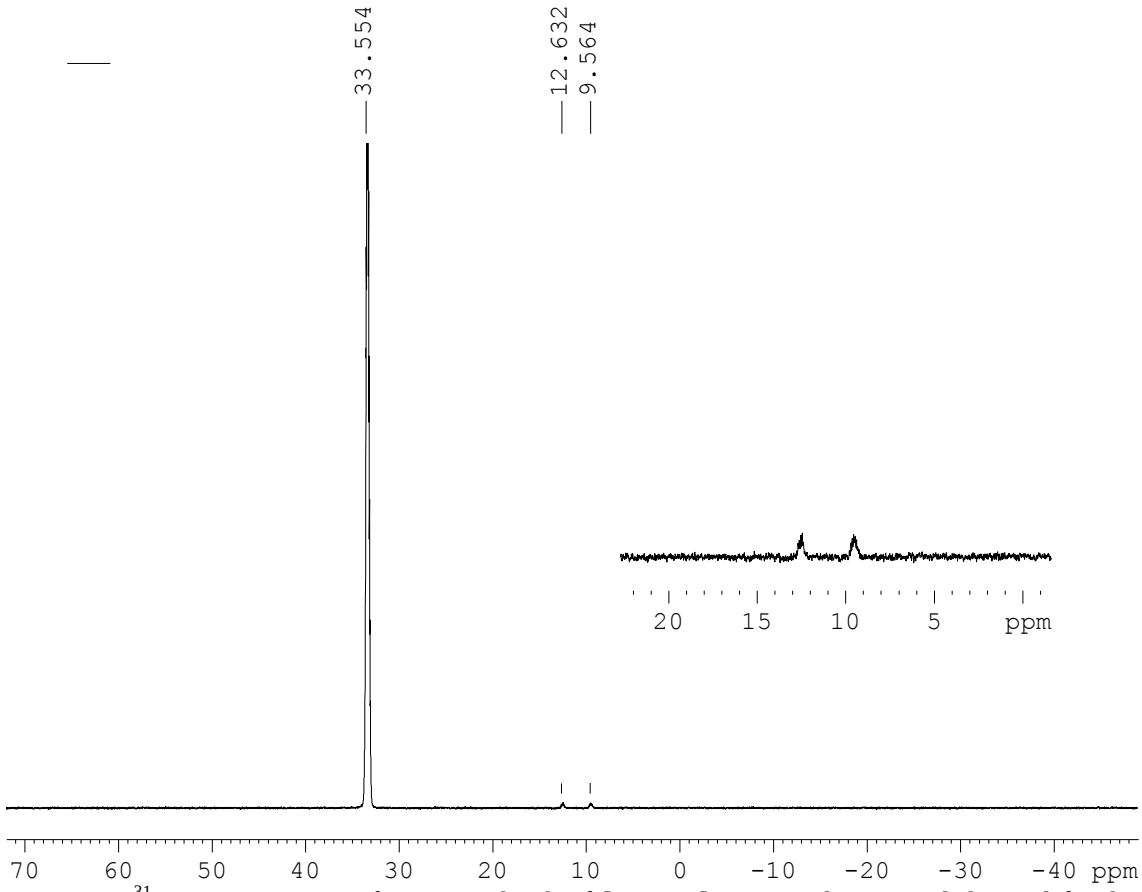

Figure 5.4. ^{31}P NMR spectrum of an active batch of [PBu$_4$]Br]. Inset is the H coupled signal for the resonance at δ 11.55 ppm.

These signals were identified to arise from tributylphosphonium bromide, [HPBu$_3$]Br, which is a protonated form of tributyl phosphine. This impurity is presumably formed during the synthesis of tetrabutylphosphonium bromide when tributylphoshine reacts with free HBr or when n-butylbromide reacts with traces di(n-butyl)phosphine (Scheme 5.1).

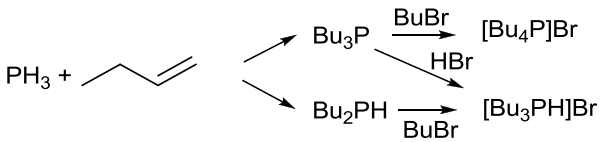

Scheme 5.1. Process for the production of [Bu$_4$P]Br and how this can lead to small amounts of [HBu$_3$P]Br as an impurity

It was anticipated that the $[HPBu_3]Br$ was not so innocent during catalysis. Since the batch of $[Bu_4P]Br$ which visibly contained $[HBu_3P]Br$ was more active than the other one, we introduced a purification procedure to treat the tetrabutylphosphonium bromide by reprecipitating it from acetone using diethyl ether. This effectively removed almost all of the $[HPBu_3]Br$ impurity.

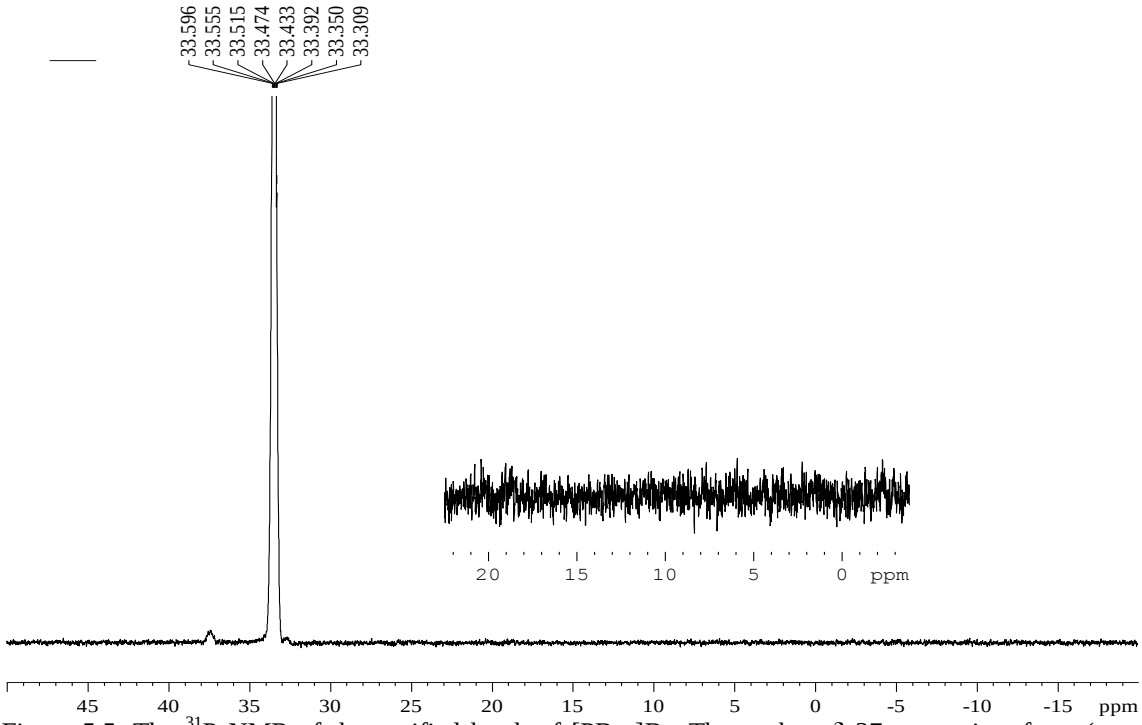

Figure 5.5. The ^{31}P NMR of the purified batch of $[PBu_4]Br$. The peak at δ 37 ppm arises from (sec-butyl)tri –(*n-butyl)*phosphonium bromide, a common side product in the synthesis of tetrabutylphosphonium bromide.

To test the hypothesis that the $[HPBu_3]Br$ was indeed the impurity causing the change in activity, some of it was generated by adding dry HBr to a solution of tributylphosphine in ether.

$$PBu_3 + HBr \xrightarrow[85\%\ \text{yield}]{\text{Diethyl ether}\ <\ -66\ ^oC} [HPBu_3]Br$$

To generate dry HBr, 85% H_3PO_3 was dried with a slight excess of P_2O_5, and reacted it with KBr to evolve HBr. The HBr was led through a tube containing a plug of P_2O_5 to a solution of tributylphosphine in diethyl ether. The reaction is slightly exothermic so the ether solution was chilled to the point where HBr condensed. After no HBr visibly evolved from the KBr anymore the reaction mixture containing a white

solid was warmed to room temperature, filtered and the solid washed three times with diethyl ether. The reaction gave a white hygroscopic powder (isolated yield, 85 %). The ^{31}P NMR spectrum (figure 5.6) showed a pure sample containing the [$HPBu_3$]Br with a doublet at δ 11.6451 J_{Ph} = 483.24 Hz. The ^{1}H NMR spectrum (figure 5.7) showed the 4 resonances at δ 0.95, 1.47, 1.61 and 2.293 ppm belonging to the butyl groups and a doublet of multiplets at δ 6.496 ppm with J_{HP} = 484.52 Hz. The integration shows 1 H-P proton to 3 butylgroups. This is consistent with the expectations for [$HPBu_3$]Br.

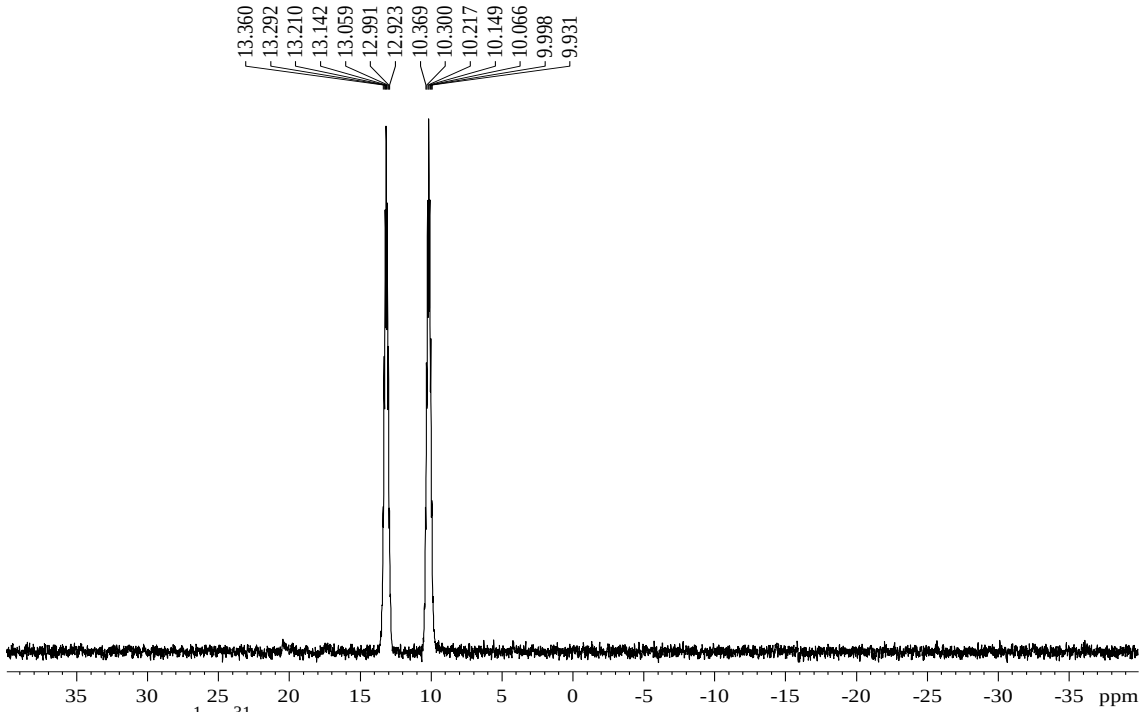

Figure 5.6. The {^{1}H}^{31}P NMR of synthesised [$HPBu_3$]Br, the chemical shift is very close to that of the impurity in the [PBu_4]Br and may be shifted because of solvent interactions with the proton. J_{HP} = 483.24 Hz.

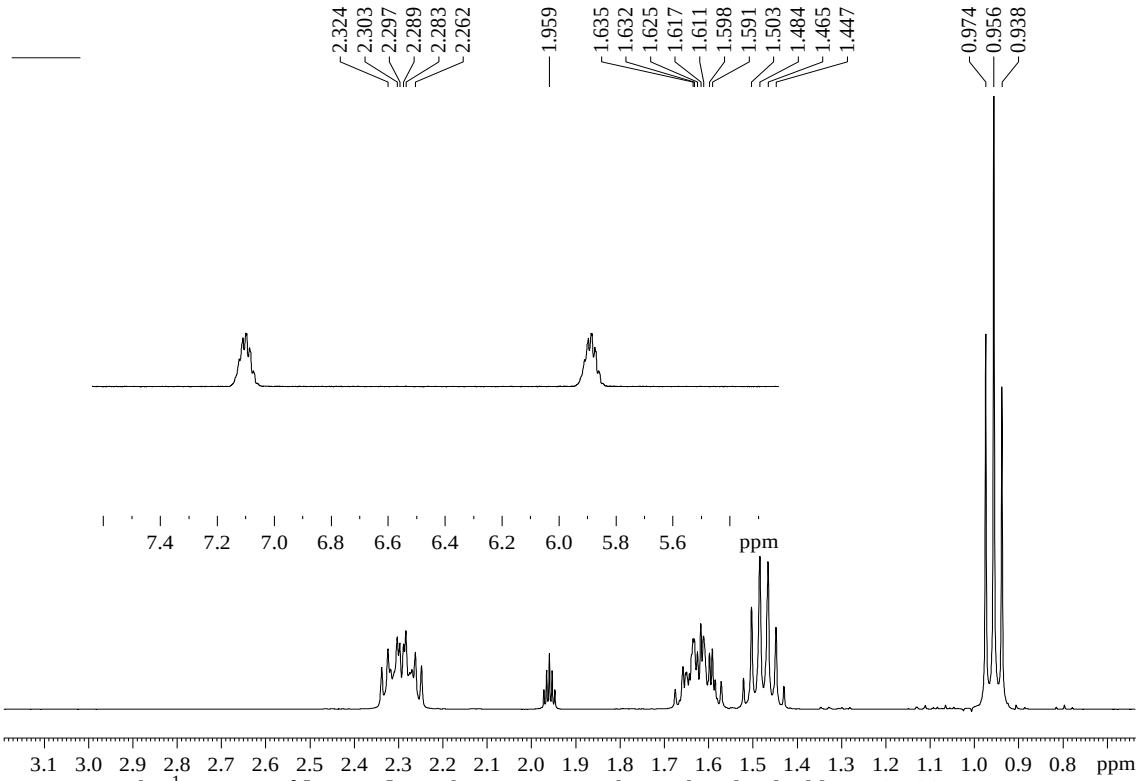

Figure 5.7. The ^{1}H NMR of [$HPBu_3$]Br. The integration shows that the doublet at 6.496 ppm is consistent with[$HPBu_3$]Br. The position of the split signal (inset) of the H-P proton is at δ 6.50, d , $^{1}J_{HP}$ is 484.52 Hz and its integration is 1 H to 3 butyl groups.

To test the influence of the impurity a set of experiments were performed where a purified sample of [PBu_4]Br was used to test activity with and without added [$HPBu_3$]Br.

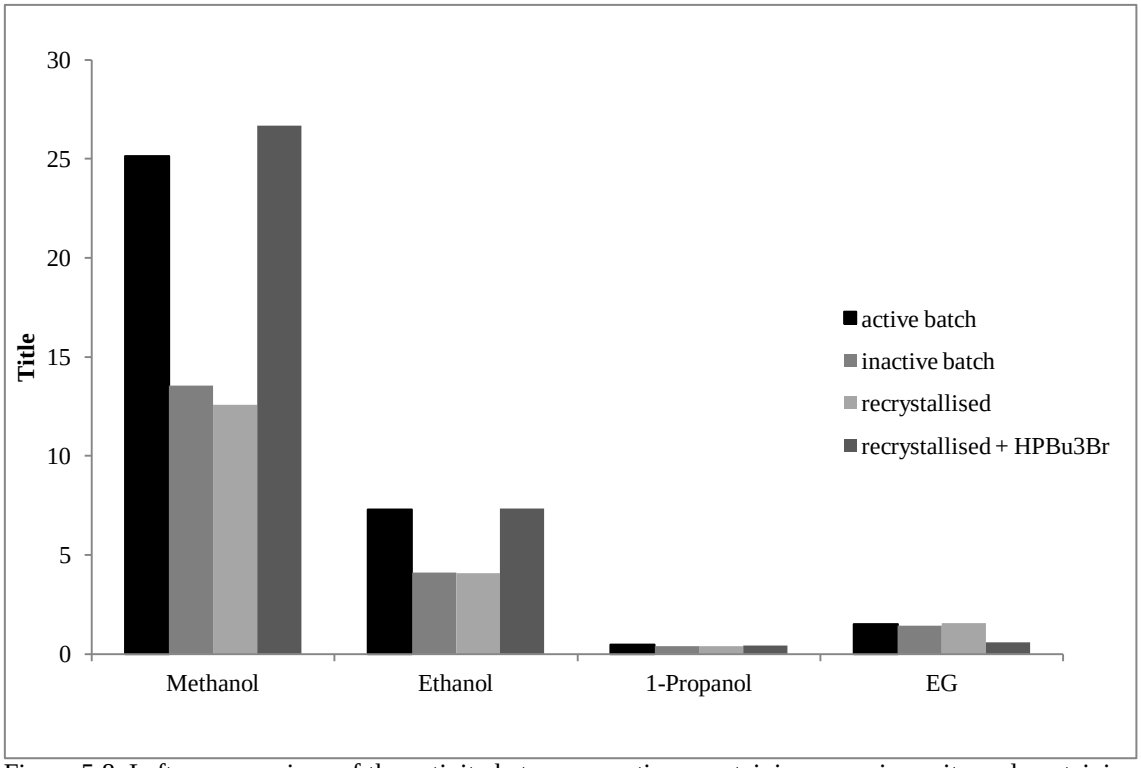

Figure 5.8. Left, a comparison of the activity between reactions containing some impurity and containing no impurity. Purifying tetrabutylphosphonium leads to reduced activity, adding $[HPBu_3]Br$ to purified $[PBu_4]Br$ increases the activity significantly. Conditions used: $[Ru_3(CO)_{12}]$ (0.5 g), $[PBu_4]Br$ (15 g), 200 ^oC, CO/ H_2 (1:1, 250 bar), 4 hrs.

As can be seen in figure 5.8 there is a significant difference between the active and inactive batch, and also between the active batch and the recrystallised batch. Furthermore, when some $[HPBu_3]Br$ was added to the reaction mixture containing recrystallised $[PBu_4]Br$ the activity was restored to the same activity as in the active batch. These results show that $[HPBu_3]Br$ is the impurity responsible for the increased activity of the active batch and that it may be capable of improving the rate of catalysis.

5.3 The method of action of the promoter

The time series discussed at the start of this chapter, and the time series discussed in the previous chapter contained different amounts of promoter. The inactive series from this chapter contained only very low levels of $[HPBu_3]Br$. These two series can be compared to better understand the action of the promoter. In the promoted series the values of k_1 ($k_1 \approx 0.005$) start out much higher than in the unpromoted series, almost double value. However, there is an induction period, which was not present in the unpromoted series. Because the methanol rate constant is calculated by the sum of the total alcohol formation over a period of time we can improve on the accuracy of the k_1-

values at any point in time by calculating them manually over each interval. This should give an accurate picture of how the methanol catalyst behaves over time, without the systematic high estimate from the model. In figure 5.9 (left) a comparison is shown between the methanol formation (k1) for the two series.

For homologation, on the right hand side of figure 5.9, the rate constants in the promoted series starts lower than the rate constants from the reactions with almost no promoter in it. Also, the k_2 decreases more rapidly than in the previous experiments. In the induction time not only the methanol catalyst improves, but comparison between the k_2-values shows that the homologation step is inhibited more and more during this induction period.

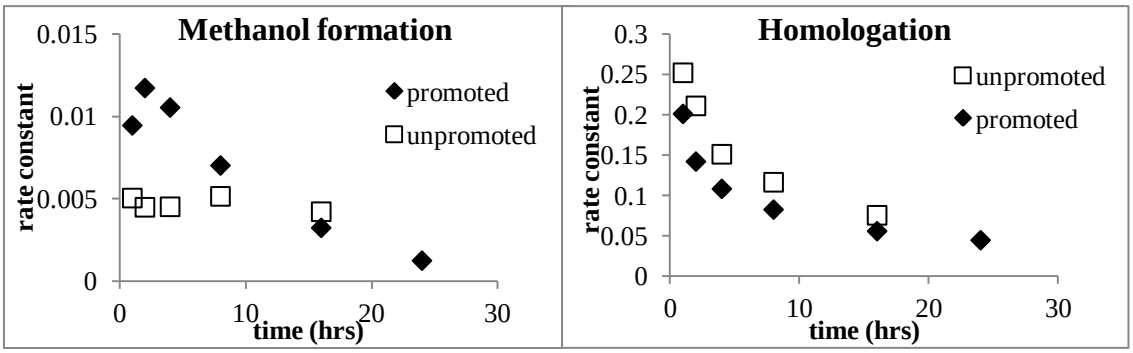

Figure 5.9. A comparison of the rate constants, k, using no promoter (white squares) and promoter (rotated tiles). Left: methanol formation. Right: ethanol formation, the promoter decreases the rate of ethanol formation significantly.

From figure 5.9 we can see another interesting clue. Both series have a reduction in activity over time, however, the promoted series shows a faster rate reduction than the unpromoted series. This effect could arise from inhibitions due to side reactions taking place in the reactor, or due to changes in the gas phase composition. The promoted reactions should be affected by this much more than the unpromoted reactions, because general activity is much higher, and the levels of synthesised products should be much higher. Again, side reactions are not taken into account during these calculations. Furthermore, the synthesis of methane from methanol is not taken into account. If the methane synthesis has a higher order in methanol than the ethanol synthesis it could be the case that methane synthesis increases with higher methanol levels. Higher levels of methane could "suffocate" the reactor gas phase, reducing the partial pressures of H_2 and CO. In later chapters the rate dependency of alcohol formation on the partial pressures of CO and H_2 is assessed.

5.4 The scope of action of [$HPBu_3$]Br

Encouraged by the results described in the previous section, it was decided to run a reaction with pure [$HPBu_3$]Br as a solvent. The system was completely inactive and there was no product formation. The product mixture was a white solid and the IR (figure 5.10) of this solid contained one set of peaks at 2033.7, 1970.2 and 1941.0 cm^{-1}, the ^1H NMR of the hydride region showed no hydrides. Assignment of this compound is difficult from IR alone, likely candidates are [$RuBr_2(PBu_3)(CO)_3$] and $[RuBr(PBu_3)_2(CO)_3]^+$, both compounds have C_s symmetry and should give rise to three active bands in the IR. Of these the former compound has higher electron density and should give rise to the lower frequency bands that we observe. Nonetheless, this species alone is not active for catalysis.

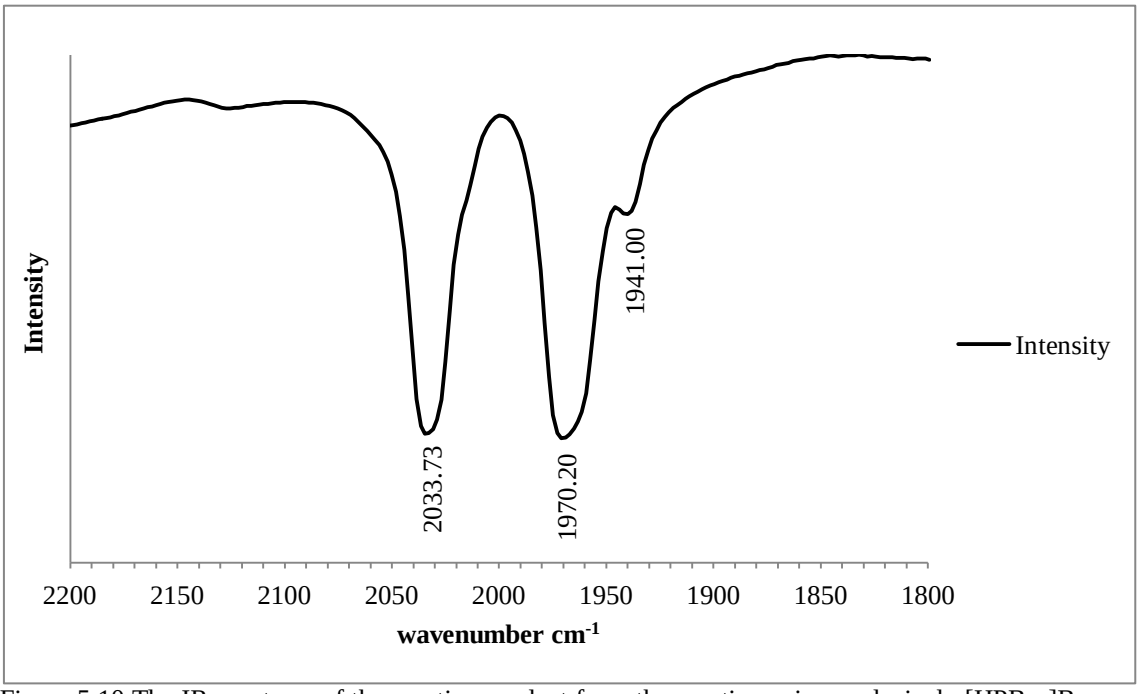

Figure 5.10 The IR spectrum of the reaction product from the reaction using exclusively [$HPBu_3$]Br as a solvent. Conditions used: [$Ru_3(CO)_{12}$] (0.5 g), [$HPBu_3$]Br (12.9 g), 200 ^oC, 250 bar, CO/ H_2 1:1, 4 hrs.

To further test the action of [$HPBu_3$]Br a series of experiments was carried out where the amount of [$HPBu_3$]Br present in the reactor was varied, using clean [PBu_4]Br as a solvent.

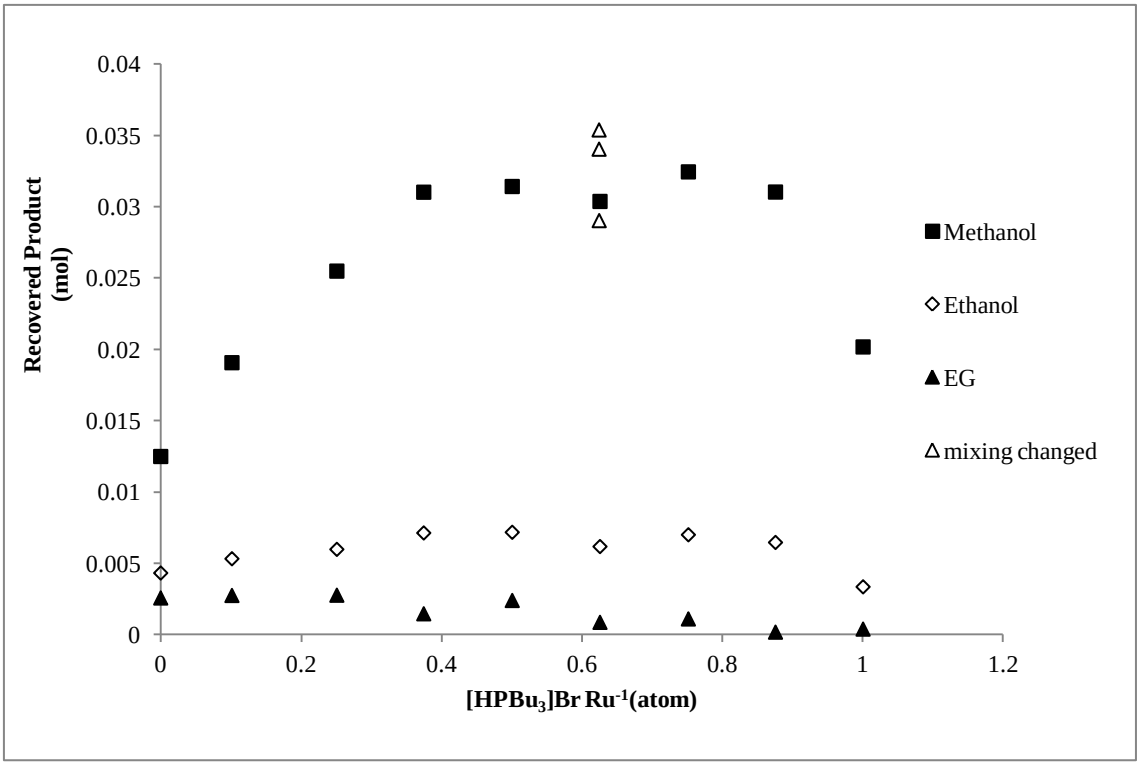

Figure 5.11. Product distribution from hydrogenation of CO catalysed by $[Ru_3(CO)_{12}]$ (0.5 g) in $[PBu_4]Br$ (15 g), CO/H_2 (1:1, 250 bar), 200 ^oC, 4 hrs with added $[Bu_3PH]Br$. Δ: experiments where we changed stirring speed, increasing the stirring yields increased product formation.

The results of this series of experiments, which are shown in Figure 5.11, clearly demonstrate that $[HPBu_3]Br$, in a limited and low concentration range, acts as a promoter for the CO hydrogenation reaction in this system. The activity increases up to a $[HPBu_3]Br$: Ru ratio of 0.4 mol/mol, reaches a plateau and then falls again above a ratio of 0.9. The plateau appears to arise because the rate of transport of gas across the liquid–gas interface becomes rate determining.

5.4.1 Addressing mass transfer issues

Because the system is showing mass transfer effects at higher activities, it was decided to start testing using lower levels of ruthenium and higher levels of H_2 in our system. Using viscous materials, like ethylene glycol we tested and designed a new stirrer and when we visually confirmed gas entrainment and proper mixing of the gas phase with the liquid phase we used this stirrer to perform our reactions. The prime feature of this stirrer is that it has larger paddles. Using these settings, we continued our research after repeating some already performed reactions for comparison. Using less ruthenium should reduce the total activity so that the rate determining step in the

catalytic reaction becomes slower than gas diffusion. A few tests were performed to verify to what extend our system is affected by the changes and the results of these are shown in figure 5.12 All further reactions were carried out with a [$Ru_3(CO)_{12}$] (0.25 g) and CO:H_2 = 1:2.

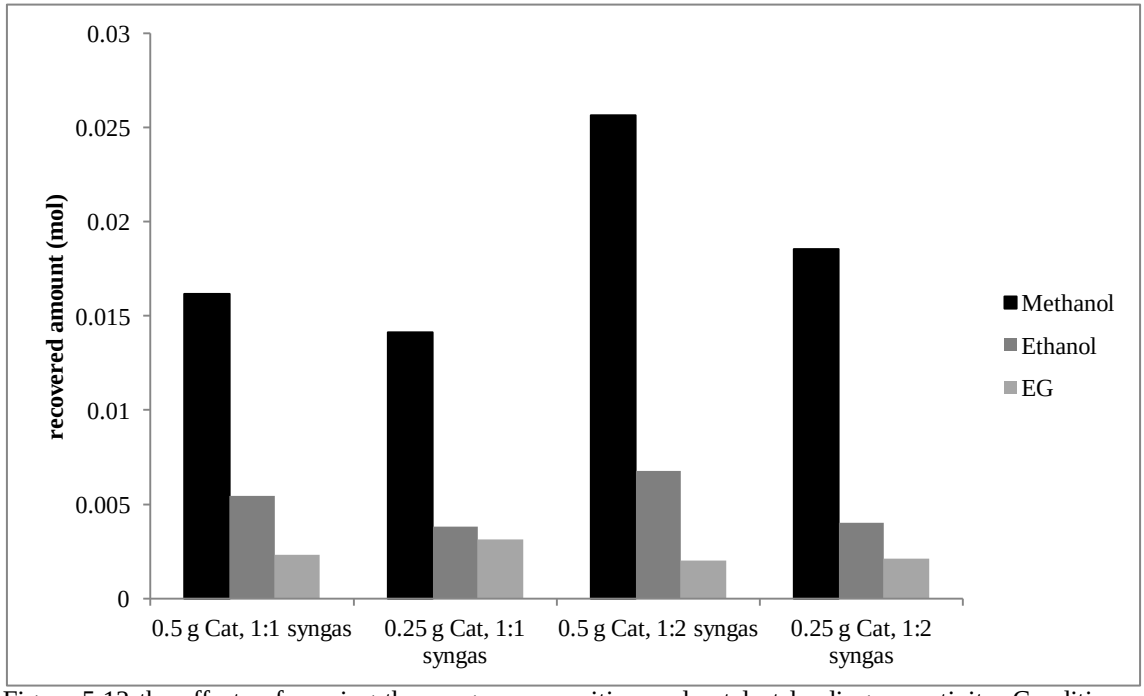

Figure 5.12 the effects of varying the syngas composition and catalyst loading on activity. Conditions: [PBu_4]Br (15 g), [$Ru_3(CO)_{12}$], 200 ^oC, 250 bar total pressure, 4 hrs.

Using different stirring rates or designs of paddles affects the reaction rate when a ratio of [$HPBu_3$]Br to Ru of 0.62 is employed (see also figure 5.11). The mass transport problem can be overcome when using lower concentrations of [$Ru_3(CO)_{12}$] and H_2/CO = 2/1. Under these conditions a more conventional curve is obtained (figure 5.13). It is notable that the peak of this plot is near the same ratio as that for the system with twice the concentration of ruthenium. It is the [$HPBu_3$]Br:Ru ratio, not the absolute concentration of [$HPBu_3$]Br that dictates its influence.

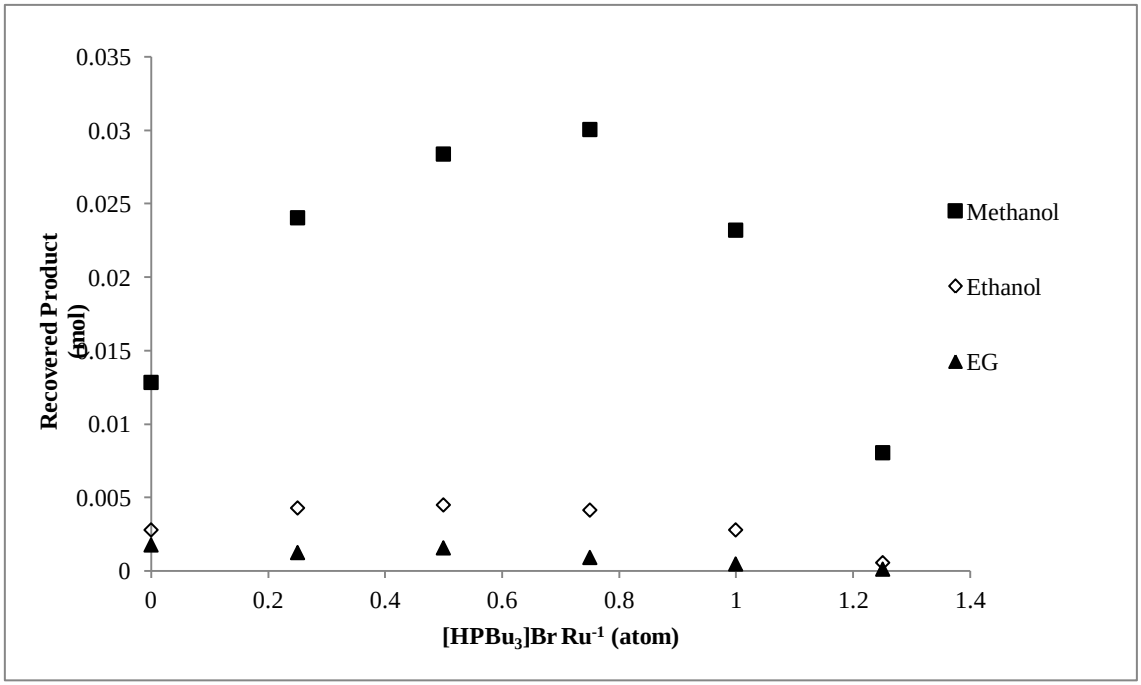

Figure 5.13 Product distribution from hydrogenation of CO catalysed by $[Ru_3(CO)_{12}]$ (0.25 g, mmol) in $[PBu_4]Br$ (15 g) with added $[Bu_3PH]Br$. CO/H_2 (1:2, 250 bar), 200 ^oC

5.4.2 Spectroscopic analysis of the product medium

At the end of the reactions depicted in figure 5.13, the colour varied markedly from dark red (no $[HPBu_3]Br$) through orange to yellow (Ru:$[HPBu_3]Br$ =1:1). This suggests a change in catalyst composition so we undertook spectroscopic analysis on these samples. When no $[HPBu_3]Br$ was added (dark-red solution obtained after the reaction), the IR spectrum (figure 5.14) showed peaks at 2112.0, 2073.1, 2014.5, 1987.7 and 1952.4 cm^{-1} and there was a peak at δ -12.67 ppm in the hydride region of the ^1H NMR spectrum.

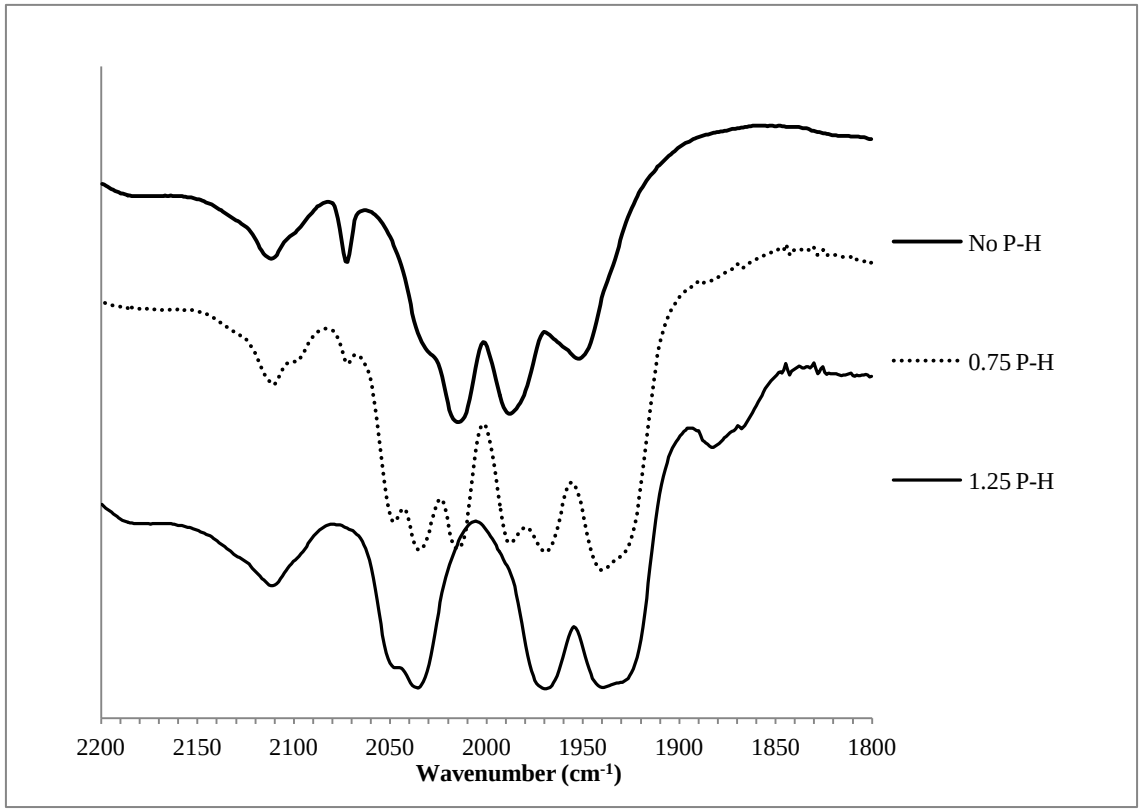

Figure 5.14. IR spectra obtained after CO hydrogenation of CO catalysed by $[Ru_3(CO)_{12}]$ (0.25 g, mmol) in $[PBu_4]Br$ (15 g) with a) no added $[HPBu_3]Br$; b) $[Bu_3PH]Br$ (0.75 mol (mol Ru)$^{-1}$ or c) $[Bu_3PH]Br$ (1.25 mol) (mol Ru)$^{-1}$. The expected vibrations for $[HRu_3(CO)_{11}]^-$, $[RuHBr(CO)_2(PBu_3)_2]$ and from $[Ru(CO)_3Br_3]^-$.

This can be assigned to $[HRu_3(CO)_{11}]^-$.[84] However, yellow post- reaction solutions obtained with $[HPBu_3]Br$ (≥ 1 mol (mol Ru)$^{-1}$, figure 5.14, lower spectrum, have IR absorptions at 2111.39, 2047.8, 2036.43, 1970.2, 1939.6 cm^{-1}, a less intense hydride resonance at δ -12.67 ppm and a new triplet hydride resonance at δ -6.30 ppm. We have assigned these to a mixture of $[RuHBr(CO)_2(PBu_3)_2]$ and $[Ru(CO)_3Br_3]^-$.[51, 84, 110]

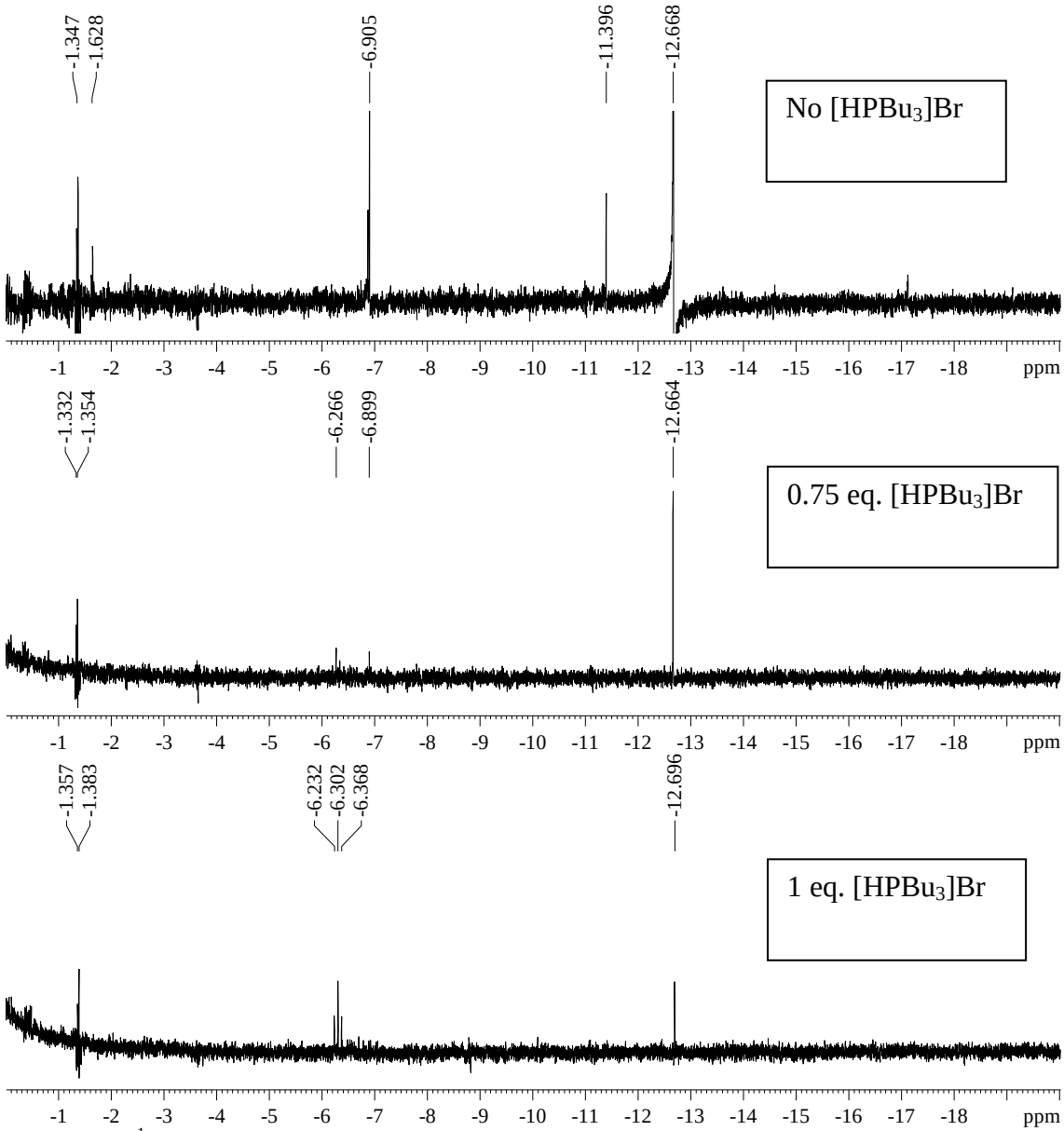

Figure 5.15. ^{1}H NMR spectra showing the hydride region of the product mixtures for three reactions where the amount of $[HPBu_3]Br$ was varied. Conditions: $[Ru_3(CO)_{12}]$ (0. 5 g, mmol) in $[PBu_4]Br$ (15 g) with added $[Bu_3PH]Br$. CO/H_2 (1:1, 250 bar), 200 ^{o}C. The amount of $[HPBu_3]Br$ relative to Ru is shown in the inset boxes.

All the spectra from successful reactions containing added $[HPBu_3]Br$ can be assigned as arising from mixtures of $[HRu_3(CO)_{11}]^-$, $[RuHBr(CO)_2(PBu_3)_2]$ and $[RuBr_3(CO)_3]^-$ with the relative intensities of the peaks belonging to each compound being dependent on the amount of $[HPBu_3]Br$ added. This suggests that, for higher reactivity, a catalyst composition is needed which contains several species and that $[HPBu_3]Br$ reacts with $[HRu_3(CO)_{11}]^-$ to give $[Ru(CO)_3Br_3]^-$ and $[RuHBr(CO)_2(PBu_3)_2]$. Catalysis may occur through intermolecular hydride transfer pathways,[49, 56, 65] since neither species alone induces optimum activity. Dombek has suggested that the

analogous iodide complexes of $[HRu_3(CO)_{11}]^-$ and $[Ru(CO)_3Br_3]^-$are present in CO hydrogenation reactions catalysed by $[Ru_3CO)_{12}]$ in the presence of iodide,[10] although no mention is made of P-H phosphonium salts. Ono and coworkers have also shown that $[Ru_3(CO)_{12}]$ reacts with bis(triphenylphosphine)iminium chloride and HCl to give $[Ru(CO)_3Cl_3]^-$, but suggest that this complex is inactive for CO hydrogenation, the active species in this system being $[HRu_3CO_{11}]^-$.[111]

5.5 The effect of $[HPBu_3]Br$ on the rates of methanol and ethanol formation

Although the model we have derived at the start of this chapter has limits, it is a capable tool for decoupling the rates of individual reactions. For instance, in assessing data at $[HPBu_3]Br$:Ru = 1.25, the drop in methanol formation would skew any visual observation based on figure 5.11 or 5.13 about the relative rate of ethanol formation. It is difficult to tell whether the rate of ethanol formation is in fact low, or that it only seems low as a result of the low methanol concentration. Because k_2 varies over time, only measurements can be compared if they had the same reaction time. This is the case in this series.

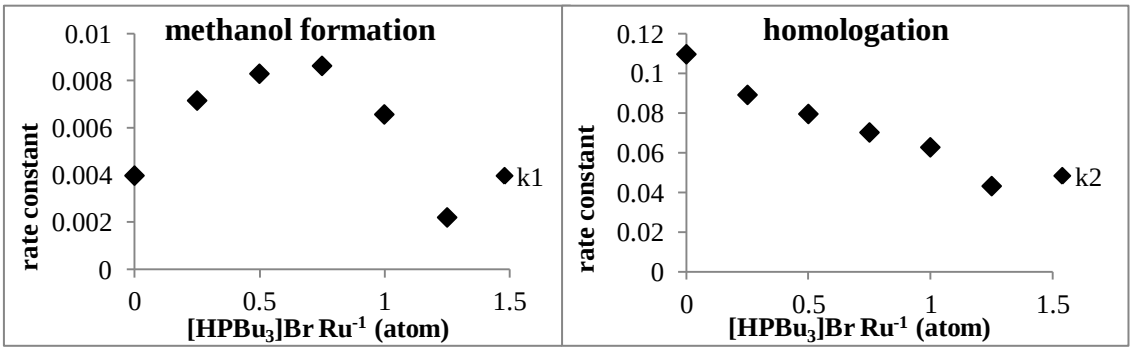

Figure 5.16. The obtained rate constants for the $[HPBu_3]Br$ series. Left the rate of methanol formation. Right, the rate of ethanol formation. Conditions: $[Ru_3(CO)_{12}]$ (0.25 g, mmol) in $[PBu_4]Br$ (15 g) with added $[Bu_3PH]Br$. CO/H_2 (1:2, 250 bar), 200 ^oC. The data in these figure is from the series displayed in Figure 3.12.

The results show that although the rate constant for methanol formation is increased significantly with low levels of $[HPBu_3]Br$ the methanol formation rate constant decreases significantly again when the levels of $[HPBu_3]Br$ are increased beyond a $[PHBu_3]Br$:Ru ratio of 0.75. The rate of ethanol formation is affected completely differently; it is not improved by the presence of $[HPBu_3]Br$, rather it

declines linearly with increasing $[HPBu_3]Br$ levels. Using $[HPBu_3]Br$ would not be favourable if the emphasis of synthesis lies towards higher alcohol formation. From the IR data we can see that $[HPBu_3]Br$ affects the ratio of species that are present after the reaction (and most likely during catalysis) from $[HRu_3(CO)_{11}]^-$ to $[RuBr_3(CO)_3]^-$ and (possibly) $[RuHBr(CO)_2(PBu_3)_2]$.

$$\underset{\mathbf{1}}{[Ru_3(CO)_{12}]} \xrightleftharpoons{H_2 + Br^-} \underset{\mathbf{2}}{[HRu_3(CO)_{11}]^-} \xrightleftharpoons{HPBu_3Br} \underset{\mathbf{3}}{[RuBr_3(CO)_3]^-} + \underset{\mathbf{4}}{[RuHBr(CO)_2(PBu_3)_2]}$$

Without $[HPBu_3]Br$ a natural equilibrium exists after catalysis where 2 and 3 are formed from 1 in the presence of H_2 and Br^- however the evolution of 4 has not been seen before. Most likely the $[HPBu_3]Br$ dissociates during catalysis to form the phosphine and HBr (catalysed by Ru or not) and HBr is known to react with 1 and 2 to form 3.[72] Dombek has already found that the rate of catalysis increases significantly when the ratio of 2 and 3 is 2:1 and perhaps the presence of $[HPBu_3]Br$ assists this.[10] We are still unsure of the effect of species 4, however we know from experiments described in the following chapters that we can achieve higher activity if we create a system where species 4 is not formed. So most likely it is an inactive form of ruthenium.

5.6 HBr series

Starting with the reaction of $[Ru_3(CO)_{12}]$ (0.25 g), $[PBu_4]Br$ (15 g) and 1:2 CO/H_2 at 250 bar for 4 hrs at 200 ^oC. The experiment with various amounts of added promoter (HBr) was repeated. To keep the level of Br^- the same for each experiment the amount of $[PBu_4]Br$ was adjusted to match the total amount of Br^- in the system equal to using 15 g of $[PBu_4]Br$. The results are given in figure 5.17:

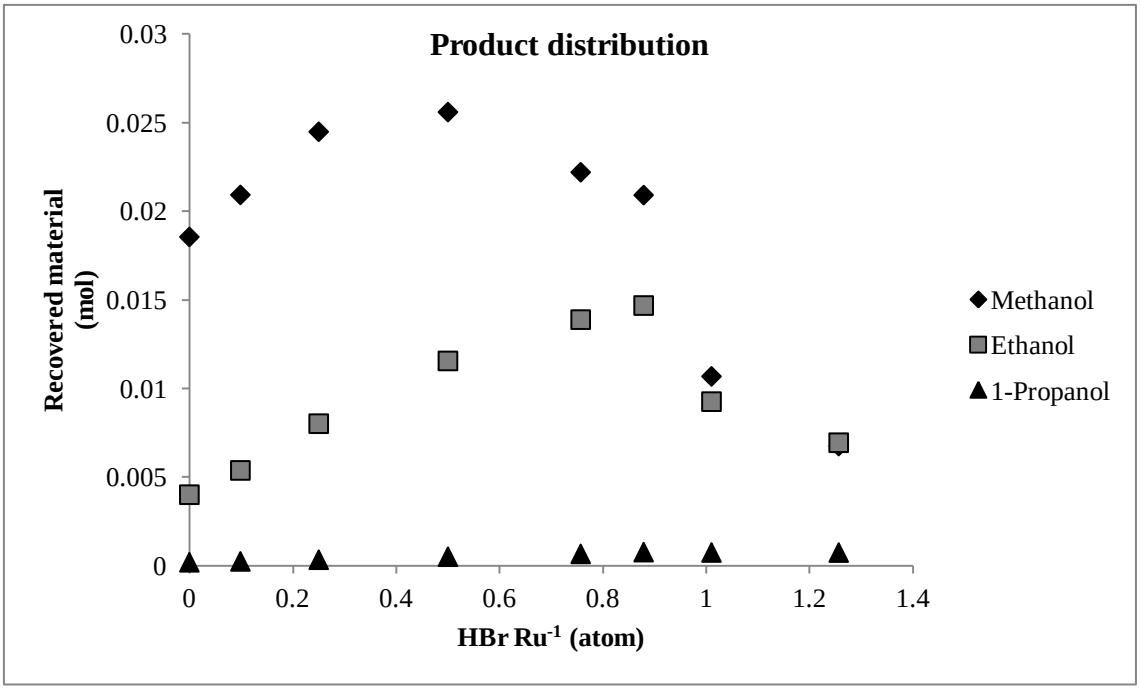

Figure 5.17. Product distribution from the HBr series. With varying levels of HBr the product dirstribution changes significantly. Conditions: $[PBu_4]Br$ (~15 g), 200 °C, 250 bar total pressure, 4 hrs. Catalyst is $[Ru_3(CO)_{12}]$ (0.25 g). Amounts of $[PBu_4]Br$ varied to keep the amount of halide constant throughout the series. HBr added as conc. aqueous HBr (48%).

The activity of the system changes significantly upon using HBr as a promoter. This is also apparent from the gas uptake measurements (not shown here). The change in activity resembles that when using $[HPBu_3]Br$, but there are a few significant differences. The increase in methanol formation using HBr is somewhat lower than with $[HPBu_3]Br$, but overall a similar polynomial curve is generated. As in the $[HPBu_3]Br$ promoted reactions, the overall activity of the system is reduced if levels of HBr are used approaching HBr/Ru =1 or higher. Overall, the increase in methanol levels is up to 150%. Furthermore, the levels of ethanol found after the reaction increases significantly and continue increase linearly throughout the series up to the point where all catalysis seems to be inhibited. Interestingly, in the region HBr $Ru^{-1} > 1$ the methanol synthesis is decreased more than the ethanol synthesis and we obtain higher levels of ethanol after the reaction than methanol. One reason that the methanol yield does not rise as high when using HBr as when using $[HPBu_3]Br$ may be that much more of the methanol is converted into ethanol. A plot of the overall conversion to methanol + ethanol when using HBr or $[HPBu_3]Br$ is shown in figure 5.18, which makes it clear that the overall promoting ability of HBr and $[HPBu_3]Br$ is very similar.

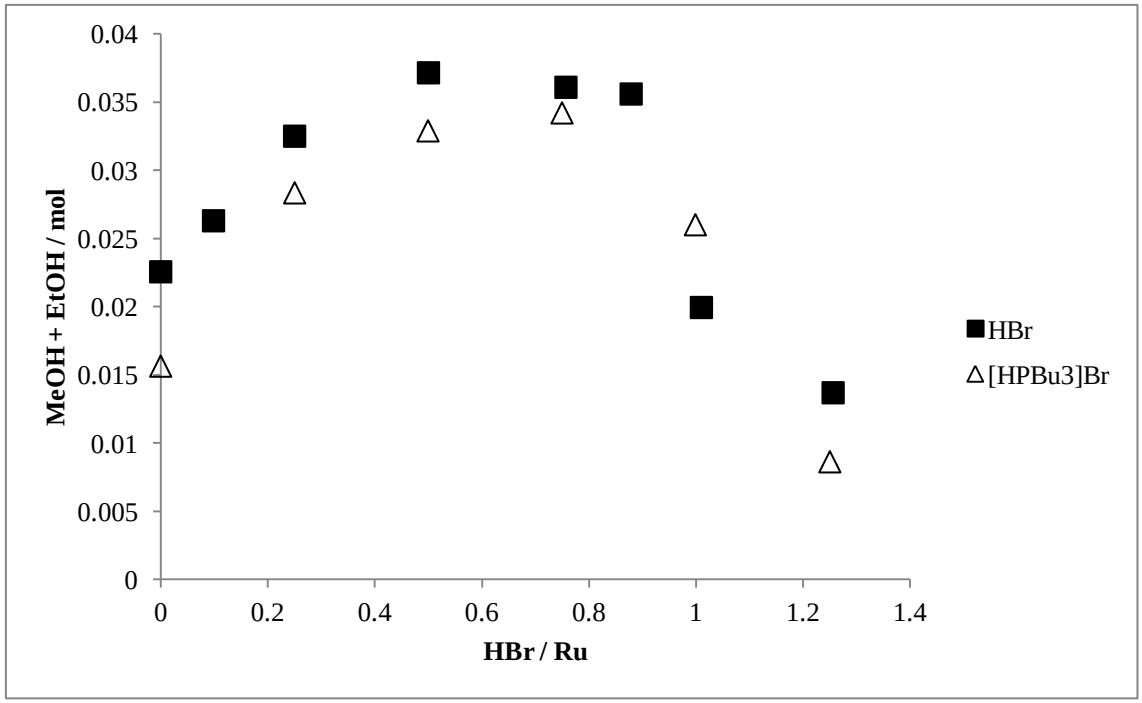

Figure 5.18. Plot of the yield of methanol +ethanol against H/Ru ratio for CO hydrogenation reactions promoted by HBr and by $[HPBu_3]Br$.

From a comparison of figures 5.13 and 5.17, it appears that the homologation reaction is promoted more by HBr than by $[HPBu_3]Br$. To confirm this we applied the results obtained using HBr to the model developed in Chapter 4 to determine the individual rate constants for methanol formation and the homologation step. The results are shown in figure 5.19.

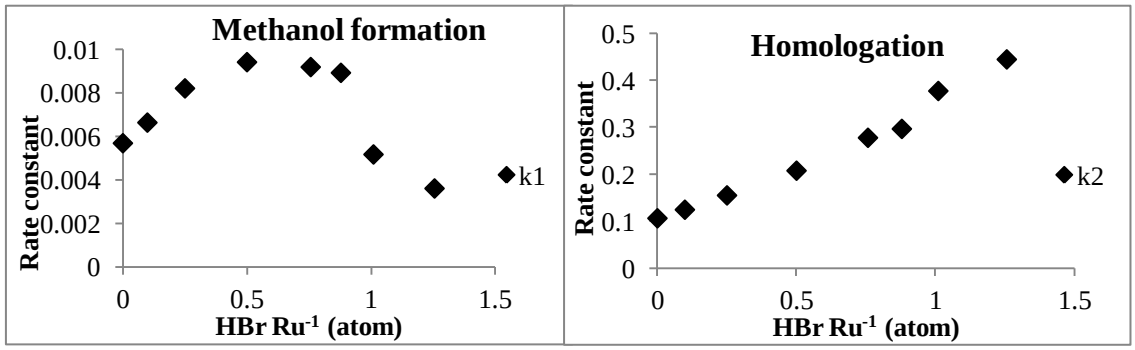

Figure 5.19. The calculated rate constants through the HBr series. As it appears there is a near linear relation between the amount of HBr added and the rate of homologation. Conditions: $[PBu_4]Br$ (~15 g), 200 ^{o}C, 250 bar total pressure, 4 hrs. Catalyst is $[Ru_3(CO)_{12}]$ (0.25 g). Amounts of $[PBu_4]Br$ varied to keep the amount of halide constant throughout the series. HBr added as conc. aqueous HBr.

The rate of methanol formation forms a curve with a maximum around a ratio of HBr Ru^{-1} = 0.625. After that, the rate of methanol production reduces gradually until the ratio is 1 when the production of methanol is halted considerably. Interestingly, the rate

of ethanol formation does not have such a curve and continues to increase almost linearly to nearly 4.5 times the starting value with increasing levels of HBr. Fitting a curve through the data for k_2 shows the best fit comes from using an exponential function. The best fit was found using excel and is a curve where the rate constant follows the expression $k_2=0.1125\ e^{1.144x}$ and x is the ratio HBr Ru^{-1}. As with $[HPBu_3]Br$, the colour of the product mixture after the reaction changed throughout the series going from dark-red at low levels of HBr to orange with HBr Ru^{-1} =0.5 to yellow at HBr Ru^{-1} = 1.25. Clearly, the composition of the catalyst mixture changes throughout the series. IR spectra of the product mixture after each reaction were measured and showed that the major species that are present to be $[HRu_3(CO)_{11}]^-$ and $[RuBr_3(CO)_3]^-$. These are the analogous two species of ruthenium carbonyls that Dombek and Warren had described in the iodide promoted system[10, 52, 72] and the level of each species is dependent on the amount of HBr introduced into the reaction. Figure 5.20 shows the IR spectra of the carbonyl region of three reactions, at HBr Ru^{-1} = 0 (dark red), 0.625 (orange) and 1.25 (yellow).[a] The levels of each species cannot be quantified, but there seems to be a gradual, continuous change.

[a] A table of peaks for these spectra can be found in the experimental section.

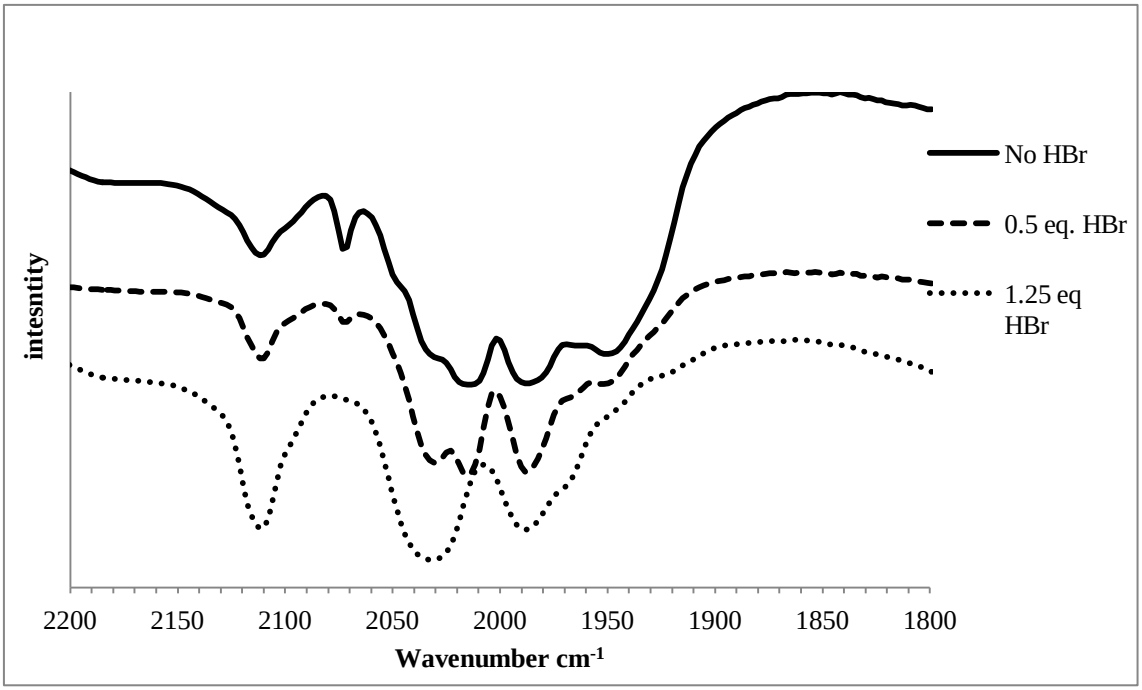

Figure 5.20. IR spectra of selected product liquids in the HBr series. Spectra taken after the reaction. In the reaction without added HBr we find that the primary compound is $[HRu_3(CO)_{11}]^-$. In the reaction with 1.25 eq. of HBr (to Ru) we find that the primary compound is $[RuBr_3(CO)_3]^-$. Conditions: $[PBu_4]Br$ (15 g), 200 ^oC, 250 bar total pressure, 4 hrs. Catalyst is $[Ru_3(CO)_{12}]$ (0.25 g). Amounts of $[PBu_4]Br$ varied to keep the amount of halide constant throughout the series. HBr added as conc. aqueous HBr.

In the unpromoted reaction we see primarily $[HRu_3(CO)_{11}]^-$ and in the reaction with very high levels of HBr (HBr Ru^{-1} = 1.25) we find almost exclusively $[RuBr_3(CO)_3]^-$. In between a mixture of both compounds is found, with the relative intensity of $[RuBr_3(CO)_3]^-$ continually increasing. Likewise, inspection of the hydride region of the ^1H NMR specrum reveals the presence of the hydride $[HRu_3(CO)_{11}]^-$ in all samples at δ -12.66 ppm (figure 5.21). The hydride signal *seems* to decrease with increasing levels of HBr, however it is difficult to tell with small hydride peaks, where intensity and the S/N ratio could be more a function of shimming and concentration than of actual composition.

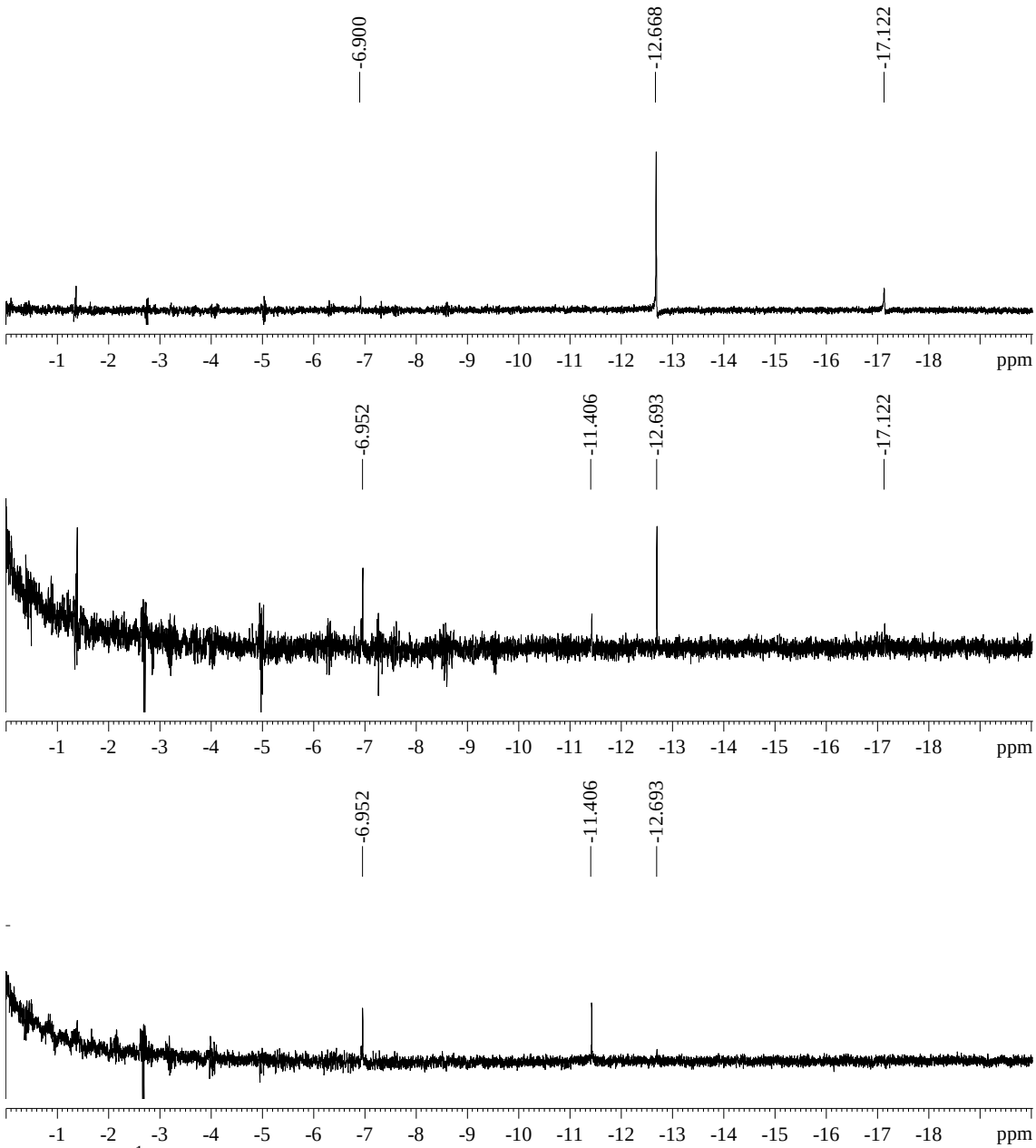

Figure 5.21 ^{1}H NMR of the hydride regions. The samples were post-reaction product liquids in Acetonitrile–d_3. From top to bottom: No HBr used, 0.75 eq. (to Ru) of HBr, 1.25 eq. (to Ru) of HBr added. Conditions: [PBu_4]Br(~15 g), 200 ^{o}C, 250 bar total pressure, 4 hrs. Catalyst is [$Ru_3(CO)_{12}$] (0.25 g). Amounts of [PBu_4]Br varied to keep the amount of halide constant throughout the series. HBr added as conc. aqueous HBr.

Taken together, these results suggest that the two species that are present have different roles and presence of HBr promotes formation of $[RuBr_3(CO)_3]^-$ from $[HRu_3(CO)_{11}]^-$ or $[Ru_3(CO)_{12}]$.

The existence of a maximum rate of methanol formation within the series suggests that there is a cooperative effect between $[HRu_3(CO)_{11}]^-$ and $[RuBr_3(CO)_3]^-$ for the formation of methanol. This is not a new concept, when Dombek found the

existence of the analogous iodide complexes he performed a series of reactions where he varied the ratio between them, the results are copied in figure 5.22.

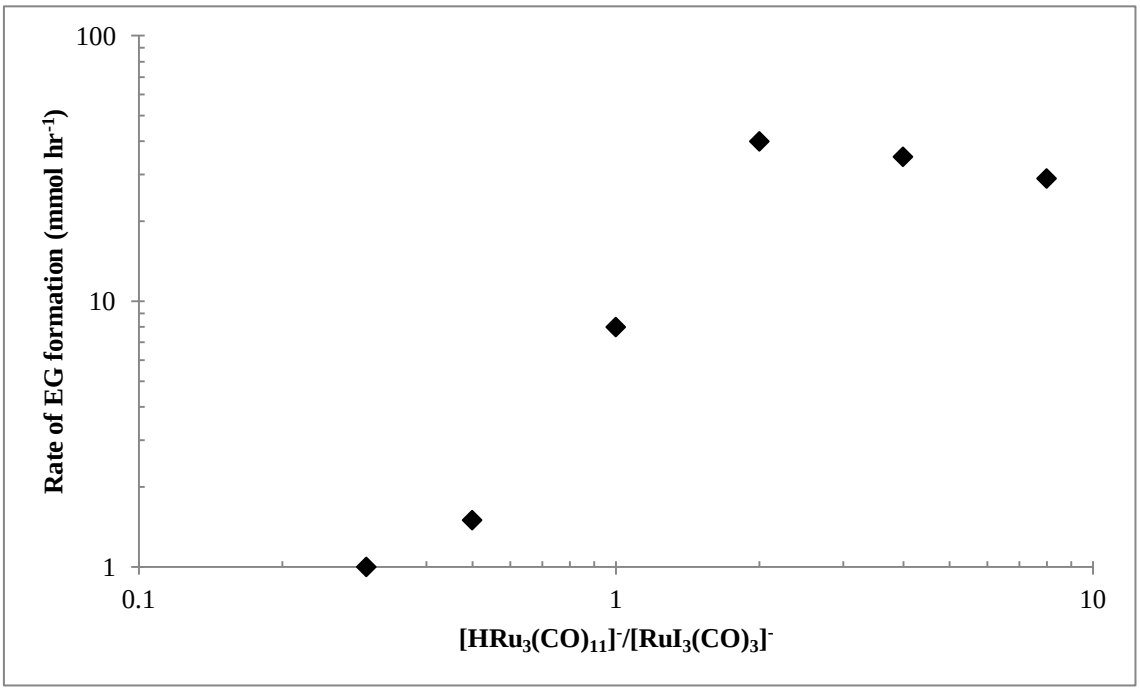

Figure 5.22. The effect of varying the ratio of $[HRu_3(CO)_{11}]^-$ to $[RuI_3(CO)_3]^-$. The data was estimated from Dombek [10], figure 2, and the scale on the rate of EG formation (y-axis) was changed to display a logarithmic scale. Using PPN salts of $[HRu_3(CO)_{11}]^-$ and $[RuI_3(CO)_3]^-$ (0.86 mmol), 36 mmol NaI in sulfolane at 230 ^{0}C, 850 atm in syngas (CO:H_2 = 1:1)

The optimum ratio of $[HRu_3(CO)_{11}]^-$ to $[RuI_3(CO)_3]^-$ for the synthesis of ethylene glycol was, in this system, 2:1 (figure 5.22), which is also the ratio in which they should be formed, from just $[Ru_3(CO)_{12}]$ halide and H_2, as shown in Scheme 5.1.[10]

$$7\,[Ru_3(CO)_{12}] + H_2 + 3\,I^- \longrightarrow 6\,[HRu_3(CO)_{11}]^- + 3\,\text{fac-}[RuI_3(CO)_3]^- + 9\,CO$$

Scheme 5.1. When $[Ru_3(CO)_{12}]$ comes into contact with H_2 and I^- at elevated temperatures it heterolytically splits the hydrogen upon loss of CO to produce $[HRu_3(CO)_{11}]^-$. Most likely the I^- acts as a base to collect the proton. HI can then react with $[Ru_3(CO)_{12}]$ to form facial $[RuI_3(CO)_3]^-$. It is very likely that the same occurs using HBr to form $[RuBr_3(CO)_3]^-$.

Our findings do not match: Dombek does not add a proton source to his system so that, if the ruthenium complex reacts the same towards bromide as it does towards iodide, we should see both $[HRu_3(CO)_{11}]^-$ and $[RuBr_3(CO)_3]^-$, whereas we mainly see $[HRu_3(CO)_{11}]^-$, although some $[RuBr_3(CO)_3]^-$ is also present, perhaps from reaction of $[HRu_3(CO)_{11}]^-$ with the HBr formed along with it:

$[Ru_3(CO)_{12}] + H_2 + [PBu_4]Br \longrightarrow [PBu_4][HRu_3(CO)_{11}] + HBr + CO$

$[Ru_3(CO)_{12}] + 6\ HBr + 3\ [PBu4]Br \longrightarrow 3\ fac\text{-}[RuBr_3(CO)_3][PBu_4] + 3\ CO + 3\ H_2$

Scheme 5.2 The formation of $[HRu_3(CO)_{11}]^-$ and $[RuBr_3(CO)_3]^-$ from $[Ru_3(CO)_{12}]$ and H_2.

Dombek's catalytic results refer mainly to ethylene glycol (EG), yet he also makes methanol in his system and it appears that the species present are also correlated with methanol formation. In our system, EG synthesis is minor, increasing slightly with increasing ratio of $[HRu_3(CO)_{11}]^-$ to $[RuI_3(CO)_3]^-$.

There are two possible explanations for the differences between Dombek's system and ours, which was based on Knifton's system: the first is that Dombek inadvertently had a source of H^+ present. We have shown above that this can easily occur, in our case from contamination of the $[PBu_4]Br$ by $[HPBu_3]Br$. However, Dombek adds his iodide as KI and his solvent is N-methyl pyrrolidone. It seems unlikely that either of these will contain an adventitious Brønsted acid. The alternative explanation is that bromide genuinely behaves differently from iodide in these systems. So that the equilibrium constant for reaction in scheme 5.3 is smaller for bromide than for iodide so that added HI is not required to generate a significant amount of $[RuI_3(CO)_3]^-$ in the KI/NMP system but added HBr is required for the $[PBu_4]Br$ system.

$[PBu_4][HRu_3(CO)_{11}] + 7\ HBr + 3\ [PBu_4]Br \rightleftharpoons 3\ [PBu_4][RuBr_3(CO)_3] + 7\ H_2 + 2\ CO$

Scheme 5.3. The net equilibrium between $[HRu_3(CO)_{11}]^-$ and $[RuBr_3(CO)_3]^-$.

This is evidently not a feature simply of iodide vs bromide, since we discuss the related $[PBu_4]I$ system later in the following chapter and the IR spectrum obtained from a solution of $[Ru_3(CO)_{12}]$ in $[PBu_4]I$ without added HI is very similar to that for $[Ru_3(CO)_{12}]$ in $[PBu_4]Br$. The result is that Knifton's and Dombek's systems are not necessarily comparable because of the use of different solvents and conditions. Further, using the model, it has been shown that the ratio of $[HRu_3(CO)_{11}]^-$ to $[RuI_3(CO)_3]^-$ significantly affects the methanol and homologation reactions in a different ways, with different optimal conditions for each of them. Usually, having two reactions taking place in tandem in one pot is desirable. However, in this situation there may be an argument for splitting up the reactions into two separate reactors. In one pot methanol is synthesised under the favourable conditions for methanol synthesis (HBr ; Ru = 0.6),

and in the second pot, the conditions will be optimised for methanol homologation (excess HBr). Splitting up the reaction may make it easier to investigate each reaction and increase the level of focus for each reaction. Even though there are good sources to ethanol through fermentation, the most interesting reaction taking place may be the ethanol formation from methanol as there are to date not many alternatives known that do this reaction efficiently. In later sections we attempt to look at the homologation step separately to try to define significant factors.

5.7 The effect of tributylphosphine

To complete the work on understanding the action of the $[HPBu_3]Br$ promoter it was necessary to perform one more experiment to assess the effect of free phosphine present if free HBr is generated under reaction conditions using $[HPBu_3]Br$. For this the reactor was set up as usual, with $[PBu_4]Br$ (15 g) and $[Ru_3(CO)_{12}]$ (0.25 g) and added PBu_3 (0.5 eq. to Ru) under inert conditions. In figure 5.23 a comparison is made between reactions that contain no added promoter, added $[HPBu_3]Br$, added HBr and added PBu_3.

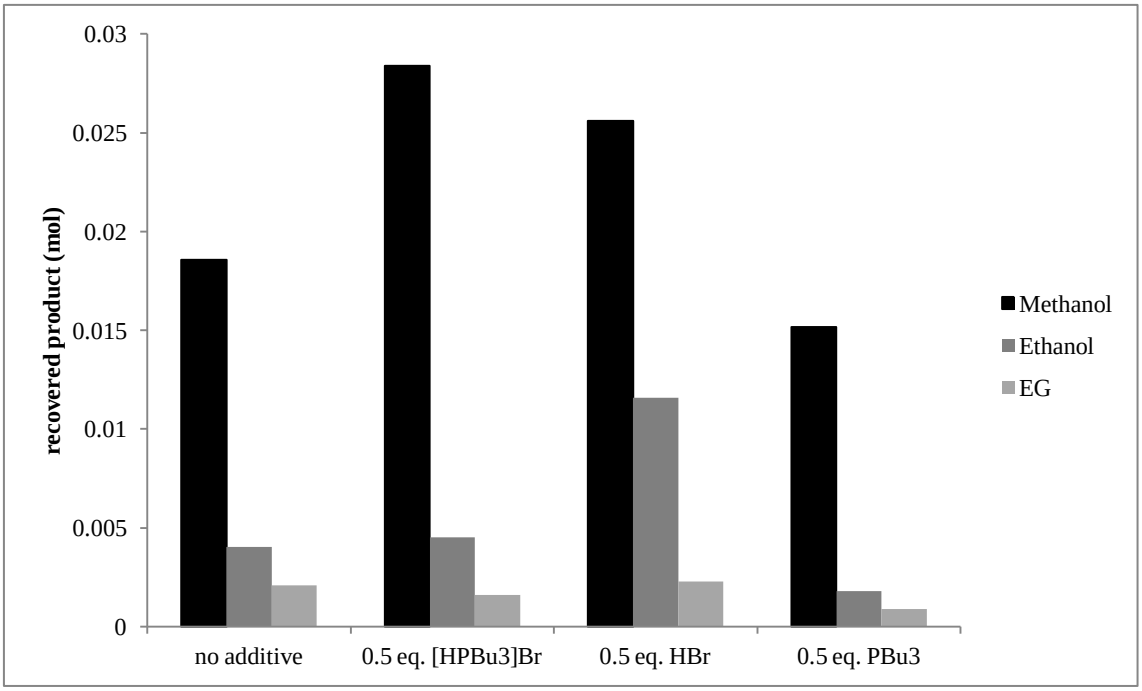

Figure 5.23 The affect of $[HPBu_3]Br$, HBr and PBu_3 on the product formation of a standard reaction. Conditions: $[PBu_4]Br$(~ 15 g), 200 ^oC, 250 bar syngas ($CO:H_2$ 1:2) total pressure, 4 hrs. Catalyst is $[Ru_3(CO)_{12}]$ (0.25 g). Amounts of $[PBu_4]Br$ varied to keep the amount of halide constant. HBr added as conc. aqueous HBr.

From the histogram it can be seen that in both the $[HPBu_3]Br$ and HBr promoted reactions the total methanol synthesis is increased significantly. For the reaction using HBr the homologation step is increased too, and so the total level of methanol is lower, but the ethanol levels are doubled. Compared to the unpromoted reaction the PBu_3 has almost no effect, other than inhibiting catalysis slightly, especially the ethanol formation. The IR spectra indicated that free HBr promotes $[RuBr_3(CO)_3]^-$ formation, however the product analysis shows that if there is any free phosphine present it will react with this species to form an inactive species that does not participate in catalysis. Therefore, the concentration of homologation catalyst is reduced, and thus homologation is reduced. A logical set of products from the reaction of $[RuBr_3(CO)_3]^-$ and PBu_3 would be $[RuBr_2(CO)_3(PBu_3)]$ or $[RuBr(CO)_3(PBu_3)_2]^+$. Inspection and comparison of the IR spectrum (figure 5.24) obtained from this reaction with the spectra obtained from a reaction using $[HPBu_3]Br$ and HBr tells that the species that is formed with PBu_3 has detectable CO vibrations at 2047.56, 1969.79 and 1939.73 cm^{-1}.

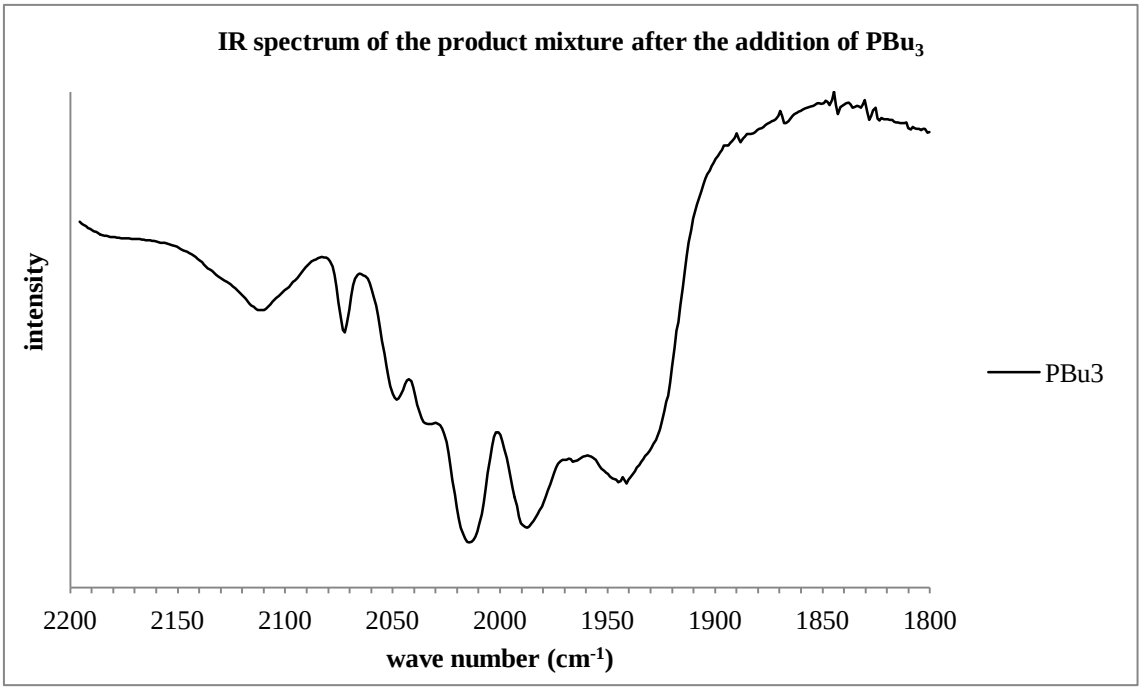

Figure 5.24 The IR spectrum of the product mixture of reaction containing PBu_3 shows the rise of peaks at 2047.56, 1969.79 and 1939.73 cm^{-1} due to coordination of PBu_3 to a ruthenium carbonyl species. These peaks are also present in the reactions with $[HPBu_3]Br$. Conditions: $[PBu_4]Br$(~15 g), PBu_3 (0.75 eq. to Ru), 200 ^oC, 250 bar syngas ($CO:H_2$ 1:2) total pressure, 4 hrs. Catalyst is $[Ru_3(CO)_{12}]$.

The lower formation of ethanol when PBu_3 is added to the system also suggests that PBu_3 could scavenge an intermediate in ethanol formation. One possibility is that ethanol is formed through MeBr, which readily reacts with PBu_3. Support for this suggestion comes from ^{31}P NMR studies of the post reaction solutions, which contains a singlet at δ 31.91 ppm, exactly the shift for an authentic sample of $[MePBu_3]Br$. A doublet at δ 1.78 ppm ($^2J_{PH}$ = 13.75 Hz) confirms that $[MePBu_3]Br$ is indeed present. This is apparent from the following NMR spectra. $[MePBu_3]Br$ was synthesised, using an analogous methods for preparing $[HPBu_3]Br$. Instead of generating HBr, MeBr was generated using acyl bromide and methanol. The product spectra are shown in figures 5.25 and 5.26.

methyl tributyl phosphonium bromide

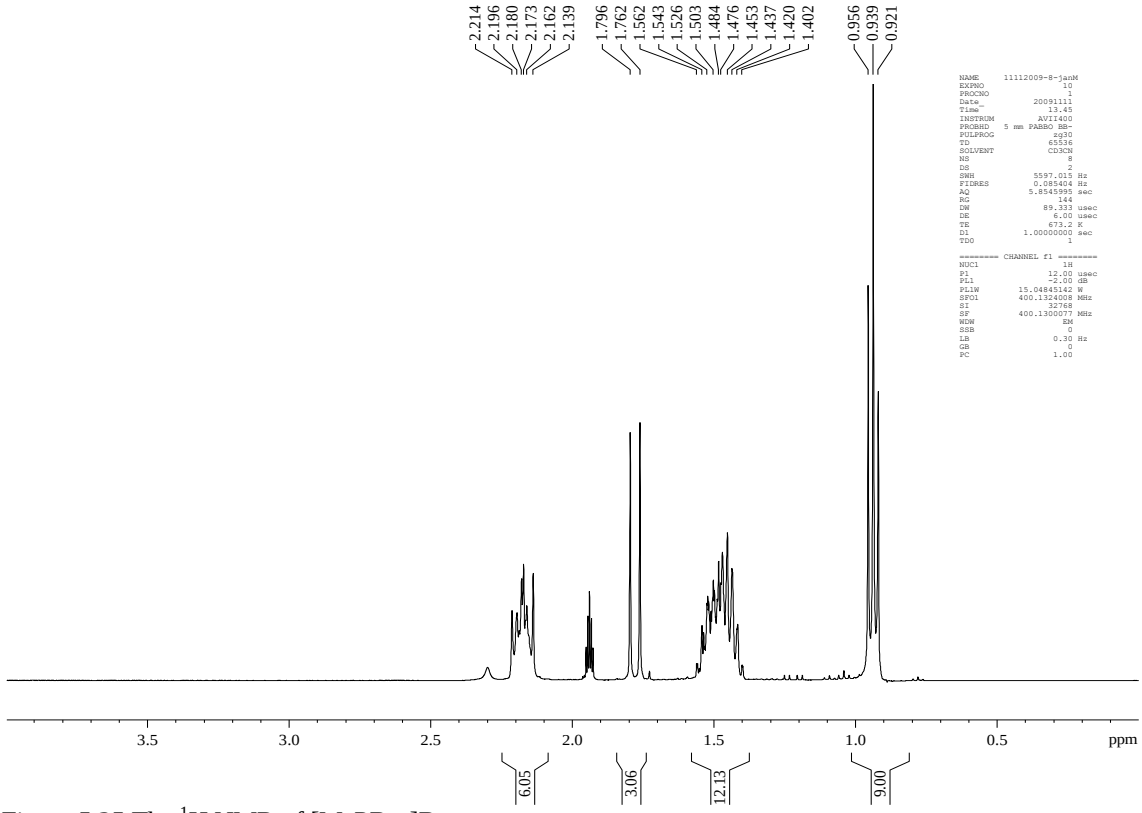

Figure 5.25 The ^{1}H NMR of [$MePBu_3$]Br.

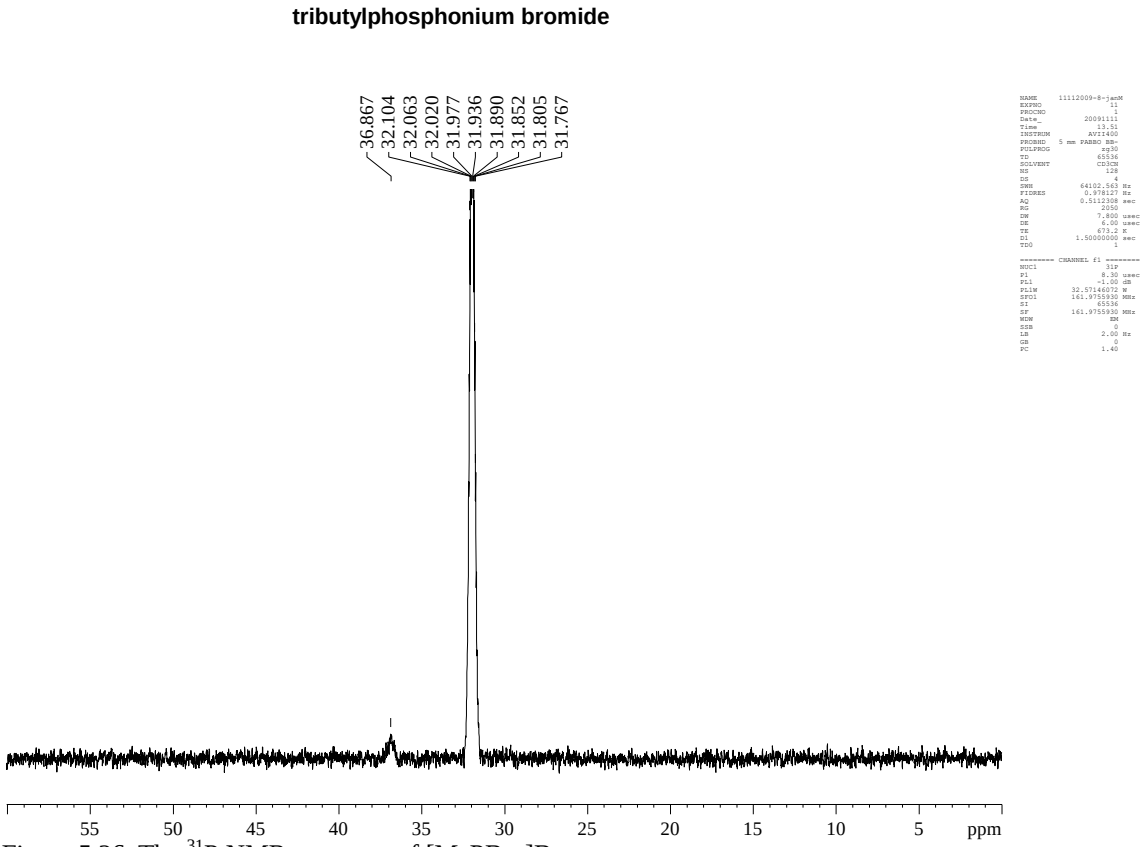

Figure 5.26. The ^{31}P NMR spectrum of [$MePBu_3$]Br.

These NMR signals with spectra can be compared with product mixtures using [$HPBu_3$]Br. When we do this, the presence of small amount of this compound after the reaction is found:

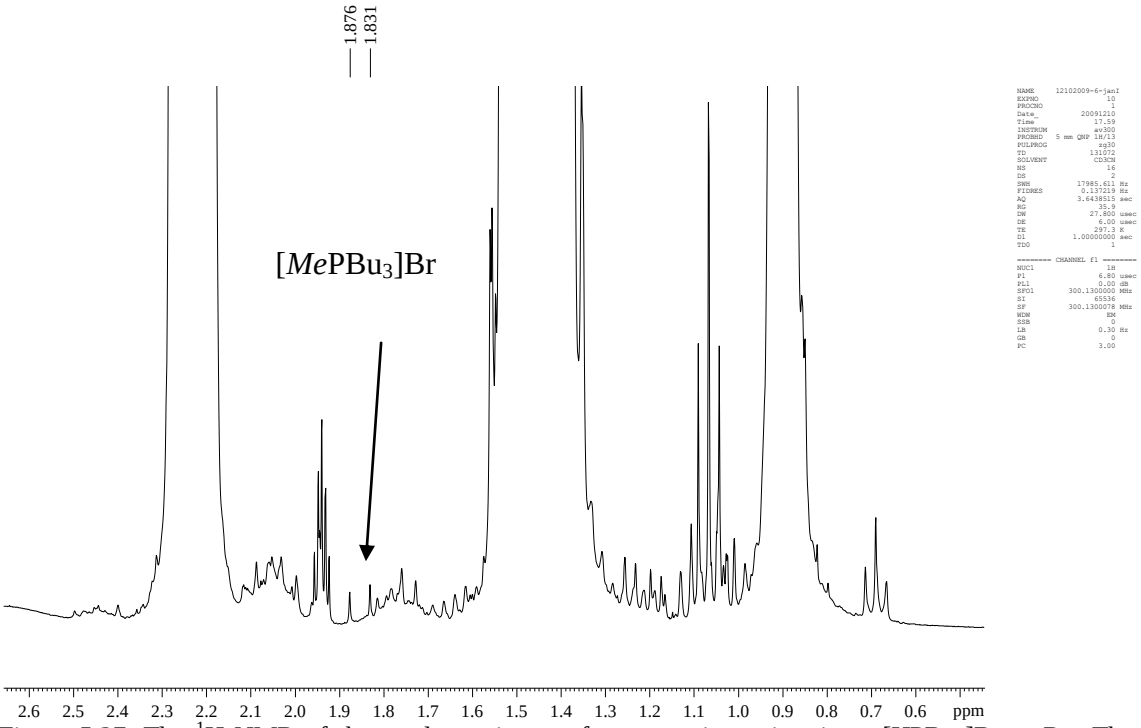

Figure 5.27. The ^{1}H NMR of the product mixture after a reaction using 1 eq. $[HPBu_3]Br$ to Ru. The doublet at δ 1.85 ppm is slightly shifted. However, a spectrum taken after a reaction using 0.75 eq. of $[MePBu_3]Br$ shows the same peaks. These peaks are absent when a reaction is performed using HBr as a promoter.

Through labelling studies it was shown that ethanol is formed through methanol as an intermediate, so the overall rate of methanol production is represented by the rate of formation of [methanol+ethanol]. The trend in [methanol+ethanol] yield together with IR studies, which show that $[HRu_3(CO)_{11}]^-$ smoothly converts to $[RuBr_3(CO)_3]^-$ as HBr is added, also reinforce the view that both $[HRu_3(CO)_{11}]^-$ and $[RuBr_3(CO_3]^-$ must be present in the solution for good activity for methanol production.

The situation for ethanol is different when using HBr compared to using $[HPBu_3]Br$. In the presence of HBr, the yield of ethanol increases as [HBr] is increased, only falling when the yield of methanol becomes low, although the ratio of ethanol/methanol continues to increase. These observations suggest that $[RuBr_3(CO)_3]^-$, which also increases at the expense of $[HRu_3(CO)_{11}]^-$ as HBr is added is the major species responsible for conversion of methanol to ethanol. In contrast the yield of ethanol remains fairly constant as increasing amounts of $[HPBu_3]Br$ are added, reducing at higher concentrations of $[HPBu_3]Br$. Since $[MePBu_3]Br$ is observed by NMR spectroscopy when $[HPBu_3]Br$ is the promoter, but not when HBr is added, we propose that the free PBu_3 liberated when HBr is formed from $[HPBu_3]Br$ acts to scavenge

MeBr, which is an intermediate in ethanol formation, thus reducing the rate of ethanol formation as more $[HPBu_3]Br$ is added.

Concluding, it appears then that the main role of $[HPBu_3]Br$ is to act as a source of HBr which converts $[HRu_3(CO)_{11}]^-$ to $[Ru(CO)_3Br_3]^-$, both of which are required for methanol formation. The system is, thus, very similar to that of Dombek, who has proposed that both species are required to form the key formyl intermediate by intermolecular transfer of hydride from $[HRu_3(CO)_{11}]^-$ to $[Ru(CO)_3Br_3]^-$ or something derived from it. In support of this he[49] and we[112] have demonstrate such H transfer to Re[49] or Ru[112] bound CO ligands from $[HRu_3(CO)L]^-$ (L = $(CO)_2$ or 1,2-bisdiphenylphosphinoethane.

5.8 Experimental

See the general notes in chapters 2, 3 and 4 for standard methods, used equipments, methods and materials.

5.8.1 Method for the purification of [PBu_4]Br

The general method for purifying a batch of crude (from the supplier (Sigma Aldrich) [PBu_4]Br was to dissolve it in warm acetone and then precipitate the [PBu_4]Br using diethylether. In the first set of experiments precipitation was considered adequate for the removal of impurities. A general method for purifying [PBu_4]Br used in this chapter can be described by the following example:

In an open flask [PBu_4]Br (59.9 g) was dissolved into 40 mL of acetone with stirring. Then 200 mL of diethyl ether was added causing the [PBu_4]Br to precipitate. The [PBu_4]Br was collected by filtration and washed 3 times using (80, 40 and 80 mL) of diethyl ether. The solid was then dried *in vacuo* to produce white soft solids (53.1 g (88.6 %)). The proton decoupled ^{31}P NMR showed significant reduction in the size of the [$HPBu_3$]Br peak see figure 5.28 A and B.

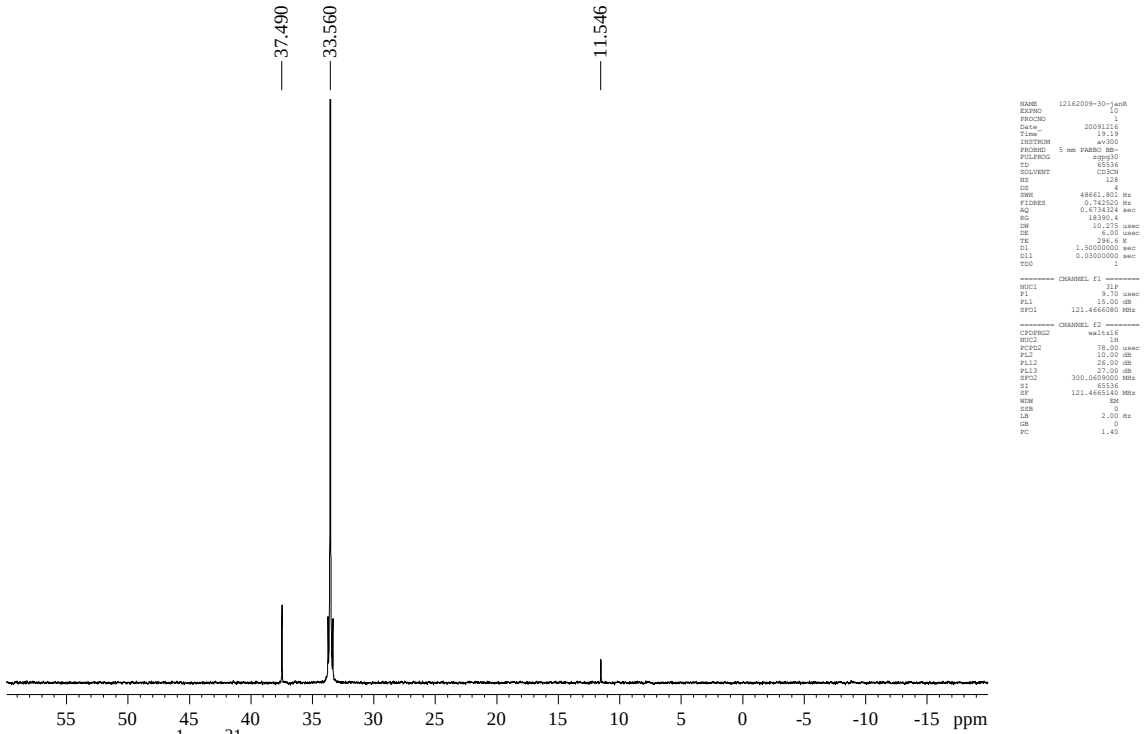

Figure 5.28 A {^{1}H} ^{31}P NMR of an unpurified batch of [PBu_4]Br. The peak at δ 11.54 ppm arises from [$HPBu_3$]Br.

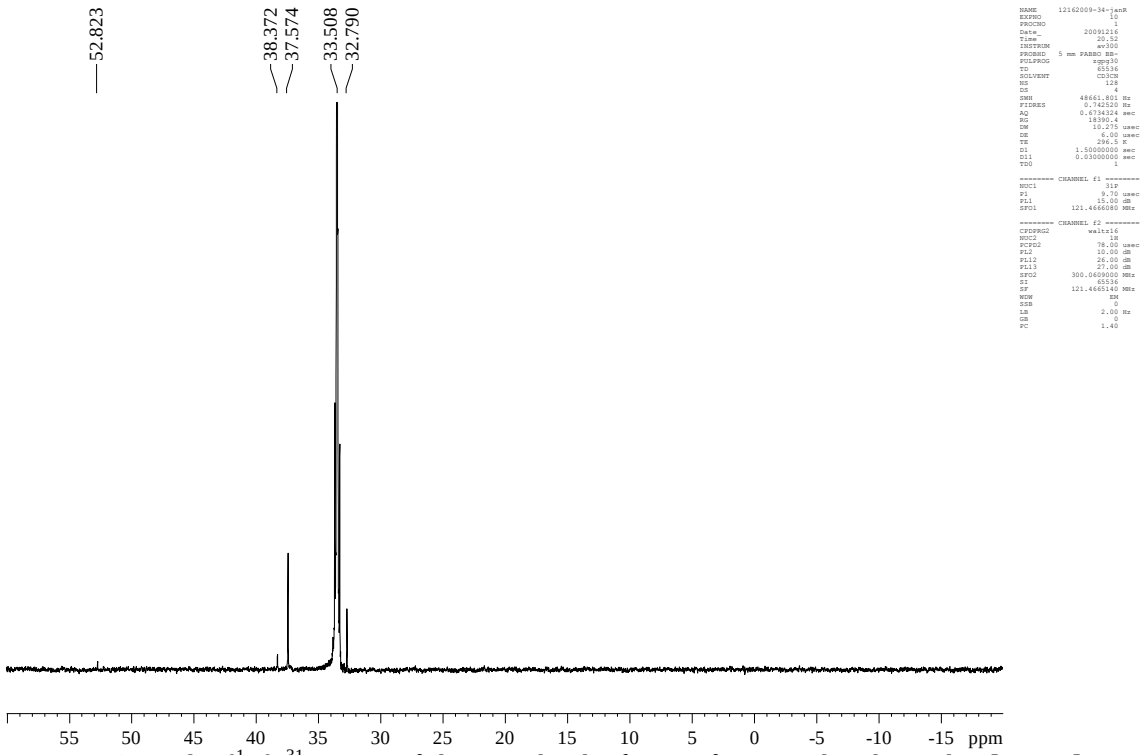

Figure 5.28 B. The {^{1}H} ^{31}P NMR of the same batch after purification. This shows that [$HPBu_3$]Br is effectively removed from the sample.

5.8.2 Synthesis of the crude [$HPBu_3$]Br for a direct assessment of the effect caused by the presence of [$HPBu_3$]Br on the catalytic activity compared to samples without added [$HPBu_3$]Br.

The first attempt to synthesise [$HPBu_3$]Br one yielded only a crude mixture of [$HPBu_3$]Br and other compounds. Later attempts yielded pure samples. However, a quantity of crude [$HPBu_3$]Br was used to determine if it had an effect on catalysis. Synthesis: to a three-necked flask containing dry and degassed methanol (15 mL, excess), 0.94 mL (1.48 g, 8.01 mmol) of benzoyl bromide was added. The flask was allowed to stir for 5-10 minutes and 1 mL (0.81 g, 4 mmol) of PBu_3 was added dropwise over the course of 5 minutes. The solution was stirred for 1 hour before drying *in vacuo*. The residue was washed 3 times with diethylether (10 mL) and dried in vacuo. This yielded a sticky white solid (1.2720 g, 112 %, hygroscopic). The ^{1}H NMR showed a mixture of products, among which were [$MePBu_3$]Br and some signals corresponding to benzyl derivatives, possibly methyl benzoate. However the main product was [$HPBu_3$]Br. This is supported by the ^{31}P NMRspectrum, which shows only [$HPBu_3$]Br and [$MePBu_3$]Br (minor peak) as P-containing compounds. Since the goal was to make a "quick and dirty" assessment of the [$HPBu_3$]Br we decided to use this in catalysis once, and if it proved to be active a better method for synthesis or purification would be developed. See figures 5.29 and 5.30.

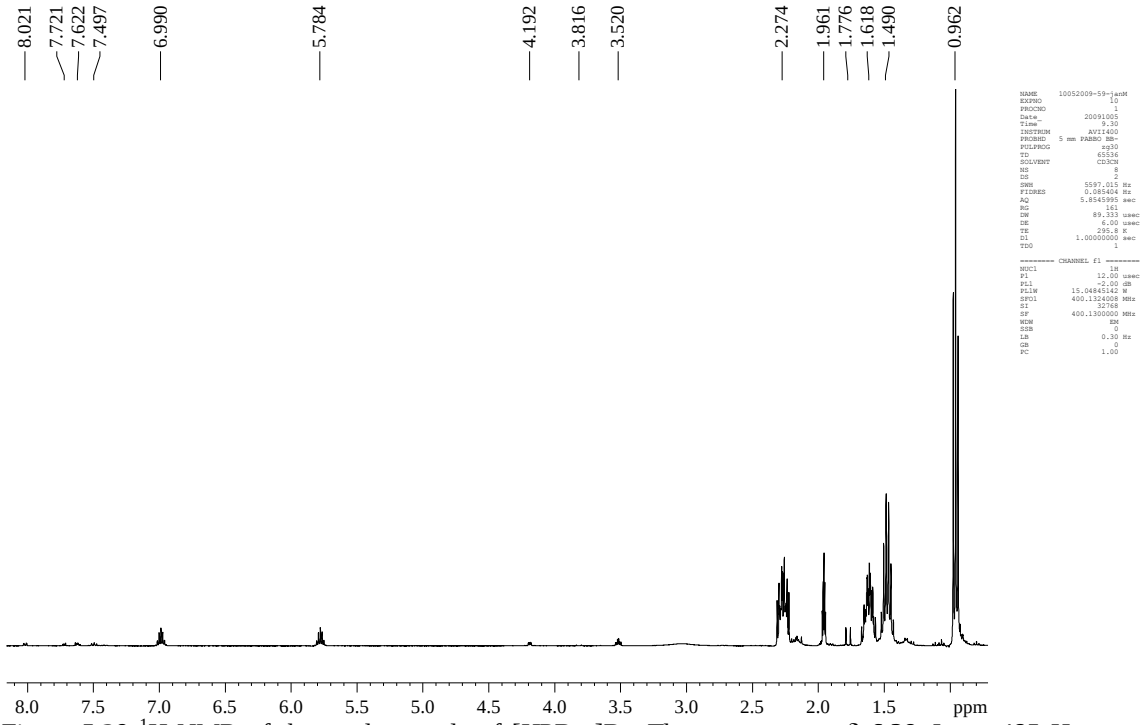

Figure 5.29 ^{1}H NMR of the crude sample of [HPBu$_3$]Br. The resonance at δ 6.38 J_{HP} = *485 Hz* ppm correspond to the H-P proton in [HPBu$_3$]Br.

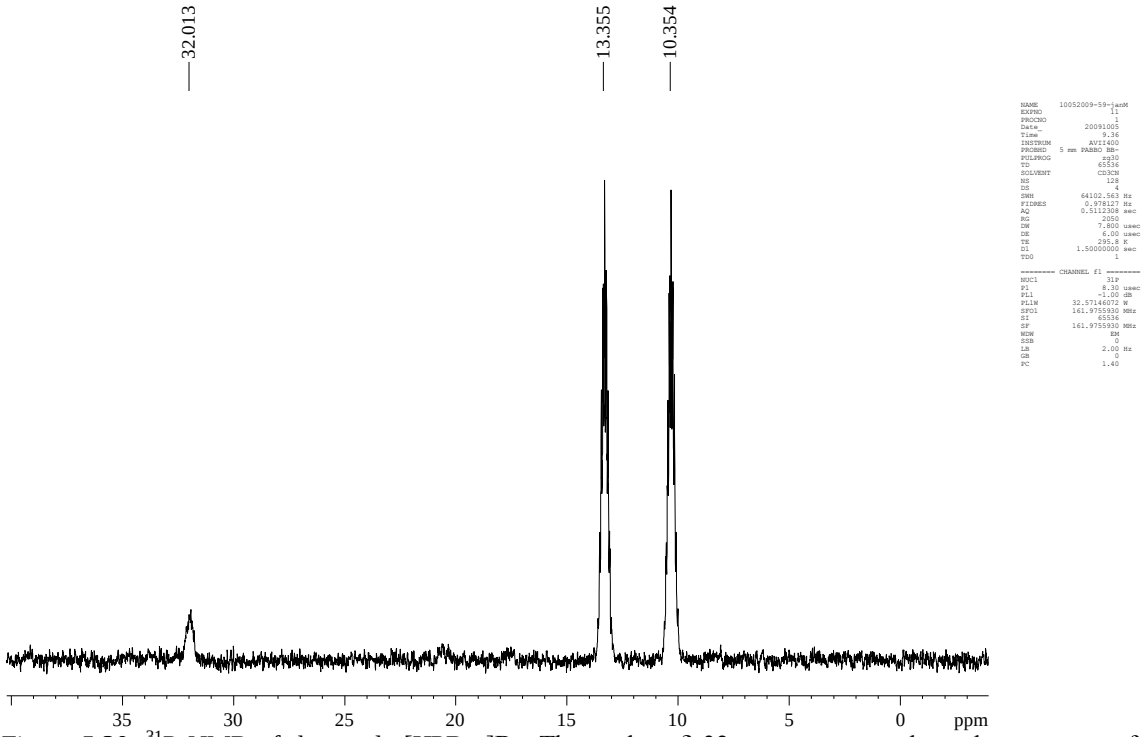

Figure 5.30. ^{31}P NMR of the crude [HPBu$_3$]Br. The peak at δ 32 ppm corresponds to the presence of minor amounts of [MePBu$_3$]Br.

5.8.3 Improved synthesis of [$HPBu_3$]Br

The synthesis of [$HPBu_3$]Br occurred in two steps, first *in situ* generation of dry HBr which was transferred continuously, bubbling into a flask containing PBu_3 dissolved in chilled diethylether. The total setup consisted of two flasks connected through a glass transfer tube, fitted with a plug of P_2O_5. To one flask fitted with stirrer bar, H_3PO_4 (33 mL, 85%) was degassed using three freeze-pump-thaw cycles, and subsequently dried using an excess of P_2O_5 (30 g). Then dry KBr (65 g) was added and the system was degassed once more before being fitted with the glass connection tube. A three neck flask was evacuated, dried, fitted with a stirrer bar and added to the other end of the glass connection tube under N_2. Next, diethyl ether (250 mL) was added followed by of PBu_3 (32 mL). The flask containing the PBu_3 was subsequently chilled using a dry ice, acetone bath. The flask containing the KBr salt was then heated until HBr was liberated. Immediately, formation of the product was visible in the flask containing the PBu_3, as a white precipitate. The reaction was controlled by control of the heating of the flask containing the KBr. This procedure was continued until no more HBr was liberated. The white product was then collected by filtration and washed 3 times using of dry diethyl ether (50-60 mL). After drying *in vacuo* this yielded fine, a white powder (31.2 g, 0.1102 mol, 85%). ^{1}H NMR (figure 5.31) (400.13 MHz, CD_3CN, δ (ppm)): 6.50 (1H, d, $^1J_{PH}$ = 485.20 Hz, Bu_3P-**H**), 2.29 (6H, m, P-($C\mathbf{H}_2$-C_3H_7)$_3$), 1.62 (6H, m, P-(CH_2-$C\mathbf{H}_2$-C_2H_5)$_3$) , 1.48 (6H, m, P-(C_2H_4-$C\mathbf{H}_2$-CH_3)$_3$), 0.96 (9H, t, $^3J_{HH}$ = 7.2 Hz, P-(C_3H_6-$C\mathbf{H}_3$)$_3$). ^{31}P NMR (figure 5.32), (161.97 MHz, CD_3CN, δ (ppm)): 11.66 (d, $^1J_{PH}$ = 484.9 Hz).

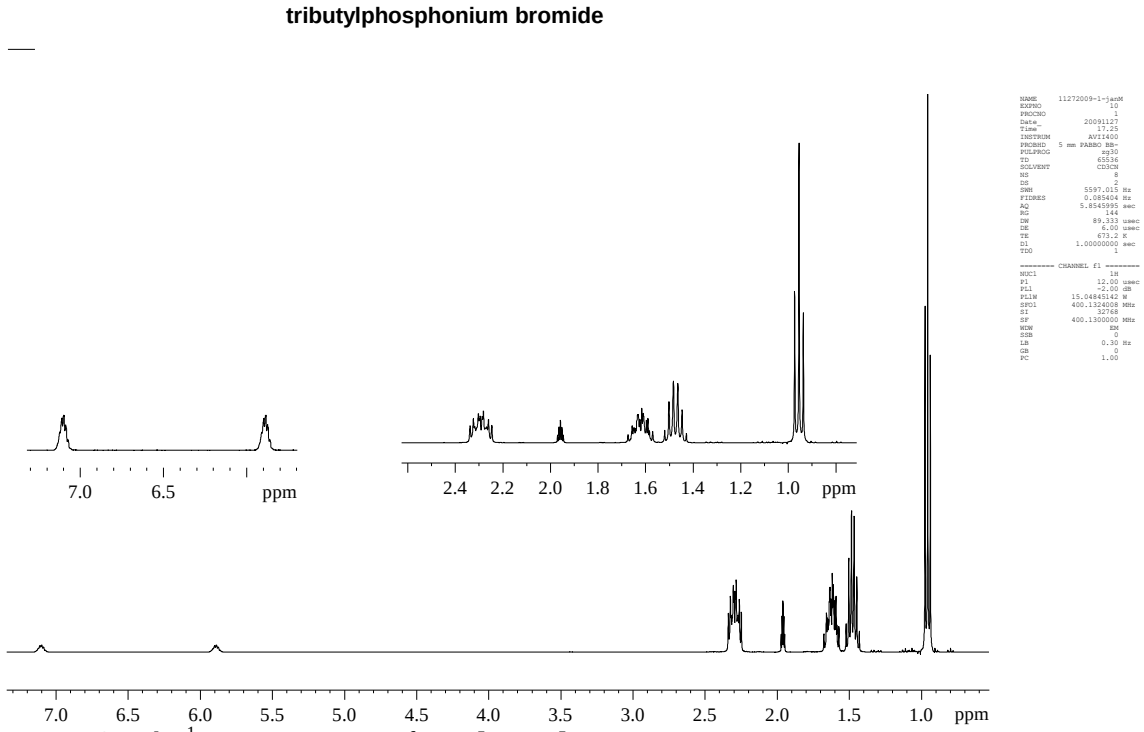

Figure 5.31. The ^{1}H NMR spectrum of pure $[HPBu_3]Br$.

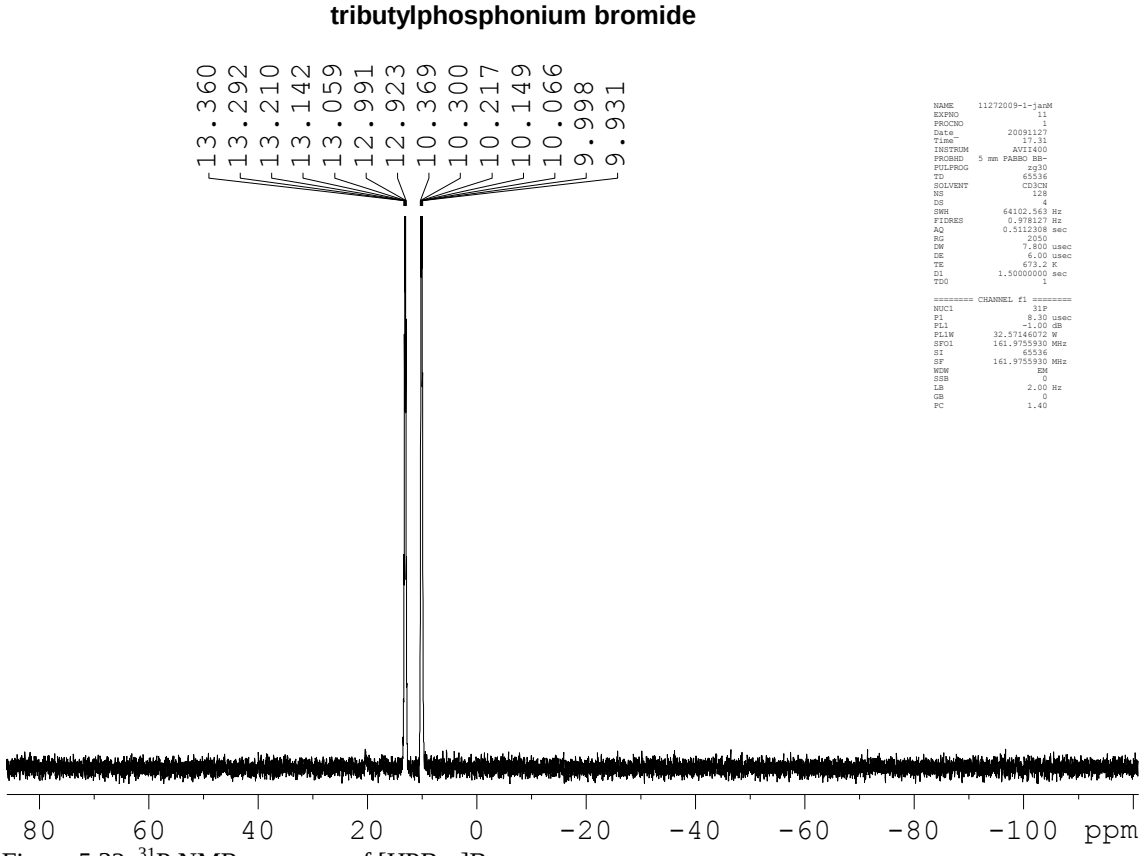

Figure 5.32. ^{31}P NMR spectrum of $[HPBu_3]Br$.

5.8.4 The Catalytic runs

5.8.5 General Procedure

In a typical reaction, the solids were weighed into the clean and dry autoclave, which was screwed onto the holder and sealed, filled with CO/H_2 (50:50 v/v, approx 11 bar) and then vented. This purging sequence was repeated at least 6 times but usually 7 times, to ensure adequate removal of air. Next, the system was filled with syngas to approximately 170 bar and tested for leaks. The heater was attached and set to 200 ^oC. The heater was switched on under continuous stirring. When the reactor had reached the desired temperature of 200 ^oC the reactor pressure was adjusted to 250 bar. During the reaction the pressure was held continuously at 250 bar by the addition of new syngas from an attached ballast vessel through a pressure controller. The pressure of the ballast vessel was monitored throughout the reaction by the use of computerised logging equipment. The reaction was allowed to run for 4 hrs after which the heater was switched off and decoupled to ensure swift cooling. When the temperature of the autoclave was below 30 ^oC the excess pressure was vented from the autoclave and the product mixture was inspected. The usual colour was red, orange or yellow depending on how much $[HPBu_3]Br$ was added. Further, the liquid was poured into a glass flask and subsequently weighed. The product mixture was distilled under reduced pressure using temperatures up to 250 ^oC. The condensed vapours were collected in a liquid N_2 cold trap. The products were diluted using a stock solution (5 mL , acetonitrile (2% v/v) internal standard in N-methylpyrrolidone (NMP)). This mixture was then analysed using GC-FID. The retention times of the products were previously determined using GC-MS.

5.8.6 Series varying time

Two series of experiments were performed where the reaction time was varied. In the first one unpurified (low $[HPBu_3]Br$ was present) $[PBu_4]Br$ was used. This series was discussed in this chapter. The other series was discussed in the previous chapter. The amounts of reagents used and conditions of operation are stated table 5.1 and the product yields in table 5.2.

Table 5.1. Used reagents and experimental conditions[a] for the first series of experiments where the reaction time was varied.

		mass [PBu4]Br		mass [Ru3(CO)12]	
Exp. No.	time (hrs)	grams	mmol	grams	mmol Ru
36	1	15.0011	44.2074	0.4997	2.3448
37	2	15.0011	44.2074	0.4997	2.3448
38	4	15.0004	44.2053	0.4992	2.3471
39	8	15.0004	44.2053	0.5002	2.3424
40	16	15.0006	44.2059	0.4995	2.3439

[a]Conditions: 200 ^{o}C, 250 bar syngas (1:1 v/v).

The recovered product yields are as following:

Table 5.2 the recovered amounts of product for the first time series.[a]

Exp. No	Methanol	Ethanol	EG	1-Propanol
36	4.4537	0.5402	0.3883	0.0441
37	7.3115	1.5212	0.8248	0.1281
38	13.5396	4.1215	1.4085	0.3725
39	26.7838	12.8034	1.3821	1.5455
40	39.1709	24.4287	3.3587	3.7645

[a]Amounts in mmol.

The catalytic runs comparing active batches of [PBu_4]Br, inactive batches of [PBu_4]Br, purified [PBu_4]Br and a run with purified [PBu_4]Br and added crude [$HPBu_3$]Br:

The catalytic runs assessing the catalytic properties of impurities in the solvent were performed in the same way as all other runs. In table 5.3 the quantities of used reagents and conditions are given. In table 5.4 the recovered material yield of each run is give.

Table 5.3. Used material for testing the effect of crude $[HPBu_3]Br$. (figure 5.8)

		mass $[PBu_4]Br$		mass $[Ru_3(CO)_{12}]$	
Exp. No.	description	grams	mmol	grams	mmol Ru
41	active batch	15.0009	44.2068	0.4996	2.3443
42	inactive batch	15.0004	44.2053	0.4992	2.3424
43	purified batch	15.0001	44.2044	0.5007	2.3495
44	purified + crude $[HPBu_3]Br$[a]	14.9995	44.2027	0.4994	2.3434

[a]Used material from the synthesis of crude $[HPBu_3]Br$ described above, 0.0568 g. Conditions: 200 ^oC, 250 bar syngas (1:1 v/v), 4 hrs.

Table 5.4. Recovered product yield from the experiments shown in figure 5.8

Exp. No.	Methanol	Ethanol	1-Propanol	EG
41	0.025150527	0.0072801	0.0004672	0.0014912
42	0.0135396	0.0041215	0.0003725	0.0014085
43	0.012593473	0.0040741	0.0004001	0.0015596
44	0.026682589	0.0073377	0.0004059	0.0005749

5.8.7 The $[HPBu_3]Br$ variation series

The amounts of reagents used and conditions of operation are stated table 5.5 and the product yields in table 5.6. Two series were performed, one where the catalyst loading was 0.5 gram and another where the catalyst loading was 0.25 gram in order to avoid the mass transfer limitation.

Table 5.5. Amounts of materials used for CO hydrogenation reactions with added [HPBu3]Br[a]:

	mass $[PBu_4]Br$		mass $[HPBu_3]Br$		mass $[Ru_3(CO)_{12}]$		
Exp. No.	grams	mmol	grams	mmol	grams	mmol Ru	$[HPBu_3]Br/Ru$
45	15.0005	44.2056	0	0	0.5001	2.3467	0
46	14.9208	43.9707	0.0674	0.238	0.4996	2.3443	0.1
47	14.8003	43.6156	0.1665	0.5879	0.4991	2.342	0.25
48	14.7022	43.3265	0.2493	0.8802	0.5004	2.3481	0.37
49	14.6019	43.031	0.3329	1.1754	0.5	2.3462	0.5
50	14.5024	42.7377	0.4155	1.467	0.4994	2.3434	0.63
51	14.4033	42.4457	0.4988	1.7611	0.4991	2.342	0.75
52	14.3034	42.1513	0.5822	2.0556	0.5	2.3462	0.88
53	14.203	41.8554	0.6642	2.3451	0.4993	2.3429	1
54b	14.5022	42.7371	0.4145	1.4635	0.4991	2.3420	0.6249
55c	14.5025	42.7380	0.4149	1.4649	0.4997	2.3448	0.6247
56d	14.5024	42.7377	0.4144	1.4631	0.4991	2.3420	0.6247
57	15	44.2041	0	0	0.2496	1.1712	0
58	14.9009	43.9121	0.0833	0.2941	0.2503	1.1745	0.25
59	14.8013	43.6186	0.1662	0.5868	0.2503	1.1745	0.5
60	14.7013	43.3239	0.2489	0.8788	0.2497	1.1717	0.75
61	14.6016	43.0301	0.3324	1.1736	0.2503	1.1745	1
62	14.5019	42.7363	0.415	1.4652	0.2497	1.1717	1.25

[a] For all experiments: conducted at 200 ^oC, 250 bar, 4 hrs. For experiments 45-56: syngas 1:1 CO/H_2. For experiments 57-62: syngas 1:2 CO/H_2 using a better stirrer. [b]using a relatively low stirring rate. [c]using a the maximum stirring rate. [d]Using the usual stirring rate, with an improved and larger impeller.

Table 5.6 Recovered product yield (mmol) form the reactions shown in table 5.5:

Exp. No.	Methanol	Ethanol	Propanol	Ethylene Glycol
45	12.5	4.34	0.29	2.59
46	19.08	5.34	0.3	2.76
47	25.5	5.99	0.29	2.78
48	31.03	7.14	0.32	1.48
49	31.43	7.19	0.3	2.41
50	30.38	6.19	0.29	0.88
51	32.45	7.02	0.27	1.12
52	31.04	6.48	0.23	0.19
53	20.18	3.37	0.17	0.4
54	29.04	6.30	0.21	0.18
55	34.05	7.42	0.28	0.43
56	35.39	7.82	0.32	2.38
57	12.85	2.81	0.21	1.79
58	24.06	4.31	0.23	1.27
59	28.4	4.51	0.23	1.59
60	30.07	4.16	0.25	0.94
61	23.22	2.81	0.21	0.49
62	8.07	0.58	0.13	0.14

5.8.8 HBr series and added PBu_3

In this series of experiments HBr was used as a promoter in incremental amounts. The catalytic runs were conducted in the same way as with the $[HPBu_3]Br$ promoter described above. The materials used are described in table 5.7. Added to this is the reaction where PBu_3 was added as a promoter together with the relevant reactions described in figure 5.23. In this case, the air-sensitive phosphine was added after purging, under a constant flow of syngas. Spectra may be found in the appendix.

Table 5.7. Used reagents and conditions[a] for the HBr series.

Exp.	[PBu_4]X X=	mass [PBu_4]Br grams	mmol	Promoter	amount of promoter grams/mL	mmol	mass [$Ru_3(CO)_{12}$] grams	mmol Ru	Promoter/Ru	H_2/CO
jhbr211	Br	14.9999	44.2038	-	-	-	0.2501	1.1736	0.00	2
jhbr212	Br	14.9608	44.0886	HBr 48% aq.	0.0094	0.1157	0.2496	1.1712	0.10	2
jhbr213	Br	14.9004	43.9106	HBr 48% aq.	0.0238	0.2937	0.2500	1.1731	0.25	2
jhbr214	Br	14.8005	43.6162	HBr 48% aq.	0.0475	0.5873	0.2501	1.1736	0.50	2
jhbr215	Br	14.7015	43.3245	HBr 48% aq.	0.0720	0.8899	0.2504	1.1750	0.76	2
jhbr216	Br	14.6024	43.0324	HBr 48% aq.	0.0958	1.1835	0.2496	1.1712	1.01	2
jhbr217	Br	14.5023	42.7374	HBr 48% aq.	0.1195	1.4772	0.2505	1.1754	1.26	2
Jhbr360	Br	15.0005	44.2056	PBu_3	0.145	-	0.2503	1.1745	0.5	2
jhbr314	Br	14.8013	43.6186	$HPBu_3Br$	0.1662	0.5868	0.2503	1.1745	0.50	2

[a] Reaction conditions 200 °C, 250 bar total constant pressure, 4 hrs.

Table 5.8 Recovered material after the reaction (given in mmol).

Exp.	Methanol	Ethanol	Propanol	Butanol	EG	2-methoxy ethanol	2-ethoxy ethanol	methyl acetate	Dimethoxymethane
jhbr211	18.5626	4.0190	0.2060	0.0910	2.0939	0.1600	0.1292	0.0043	nd
jhbr212	20.9335	5.3888	0.2559	0.0979	2.3449	0.2081	0.1486	0.0052	nd
jhbr213	24.4966	8.0253	0.3510	0.0976	2.1680	0.3007	0.1595	nd	nd
jhbr214	25.6065	11.5662	0.5206	0.0981	2.2640	0.3436	0.1059	nd	nd
jhbr215	22.2126	13.8967	0.6806	0.1045	1.7524	0.3310	0.2196	nd	nd
jhbr216	10.6951	9.2688	0.7592	0.1181	0.5317	0.1564	0.1582	nd	nd
jhbr217	6.7615	6.9516	0.7548	0.1229	0.5201	0.1116	0.1555	nd	nd
jhbr360	15.1648	1.7780	0.1297	0.2425	0.8792	0.1341	nd	0.0462	0.0154
jhbr314	28.4000	4.5149	0.2342	0.2468	1.5910	0.2495	nd	0.1328	0.1533

5.9 Conclusion

We conclude that the irreproducibility, which is often found when studying CO hydrogenation reactions especially in molten phosphonium halides, may arise because of minor impurities that are present in the salt. We have discovered that $[HPBu_3]Br$ can act as a promoter of the reaction when added in small amounts (< stoichiometric with respect to ruthenium). To our knowledge, the use of such compounds as promoters for catalytic reactions has not been reported, although P-H phosphonium salts have been used as air stable alternatives to highly basic phosphines,[113] especially where both phosphine and acid are required in the system.[113-115] In the CO hydrogenation reactions, $[HPBu_3]Br$ acts to convert $[HRu_3(CO)_{11}]^-$ into $[Ru(CO)_3Br_3]^-$ and both of these ruthenium complexes are required for active catalysis. Since hydrogen halides have also been shown to act as promoters for CO hydrogenation in ruthenium systems containing halide,[111, 116] it is possible that $[HPBu_3]Br$ acts as a source of HBr in the system. The HBr shifts the composition of the ruthenium species towards more $[RuBr_3(CO)_3]^-$. Based on the correlation between the presence of this species and the rate of homologation we assume that this species plays an important role in the homologation reaction. We have applied the model to establish that there is a linear relation between the ratio of HBr added (to ruthenium) and the rate of homologation. However, when we promote the formation of this species by the addition of an excess of HBr we can see the catalytic activity of the system drop significantly due to a lack of $[HRu_3(CO)_{11}]^-$. This supports Dombek's finding that there is a hydride donor and a hydride acceptor needed for intermolecular hydrogenation of CO, and for the homologation. Although the role of the phosphine is not fully understood yet, it may coordinate to ruthenium giving inactive complexes and thus reducing the effective concentration of catalyst in the system. Furthermore, the phosphine specifically inhibits methanol homologation and not methanol formation.

Chapter 6
The effect of various promoters on the activity of the system

The effect of halide concentration, halide type and acidic promoters on catalysis and a discussion on possible mechanisms of product formation.

6.1 Introduction

In the previous chapters, the gas phase compositions have been charted over time. In addition, reaction pathways have been uncovered and kinetic models were developed based on those pathways, which proved useful in understanding processes that are taking place in during the reaction. However, finding a pathway does not equate to finding a mechanism. In this chapter we attempt to vary the conditions and reagents in the reactor medium in order to elicit changes in product distribution and kinetics. This in turn should lead to better understanding of possible mechanisms that play a role.

6.2 The effect of bromide concentration on the catalytic activity

To measure how the bromide concentration affects catalytic activity of the ruthenium melt catalyst the bromide level during the reaction was incrementally increased in a series of experiments. To do so, tetrabutylphosphonium triflate and tetrabutylphosphonium bromide were added in varying amount to act as solvents. The total amount of phosphonium salt was held at constant weight of 15 g constant weight and the ratio of bromide to triflate was varied. Using $[Ru_3(CO)_{12}]$ as a catalyst at 200 ^oC and 250 bar of syngas pressure (1:1). The results are shown in figure 6.1 where the x-axis is the ratio of bromide to ruthenium. The 20:1 ratio of bromide to Ru was obtained by using only $[PBu_4]Br$ and adjusting the total weight of the solvent to 15.9 g.

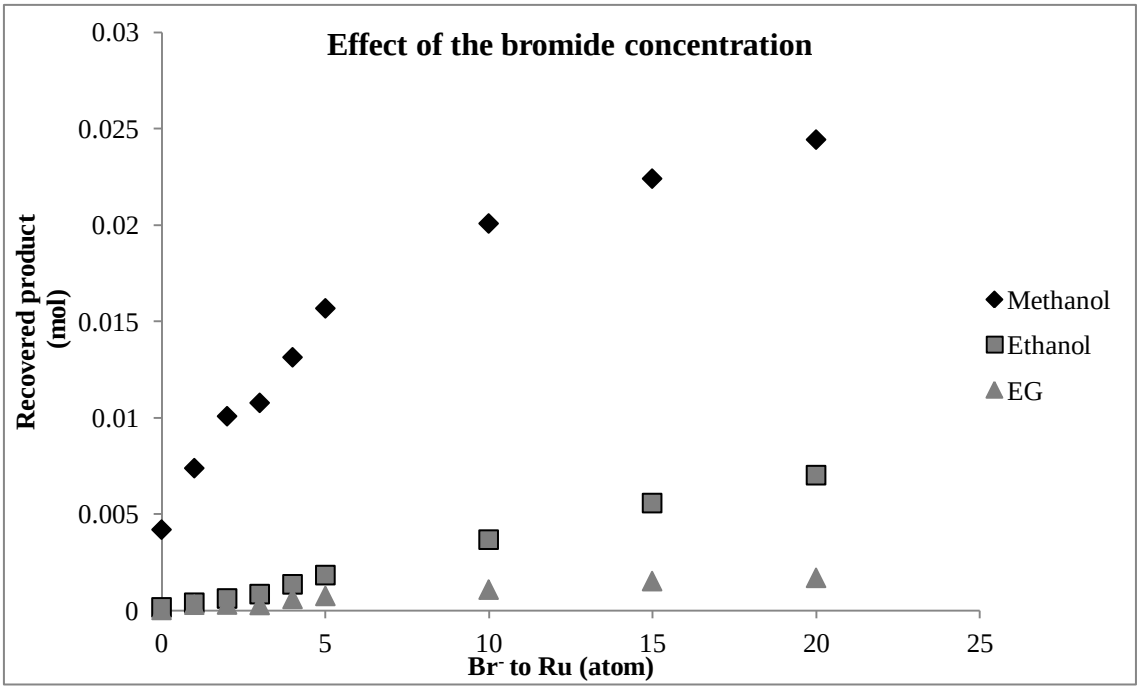

Figure 6.1. The product formation after 4 hours of a series of experiments where the bromide level in the solvent was varied using phosphonium triflate. Conditions: $[PBu_4]Br/[PBu_4][CF_3SO_4]$ (~15 g), 200 °C, 250 bar syngas ($CO:H_2$ 1:1) total pressure, 4 hrs. Catalyst is $[Ru_3(CO)_{12}]$ (0.5 g). The reaction with 20 Br to 1 Ru was exceptional and contained 15.9 g of phosphonium bromide.

To our surprise, changing the solvent to $[PBu_4][CF_3SO_4]$ does not reduce the activity completely to zero. Minute amounts of methanol were still measured after the reaction. The $[PBu_4][CF_3SO_4]$ was prepared from $[PBu_4]Br$ by ion exchange and it is possible that the ion exchange did not yield a 100% conversion and some bromide salt co-precipitated. Analysis of the bromide content was attempted using $AgNO_3$. However, precipitation of the silver bromide did not result in large enough flocks for filtration. We could nonetheless visibly detect that the amount of silver bromide was very small and resulted in only slight discolouration over time. Nonetheless, the bromide content may be sufficient to explain the small amount of catalysis observed.

The methanol production increases significantly when the bromide content increases. According to Dombek's chemical equation(for the I^- system) for every 7 ruthenium atoms 3 halide ions are needed to produce the needed mixture of $[HRu_3(CO)_{11}]^-$ and $[RuBr_3(CO)_3]^-$, to see that breaking point we need levels of bromide that are outside the range of this set of experiments. However, there seems to be a curious breaking point in the methanol curve at Br:Ru = 7, for which no explanation has been found. As for the ethanol production, the line seems to increase linearly with the bromide concentration, there is no point where the ethanol formation increases more

than the methanol formation. The rate constants can be plotted throughout the series (figure 6.2).

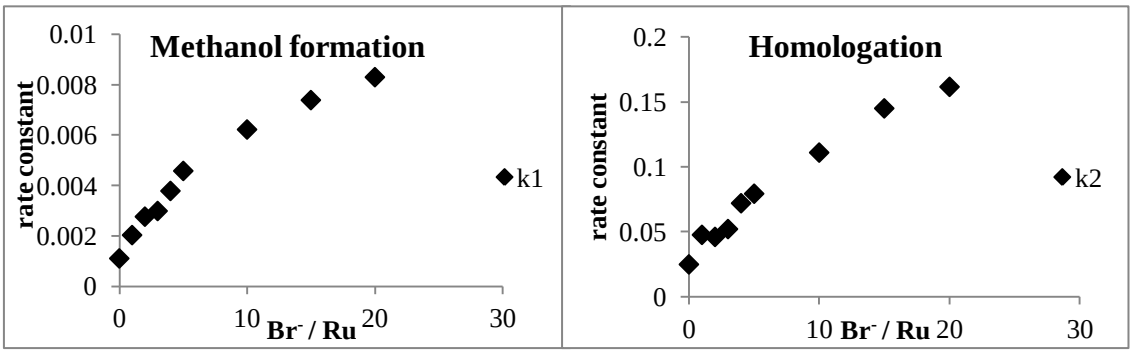

Figure 6.2. The calculated rate constants for methanol formation (left) and homologation (right) with varying bromide to ruthenium levels. Conditions: $[PBu_4]Br/[PBu_4][CF_3SO_4]$ (~ 15 g), 200 ^oC, 250 bar syngas ($CO:H_2$ 1:1) total pressure, 4 hrs. Catalyst is $[Ru_3(CO)_{12}]$ (0.5 g). The reaction with 20 Br to 1 Ru was exceptional and contained 15.9 g of phosphonium bromide.

The rate constants for methanol production seem to grow a little bit more linearly than before but it still has the unmistakable bend in the curve. This series of experiments was performed before it was discovered that there was an impurity in the phosphonium bromide and before we were aware of any mass transport limitation issues. However, because the activity is not increased by replacing bromide for triflate the mass transport limitation should have no role in this range of activity. Additionally it was not yet discovered that minute amounts of $[HPBu_3]Br$ were present in the solvent at this was also not taken into consideration. Therefore, throughout the series not only the amount of bromide in the series was increased, but also the amount of $[HPBu_3]Br$. It is already shown that the concentration of $[HPBu_3]Br$ has a significant effect on the methanol production and therefore it should also have a significant affect in this series. Perhaps this explains the break in the curve at Br/Ru= 7. At that point perhaps the $[HPBu_3]Br$ levels become so significant that the increase in methanol production levels off as shown in figure 5.13 with $[HPBu_3]Br/Ru$ near 0.5. As only a very rough estimate of the $[HPBu_3]Br$ levels in that particular batch of solvent can be made (the same activity as a reaction containing approximately 0.25 eq. of $[HPBu_3]Br$) we can only say that a break would be expected to occur only after reaching more than 15 g $[PBu_4]Br$, or a ratio higher than 18:1.

6.3 The halide anions

Dombek preferred the use of iodide, and in most ruthenium halide systems the use of iodide promoters is preferable because of the usual higher kinetics in organic reactions such as substitutions and eliminations and seemingly higher catalyst activity. Ono[73] shows high activity using the chloride. Knifton has shown that the bromide salts are preferable.[11] Because of this variation in the activity with changing halide it was necessary to inspect the activity of each system independently. $[PBu_4]I$ was synthesised by the addition of freshly distilled and degassed butyliodide to a solution of PBu_3 in ether. The solution was stirred for 48 hrs and the white $[PBu_4]I$ was collected by filtration and washed three times with ether. The product was dried *in vacuo* overnight to yield (77%) white powder. $[PBu_4]Cl$ was synthesised by the addition of butylchloride to a solution of PBu_3 in ether.

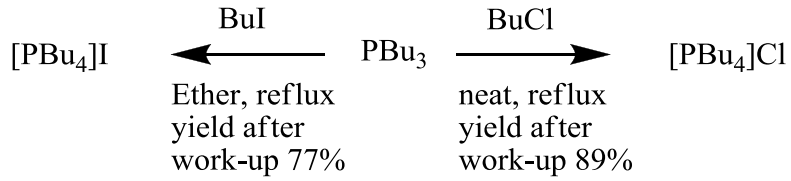

Scheme 6.1. Synthesis of $[PBu_4]Cl$ and $[PBu_4]I$ from PBu_3.

For the iodide and the bromide salts the quaternisation step is fast, but when using the chloride, the reaction was very slow. Therefore, in the case of the chloride, the ether was removed by distillation and the temperature was raised to run the reaction under (neat) reflux conditions (80 ^{o}C). The reaction proceeds quantitatively over 6 hours and the product was *in vacuo* for purification. An additional purification step was added by dissolving the $[PBu_4]Cl$ in acetone and reprecipitating it with ether. This was to make sure no additional butyl chloride or phosphine remained in the solvent. The product was collected by filtration, washed three more times with ether, and dried *in vacuo* to yield (89%) a white hygroscopic solid. ^{31}P NMR spectra (figures 6.3 and 6.4) show the presence of the desired compounds

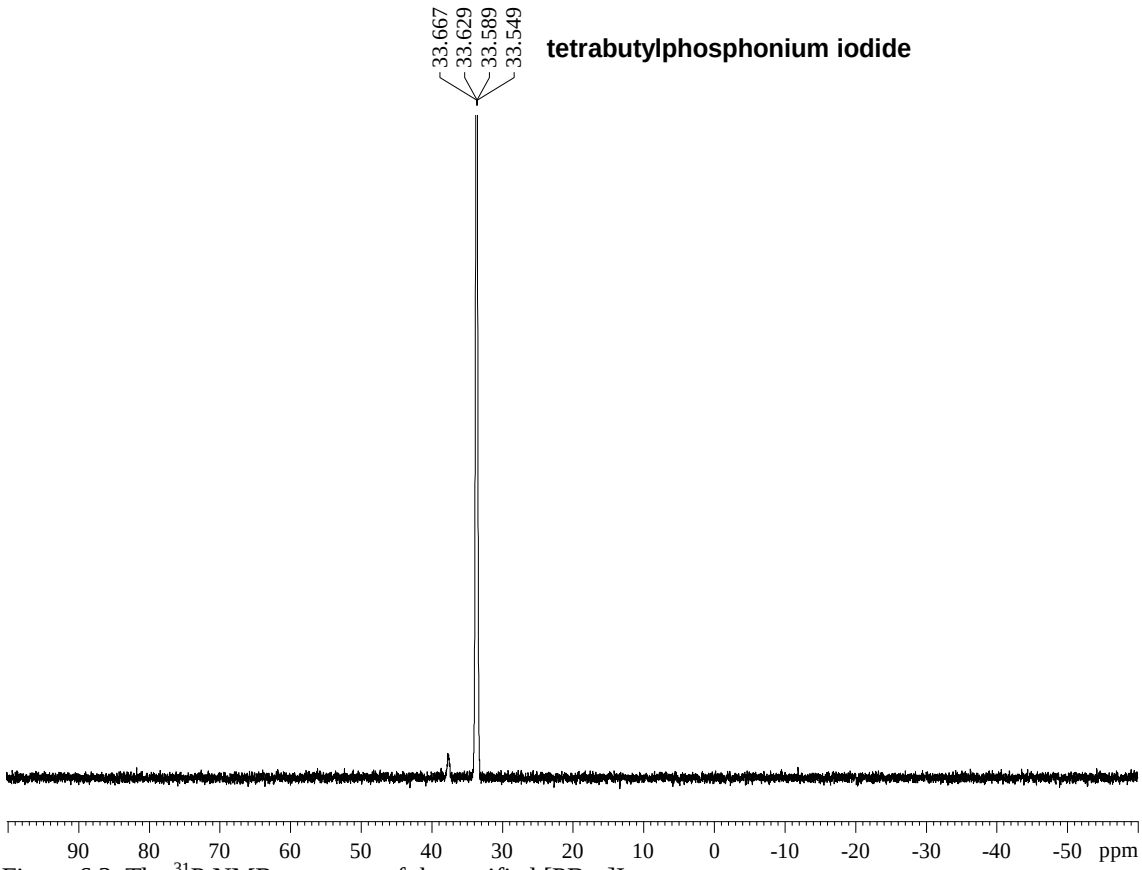

Figure 6.3. The ^{31}P NMR spectrum of the purified $[PBu_4]I$

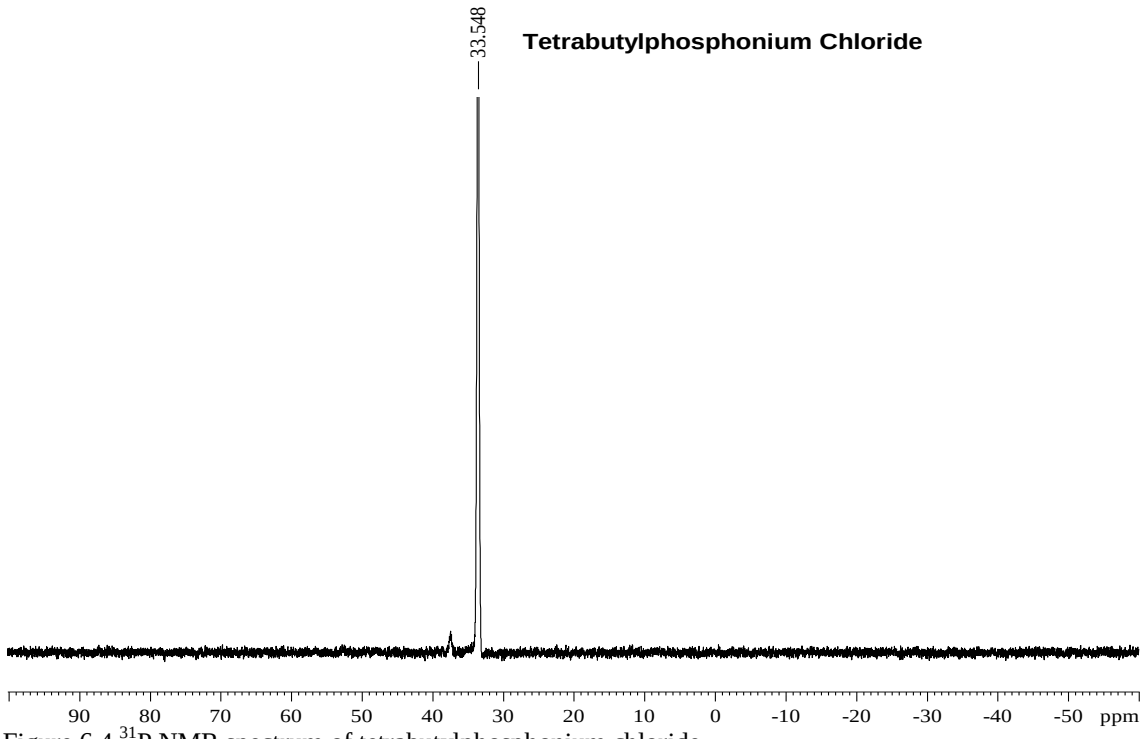

Figure 6.4 ^{31}P NMR spectrum of tetrabutylphosphonium chloride

Interestingly, there is very little difference between the chemical shift of the ^{31}P signal of both phosphonium salts, which indicates that the phosphorous atoms are relatively isolated and have little interaction with the anion while dissolved in the acetonitrile-d_3 solvent. The activity was assessed in a set of 4 experiments. In two experiments either neat $[PBu_4]Cl$ or $[PBu_4]I$ (13.035 g and 17.078 g respectively, 1 eq. to using 15 g of $[PBu_4]Br$), were used with $[Ru_3(CO)_{12}]$ (0.25 g) at 200 ^oC and 250 bar of CO/H_2 (1:2) for 4 hrs. In two other reactions, aqueous HI and HCl were added in a similar fashion to the HBr experiments (0.75 eq. to Ru). To assess the total activity of the reactions it is often easy to compare the normalised uptake curves from each reaction as shown in figure 6.5.

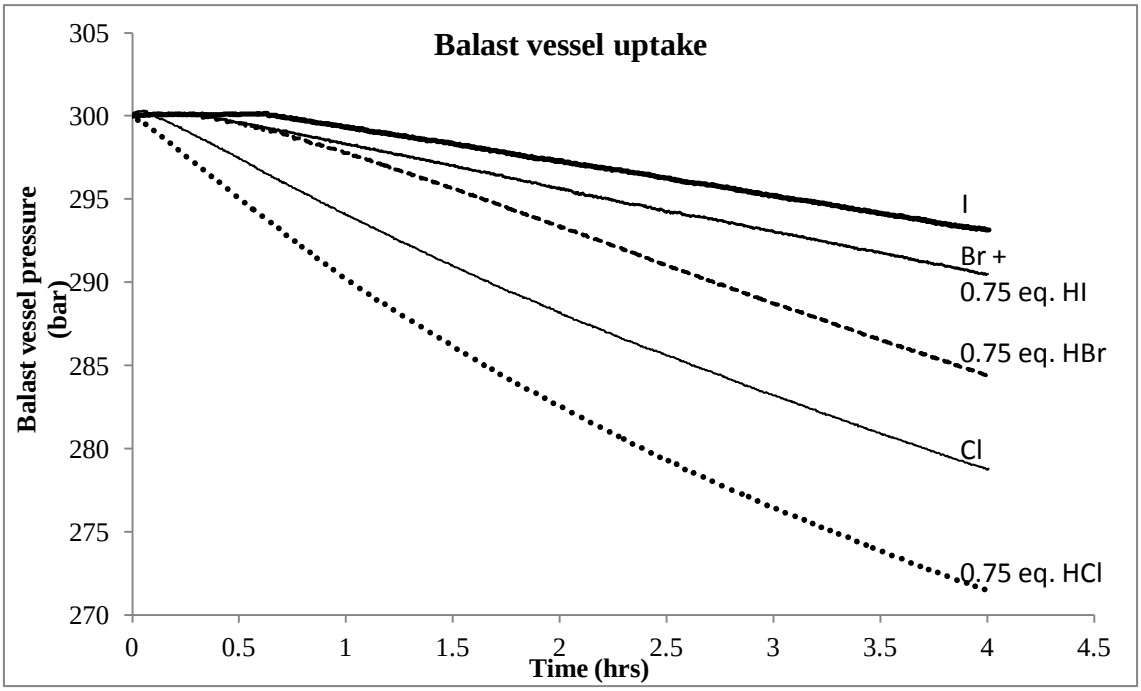

Figure 6.5 Normalised gas uptake curves: ballast vessel pressure throughout reactions containing phosphonium iodide, bromide or chloride as solvent, with or without the presence of HCl, HBr and HI. Conditions: $[PBu_4]X$ (44 mmol), $[Ru_3(CO)_{12}]$ (0.25 g), 200 ^oC, 250 bar syngas ($CO:H_2$ 1:2) total pressure, 4 hrs. Amounts of $[PBu_4]X$ varied with HX to keep the amount of halide constant. HX added as conc. aqueous HX. Where X = Cl, Br, I.

The least reactive system is the unpromoted bromide system, while the most productive reaction is the chloride reaction promoted with HCl, which has a gas uptake of about 30 bars over 4 hours, which is equivalent to around 15 L of 1:2 syngas or 0.56 moles of gas. Even when no promoter is added, the chloride solvent leads to a threefold increase in activity and high gas uptake - more than 22 bar (0.5 L volume) in 4 hours. The iodide system has intermediate reactivity and in addition, appears least affected by

using a promoter. When the product formation was assessed, it was observed that using the different halides leads to large changes in the relative rates of methanol and ethanol formation.

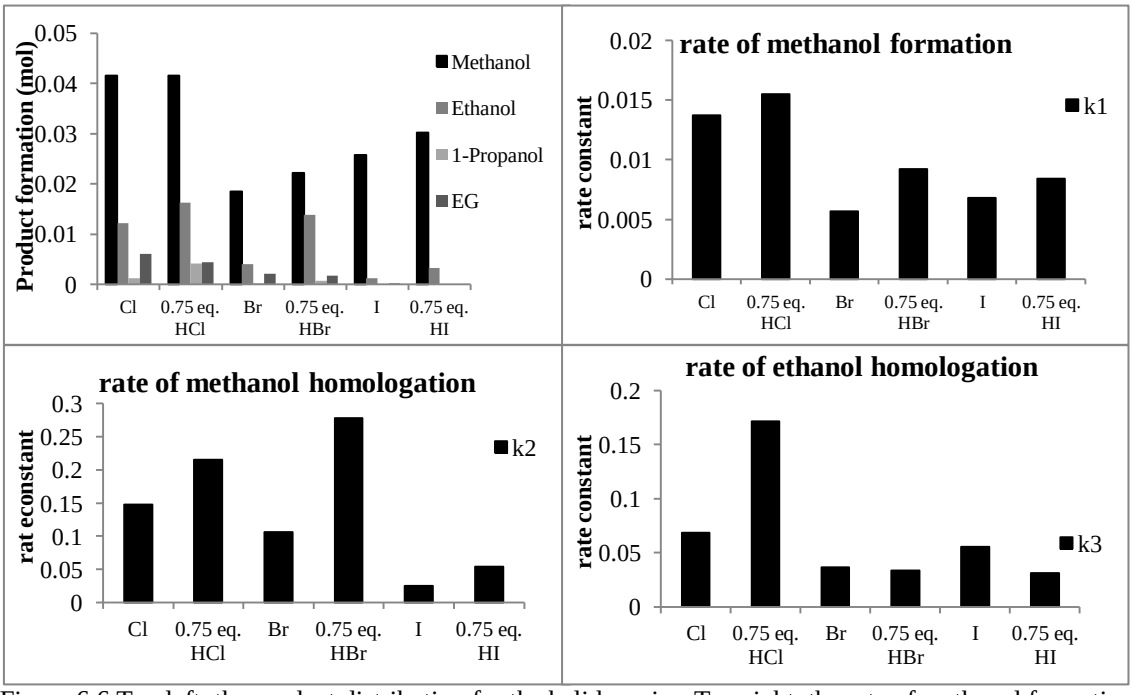

Figure 6.6 Top left, the product distribution for the halide series. Top right, the rate of methanol formation for each solvent and promoter. Bottom left, the rate of ethanol formation for each solvent. Bottom right, the rate of propanol formation for each solvent. Conditions:[PBu_4]X (44 mmol), [$Ru_3(CO)_{12}$] (0.25 g), 200 ^oC, 250 bar syngas ($CO:H_2$ 1:2) total pressure, 4 hrs. Amounts of [PBu_4]X varied with HX to keep the amount of halide constant. HX added as conc. aqueous HX. Where X = Cl, Br, I

Figure 6.6, top left, shows the product distribution for each reaction. Using [PBu_4]I as a solvent leads to formation of high levels of methanol, but the formation of ethanol is relatively slow. Even upon addition of HI the levels of ethanol remain low. Of all the halides, the iodide systems leads to the least amount of homologation. The low uptake also points to low conversion to methane. On the other hand, using chloride leads to the highest product yield, and the amount of ethanol found at the end of the reaction is very high, even when it is not promoted by HCl. Knifton never reported such high activity and nearly always used bromide salts, perhaps due to the relatively high selectivity towards ethanol.

To assess the relative reaction rates it is convenient to compare the rate constants of the reactions, which are also displayed in figure 6.6. Because the rates are relatively high in the chloride system, it is good to keep in mind that the "batch-effect"

(suffocation, gas phase composition changes, solvent composition changes, etc.) will play a role.

6.4 Rate constants

In the chloride reactions, the rate constant, k_1, for methanol formation is nearly twofold higher than in the reactions using bromide or iodide (figure 6.6 top right). This is reflected in the high uptake and the large amount of products found after the reaction. Between the bromide and the iodide reactions the difference is relatively small, however the levels of methanol are higher after the reaction in the iodide system. The reason seems to be the lower rate constant for ethanol formation in the iodide system compared to the bromide system. Therefore, more methanol remains in the iodide system: because less of it is converted. Compared to the bromide system the chloride system may have higher overall product levels, but as determined by the model, the methanol homologation step is slower in the chloride system than in the promoted bromide system, even though the levels of ethanol found after the reaction are nearly the same. Thus, because the methanol levels are higher during reaction using chloride the rate of ethanol formation is high even though the rate constant is lower than in the promoted bromide reaction. Usually there is limited value in looking at the rate constant for propanol formation because the relatively low levels of propanol make conclusions about the rates less certain. However, in this case we find interesting results that are worth reporting. The reaction using chloride and HCl shows a very high rate constant for propanol formation. Of all the halides, the chloride ion is the lesser nucleophile and it should have the lowest levels of methyl chloride and ethylchloride present during catalysis. Apparently, that is not an issue and catalysis occurs readily. For this reason we suspect that halogenation of the alcohols is not the rate determining step in the homologation. Because there is such a difference between the use of different halides we decided to repeat the HX series for the $[PBu_4]Cl$ and $[PBu_4]I$ solvents, but then using HCl and HI respectively.

6.5 Catalytic runs using $[PBu_4]I$ and HI

For this series, the level of HI at the start of the reaction were varied by addition of aqueous HI to the reaction mixture whilst keeping the level of iodide constant

throughout the series. As with using HBr and $[PBu_4]Br$ the added amount of water included in the aqueous HI is catalytic and very small (<80 µL) and therefore the extent of CO_2 formed by the WGS reaction (or the amount of CO removed) is very small and negligible. The same amount of halide was used in the reactor as in the HBr series. For example, $[PBu_4]I$ (16.8510 g, 43.6 mmol) and $[Ru_3(CO)_{12}]$ (0.25 g, 1.174 mmol Ru) were added to the reactor. The autoclave was purged using CO and H_2 and then 80 µL of HI (freshly distilled, 55% in water), 0.5 eq. to Ru) was added. The reactor was pressurised to 170 bar of syngas ($CO:H_2$ 1:2) and the autoclave was heated under stirring to 200 ^oC. The temperature and pressure were held constant for 4 hrs at 200 ^oC and 250 bar, before cooling , venting and analysis of the product mixture. The results of the series are shown in figure 6.7.

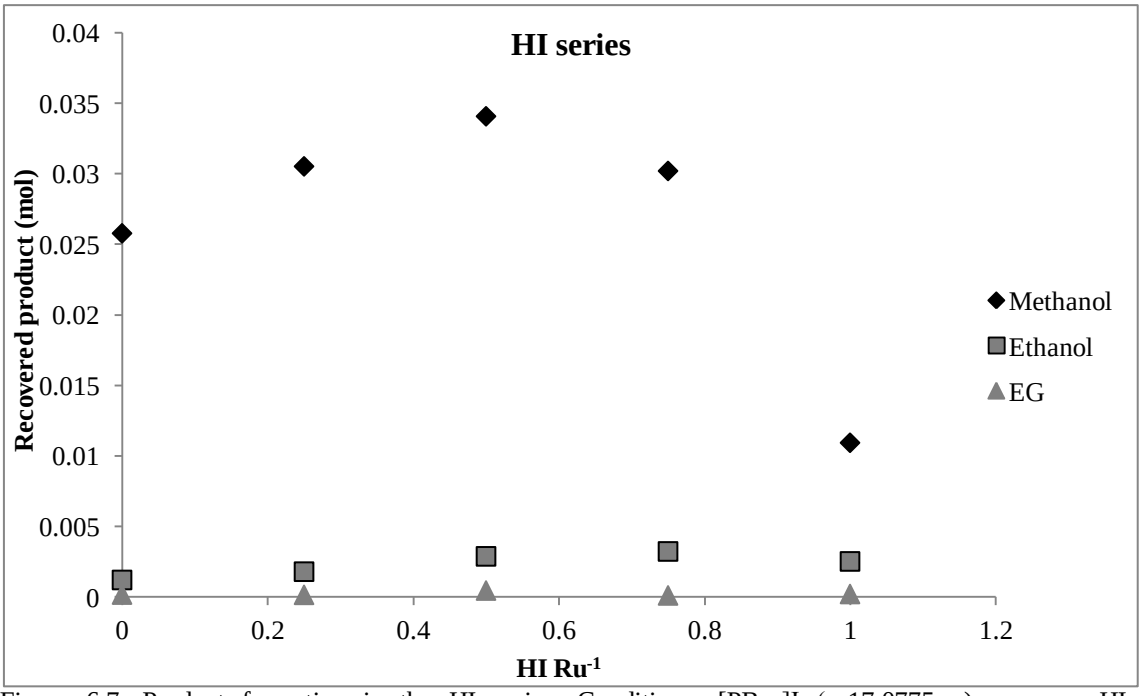

Figure 6.7. Product formation in the HI series. Conditions: $[PBu_4]I$ (~ 17.0775 g), aqueous HI, $[Ru_3(CO)_{12}]$ (0.25 g), 200 ^oC, 250 bar ($CO:H_2$ 1:2) total pressure, 4 hrs. Amounts of $[PBu_4]I$ varied to keep the amount of halide constant throughout the series. HI added as conc. aqueous HI.

The methanol production shows a very similar profile as in the HBr series. With the addition of incremental amounts of HI the reactivity increases significantly and peaks at a ratio of HI to Ru ≈ 0.75 after which reactivity declines again. However, the ethanol formation has a very different profile compared to the HBr series. Instead of significantly increasing throughout the series, the ethanol formation is only moderately affected by the HI. This is reflected in the relative rate constants, k_1 and k_2 in figure 6.8.

The rate constants for methanol formation are very close to those in the HBr series, but the homologation rate constants consistently low. The rate constant k_2 of the final datapoint at HI to Ru = 1 seems much higher than the other rate constants, which may be an experimental uncertainty, but in fact they are all at the same level or lower than in the HBr series and the difference should be close to the uncertainty levels of analysis.

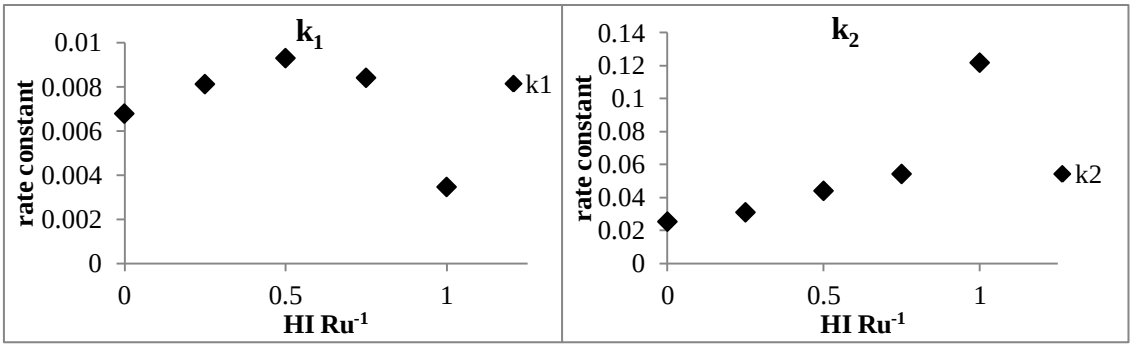

Figure 6.8 The calculated rate constants for the HI series. Conditions: $[PBu_4]I$ (~17.0775 g), aqueous HI, $[Ru_3(CO)_{12}]$ (0.25 g), 200 ^oC, 250 bar ($CO:H_2$ 1:2) total pressure, 4 hrs. Amounts of $[PBu_4]I$ varied to keep the amount of halide constant throughout the series. HI added as conc. aqueous HI.

Since the rate constant to methanol is in the same order as the bromide system, this system would be a suitable choice if one was looking for a system that homogeneously synthesises methanol selectively. To see how the activity relates to the species that we form throughout the system the IR spectra of the product liquids after catalysis were measured.

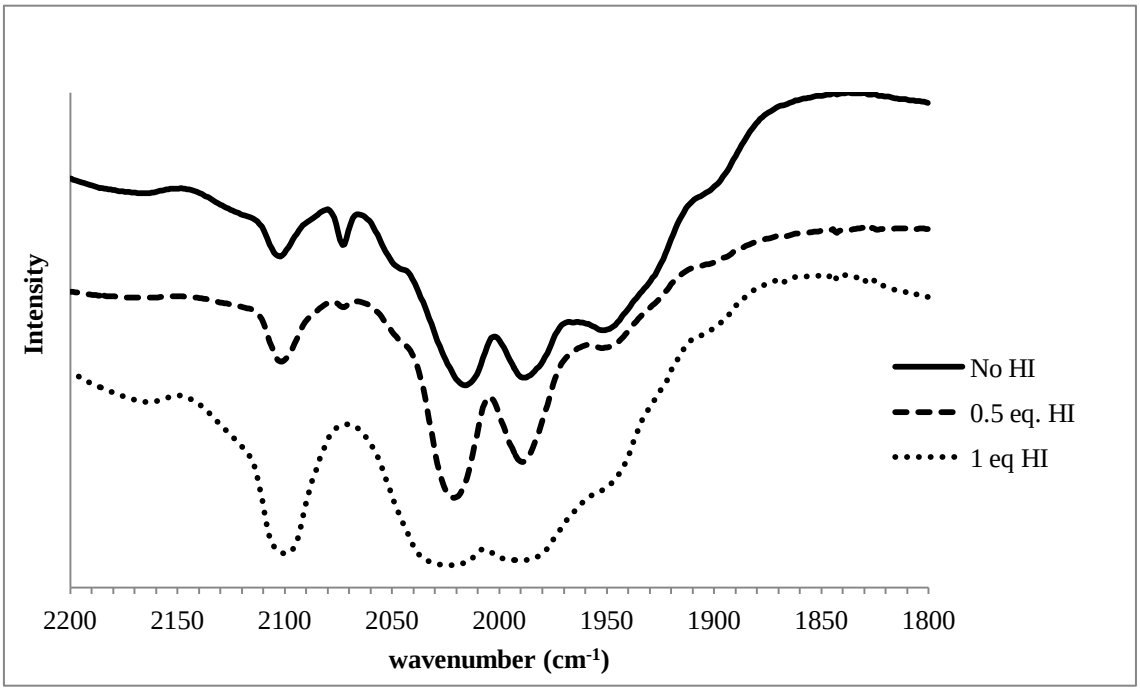

Figure 6.9 the IR spectra of selected samples from the HI series taken after reaction. Conditions: $[PBu_4]I$(17.0775 g), aqueous HI, $[Ru_3(CO)_{12}]$ (0.25 g), 200 ^oC, 250 bar ($CO:H_2$ 1:2) total pressure, 4 hrs. Amounts of $[PBu_4]I$ varied to keep the amount of halide constant throughout the series. HI added as conc. aqueous HI.

Figure 6.9 demonstrates that upon addition of HI to the system containing $[PBu_4]I$ and $[Ru_3(CO)_{12}]$ the composition of the ruthenium species is adjusted in the same way as in the HBr series. The series begin with a system that shows mostly the presence of $[HRu_3(CO)_{11}]^-$ and after addition of HI more and more $[RuI_3(CO)_3]^-$ is formed. However, in this case, formation of $[RuI_3(CO)_3]^-$ does not lead to higher rates of ethanol formation. When the spectra of the HX to Ru = 1 experiments from the HI and HBr are compared similar curves and relative intensities of each compound are observed. The iodide species shows absorptions at lower wave numbers than the bromide species indicating a lower average bond order in the CO ligands and a higher amount of back bonding from the ruthenium centre. We can conclude that there is a profound difference in the activity of the $[RuX_3(CO)_3]^-$ species depending on the halide used. Since $[HRu_3(CO)_{11}]^-$ does not contain any halides, this species should not be affected at all by the presence of different kinds of halides in the solution. Furthermore, as it is negatively charged the $[HRu_3(CO)_{11}]^-$ should interact mostly with $[PBu_4]^+$ which is the same in both systems. The reason why $[RuX_3(CO)_3]^-$ behaves different for each halide can lie in differences in electronic effects, in steric effects or in effects caused by

the solvent, for instance when there is a lower solubility of one of the gases in the solvent.

6.6 Catalytic runs using [PBu$_4$]Cl and HCl

To assess how the presence of HCl affects the reaction mixture containing [PBu$_4$]Br a series of experiments was performed where the level of HCl at the start of the reaction was varied. Due to the high intrinsic activity of the reaction using [PBu$_4$]Cl, this test was performed using half of the amount of ruthenium, while using the same molar amounts of [PBu$_4$]Cl as in the bromide and iodide series. Thus, 0.125 g of [Ru$_3$(CO)$_{12}$] at 200 ^{o}C and 250 bar of syngas (CO/H$_2$ 1:2) for 4 hrs. The results are shown in figure 6.10.

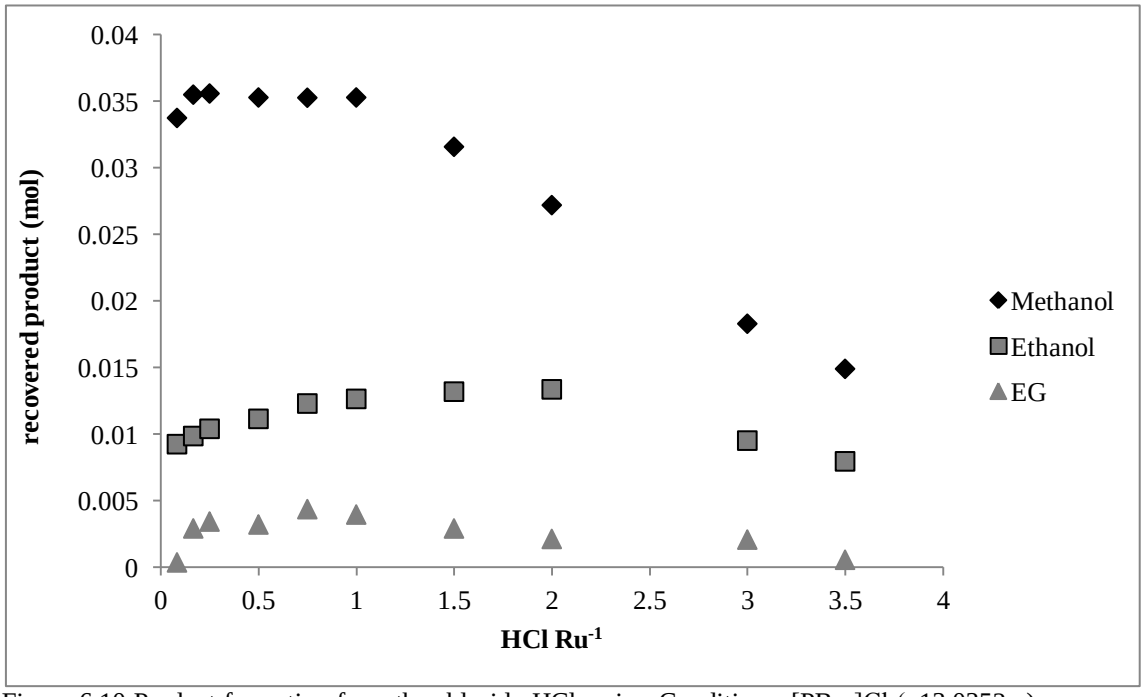

Figure 6.10 Product formation from the chloride-HCl series. Conditions: [PBu$_4$]Cl (~13.0352 g), aqueous HCl, [Ru$_3$(CO)$_{12}$] (0.125 g), 200 ^{o}C, 250 bar (CO:H$_2$ 1:2) total pressure, 4 hrs. Amounts of [PBu$_4$]Cl varied to keep the amount of halide constant throughout the series. HCl added as conc. aqueous HCl.

Taking into account that only half the amount of catalyst is used, this system shows a remarkably high activity. The activity of this series goes up upon using HCl and then lowers gradually. While in the other series the activity is nearly halted after adding more than 1 eq. of HCl to ruthenium, in the case of HCl this does not occur. Only after adding more than 2 equivalents of HCl does the activity of the system reduce significantly, but the reduction is much less defined compared to the other series. Where

normally a peak in methanol production is expected, flattening of the curve occurs which is indicative of either mass transport limitations or that the equilibrium amount of methanol formation has been achieved. Because the equilibrium amount of methanol can be estimated it can be shown that the latter should not be the case. Theoretically, the equilibrium value of methanol is the value where the methanol synthesis has the same rate as methanol conversion. For case two kinetics, this is k_1/k_2. In figure 6.11 the calculated rate constants k_1, k_2, k_3, and the ratio k_1/k_2 over the range of the series are shown.

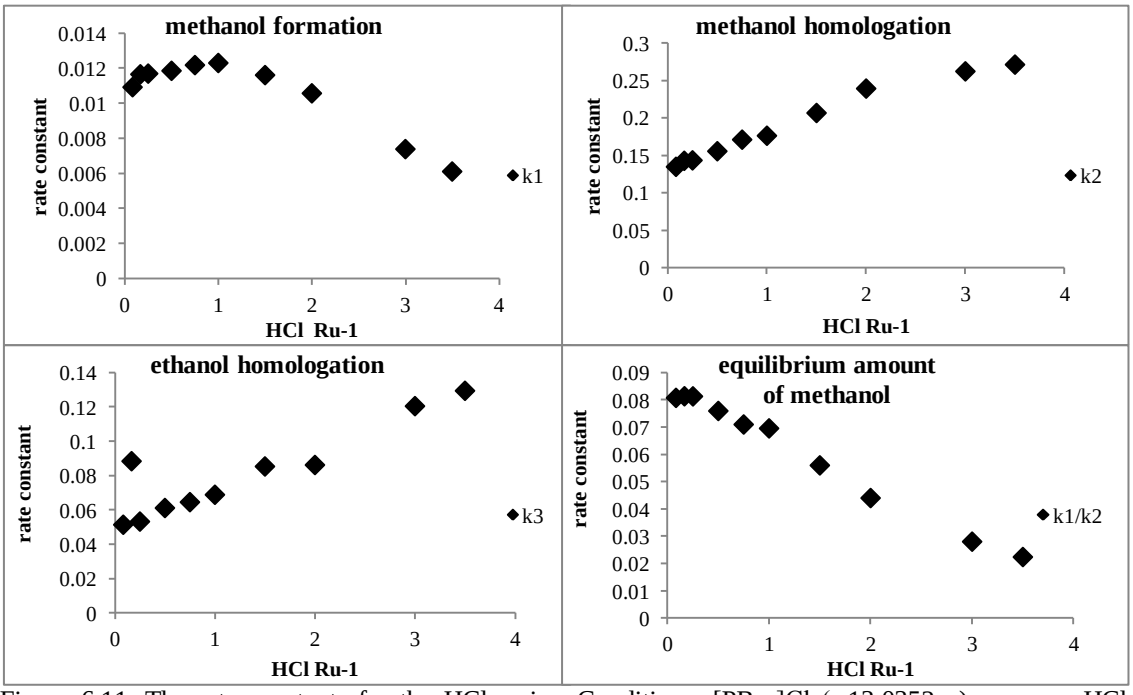

Figure 6.11. The rate constants for the HCl series. Conditions: $[PBu_4]Cl$ (~ 13.0352 g), aqueous HCl, $[Ru_3(CO)_{12}]$ (0.125 g), 200 ^oC, 250 bar ($CO:H_2$ 1:2) total pressure, 4 hrs. Amounts of $[PBu_4]Cl$ varied to keep the amount of halide constant throughout the series. HCl added as conc. aqueous HCl.

The rates are relatively high; the methanol formation, k_1, starts out higher than the top of the HBr series (k_1=0.0109 (HCl) against 0.0094 (HBr),8.6 % higher), but the increase with rising HCl levels is not as high compared to the HBr series. In addition, the k_2 or the homologation increases gradually over the course of the series, however the values never rise above the values that were obtained over the HBr series. That makes the bromide system the best system for generating ethanol from methanol under these conditions. Because for this series the conversion were high enough to get reasonable quantities of propanol we decided to add a plot of the k_3 values as well. A similar profile exists in the k_2 values, which indicates that both follow a similar

mechanism. Finally, we arrive at the k_1/k_2 levels, which is the theoretical equilibrium value for methanol formation ignoring methane formation. The ratio changes over the series, because the rate for homologation increases throughout the series while the methanol formation slows down.

6.6.1 Additional work on the mass balance

One issue is the formation of dimethyl ether and methyl ethyl ether, which are gases at room temperature, but could contribute significantly in the uptake. In attempt to consider this and to get closer to the mass balance two reactions were considered. For these two reactions, the amount of CO locked up in the know liquid products was determined by GC. Then it was assumed that the remainder of the liquid products that were not identified were similar to the known products. It was assumed that the response factor per incorporated CO was the same. This way the total amount of CO in the liquid fraction could be estimated. This number was compared to the total amount of CO taken up during the reaction as determined by the ballast vessel pressure drop. This is shown in Table 6.1 in the upper two lines, it shows the calculated amounts of syngas consumed by estimation from recovered product analysis and by estimation from syngas uptake.

Table 6.1. Estimated amounts of syngas consumed (mol) from calculation from the product formation or from calculation of the total pressure drop of syngas.

reaction	identified liquids	total liquids	methane	total CO in analysis	gas uptake CO
Br	0.0271	0.0355	0.0053	0.0408	0.0547
0.75 eq. HBr	0.0578	0.0736	0.0077	0.0813	0.1037
Br*	0.0389	0.0472	0.0053	0.0525	0.0547
0.75 eq. HBr*	0.1801	0.1959	0.0077	0.2036	0.1037

*CO held up in the liquids when the amount of ethers that are formed are taken into account.

In the lower two lines the equilibrium values of dimethyl ether and diethyl ether were calculated as a function of how much liquid alcohols were present using the following relation:

$$K = \frac{[Et_2O][H_2O]}{[EtOH]^2}$$

Where K is the alcohol-to-ether equilibrium constant as determined via regular thermodynamical calculations. Ethanol is used as an example here. Using this information the amount of ether present is estimated and added to the amount of CO that is present. In table 6.1 this is shown in the lower two lines. Accounting for the ether formation leads to good mass balance in the unpromoted reaction, but to bad results in the promoted reactions. This made us realise that it is important to consider the WGS reaction, as the water produced in the ether formation should be used in the WGS reaction. This leads to a set of equations showing how the ether formation and the WGS reaction is an intricate system of equations and conversions. Easy insights are obtained when the set of equations are multiplied, leading to a single equilibrium value for the set of products:

$$K_1K_2K_3 = \frac{[Et_2O]\ [Me_2O][H_2][CO_2][H_2O]}{[EtOH]^2[MeOH]^2\ [CO]} \approx 100$$

Where K_1, K_2, and K_3 are the equilibrium constants for the diethyl ether formation, dimethyl ether formation and WGS reaction respectively. As can be seen the shift is significantly towards the ether side. This equilibrium may prove to limit the ether formation under reaction conditions. However, attempts to quantify this were unsuccessful up to now. A further problem could be the formation of ethane, possibly through dehydration followed by hydrogenation. A quantification was attempted. In two separate experiments, a small amount of butanol was added at the start of one reaction, while none was added in the second reaction. The reason of choosing butanol is that it has a relatively low vapour pressure, it is soluble in the reaction mixture, easily quantified and only very small amounts are formed during the reaction. The amounts of butanol and pentanol were compared after reaction and this showed that approximately 34.8 % of the added butanol could not be accounted for after the reaction. This missing part can be contributed to experimental error, ether formation, butyl acetate formation, and perhaps also butane or butene formation and even venting.

6.7 Species and reactivity

For the chloride series, IR spectra were taken after reaction. In the HBr and HI series it was found that the we formed $[HRu_3(CO)_{11}]^-$ and $[RuX_3(CO)_3]^-$ and that the

relative levels of each compound changed by the addition of HX affecting the activity. Upon addition of HX levels higher than 1 eq. relative to ruthenium, activity was halted, because of the reduced presence of $[HRu_3(CO)_{11}]^-$ and increased levels of $[RuX_3(CO)_3]^-$. However, in the chloride series the addition of HCl does not cause such a sharp change in catalyst composition. Figure 6.12 shows that even though the same species are formed, the composition of the ruthenium species after the reaction is much less sensitive to the levels of HCl. and as a result, significantly higher amounts of HCl need to be added in order to achieve the same change in the composition of species than needed for HBr and HI.

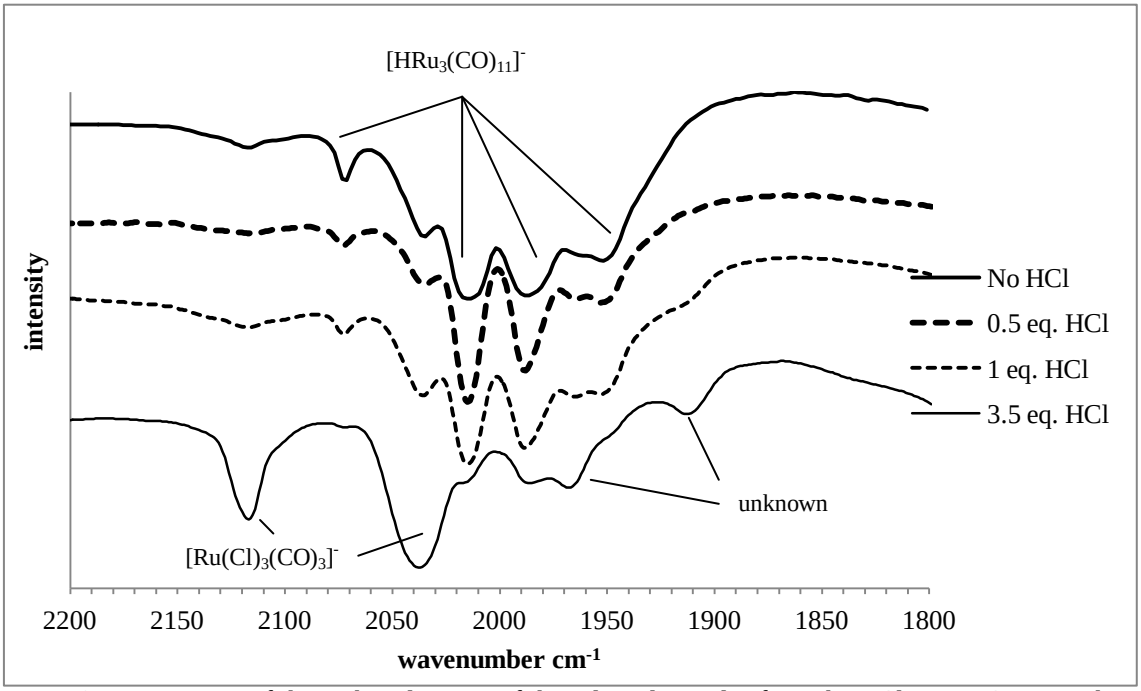

Figure 6.12 IR spectra of the carbonyl region of the selected samples from the HCl series. Spectra taken after reaction.

The first observation is the formation of the same species that were observed in the other halide series, $[HRu_3(CO)_{11}]^-$ and $[RuCl_3(CO)_3]^-$. However, we can see the rise of a new compound upon addition of HCl. When the IR spectra of the samples from the bromide and iodide series are inspected it can be seen that this compound is apparently also present in the other series, albeit at much lower levels. Comparison to known literature does not lead to a match with ruthenium carbonyls with similar absorptions (peaks at 1964 and 1912 cm^{-1}). Thus, the identity remains unknown. Most likely this is a species with either a high charge, or few carbonyls, and most likely a combination, much like $[RuCl_4(CO)_2]^{2-}$, for which the reported numbers[51] do not correspond.

Interestingly, the results from investigations by Ono also using HCl and chloride salts show the presence of the same high activity and the same set of peaks, although he does not identify them either.[74] HX is a by product from the reaction of H_2 with $[Ru_3(CO)_{12}]$ in the presence of halide. For every six $[HRu_3(CO)_{11}]^-$ formed six HX are formed and they react with one $[Ru_3(CO)_{12}]$ and three additional halide salts to form three $[RuX_3(CO)_3]^-$ (Scheme 5.2 and 5.3). Therefore, in the presence of H_2 and halide this mixture of $[HRu_3(CO)_{11}]^-$ and $[RuX_3(CO)_3]^-$ forms. However, the action of HCl on $[Ru_3(CO)_{12}]$ must be less efficient than HBr or HI. There are either thermodynamic limitations, kinetic limitations or a combination of both. Addition of aqueous HBr to a suspension of $[Ru_3(CO)_{12}]$ leads to the formation of $[RuBr_3(CO)_3]^-$ over the course of a few days or hours depending on the concentration of ruthenium. The reaction *appears* to be of zero order kinetics, dependent on the rate of dissolution of $[Ru_3(CO)_{12}]$ in the solvent, the reaction with dry HBr occurs more rapidly over the course of one night. The reaction using dry HCl at room temperature is much slower, if it proceeds at all, while the reaction with aq. HI and $[Ru_3(CO)_{12}]$ is fast.[52] So the rate for the formation of $[RuX_3(CO)_3]^-$ follows a familiar pattern; I > Br > Cl. Although we do not understand the exact mechanism of fragmentation and oxidation, we can still conclude that the reaction proceeds slower to completion within than with Br and I. This must mean that there is more "free" HCl present during catalysis. This could be an important factor during catalysis and formation of products. Furthermore, there may be an additional fundamental difference between ruthenium chloride species and ruthenium iodide and bromide species.

6.8 Correlation between mechanisms, species and activity

To this date, only a few attempts have been made to determine the exact mechanistic pathway of methanol formation. We also understand now that there should also be a separate mechanistic pathway for the homologation. Because the temperatures and pressures are high, spectroscopic analysis is very difficult. The most valuable tool has been IR spectroscopy, but it has only revealed the presence of the well known species $[HRu_3(CO)_{11}]^-$ and $[RuX_3(CO)_3]^-$ and intermediates cannot be trapped. First, the $[RuX_3(CO)_3]$-CO absorption bands can be compared for a possible explanation for the higher activity of the chloride complex compared to the bromide and iodide species,

figure 6.13. The $[HRu_3(CO)_{11}]^-$ species is the same in each reaction so this should not cause the higher activity when using different solvents, although we note that ion pairing can affect intermolecular hydride transfers from the related species, $[HRu_3(CO)_9$(1,2-bis(diphenylphosphino)ethane)$]^-$.[112] For this comparison the spectra of the product liquids after reaction that contain the highest HX content are used from each series. These contain the highest levels of $[RuX_3(CO)_3]^-$ and are easiest for comparison.

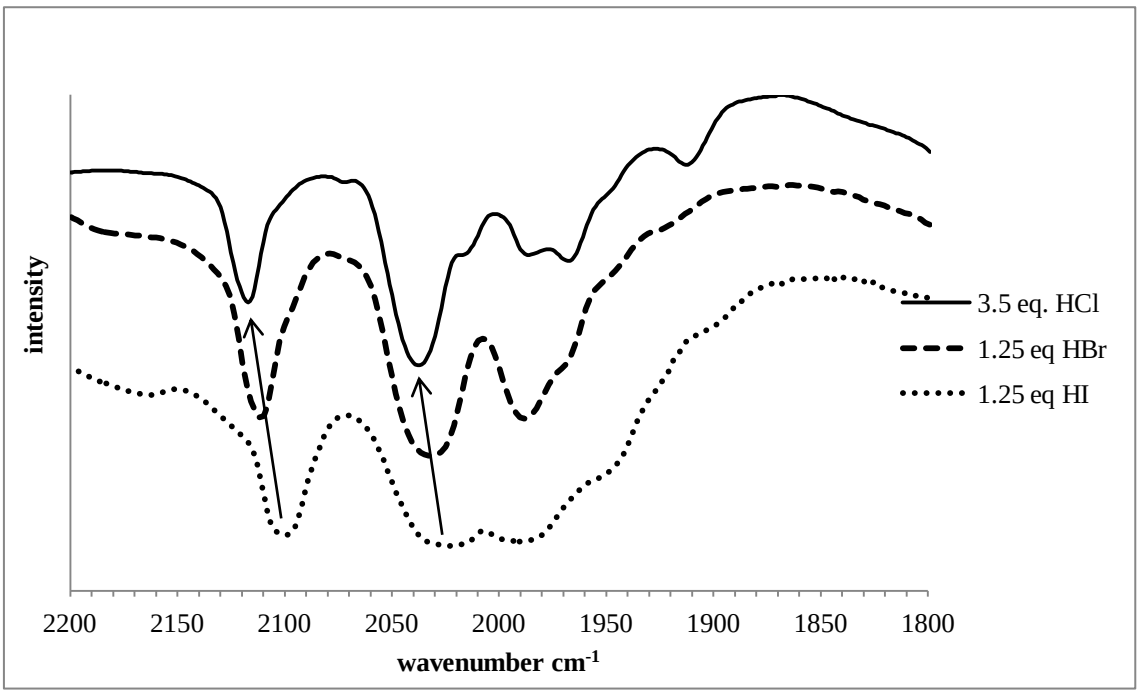

Figure 6.13 comparison of the IR spectra of product mixtures containing high levels of $[RuCl_3(CO)_3]^-$, $[RuBr_3(CO)_3]^-$ and $[RuI_3(CO)_3]^-$.

It shows that the position of the carbonyl absorption bands are at slightly higher energy for the chloride compound, indicating a lower overall electron density on the ruthenium metal centre, as expected because chloride is the most electronegative of the halides used. This will reduce the back bonding into the CO π*-orbitals and give a slightly higher ν_{CO}. Methanol synthesis appears to benefit from generating the "right" mixture of $[HRu_3(CO)_{11}]^-$ and $[RuX_3(CO)_3]^-$. For this reason of synergism, the mechanism is thought to occur via intermolecular interactions. Dombek suggested addition of a hydride from a hydride donor (such as $[HRu_3(CO)_{11}]^-$) to a hydride acceptor (such as $[RuCl_3(CO)_3]^-$ or something derived from it).[49] In this reaction a ruthenium formyl intermediate has to be formed that is usually very unstable and readily dissociates.[45, 56, 61, 112] He also demonstrated that $[HRu_3(CO)_{11}]^-$) can transfer its hydride to a carbonyl on rhenium to give an isolable formyl complex whilst Barratt and Cole-

Hamilton showed that isolable formyl complexes of ruthenium could be formed by hydride transfer from $[HRu_3(CO)_9(1,2\text{-bis(diphenylphosphino)ethane})]^-$ to ruthenium dicarbonyl dications.[112] We can only speculate about the real species that undergoes hydride addition, and it has been suggested that it is either $[RuX_3(CO)_3]^-$ or a species derived from it that is more capable of accepting a hydride, but no spectroscopic evidence of such a species exists yet. For the chloride complex there is lower electron density on CO than for the bromide and iodide complex, nucleophillic attack of a hydride to the carbonyl would be best for the $[RuCl_3(CO)_3]^-$ species, rather than the bromide or iodide analogues.

Other valuable insights may be obtained by measuring the effect of additives and promoters and considering how they might affect the various possible mechanistic pathways. Therefore, it may be easier to use the compounds that we know exist and try to build a mechanistic picture from there. If the "real" hydride acceptor has a different form, the mechanism should still be very similar, but may produce more stable species. We will start from $[HRu_3(CO)_{11}]^-$ and $[RuCl_3(CO)_3]^-$ and confine the discussion to the activation and subsequent stabilisation of CO. For the synthesis of formaldehyde from CO one hydride and one proton is needed. $[Ru_3(CO)_{12}]$ reacts readily with H2 to form $[HRu_3(CO)_{11}]^-$ under release of one CO and a proton. When enough protons have been generated, $[RuCl_3(CO)_3]^-$ can be formed and catalysis can occur. $[RuCl_3(CO)_3]^-$ is an 18-electron complex with a net -1 charge. The ruthenium has an oxidation state of 2+ and the negative charge is spread over three carbonyl moieties. Loss of one chloride anion should lead to a neutral 16-electron complex, with even lower electron density on the carbonyls. This complex dimerizes readily to form the well-known $[RuCl_2(CO)_3]_2$ dimer. The dimerisation reaction occurs with loss of one Cl^- per monomer, but because the concentration of $[PBu_4]Cl$ and the pressure are so high we will assume that the equilibrium of this reaction will be far to the side of the monomer. It may be interesting to keep in mind that this reaction *can* occur and could be used as an argument for the high dependence of the reaction rate on the concentration of the monomer! Scheme 6.2 shows what happens after hydride addition. The resulting species that is formed from this reaction is a ruthenium-formyl species and it has a carbene resonance structure.

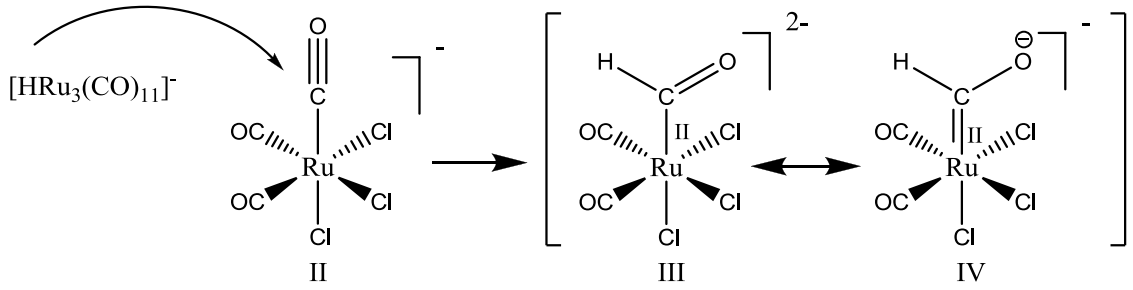

Scheme 6.2 Hydride addition to $[RuX_3(CO)_3]^-$ leads to formation of a ruthenium formyl species.

After hydride addition a $[Ru_3(CO)_{11}]$ species is formed and can bind CO, halide or H_2 again and is ready to repeat the cycle. The resulting ruthenium formyl species after hydride transfer, III, is very unstable. Because the chlorides are labile the formyl readily dissociates by α-hydride abstraction to a cis-position. To prevent degradation, stabilisation should occur when the cis-positions are blocked. However, if the cis-position is blocked the formyl group readily dissociates homolitically.[61] Further stabilisation of the formyl group can occur by ion pairing[45], or by competitive reaction of the formyl to form a more stable species.[45] By ion pairing, stabilisation occurs by promoting a more stable resonance structure; the methoxycarbene ruthenium species, IV. This leads to a formal Ru(II) oxidation state with electron density away from the metal centre, which could have a significant contribution, because of the high electron density throughout the complex. Therefore, for the iodide and bromide complexes the contribution of this resonance structure should be higher than for the chloride complex. Interestingly, the charge density on the formyl-carbon should be quite different for III than for IV. Species III has a formal negative charge and is nucleophillic and can undergo protonation, species IV has a carbon that is electrophillic as this releases the high charge on the ruthenium. We have drawn three possible pathways towards formaldehyde or methanol starting from these species. Other mechanisms are possible but are too elaborate and yield similar species, so they do not contribute much to this discussion.

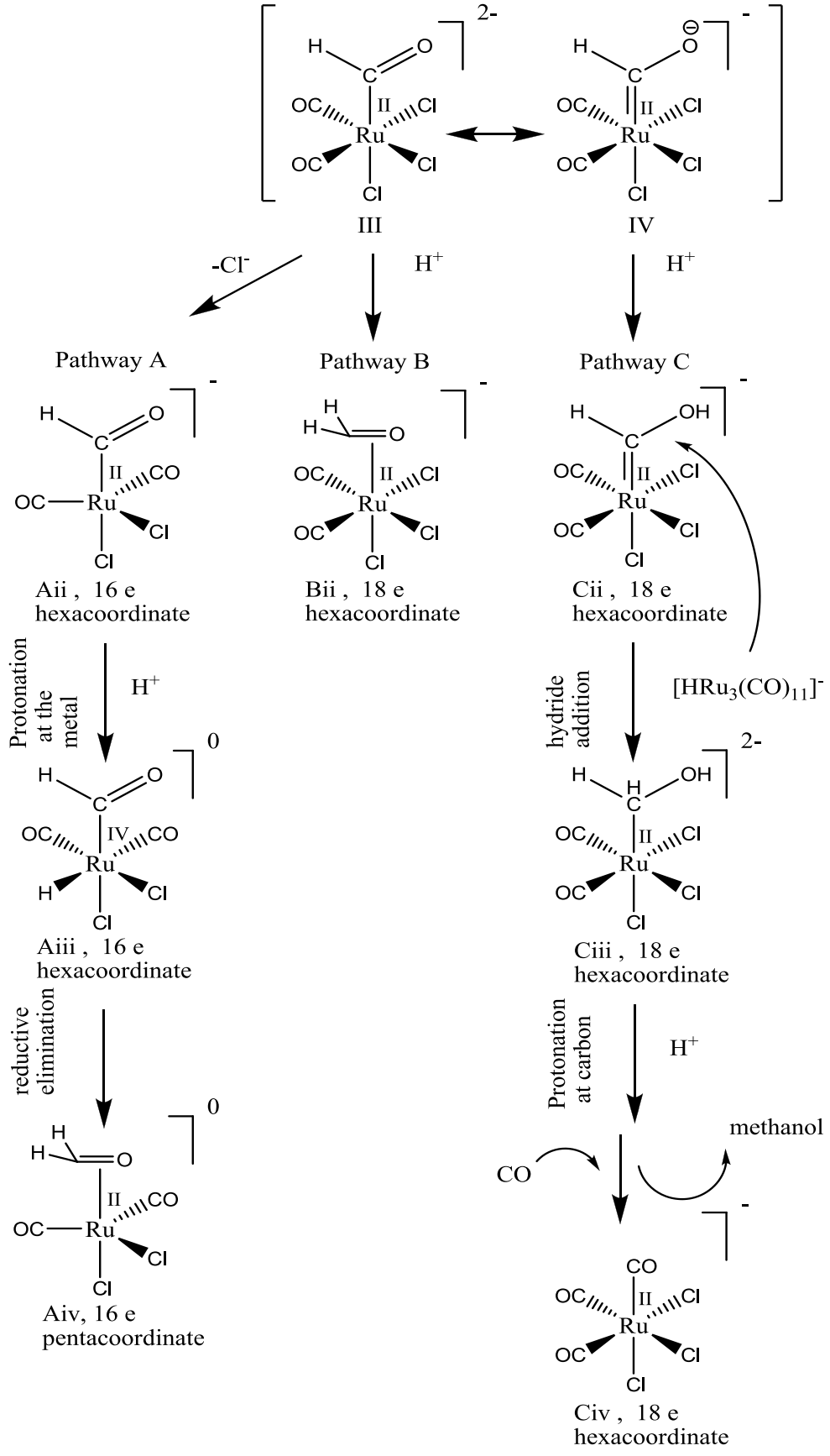

Scheme 6.3 A selection of possible pathways toward methanol.

Of the pathways shown above we have started from the proposed formyl species. Because species III is an 18-electron octahedral complex with relatively high charge density and labile chloride ligands, loss of a halide ligand could occur, although perhaps not readily in an ionic liquid solvent. This leads to pathway A. This species has an electron count of 16 and of a trigonal bipyramidal geometry. For this species, hydride migration from the formyl to a cis position should be very rapid leading to regeneration of unactivated carbonyl, and restoring the 18 electron comlpex. This pathway is counterproductive. In scheme 6.4 two competing pathways are shown, where only one pathway could lead to production of methanol. To make the scheme more general we start from III, which loses a chloride ligand during the hydride migration. Because the protonation of III is in competition with the formyl dissociation reaction the overall reaction rate should benefit considerably from high Brønsted acidity. The hydride abstraction reaction would be inhibited by the presence of excess chloride.

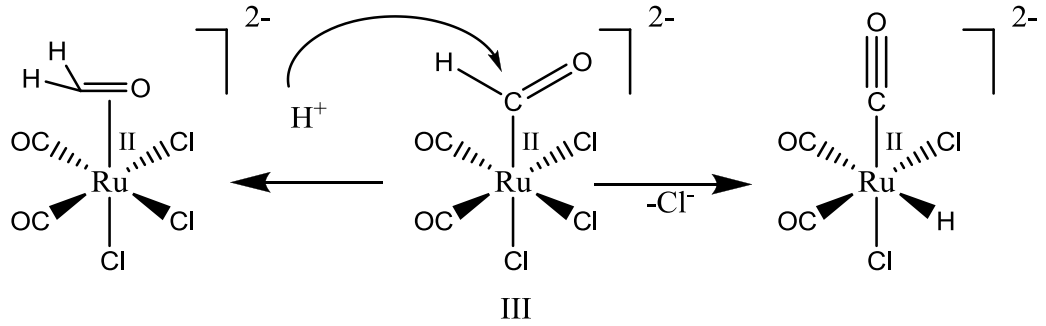

III

Scheme 6.4. two competing pathways, the right hand side leads to a ruthenium hydride, but there is no CO activation. The left hand side leads to formation to a "stable" precursor of methanol.

In the case of the chloride reactions we anticipate that the level of "free protons" is higher, which leads to a higher participation of the protonation of III and Aii (scheme 6.4 left, scheme 6.3 pathways A and B). This could help explain the higher overall rate. A more probable mechanism is shown in scheme 6.3, pathway B, where direct protonation occurs on the formyl carbon yielding formaldehyde which can be hydrogenated to form methanol. We have not covered how the formaldehyde is hydrogenated to methanol, but we have shown that ketone hydrogenation in this reaction medium is very rapid. In chapter 2 we described this experiment and discussed the presence of dimethoxymethane which points to the presence of formaldehyde in the system. In most reactions we find minor amounts of methylformate, by GC, which we

think is formed from a ruthenium formyl species that has undergone nucleophillic attack from methanol or water. This would indicate that a ruthenium formyl species is a plausible intermediate.

Pathway C follows protonation/stabilisation of the resonance structure IV to give a hydroxycarbene intermediate. (Cii). It has been shown that formyl complexes of ruthenium readily undergo protonation to give hydroxycarbenes even if they are positively charged[117], so it seems very likely that protonation of the formyl in the dianion, Cii would be highly favourable. Species Cii has a electrophillic carbene that should readily undergo nucleophillic attack from a hydride source to form Ciii. Protonation at the carbon yields methanol. Such a pathway has previously been proposed for methanol formation in reactions catalysed by $[Ru_3(CO)_{12}]$ in the presence of iodide.[65] Pathway C shows direct protonation, however because of the labile chloride ligands another possibility is dissociation of chloride followed by protonation at the metal centre followed by relatively quick reductive elimination of methanol as shown in scheme 4.3.

6.9 Discussions on the rates

In discussing rates of reactions the emphasis should lie in the slowest step of the entire mechanism. Because we do not really know the mechanism, nor the exact nature of the species involved this is difficult. However, there are some clues about the relative stability of species and from experience and textbooks it is known which type of species are likely to be stable, and which are not. Because evidence points to a very low stability of metal formyl species, our presumption is that rate in our system is mostly affected by this. Under the conditions of catalysis the hydride transfer should occur relatively fast, but the resulting formyl should degrade so quick that the efficiency towards methanol is actually very low. The rate of methanol synthesis is therefore most likely dependent on the race between formyl degradation and conversion to more stable intermediates.

6.9.1 Pathway B

Of the mechanisms, mechanism B leads to methanol in the easiest way, on paper. It has no intermediates that go through 16 electron complexes and it has the least amount of steps. However, we do not know if the formyl carbon is in reality negatively charged, and neither is it known if it is reactive enough towards protonation. It seems unlikely, given the known reactivity of formyl and acyl complexes towards electrophiles, which occurs at O. A high proton concentration would be beneficial in catalysis in order to provide a competitive pathway as depicted in figure scheme 6.3. Because we expect the acidity in the chloride reaction to be higher than in the other reactions the productive pathway would be favoured compared to the reactions containing bromide and iodide. Also, if this mechanism is important than it should lead to protonation the quickest if the electron density on the metal centre is moderate, making the III resonance structure dominant over the IV resonance structure, yet being high enough for a negatively charged formyl carbon. Comparing the activity of catalysis with these arguments, we can see that mechanism B seems does fit the observations made earlier, but is less likely on the basis of the probably charge distribution within the formyl group.

6.9.2 Pathway A

Likewise, prevalence of structure III is preferable in Mechanism A. Additionally mechanism A should benefit from increased steric bulk around the metal centre leading to dissociation of a halide anion, i.e. using the iodide rather than the chloride anions, having a high negative charge on the metal should increase protonation. In this sense, bromide and iodide should be the preferred anions. Interestingly, this trend does not occur in catalysis. Instead, the inverse is observed. Furthermore, in the series of experiments where the bromide level was varied, it was observed that with decreasing halide content the activity decreased as well. In case of mechanism A we would expect that formation of the pentacoordinate 16 electron species through loss of a halide anion would be energetically uphill and improved by low halide concentrations. For these reasons mechanism A is most likely not responsible for most of the methanol synthesis.

6.9.3 Pathway C

Finally, pathway C would benefit from a high electron density on the metal centre to favour formation of IV. If resonance structure IV is dominant, then protonation should occur readily on the oxygen, and this should stabilise the formyl species, as has previously been observed for isolated cationic formyl complexes of Ru. Given that formation of the active site for Pathway A is unlikely under the reaction conditions and the polarity of the CO bond in the coordinated formyl group mitigates against Pathway B, it seems more likely that Pathway C is followed, although the exact nature of the carbonyl complex that is attacked by hydride in $[HRu_3(CO)_{11}]^-$ remains undecided. The different rates of methanol formation obtained under the optimum conditions with different halides are in the order $Cl^- > Br^- > I^-$. Thus the complex with the lowest electron density is favoured. The carbonyl groups in the chloride are the least electron rich (the carbonyls absorb at the highest energy in IR) so should be the most susceptible to nucleophilic attack. The observed relative rates, therefore, suggest that hydride transfer from $[HRu_3(CO)_{11}]^-$ to $[RuX_3(CO)_3]^-$ is the rate determining step in methanol production.

6.10 Homologation

How the homologation reaction occurs is also of significant interest in our system. There is already a good source of ethanol through fermentation of biomass, however, there may be interest in converting methanol to ethanol for companies that do not have such technology or equipment in place, and if they have access to a cheap methanol source. In addition, there is concern that bioethanol may become disfavoured as the demand for land for food increases. In this and previous chapters we have discussed some of the rates involved with the reactions, however, we do not know how the methanol to ethanol conversion occurs mechanistically. Because of the relationship between the presence of $[RuBr_3(CO)_3]^-$ and the rate of ethanol formation we suspect that $[RuBr_3(CO)_3]^-$ plays an important role. The labelling studies reported in chapter 2 show that, instead of direct formation of ethanol on the metal centre from CO, ethanol is formed by the homologation of free methanol. The usual way of activating methanol for transition metal catalysis in the presence of halides is the formation of a methylhalide

species, which then undergoes oxidative addition over the metal centre forming a metal alkyl species.[118, 119] Migration to a coordinated CO can occur forming an acyl-metallate. After hydride transfer acetaldehyde can be released and hydrogenated. A good place to start investigations is by drawing out some possible mechanisms leading to ethanol. We can then compare observations from previous experiments with these mechanisms and see if they meet expectations, it must be clear that such mechanism are speculations until an investigator does proper mechanistic studies. Because we know the predominant species in our system we can start out from them; $[HRu_3(CO)_{11}]^-$, $[RuBr_3(CO)_3]^-$, $[RuBr_2(CO)_3]_2$ and methylbromide.

6.10.1 Ru(IV) mechanism

We will start from $[RuBr_3(CO)_3]^-$ which will yield a Ru(IV) species after addition of methyl bromide.

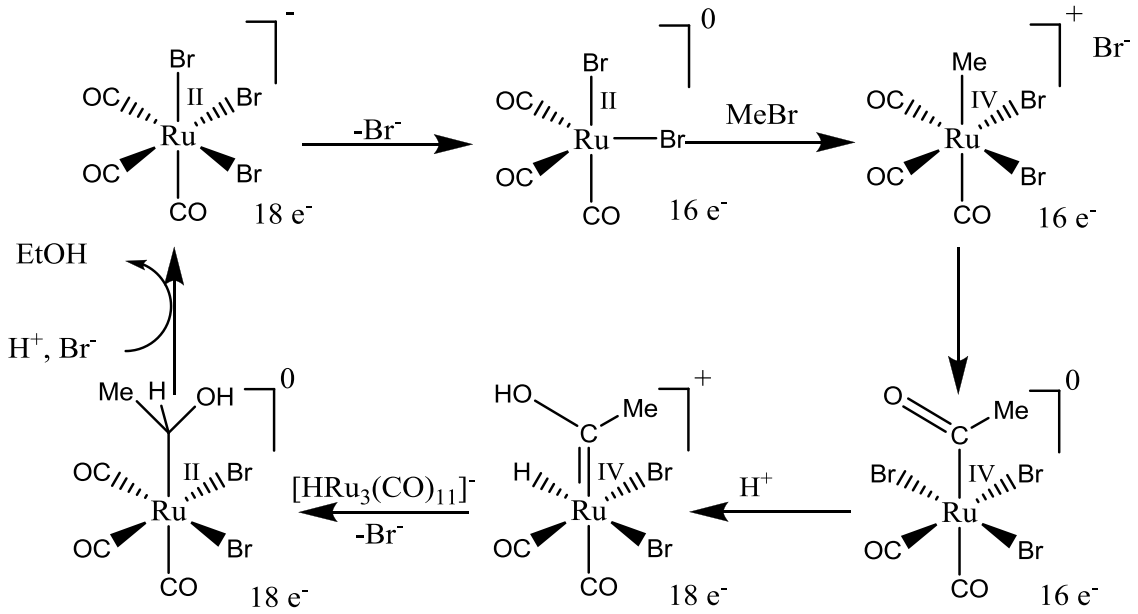

Scheme 6.5 Mechanism for the formation of acetaldehyde from methanol and $[RuBr_3(CO)_3]^-$.

Therefore, we will call this mechanism the Ru(IV)-mechanism (the ruthenium species after MeBr addition). In this mechanism $[RuBr_3(CO)_3]^-$ first loses on bromide ion to make place for oxidative addition of methylbromide. The resulting complex is a 16 e^-, octahedral ruthenium methyl species, which should be relatively unstable. The low electron density should promote CO insertion, because of the relatively electropositive charge on the carbonyl carbon (mainly sigma donation and little π-

backdonation). Ion exchange leads to a ruthenium hydride complex that should undergo easy reductive elimination to yield coordinated acetaldehyde. Alternatively, the hydride addition could occur directly in a nucleophillic attack on the ruthenium acyl species to yield a species similar to 6 but with a bromide instead of a CO ligand. Release of acetaldehyde and coordination of a bromide or CO ligand leads to the starting species. The mechanism goes through some seemingly unstable species before the product is released and the 18 e^- species is reinstated.

6.10.2 Ru(III) mechanism

The second mechanism should start from the same starting material, but then dimerised. Oxidative addition of MeBr then leads not to a Ru(IV) species but to two Ru(III) species, as shown in Scheme 6.6.

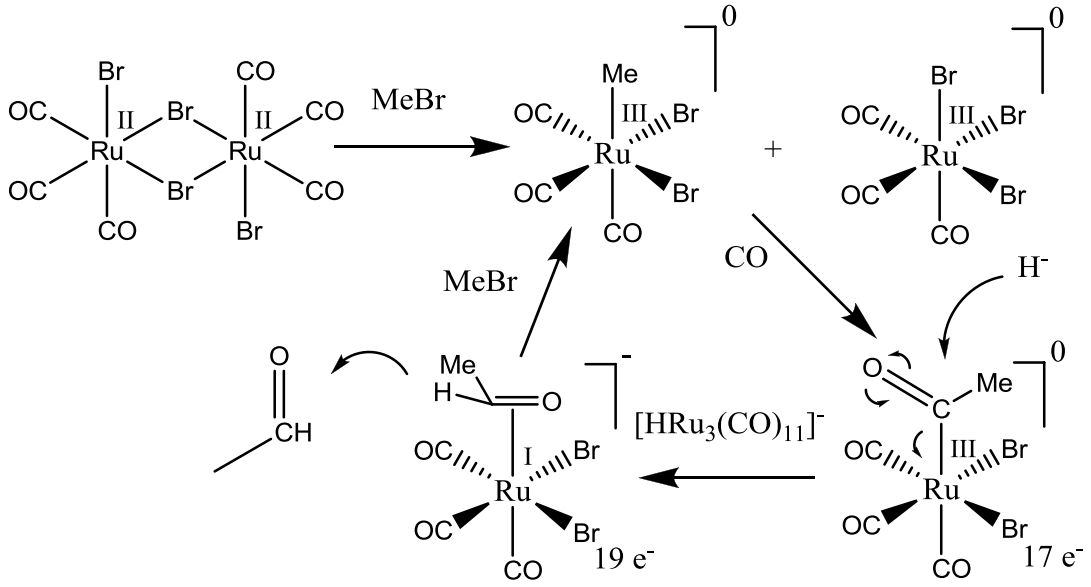

Scheme 6.6 the formation of acetaldehyde starting from $[RuBr_2(CO)_3]_2$ and methyl bromide.

We will refer to this mechanism as the Ru(III) mechanism. Because of the use of two ruthenium centres the oxidation step from the addition of methyl bromide can be shared between the metals, yielding two species. The resulting ruthenium alkyl species has a formal oxidation state of 3+ and yields a 17 e^- species. The usual step is CO migration, however this would lead to a 15 e^- species and seems unlikely, therefore this should only occur if another ligand approaches the complex, for instance a CO ligand. Subsequent nucleophillic hydride attack on the ruthenium acyl leads to coordinated acetaldehyde on a Ru(I) 19 e^- complex. Alternatively, a pathway much like C could be

followed in forming the alcohol. Loss of acetaldehyde followed by dimerisation with $[Ru(III)Br_3(CO)_3]$ with concomitant electron transfer leads to the starting dimer.

6.10.3 Ru(II) mechanism

The third mechanism involves the use of $[HRu_3(CO)_{11}]^-$. It should have enough electron density to oxidatively add methyl bromide at relatively low temperatures, because it has enough electron density to add HBr. This could break up the cluster and lead to a ruthenium species containing a hydride, a methyl and a bromide ligand with ruthenium in oxidation state 2+. A possible mechanism leading to acetaldehyde or ethanol is shown in a complete cycle below.

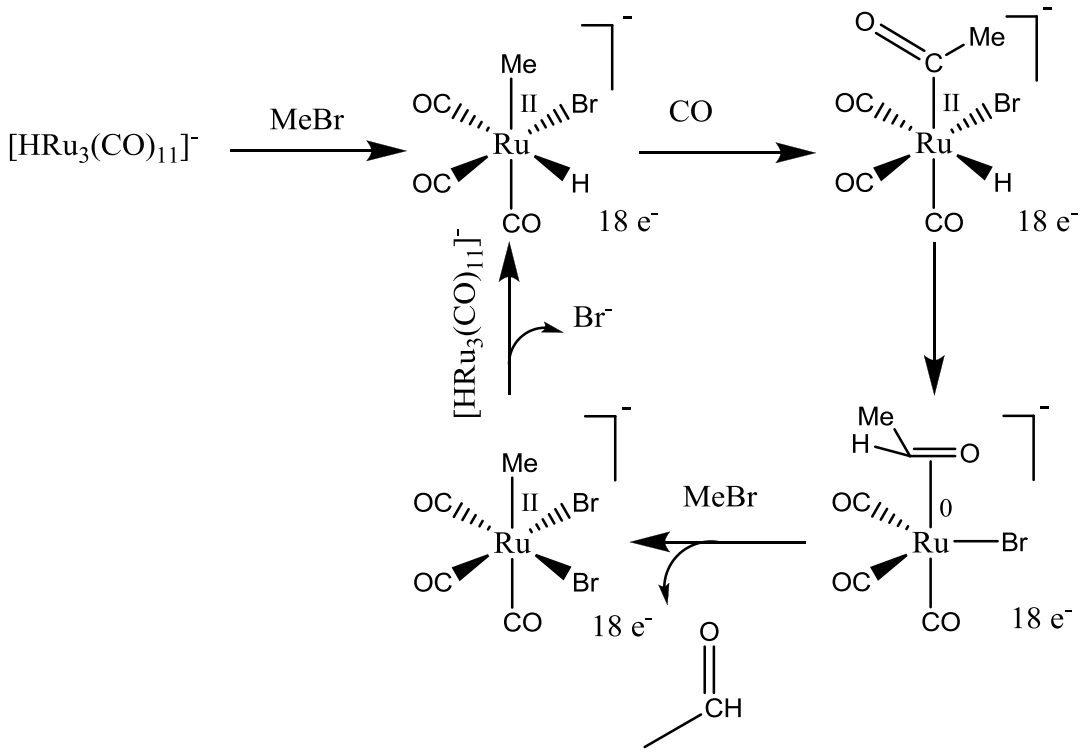

Scheme 6.7 the synthesis of acetaldehyde and ethanol starting from $[HRu_3(CO)_{11}]^-$ and methyl bromide.

This cycle starts with the formation of $[HRuMeBr(CO)_3]^-$. The CO migration leads to a 16 e^- complex, so if this reaction occurs with quick addition of CO we would get the second species, which is also an 18 e^- complex. Reductive elimination of the acyl group with the hydride leads to coordinated acetaldehyde in a pentacoordinated 18 e^- ruthenium (0) complex, which should be able to undergo oxidative addition with methyl bromide leading to the formation of the starting complex. Each of the three

mechanisms could have variations at any point, making a useful discussion about which mechanism is "real" pointless. For instance, in this last mechanism hydrogenation of the coordinated acetaldehyde could occur starting from the pentacoordinate species by adding H_2 to the vacant site. Overall, the point is to identify desirable or likely hypothetical species or reactions and to compare them with observations. In Table 6.4 some of these features are grouped.

Table 6.4 some advantages and disadvantages of the described mechanisms

Mechanism	Advantages	Disadvantages
Ru(IV)	Cycle starts from $[RuBr_3(CO)_3]^-$	Likely to yield acetic acid through premature reductive elimination with halide
	Low electron density labilises CO for exchange	Cycle goes through high oxidation state
	Low electron density promotes CO migration	Large deviations from 18 electron rule
		Need for intermolecular hydride transfer to a negatively charged species
Ru(III)	Cycle starts from $[RuBr_3(CO)_3]^-$	Formation of a dimer precursor necessary under conditions where the monomer is favoured
	MeBr activation "burden" shared over two metal centres	One additional inactive species formed
	No extreme oxidation states	Intermolecular hydride transfer needed for product formation
	Hydride addition occurs to a neutral species	Mechanism does not easily return to $[RuBr_3(CO)_3]^-$ species that is observed
	Few steps needed to get to product	
Ru(II)	The cycle does not involve any extreme oxidation states	Does not account for the beneficial presence of $[RuBr_3(CO)_3]^-$
	No deviation from the 18 electron rule	
	Activation of MeBr relatively easy step	
	Full formation of ethanol possible with additional hydrogenation step using the same species	

One mechanism stands out in terms of species, and that is the mechanism involving Ru(II) after methyl bromide addition. The species involved are much more likely to exist and to be stable. Furthermore, the methyl bromide addition to a Ru^0 species should be facile at the conditions used, shifting the slow step to one of the other reactions. Through the labelling studies it was found that the CO insertion step must be relatively slow, or beta hydride abstraction from the ruthenium alkyl species must be relatively quick. We have drawn addition of a neutral ligand to accompany the CO migration as we think that the addition of bromide to a species that is already negatively charged would be less likely. Addition of hydrogen would most likely result in the further reduction of the metal acyl species to ethanol. Because we want to compare

cycles to the same product (acetaldehyde) we propose the coordination of CO. Also, we think that addition of H_2 may reduce the electron density on the complex more than CO does, and therefore the reductive elimination to coordinated acetaldehyde would be increased. This mechanism may be a good starting point for further investigation into the homologation reaction. From Ono's work, there is additional evidence that the ethanol production in his system is increased by addition of phosphoric acid. If he added methyl phosphate the same reactivity occurs, however, then without an induction period. Therefore, we decided to test if methyl phosphate increases the homologation rate in our system too.

6.11 Phosphoric acid and trimethylphosphate as promoters

First the addition of phosphoric acid was tested by setting up a reaction using $[PBu_4]Br$ (14.702 g), $[Ru_3(CO)_{12}]$ (0.25 g) and HBr (100 µL, 48% aqueous, 0.75 eq to Ru) and of phosphoric acid (60 µL 85% aqueous, 0.75 eq. to Ru). The results are shown in figure 6.14.

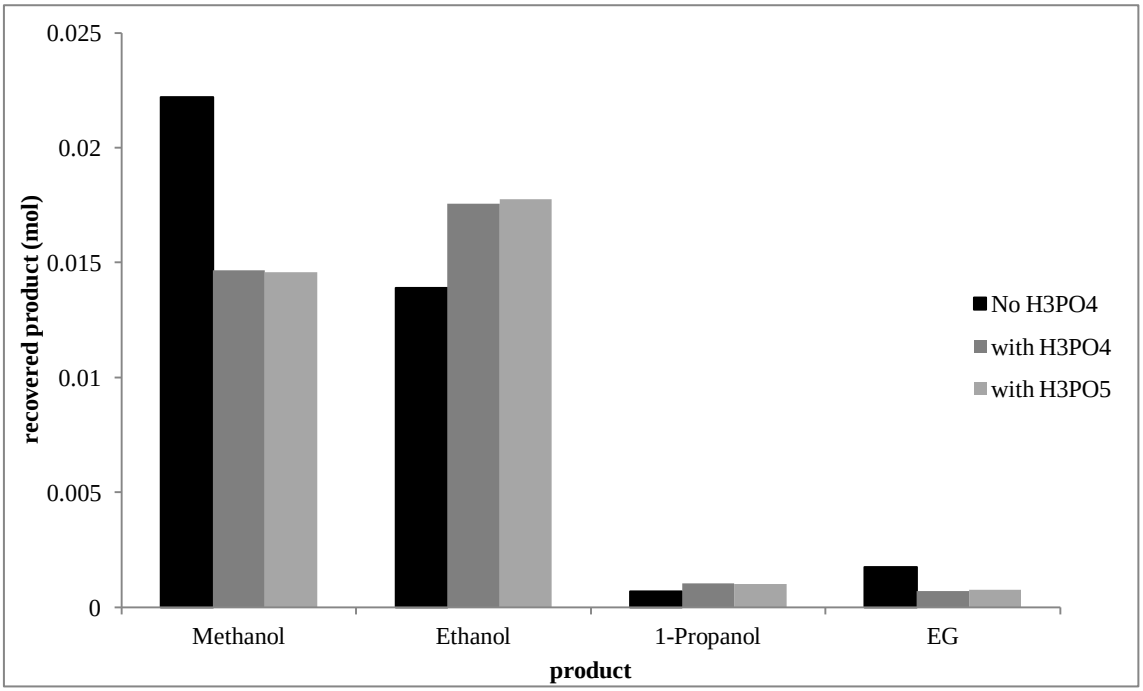

Figure 6.14 Two reactions showing the effect of using phosphoric acid during catalysis. Conditions: $[PBu_4]Br$ (44 mmol), $[Ru_3(CO)_{12}]$ (0.25 g), H_3PO_4 (85%, aqueous, 0.75 eq. (to Ru) aq. HBr, 250 bar 1:2 (CO to H_2) syngas constant pressure, 200 ^oC, 4 hrs.

The reaction shows a marked increase in homologation. A series of reactions using incremental amounts of trimethyl phosphate was performed to determine the effect of trimethyl phosphate concentration in the system. See figure 6.15.

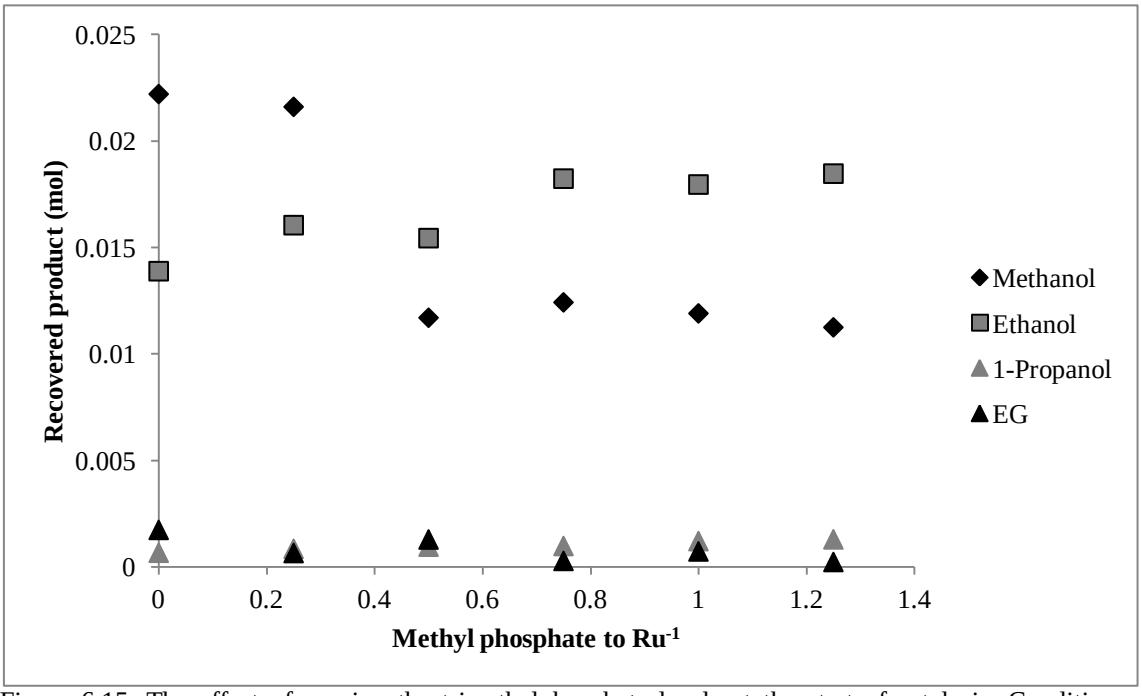

Figure 6.15. The effect of varying the trimethylphosphate levels at the start of catalysis. Conditions: $[PBu_4]Br$ (44 mmol), $[Ru_3(CO)_{12}]$ (0.25 g), HBr and Methyl phosphate(0.75 eq. (to Ru) aq.), 250 bar 1:2 (CO to H_2) syngas constant pressure, 200 ^oC, 4 hrs.

The addition of trimethylphosphate significantly changes the selectivity of catalysis. Overall, the total activity for methanol formation does not seem to be affected much, but the homologation is increased significantly. There is a crossover point where the homologation seems to be "switched on". For better insight, the rate constants were calculated, as shown in figure 6.16.

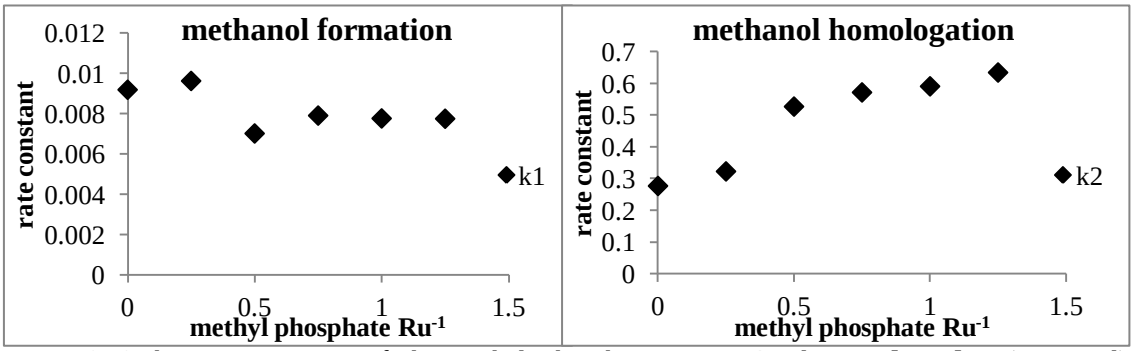

Figure 6.16 the rate constants of the methyl phosphate series. Conditions: $[PBu_4]Br$ (44 mmol), $[Ru_3(CO)_{12}]$ (0.25 g), HBr and Methyl phosphate(0.75 eq. (to Ru) aq.), 250 bar 1:2 (CO to H_2) syngas constant pressure, 200 ^oC, 4 hrs.

The calculated rate constants show that the methanol formation is relatively constant throughout the series. The homologation rate constant however, is increased significantly and continuously. IR spectra taken of the solutions after catalysis show a spectrum that is similar to a spectrum taken of the reaction where no trimethyl phosphate was added, see figure 6.17.

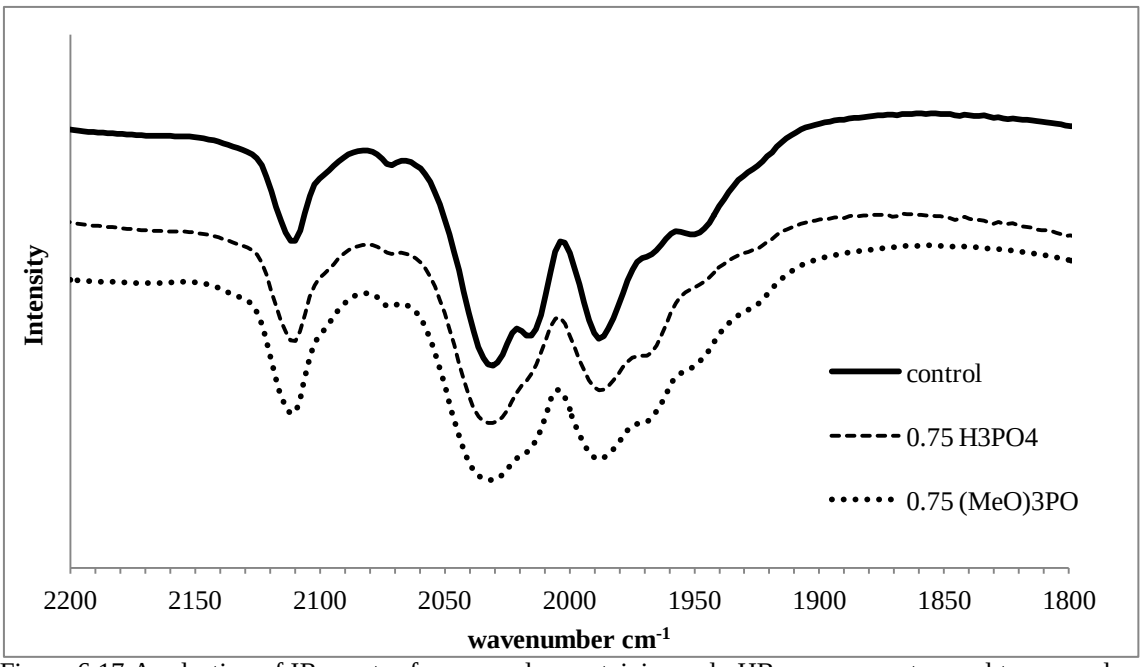

Figure 6.17 A selection of IR spectra from samples containing only HBr as a promoter, and two samples that additionally have phosphoric acid or trimethylphosphate. The IR indicates that there is little difference in the catalytic composition.

These IR data indicate that trimethyl phosphate does not change the composition of the catalytic species but instead improves the homologation rate in an alternative fashion. ^{31}P NMR spectra taken of the solutions after catalysis show that the

trimethylphosphate is converted to methylphosphates (hydrolised or not) and protonated phosphates (figure 6.18)

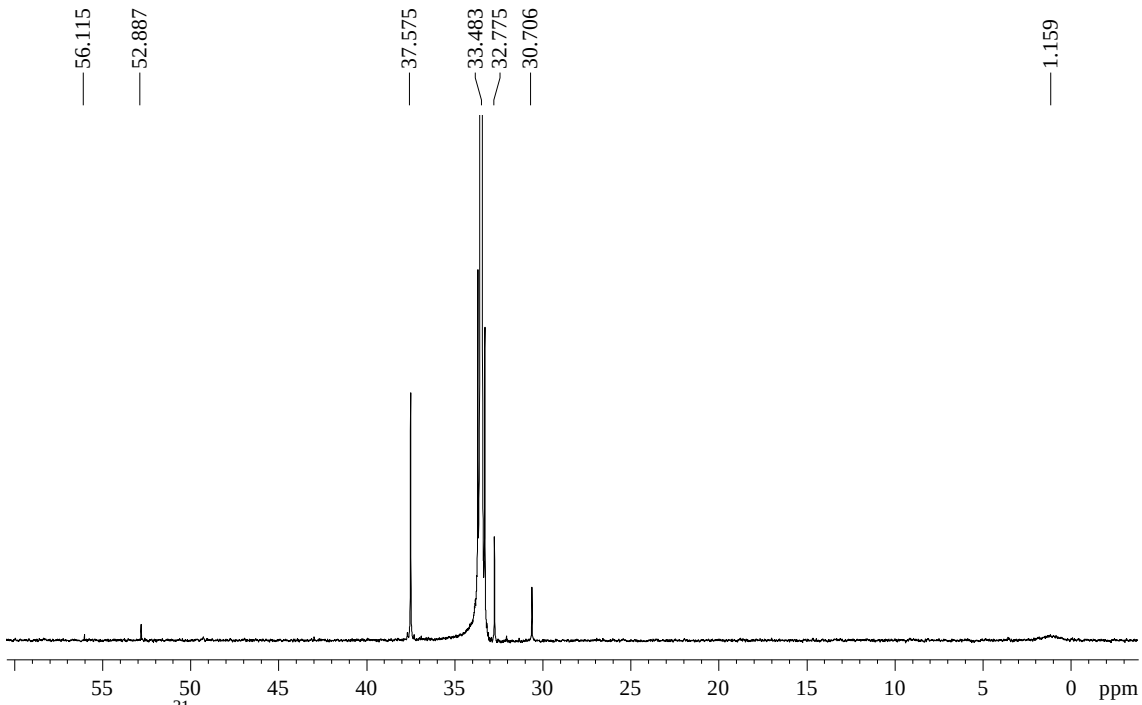

Figure 6.18 the ^{31}P NMR of the product liquid after catalysis. The peaks in the centre (between 30 and 40 ppm correspond to phosphonium salts. The peaks near 1 ppm correspond to phosphoric acids and the peaks at 52 and 56 ppm are from methyl phosphates.

The ^{1}H NMR shows very little difference from spectra obtained without the use of methyl phosphate, the relative intensity of $[HRu_3(CO)_{11}]^-$ (δ -12.67 ppm) hydride signal is low, because of the added HBr. Interestingly the peak at -11.4 ppm is relatively large, even when compared to the HBr series spectra. This suggests that presence of the species that has the hydride resonance at δ -11.4 ppm is beneficial for homologation, because not only can its presence be associated with an increase in homologation in the HBr series, but also, within the methyl phosphate series this trend is continued.

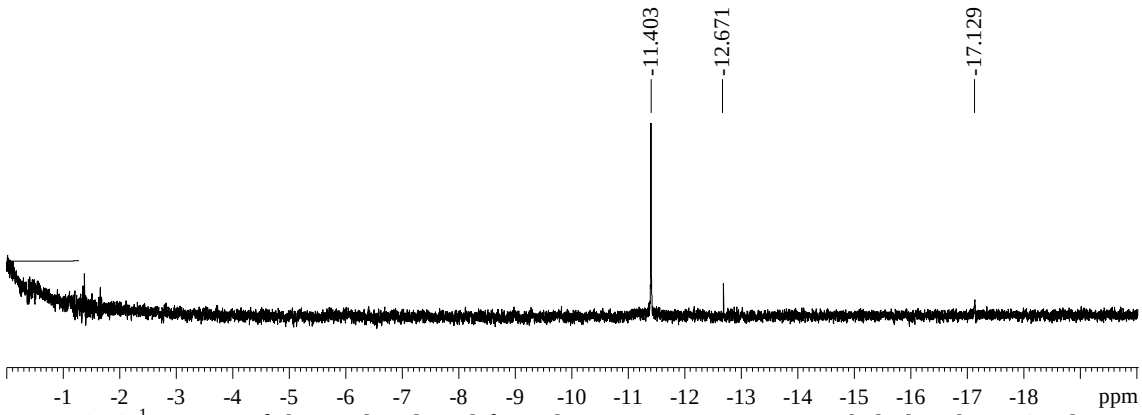

Figure 6.19 ^{1}H NMR of the product liquid from the reaction containing methyl phosphate. Conditions used: 44 mmol $[PBu_4]Br$, 0.25 g $[Ru_3(CO)_{12}]$, 0.75 eq. (to Ru) aq. HBr, methyl phosphate, 250 bar 1:2 (CO to H_2) syngas constant pressure, 200 ^{o}C, 4 hrs.

Thus, even while the IR spectra indicate the presence of predominantly two ruthenium containing species, $[HRu_3(CO)_{11}]^-$ and $[RuBr_3(CO)_3]^-$, according to the NMR this is not the case; the primary hydride is the unknown compound with a resonance at δ -11.4 ppm.

IR spectra of the reaction products when using $[PBu_4]Cl$ had revealed the presence of one more compound at higher HCl levels (figure 6.12). The coexistence of the peak at δ -11.4 ppm and the IR signals suggests that they may be from the same compound. In terms of catalysis it is good to keep in mind that there is an additional possibility that the relative amount of $[HRu_3(CO)_{11}]^-$ could be lower because the trimethylphosphate facilitates hydrogenation or hydride transfer to an intermediate that only occurs in the homologation cycle. Because this process is improved the steady state concentration of $[HRu_3(CO)_{11}]^-$ would be lower, so association of the unidentified compound with catalysis is not proven. We could try to find out a little more about the nature of the unknown hydride complex by comparing its shift to the species from reactions with other chloride and iodide reactions. Figure 6.20 shows a comparison of ^{1}H NMR spectra from the chloride and iodide series with high levels of HCl or HI. Both spectra contain a signal of a secondary species next to $[HRu_3(CO)_{11}]^-$, but with a different chemical shift. The change in chemical shift suggests that this is more than just a solvent effect, but originates from coordinated halides on this particular ruthenium hydride.

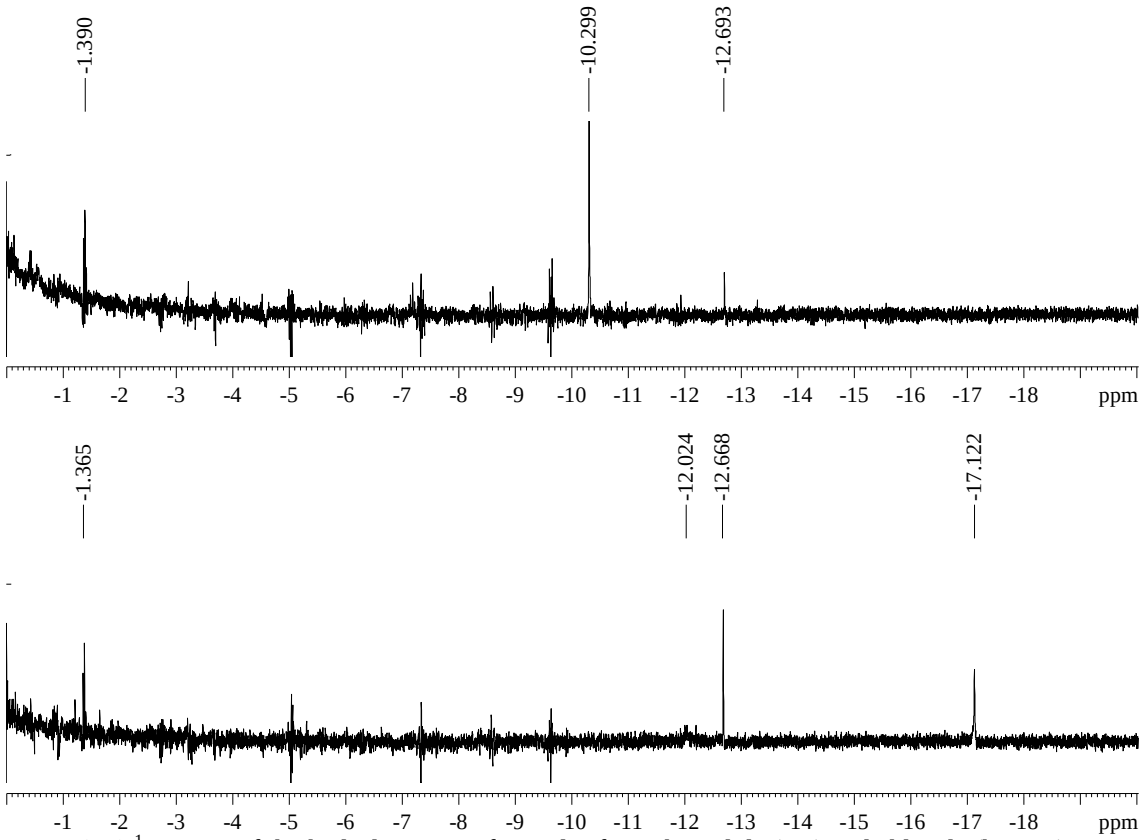

Figure 6.20 ^{1}H NMR of the hydride region of samples from the iodide (top) and chloride (bottom) series where 0.75 eq. (to Ru) HX had been added.

The iodide complex has a resonance at δ -10.299 ppm, the bromide at δ -11.4 and the chloride possibly at δ -12.02 ppm, so the basicity of the hydride increases in the order Cl> Br> I. Interestingly, comparing the series of NMR spectra between solvents also reveals the presence of a hydride species that resonates at δ -17.1 ppm that does not have the same chemical shift-shift in different [PBu_4]X (X = Cl, Br or I) solvents, but its presence appears to correlate with the rate of methanol formation.

6.12 Using similar structural features

H_3PO_4 is an acid, but trimethyl phosphate is not. However, they both affect the reactivity in the same way. Furthermore, we do not see the change in catalyst composition that was observed when adding HBr, therefore we feel that the acidity change effected by the phosphates does not affect a change in the catalyst. Rather, another property of the phosphates must be responsible for the increase in catalytic activity towards ethanol. Trimethylphosphate could act as a methyl (CH_3^+-) donor (the phosphate as a leaving group) or as a methoxy (MeO^-) donor/shuttle (esterification).

Alternatively, a combination of structural features may cause the effectiveness of methyl phosphate. For a little more information, we examined other additives containing similar structural features. Below we have drawn three compounds with similar structures.

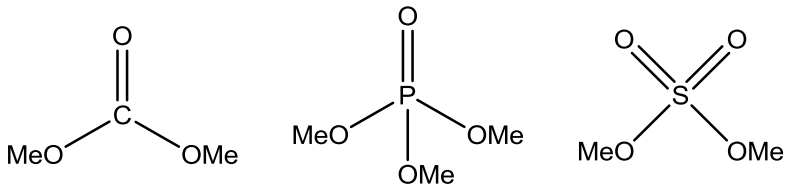

The acidity of the acids of these compounds differs significantly. Furthermore, there is a difference in the central atom. We chose to test the addition of sulfuric acid first, which also has a heteroatom centre connected with a double bond to oxygen and a single bond acidic hydroxyl group. Interestingly, the results were not what first was expected. A reaction containing $[Ru_3(CO)_{12}]$, $[PBu_4]Br$ and HBr (0.75 eq. to Ru) together with additional sulfuric acid (0.75 eq. to Ru) was initiated. However, sulfuric acid proved acidic enough to imitate the action of HBr. Thus in an experiment that already contains HBr the activity is almost halted, as if a reaction was performed with an excess of HBr. A yellow, pungent product mixture was observed, indicative of formation of $[RuBr_3(CO)_3]^-$ from $[HRu_3(CO)_{11}]^-$. Most likely HBr is formed from the sulfuric acid and phosphonium bromide. Analysis of the IR spectrum after the reaction shows that there is primarily formation of $[RuBr_3(CO)_3]^-$ and very little $[HRu_3(CO)_{11}]^-$, as expected. The experiment was repeated without added HBr, but with just sulfuric acid in its place. Different amounts of sulfuric acid were used to do a rough optimization of the conditions, also to see if the second proton of sulfuric acid plays a role too.

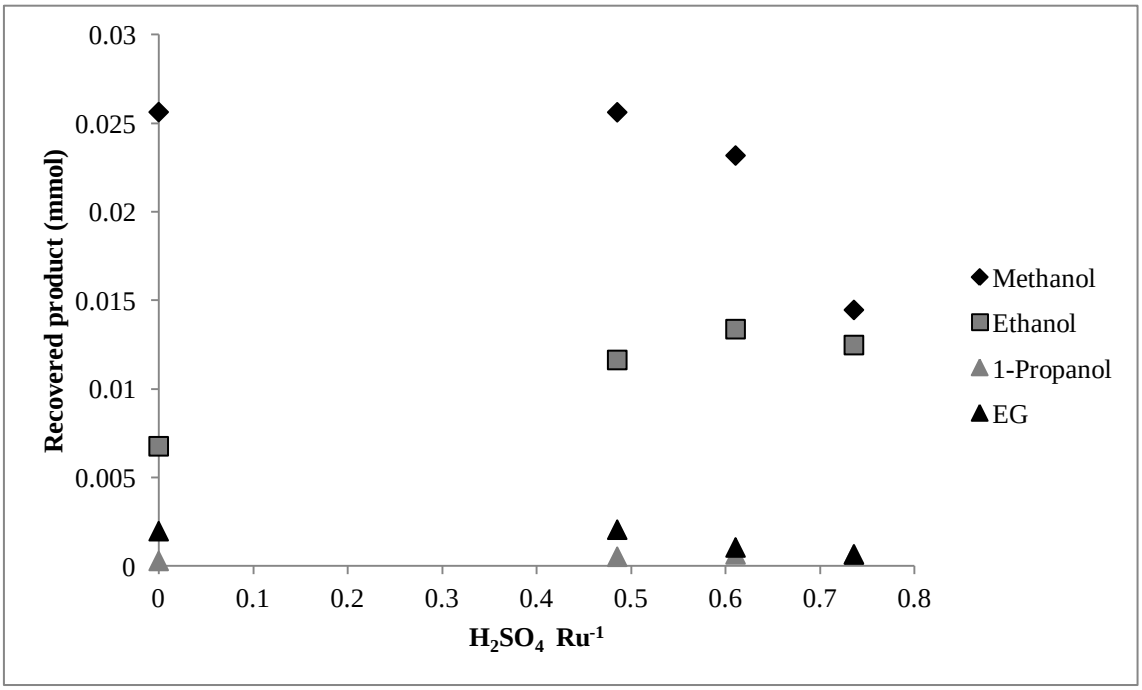

Figure 6.21 Product recoveries from the series of reactions with varying amounts of added H_2SO_4. Conditions: (0.25 g) $[Ru_3(CO)_{12}]$, (15 g) $[PBu_4]Br$, H_2SO_4, 250 bar syngas ($CO:H_2$ 1:2), 200 ^oC, 4 hr.

The shape of this curve resembles the shape of the HBr series, suggesting that only the first deprotonation of H_2SO_4 is has the acidity to effect major change in the catalyst composition. While the second proton only contributes to changes only up to a minor extent. Therefore, the reaction with ± 0.75 eq. of sulfuric acid should resemble the reaction with phosphoric (0.75 eq.) acid, which had added HBr (0.75 eq.), but no additional protons to change the catalyst mixture.

Despite the similarity between the phosphoric acid and sulfuric acid structures, there is no marked increase in homologation that was observed using phosphate. The IR spectrum taken after the sulfuric acid series shows a marked difference in species. Visibly present is the $[RuBr_3(CO)_3]^-$ species, but the IR reveals formation of an additional species with the most significant peaks at 1997.07 cm^{-1} and 1972.59 cm^{-1} and a reduction of the presence of $[HRu_3(CO)_{11}]^-$. Possibly, the sulfuric acid reacts with $[HRu_3(CO)_{11}]^-$ and converts it to another species.

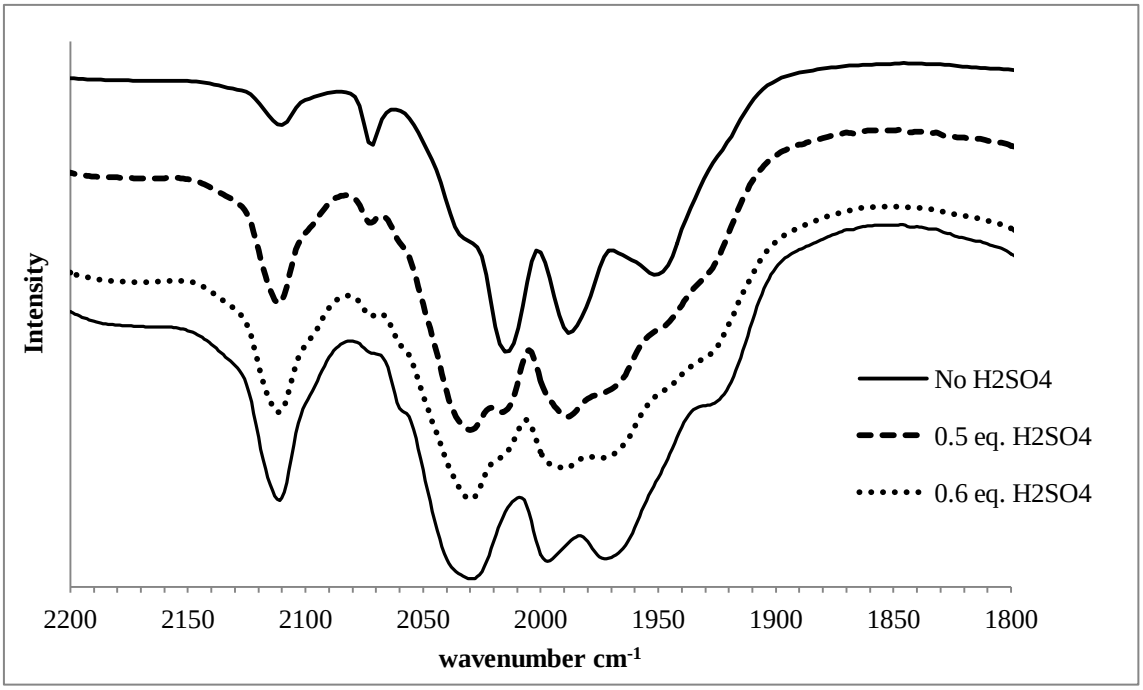

Figure 6.22. The IR spectra of the reactions with sulfuric acid present. The presence of sulfuric acid increases formation of $[RuBr_3(CO)_3]^-$, but also of another compound with carbonyl absorption at 1997.07 cm^{-1} and 1972.59 cm^{-1}.

^{1}H NMR analysis of one of the reactions shows that there is reduced formation of what we presume is $[HRu_3(CO)_{11}]^-$ (resonance at -12.67 ppm) but increased levels of a species that resonates at δ -18.8 ppm. It looks like this peak has shifted from the hydride at δ -17.12 in the HBr series due to possible coordination of sulfate ions. Furthermore, in the spectrum of the sulfate reaction no peak at δ -11.4 ppm is present. The lack of the compound that resonates at δ -11.4 ppm, which was until now associated with the homologation, shows that even though none of this compound is spectroscopically present, homologation still takes place.

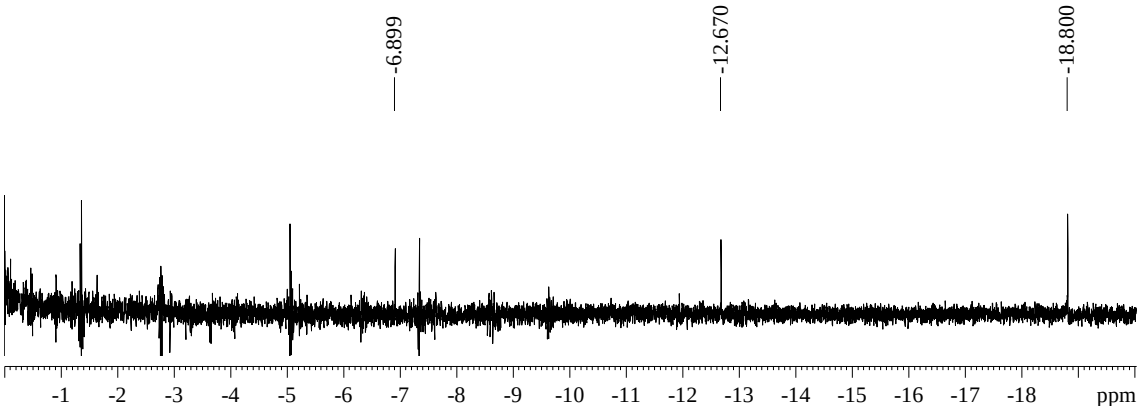

Figure 6.23. ^{1}H NMR spectrum of the product liquid from the reaction containing 0.72 eq. of H_2SO_4 to Ru.

In addition to sulfuric acid we also turned to using dimethyl sulfate as a possible promoter. To our surprise, the reaction with the dimethyl sulfate and HBr also behaves like a reaction where too much HBr is added. Under reaction conditions water is formed, capable of converting dimethyl sulfate into sulfuric acid, which in turn is a source of protons for the conversion of the ruthenium. The product yield was again a strong smelling (SO_2/SO_3 type smell) yellow paste.

The infrared showed a change in the catalytic composition but now with more defined peaks at 1999 and 1975 cm^{-1}. Furthermore the signals for $[HRu_3(CO)_{11}]^-$ cannot be found and the peaks for $[RuBr_3(CO)_3]^-$ are reduced significantly too, suggesting that the remaining peak at 2032.75 cm^{-1} also belongs to the compound that is also responsible for the peaks at 1999 and 1975 cm^{-1}.

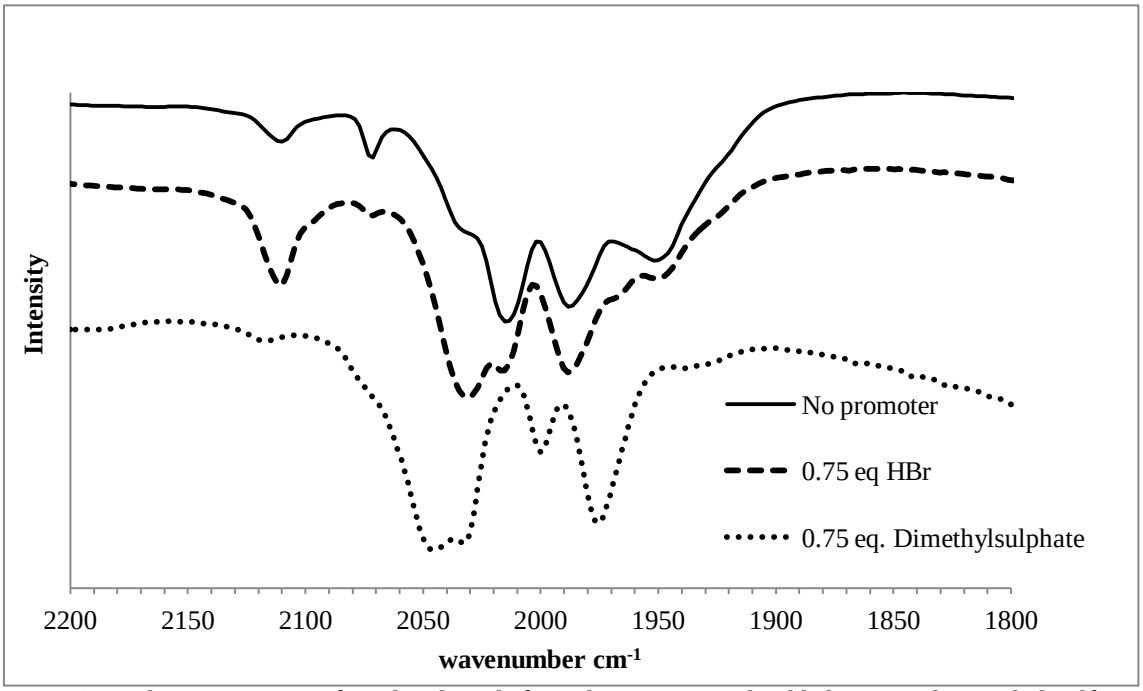

Figure 6.24 The IR spectrum of product liquids from the reaction with added, HBr and Dimethyl sulfate. It clearly shows the presence of an unknown compound at 1999 and 1975 cm^{-1}.

Because using sulfates does not increase the homologation reaction in the same way as using phosphates, dimethyl carbonate, which also has the same structural features that the phosphate and sulfate moieties, but derives from the weakest acid of the three, was employed as the promoter. A mixture of $[Ru_3(CO)_{12}]$ (0.25 g), $[PBu_4]Br$, HBr (0.75 eq. to Ru) and dimethyl carbonate (0.75 eq. to Ru) was reacted for 4 hours at 200 ^oC and 250 bar of 1:2 H_2:CO syngas.

The presence of dimethyl carbonate does not affect product formation relative to a reaction using HBr but without dimethylcarbonate (figure 6.25). The IR and NMR spectrum of the product liquid show no difference between the control and reaction with dimethyl carbonate (not shown).

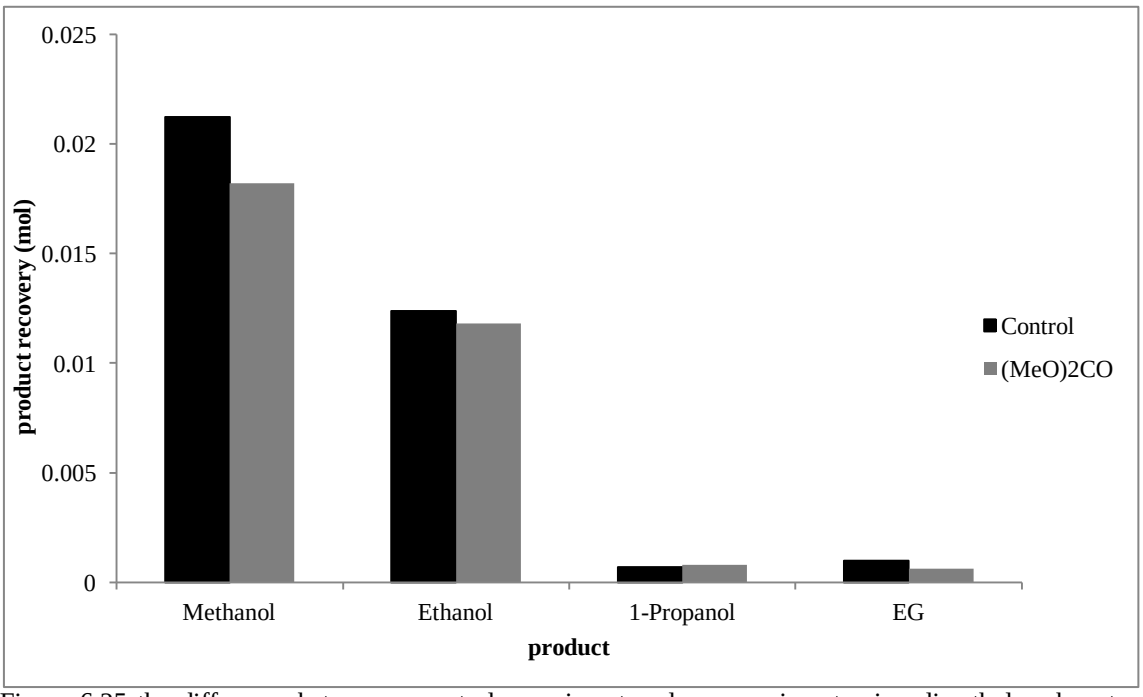

Figure 6.25 the difference between a control experiment and an experiment using dimethyl carbonate. Conditions: $[Ru_3(CO)_{12}]$ (0.25 g), $[PBu_4]Br$ (15 g), dimethyl carbonate (0.75 eq. (to Ru)), 250 bar syngas ($CO:H_2$ 1:2), 200 ^oC, 4 hr.

In fact, the activity even seems to be slightly reduced, although this appearance could be due to experimental error. Dimethyl carbonate will easily convert to CO_2 and methanol in the presence of water. We hoped that if this conversion is slow compared to the homologation, we would see an effect. Because there is no effect during catalysis we can assume that either dimethyl carbonate decomposition is fast or that dimethyl carbonate plays no role in homologation. At this point we cannot distinguish between the two possibilities, but the effect is the same: dimethyl carbonate does not improve homologation. Additionally, these studies have not yielded any significant insight to the working mechanism of trimethylphosphate. We still suspect that the action of trimethylphosphate is by facilitating esterification or methylation of crucial intermediates in the homologation cycle. One more alternative is that the doubly bonded oxygen from trimethylphosphate acts as a base or facilitates coordination. To rule out this possibility we decided to test one further compound with a structural similarity,

namely tributylphosphine oxide. If this species increases the activity for homologation then we could assign the increased activity to the presence of the doubly bonded oxygen in trimethylphosphate, alternatively it must be one of the other options. Others[72] had shown that in their systems the presence of phosphine oxides could be advantageous to catalysis, especially homologation. Dombek had significant increases in homologation using trialkylphosphine oxides, but only at very high concentrations. At low concentrations, as in our system, activity increases were not observed.

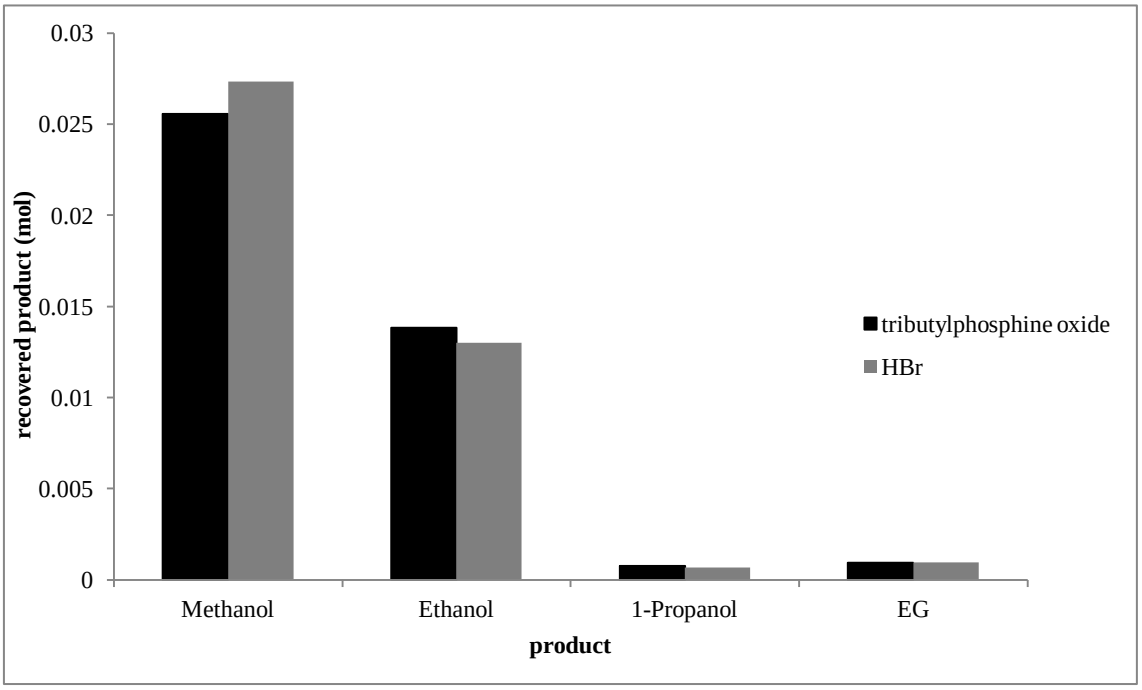

Figure 6.26 The effect of adding tributyl phosphine oxide to the reaction mixture does not lead to significant improvements in catalysis. Conditions: $[Ru_3(CO)_{12}]$ (0.25 g), $[PBu_4]Br$ (15 g), $OPBu_3$ (0.75 eq. to Ru), 250 bar syngas ($CO:H_2$ 1:2), 200 ^oC, 4 hr.

The selectivity *appears* improved in the reaction with added tributylphosphine oxide, however these differences are within experimental error and the effect for trimethylphosphate was much more dramatic. It is more likely that perhaps the phosphate can coordinate through one of the oxygen atoms presenting the basic oxide group as a ligand to the catalyst in a convenient orientation. This would increase the local "concentration" of the basic oxide to the ruthenium accounting for the high concentration effect in phosphine oxide and the low concentration effect in phosphate. Alternatively, the action of trimethylphosphate could lie with the combination of features that are present in trimethylphosphate.

Given that the mechanism of homologation probably involves nucleophilic attack of a ruthenium centre, possibly $[RuBr_3(CO)_3]^-$ itself on MeBr, it could be that this attack is promoted by the use of $(MeO)_3P=O$, if dimethylphosphate anion is a better leaving group than Br^-. The acidity of the formed phosphoric acid is then not sufficient to upset the balance of acidity required for the methanol forming reaction. It appears that trimethylphosphate has just the right balance of leaving group (from Me^+), acidity of the formed acid and stabilblity to make it the ideal activator.

Alternatively, because dimethyl sulfate is also a very good methylating agent, but is not active in increasing the homologation step we may be able to assume that it is not the methylating function that improves catalysis. Instead, it could be the ester feature that is beneficial. In earlier experiments Gresham and Dombek had shown the beneficial effects of carboxylic acids.[7, 16, 46, 120] It was proposed that the carboxylic acid activated the hydroxymethyl or the hydroxycarbene intermediate. But none of these effects are as dramatic as with the phosphate promoter. Concerning a hypothetical mechanism, a possibility could be that as the trimethylphosphate approaches a ruthenium centre, like $[HRu_3(CO)_{11}]^-$, or $[RuBr_3(CO)_3]^-$ the methyl-oxygen bond could be activated through oxidative addition, leaving a coordinated phosphate ruthenium(II) alkyl species. Hypothetically, the phosphate could then activate a cis-carbonyl via C=O-P interactions, possibly speeding up the methyl addition; a form of trans-esterification where the product alcohol is formed on the phosphate. A suggested pathway has been drawn below, were the first step is the fragmentation of the triruthenium species to a mononuclear ruthenium phosphate species. The combination of the vicinity of oxygen donating ligands and the stabilising effect of the phosphate ester could increase the methyl insertion step and reduce the reverse reaction by stabilising the product. It is well-known that transition metal catalysts can be used to activate phosphates for hydrolysis or esterfication.[121, 122]

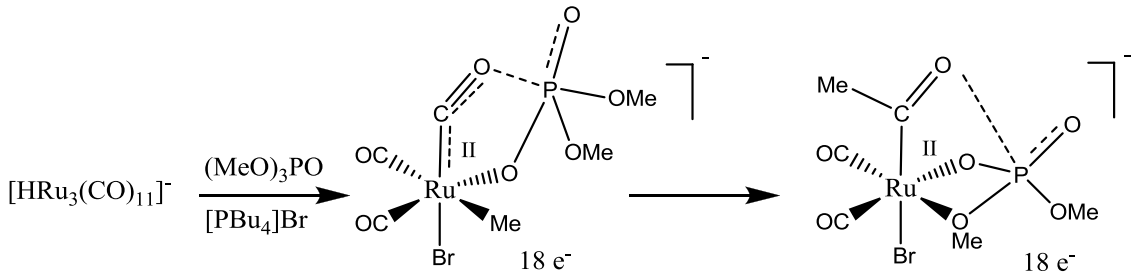

Scheme 6.8 A suggested pathway for phosphate promoted CO alkylation.

Despite not having evidence of any mechanisms or steps, we can conclude the latest studies with one very significant additional find, which is that this system is exceptionally sturdy towards the presence of sulfur. If the acidity of the mixture does not increase significantly by the presence of sulfur compounds, the reactivity of the system remains mostly unchanged. This is in contrast to most other syngas conversion processes, which need rigorous sulfur scrubbing stages before the syngas can be applied. It could lead to significant cost reductions in plant operations when there is no need for such rigorous sulfur removal or if it can be combined with a methanol/ethanol formation step. Further investigations into such a process is outside the scope of this project.

6.13 A final study on alcohol homolgation

Because we did not uncover how trimethylphosphate improves catalysis, it may be useful to look at the homologation product formation. Presenting different substrates to the homologation catalyst and seeing what products are formed from these substrates could provide more background information. In chapter two, isotopic labelling experiments were discussed showing scrambling of the carbons during homologation from from ethanol to propanol. This suggests that from the metal alkyl species rapid β-hydride abstraction and rotation of the alkene can occur before the CO insertion step. This suggests that the CO insertion step is relatively slow. In addition, this metal alkyl/alkene intermediate presents a pathway to the formation of free alkanes and alkenes. The lack of branched alcohols that is found in the product analysis shows that CO insertion always occurs at the 1-position, indicative of high steric influence around the metal centre. We were curious to find out if what products are formed when we present 2-alcohols to the catalyst mixture. Does this lead to alcohol products at the 1-position or does this lead to branched alcohols? To understand the insertion better step

we decided to add 1- and 2-butanol to two separate experiments. The levels of pentanol formed in a regular reaction are very low, so even if the homologation step of larger alkanols is slow, differences are visible in case they occur. Possible product outcomes would be 1-pentanol, 2-pentanol, and perhaps butene and butane if the ruthenium-alkyl is a true intermediate, although there was no good means to quantify the gases. Because 2-butanol overlaps with the internal standard, there is no good quantitative data, but from the GC traces (figure 6.27) it significant effects can be observed.

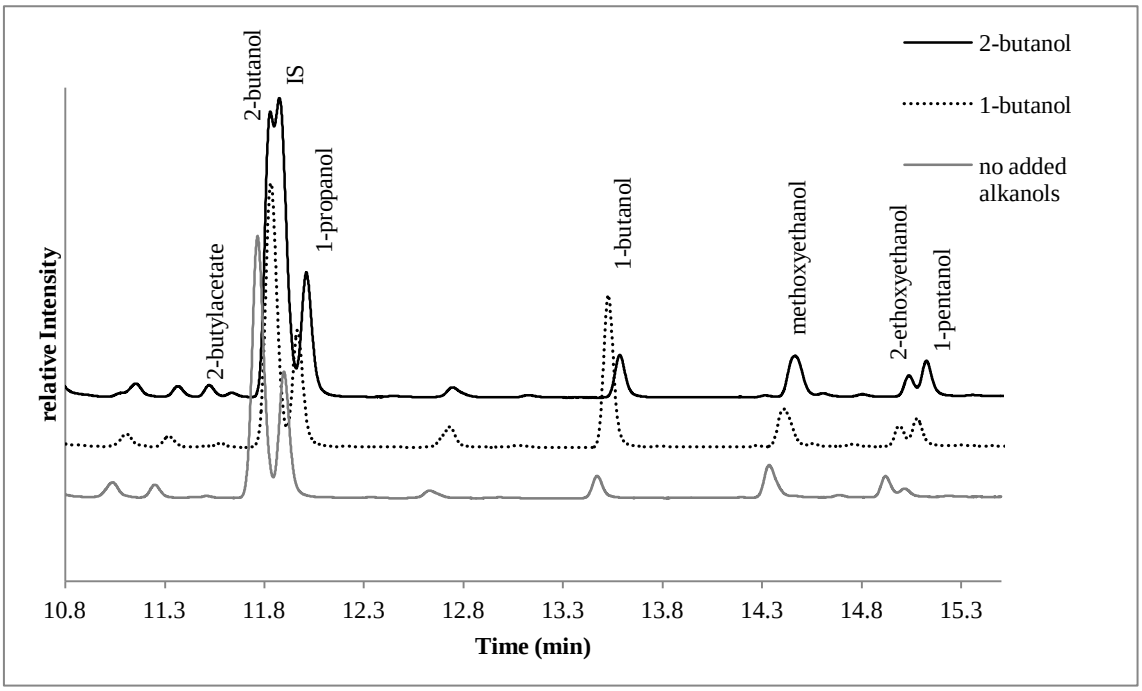

Figure 6.27 The GC trace of reactions with added higher alcohols for homologation. Conditions: $[Ru_3(CO)_{12}]$ (0.25 g), $[PBu_4]Br$ (15 g), HBr (0.75 eq. to Ru), 1-butanol (0.75 eq. to Ru) or 2-butanol (1.5 eq. to Ru), 250 bar syngas ($CO:H_2$ 1:2), 200 ^oC, 4 hr.

For comparison, the GC trace of a reaction without added alkanols was added. This reaction was also used to assess the mass balance as discussed above. There are some interesting outcomes. The addition of 1-butanol at the start of the reaction leads to higher levels of 1-pentanol compared to the reaction without added alcohols. As suspected, the addition of 2-butanol leads to higher levels of 1-pentanol too. This shows that, in the homologation reaction linear alkyl groups migrate preferentially onto CO relative to branched alkyls. It also provides another indication that β-hydride abstraction and double bond isomerisation occurs. We have looked for the presence of 2-methyl-1-butanol, but the levels are very low, barely detectable, and in all reactions the peak intensities are very similar. We were intrigued by the presence of a new significant peak

in the 2-butanol reaction. GC-MS analysis showed that this compound is in fact 2-butylacetate from the esterification of acetic acid and 2-butanol. We also looked at the first set of peaks in the GC which usually contain peaks from a mixture of permanent gases, which GC-MS indicates are C_{1-4} alkanes and alkenes. Especially for these gases the quantification is impossible through this GC because the intensity will also depend on how long the samples have been stored before analysis. The gases escape in the mean time. However, when we look at relative intensities for this set of peaks we can find no significant differences between the set of reactions, indicating no particular compound has a better presence.

Developing a good methodology for analysing the methane content was quite difficult. We could not rely on regular access to microGC equipment operated by other groups, therefore we set out to use our own equipment. Using a gas syringe and a regular GC fitted with the same column for analysis of the liquid samples, operated at a temperature of 40 ^{o}C, we managed to get regularly reproducible peak areas for injected gas mixtures. However, this analysis relied on the peak area for quantification without internal standard. Therefore, the analysis is less precise than with the liquid samples. Furthermore, there was an additional problem where occasionally the rubber septum would not seal sufficiently during injection. This results in considerably lower peak areas as the injected gas is immediately pushed out back through the septum. However, the measurement would often show a clear and significant difference compared to analyses where this was not a problem. Because of this, we cannot use many of the gas phase measurement that were performed near the end of the project, simply because they cannot be trusted. We will discuss the results that we do trust. One set of experiments considered the use of different halides. Earlier it was demonstrated that there are significant differences in both activity and selectivity. For instance, using iodide we get a fast methanol formation step, but the homologation step is very slow. We suspect that ethanol and methane share a common intermediate in their synthetic cycle. Logically, it follows that the catalyst selectivity says something about the relative rates of each step. In other words, going from methanol, at one point an intermediate "chooses" to go towards ethanol or to go to methane, and we suspect it may be the Ru-methyl species. It either undergoes CO insertion to form ethanol, or it undergoes either

(in)direct protonation or reductive elimination with a cis-hydride to form methane. See scheme 6.8.

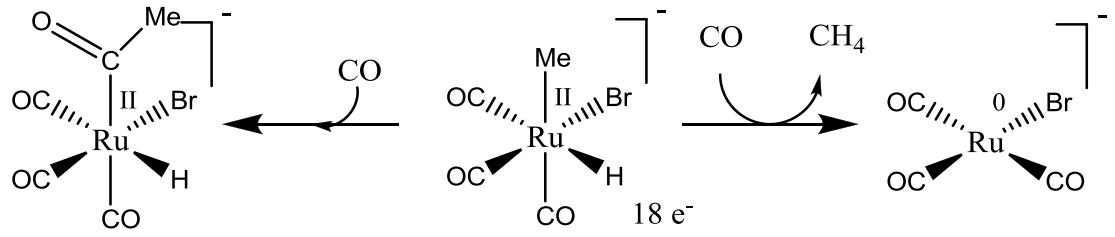

Scheme 6.8 How a proposed common intermediate towards ethanol (to the left) could also lead to methane. Alternatively, direct protonation of the complex in the middle could also lead to formation of methane.

6.13.1 The effect of the halide on methane synthesis

It is a general rule that if the electron density is increased on a metal centre, it is less likely to undergo a reductive elimination reaction. Additionally, if the concentration of free protons is increased, the likelyhood of direct protonation occurring is also increased. It is less clear how to promote CO insertion reactions. However, a very thorough study by Haynes et al.[95] suggest that lowering the electron density on metal carbonyls leads to more electropositive carbonyl carbons, facilitating electrophillic attack of the methyl. Similar work has revealed that 1-electron oxidations can also increase CO insertion steps.[123, 124] This suggests that both reactions should benefit from decreased electron density at the metal centre. Furthermore, because propanol is labelled in both C_1 and C_2 when starting from $^{13}CH_3OH$, we know that, even though it may or may not be a rate limiting step, the CO insertion step must be slow or reversible. To see how changing the halide ion affects the ratio between methane and ethanol formation, we repeated the reactions using $[Ru_3(CO)_{12}]$ and $[PBu_4]X$ where X = Cl, Br, I and measured both the liquid and gaseous product formation. The results are shown in figure 6.28.

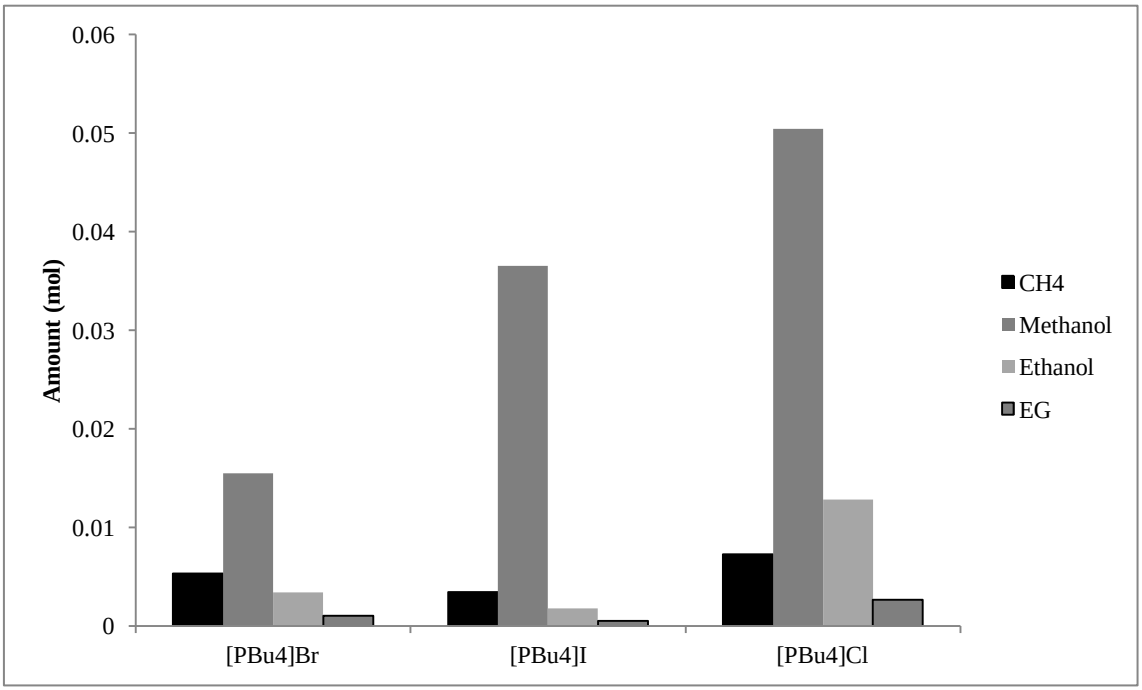

Figure 6.28 the product formation using different halide solvents under equal T/P conditions. Conditions: [PBu_4X] (Cl, 13.0352, Br, 14.9998 g, I, 17.0769 g), [$Ru_3(CO)_{12}$] (0.25 g, 0.125 g using Cl), 250 bar syngas (H_2:CO 2:1), 200 ^oC, 4 hrs.

Besides the interesting properties with respect to the homologation rate, it can be seen that the methane formation follows a similar trend, the higher the rate for homologation, the higher the rate to methane formation. The iodide reaction has very low homologation rates and similarly low amounts of methane were detected. The highest levels of methane were found in the chloride reaction, but overall the rate of the chloride reaction is much higher. It is important to keep in mind that the chloride reaction always had half the amount of catalyst compared to the other reaction, to prevent mass transfer limitations. The most significant figure in comparing these data is the ratio of rate of ethanol formation to the rate of methane formation, as this would tell us something about their relative rates of formation.

Table 6.5. The determined rate constants of the reactions shown in figure 6.28, using case one methodology.

reaction	k_1	k_2	k_3	k_4
Cl	0.0178	0.1210	0.0486	0.0640
Br	0.0061	0.0996	0.0439	0.1477
I	0.0105	0.0249	0.0486	0.0448

A number greater than 1 indicates a higher rate of ethanol formation than methane formation. We have calculated these ratios using the case one model and we can find a trend that the selectivity toward ethanol increases in going from I<Br<<Cl (0.55, 0.67 and 1.89, respectively).

Such a trend is a common feature in halide chemistry and is often attributed to the size or electronegativity of the halide ions. The differences in electronegativity and ionic radii between chloride and bromide are smaller than between bromide and iodide. As a result, a relatively delicate balance between size and electronic properties must cause the changes in activity.

It was decided to see how the ratio of ethanol to methane is affected by changing the catalyst composition. We took the bromide reaction and added 0.625 eq. (to Ru) of HBr at the start of the reaction. This should be enough HBr to change the catalyst composition, but not too much to leave "free" acid.

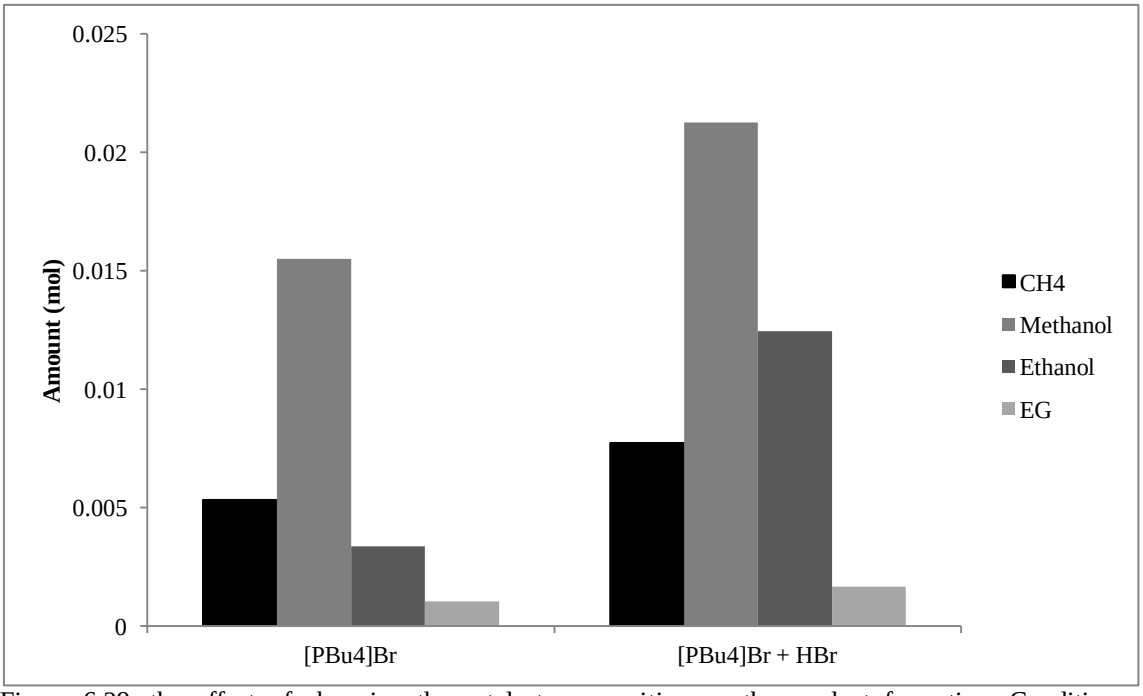

Figure 6.29. the effect of changing the catalyst composition on the product formation. Conditions: $[Ru_3(CO)_{12}]$ (14.9998 g and 14.7016 g), HBr(48% aq. 0 and 99 µL), 250 bar syngas (2:1 (H_2:CO)), 200 ^oC, 4 hrs.

This result shows that changing the catalyst composition increases both homologation and methane formation. However, the rate increase was less profound for

the methane formation compared to the increase in ethanol formation. The ratio between ethanol and methane has now changed from 0.63 to 1.61, which is a promising result.

There is another very interesting conclusion that can be drawn. We suggested earlier, that the same complex was responsible for both methane and ethanol formation through a common intermediate species, and therefore changing the catalyst composition should not alter the selectivity over one or the other. However, we find that it does. We can only conclude that the ruthenium centre that leads to formation of methane is not the same as the species that is responsible for homologation, although they are both formed in the presence of methanol and a bromide source, and they both probably have very similar properties. For instance, the difference may be where we have a species like the centre species in scheme 6.8, with either a hydride and one bromide cis to the methyl or instead two bromide ligands cis to the methyl; the former leading to methane and the latter to ethanol. In this case, the formation of these species would have to be dependent on the catalyst composition or on the level of HBr when these species are formed.

6.14 Extending the HBr series: effect on homologation and methane formation.

The concept of creating two separate reactors for making ethanol from syngas could be very interesting if the efficiency of creating two optimised processes outweighs the difference in building and operating a single reactor with intermediate efficiency. This depends heavily on being able to optimise the homologation step and reduce methane formation. The results from the series where we varied the catalyst composition by adding HBr showed a near linear increase in the homologation rate with increasing HBr levels. We therefore decided to test this reaction separately from the methanol synthesis. We estimated that changing the catalyst composition with levels of 1.5 HBr equivalent to ruthenium should incapacitate methanol formation but may be very good for the homologation step. Therefore, we decided to run a reaction with 5 mL added methanol and 1.5 eq. of HBr to see if we could convert the methanol to ethanol. Furthermore, the results from the gas analysis show that the rate of ethanol formation increases more than the rate of methane formation on addition of HBr. A positive result

would produce a lead for new investigations for future workers. The results are shown in figure 6.30.

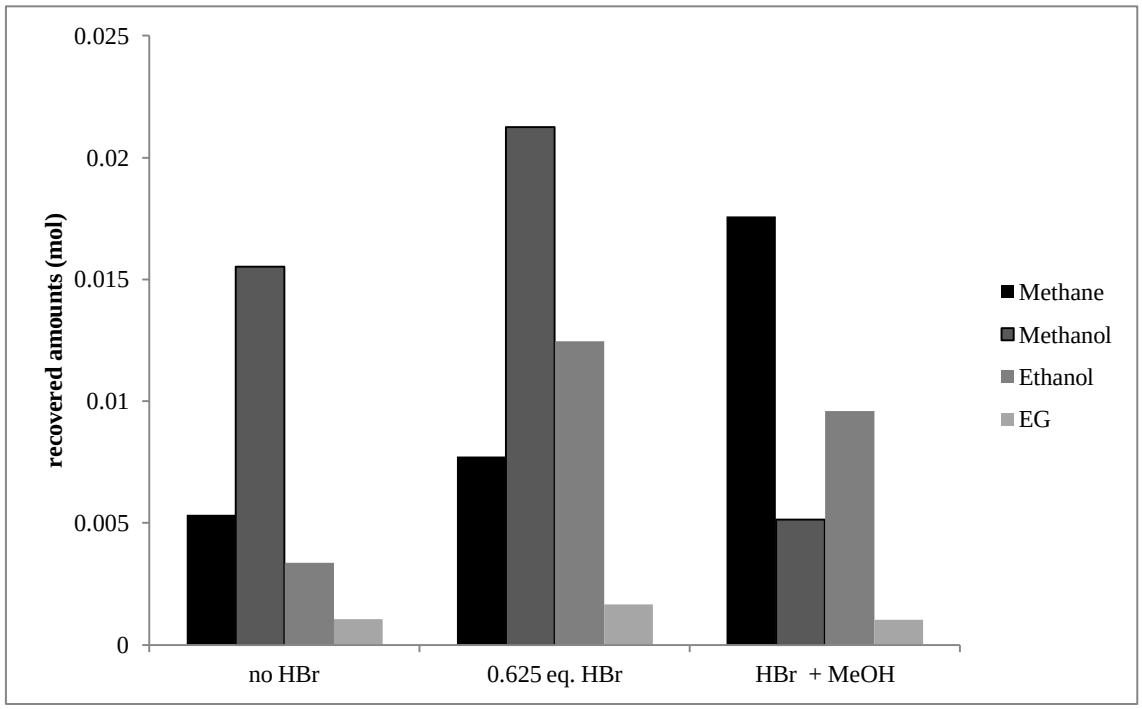

Figure 6.30 the product formation for a homologation reaction (right) in comparison to two control reactions without added methanol. Conditions: For the reactions containing no HBr and 0.625 eq. of HBr see figure 6.29. For the reaction containing 1.5 eq. of HBr: $[Ru_3(CO)_{12}]$ (14.4032 g), HBr(48% aq. 198 µL), Methanol (5 mL), 250 bar syngas (2:1 (H_2:CO)), 200 ^oC, 4 hrs.

Figure 6.30 shows that the reaction with 5 mL of added methanol and 1.5 eq. HBr to Ru leads to formation of ethanol. However, the production of ethanol in the setup designed for homologation is not as large as the production of ethanol in the system with 0.625 eq. of HBr and where no methanol is added. Thus, in the system where methanol is generated in situ, the conversion to ethanol is eventually greater than in the setup where methanol is added from the start. Also, the formation of methane is favoured over the production of ethanol. This is not what we hoped for. The previous trends suggested that the formation of methane should be lowered by changing the catalyst composition. However, the level of methanol is very high from the start. Furthermore, a quick calculation on the mass balance shows that we introduced 0.12 mol of methanol into the reactor, and these products amount to only 0.038 mol, which is significantly less. Inspection of the GC trace shows the formation of other products such as methyl acetate, acetic acid, dimethoxymethane and other products that are usually encountered after ruthenium melt experiments, but not in the amounts that could explain

such a difference. Further, we see significant amounts of dimethyl ether where the peak of dimethyl ether is much larger than the peak for methanol, however we could not quantify the exact amounts as it is a soluble gas at room temperature. The formation of ethers leads to the formation of water, and this in turn shifts CO into H_2. We think that because of this, the homologation step is lower. Furthermore, we think that methane production would benefit from a higher H_2 partial pressure, and that this could explain the difference. Even though the experiment leaves many questions unanswered, we do know that the homologation was not very successful in terms of selectivity. We therefore tried a homologation reaction in the exclusive presence of CO and with added methanol. We reasoned that some methanol would convert to ethers and form water for the synthesis of H_2; the high p_{CO} would lead promote the homologation reaction. However, the outcome of this reaction was a dry paste, indicating that no liquid products are there. The gas analysis showed the formation of high levels of methane and ethers (with the largest component being diethyl ether), but we have no quantitative information. We think that because the gas phase composition was on the opposite spectrum of the WGS equilibrium, there is a significant driving force to produce water in the system, causing the formation of ethers. So in the end, the result is that we form significant amounts of both diethyl ether and methane (similar peak area's) but quantification was not possible, so we cannot tell how the gas phase composition affecting the methane formation or ethanol formation. To return to the previous results, an additional factor in producing the high amounts of methane could be the presence of free acid. Because of the high levels of HBr, significant amounts of free acid could have remained as a result of incomplete formation of $[RuBr_3(CO)_3]^-$, because of an unfavourable equilibrium or lack of $[Ru_3(CO)_{12}]$. This would also explain a high formation of ethers. Additionally, there may be a lack of $[HRu_3(CO)_{11}]^-$ resulting in inefficient transfer of hydrides for the final step in ethanol formation. In order to find an answer to these questions much more research is needed, which are beyond the scope of this project. Instead, we chose to finalise the investigations by exploring the scope of this reaction. For instance, an interesting route from C_1-chemicals to ethanol could be the homologation reaction using dimethyl ether (DME) as a source.

6.15 Using alternative substrates

DME is an interesting choice, as it is easy to obtain and to transport, furthermore it provides a dry environment for catalysis. Because the system is so active for the WGS reaction reducing the amount of water present during catalysis is beneficial for reducing the use of CO as it is immediately converted to CO_2. One source of water is the formation of ethers from methanol in the system. Having large amounts of DME present would prevent this from occurring. Furthermore, it takes half a mol of water to form one mol of methanol. Even though the net reaction from DME to ethanol produces one mole of water for every mole of ethanol formed, it could still present an interesting opportunity to lower the use of CO. However, because dimethyl ether is a difficult gas to handle the exact amount of dimethyl ether that entered the reactor is difficult to estimate. We set up a reactor containing $[PBu_4]Br$, 0.25 g $[Ru_3(CO)_{12}]$ and 1.5 eq. of HBr and purged it using 1:2 syngas. Next we added dimethyl ether using a measuring device for easily compressible gases. The error bar on using this equipment is very high, although the liquid gas can be tracked through windows. This way we aimed for that at least 5 mL of pressurised dimethyl ether entered the reactor, using gravity, but with a low degree of accuracy. The pressure was then further increased using 1:2 CO/H_2 to 150 bar and tested for leaks. The following day the reactor was heated to 200 ^oC and the pressure was topped up to 250 bar using syngas and subsequently stirred for 4 hours under constant pressure. Because the gas analysis is not trustworthy, the most indicative compound to track is the formation of ethanol. A good homologation catalyst would still produce ethanol, and it is interesting to see how much of it is generated, compared to the same reaction where methanol was added. To see the effect of adding HBr we also set-up two reactions where we pre-formed the ruthenium-dimer, $[RuBr_2(CO)_3]_2$ and mixed it with $[Ru_3(CO)_{12}]$ to generated a catalyst composition equal to that after the addition of 1.5 eq. HBr. In this case there should be no free HBr from incomplete formation of the catalyst, at least at the start of the reaction. The product outcome is shown in figure 6.31, we have only included the results for the liquid products.

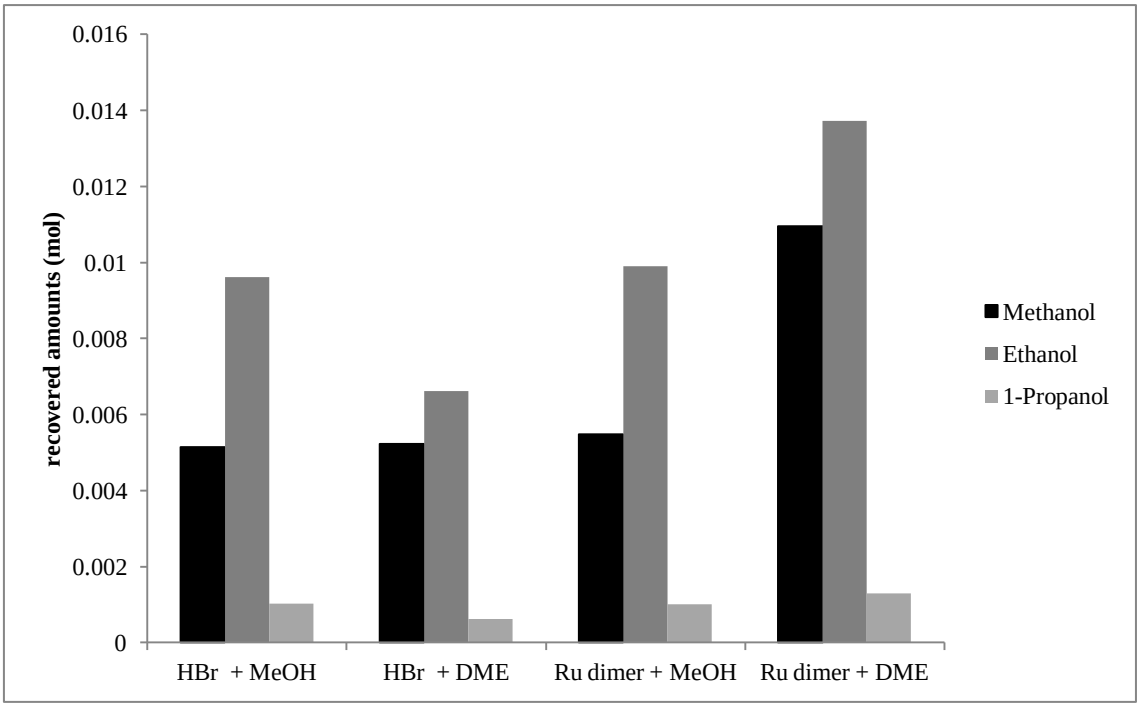

Figure 6.31 The recovered products from three homologation reactions. Conditions:5 mL of Methanol or *ca.* 5 mL of Dimethylether, 198 μL of HBr and $[Ru_3(CO)_{12}]$ (0.25 g) or $[Ru_2Br_4(CO)_6]$ (0.3033 g) and $[Ru_3(CO)_{12}]$ (0.0625 g), 250 bar syngas (H_2:CO 2:1), 200 ^oC, 4 hrs.

Because the level of DME introduced is so uncertain looking at the levels of methanol can be misleading, since it could be a direct result of the amount of DME added. However, the levels of ethanol found after catalysis are a good indication of how well the homologation step occurred. The first observation to be made is that indeed ethanol is formed in the reaction where DME is offered as a substrate. Because we do not know the exact levels of methanol present during the DME reactions there is no point in establishing kinetic constants. This means we cannot tell with precision which is the better homologation system, by comparison of the rate constants. One interesting feature of these experiments is that with the methanol added reactions, the relative levels (compared to methanol) of ethanol are higher than in the reactions using DME. This indicates that formation of methanol from DME is relatively fast compared to the methanol homologation reaction. Presumably, the reaction proceeds by formation of methanol first, which is followed by homologation. Obviously, the data is not conclusive and only hints at this mechanism. Further work could focus on this. With this, we would like to conclude the presentation of the experimental results.

6.16 Experimental Section

See Chapters 2 and 3 for general notes on experimental procedures.

6.16.1 Preparation of [PBu4]I

To a flask fitted with a stirrer and reflux condenser, containing dry and degassed diethylether (100 mL), PBu_3 (135 mL, 110.7 g, 0.547 mol) and subsequently butyl iodide (75 mL, 120.8 g, 0.657 mol) was added and the solution was allowed to stir for 48 hours. This yielded a white precipitate, which was filtered, and then washed 3 times with 100 mL diethylether. The product was then filtered again and dried *in vacuo* to yield a white soft solid (154.8 g, 0.401 mol, 73.2%) ^{1}H NMR (Figure 4.40) (400.13 MHz, CD_3CN, δ (ppm)): 2.19 (8H, m, P-(C**H$_2$**-C_3H_7)$_4$), 1.50 (16H, m, $^3J_{HH}$=7.0 (C3) and 7.2776 (C2), P-(CH_2-C**H**$_2$-C**H**$_2$-CH_3)$_4$) , 0.9579 (12H, t, $^3J_{HH}$ = 6.9 Hz, P-(C_3H_6-C**H**$_3$)$_4$). ^{31}P NMR (figure 4.15), (161.97 MHz, CD_3CN, δ (ppm)): 33.6287 (d, $^2J_{PH}$ = 6.5 Hz, [**P**Bu_4]I) 37.6325 (impurity: sec butyl [PBu_4]I).[a] [PBu_4]I can be stored under N_2 for prolonged times without discoloration.

[a] Internal communication with a manufacturer of [PBu_4]Br

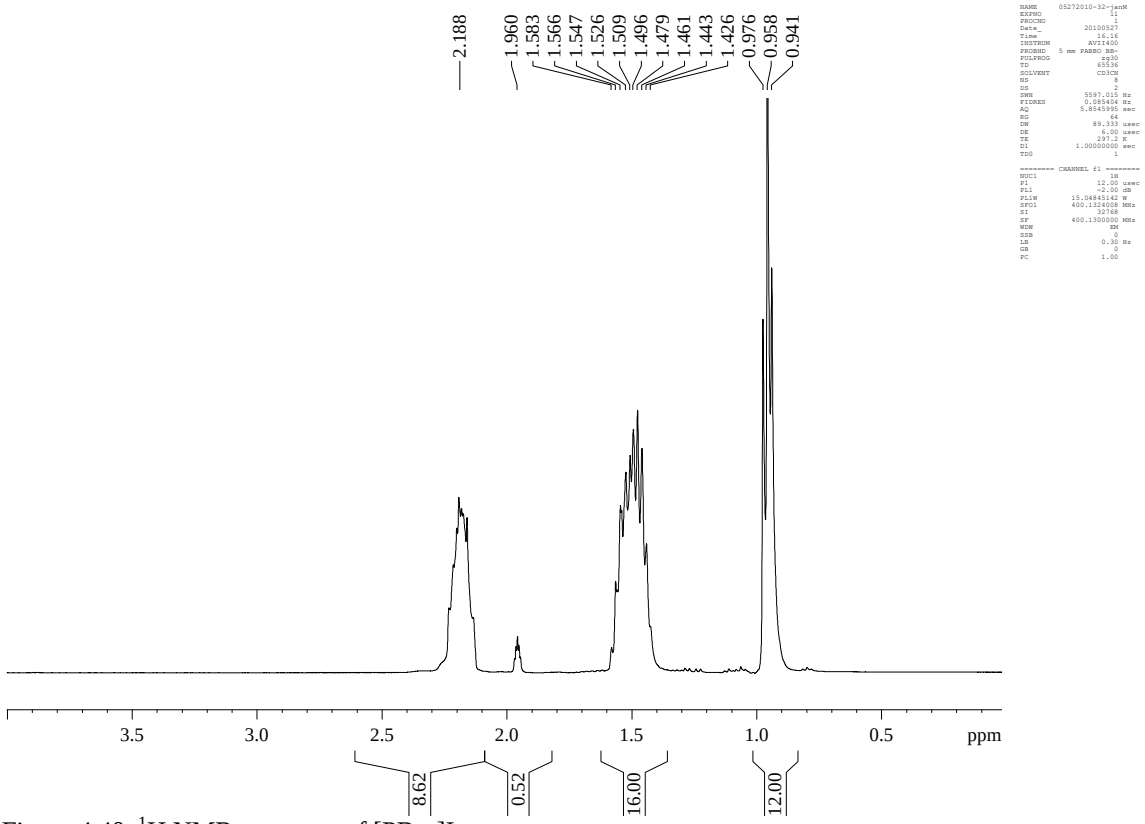

Figure 4.40. ^{1}H NMR spectrum of [PBu_4]I.

6.16.2 Preparation of [PBu4]Cl

To a flask fitted with a stirrer and a reflux condenser, containing dry and degassed diethylether (100 mL) 190.9 mL PBu_3 (154.7 g, 0.764 mol) was added. 96.5 mL of butyl chloride (84.938 g, 0.918 mol) was added and the solution was allowed to stir under reflux for 2 weeks. This yielded very small amounts of crystalline white product. To speed up the reaction the diethylether was stripped off by distillation and the reaction was continued under reflux for 1 and a half days, while the product layer continuously grew in size. The mixture was cooled to room temperature leading to the formation of a solid product layer and this was topped by 50 mL of diethylether (for storage). The diethylether was later decanted and the product was then dissolved in 100 mL of acetone. After addition of 1200 mL of diethylether the product precipitated. The precipitate were filtered and then washed with 3 x 150 mL of diethylether. The precipitate was dried in vacuo to yield white powder (161.8 g, 0.68049 mol, 89%). ^{1}H NMR (Figure 4.41) (400.13 MHz, CD_3CN, δ (ppm)): 2.222 (8H, P-(C**H**$_2$-C_3H_7)$_4$), 1.491 (16H, m, P-(CH_2-C**H**$_2$-C**H**$_2$-CH_3)$_4$) , 0.948 (12H, P-(C_3H_6-C**H**$_3$)$_4$). ^{31}P NMR

(figure 4.16), (161.97 MHz, CD_3CN, δ (ppm)): 33.5471 ([**P**Bu_4]Cl) 37.51 (impurity: sec butyl [**P**Bu_4]Cl).

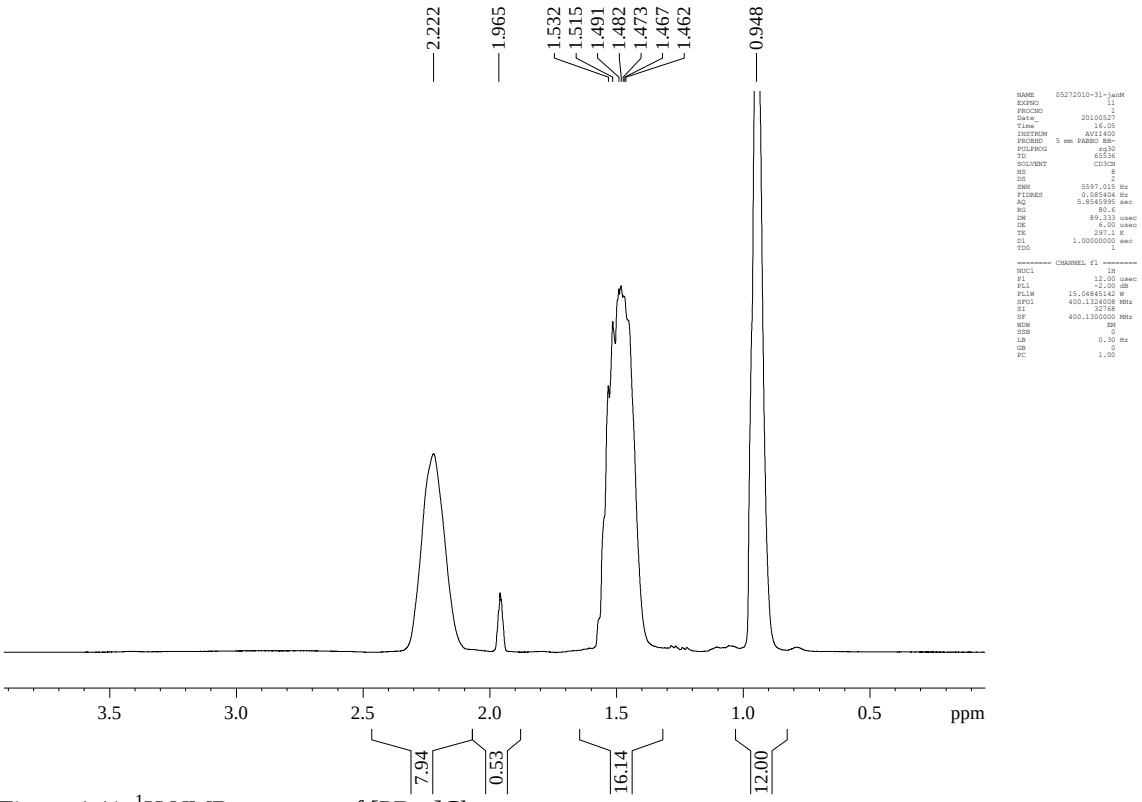

Figure 4.41. ^{1}H NMR spectrum of [PBu_4]Cl.

6.16.3 Preparation of tetrabutylphosphonium triflate

The preparation of [PBu_4][CF_3SO_3] was performed before we knew of the existence of impurities in [PBu_4]Br from the supplier. We used this [PBu_4]Br without purification. In a flask fitted with a stirrer of KCF_3SO_3 (50.233 g, 0.2670 mol) was added to [PBu_4]Br (82.3536 g, 0.2427 mol). The mixture was dissolved in 100 mL of water, and a precipitate was formed almost instantly, but the mixture was stirred overnight. The liquid was decanted and the precipitate was washed 3 times using 30 mL of water. After filtration, the mixture was dried in vacuo yielding off-white solid (97.5 g, 0.239 mol, 98 %).

6.17 The Catalytic runs

6.17.1 General Procedure

The catalytic experiments were performed in the same way as described in the experimental section of chapter 5. Changes in the amounts of used reagents and conditions will be described in the next sections. Table 6.6 shows the used amounts of reagents and the conditions applied. Table 6.7 shows the recovered products after each reaction. For most of these reactions, IR spectra and NMR spectra were taken of the product liquids they can be found in the electronic supplementary. Table 6.6 also shows where the cited reaction is used in the text in order to provide a key between the reaction and the name of the reaction.

Table 6.6.. Used reagents and conditions[a] for the reactions in Chapter 6.

Exp.	$[PBu_4]X$ X=	mass $[PBu_4]Br$ grams	mmol	Promoter	amount of promoter grams/mL	mmol	mass $[Ru_3(CO)_{12}]$ grams	mmol Ru	Promoter/Ru	H_2/CO	Relevant To[b]
jhbr92	Br	0.0000	0.0000	$PBu_4CF_3SO_3$	15.0010	36.7221	0.4994	2.3434	15.67	1	F 6.1
jhbr93	Br	11.9420	35.1924	$PBu_4CF_3SO_3$	3.0577	7.4852	0.5003	2.3476	3.19	1	F 6.1
jhbr94	Br	7.9613	23.4615	$PBu_4CF_3SO_3$	7.0380	17.2288	0.5002	2.3471	7.34	1	F 6.1
jhbr95	Br	3.9803	11.7297	$PBu_4CF_3SO_3$	11.0201	26.9769	0.4993	2.3429	11.51	1	F 6.1
jhbr96	Br	3.1843	9.3839	$PBu_4CF_3SO_3$	11.8153	28.9236	0.4995	2.3439	12.34	1	F 6.1
jhbr97	Br	2.3877	7.0364	$PBu_4CF_3SO_3$	11.6123	28.4266	0.5000	2.3462	12.12	1	F 6.1
jhbr98	Br	2.3881	7.0376	$PBu_4CF_3SO_3$	12.6122	30.8743	0.5002	2.3471	13.15	1	F 6.1
jhbr99	Br	1.5927	4.6936	$PBu_4CF_3SO_3$	13.4084	32.8234	0.4994	2.3434	14.01	1	F 6.1
jhbr100	Br	15.9237	46.9262	-	-	-	0.5000	2.3462	0.00	1	F 6.1
jhbr101	Br	0.7968	2.3481	$PBu_4CF_3SO_3$	14.2036	34.7701	0.5001	2.3467	14.82	1	F 6.1
jhbr210	Br	15.0008	44.2065	-	-	-	0.4999	2.3457	0.00	2	F 6.6
jhbr221	Cl	13.0352	44.2046	-	-	-	0.2495	1.1708	0.00	2	F 6.6
jhbr222	Cl	12.7747	43.3212	HCl 36% aq.	0.0319	0.8738	0.2500	1.1731	0.74	2	F 6.6/30
jhbr226	Br	14.7019	43.3256	HBr 48% aq.	0.0720	0.9008	0.2495	1.1708	0.77	2	F 6.15
jhbr227	Br	14.7012	43.3236	HBr 48% aq.	0.0720	0.9008	0.2502	1.1740	0.77	2	F 6.15
jhbr228	Br	14.7016	43.3248	HBr 48% aq.	0.0720	0.9008	0.2502	1.1740	0.77	2	F 6.15
jhbr229	Br	14.7017	43.3251	HBr 48% aq.	0.0720	0.9008	0.2502	1.1740	0.77	2	F 6.15
jhbr230	Br	14.7012	43.3236	HBr 48% aq.	0.0720	0.9008	0.2497	1.1717	0.77	2	F 6.15

[a] Reaction conditions 200 ^oC, 250 bar total constant pressure, 4 hrs. [b] F= figure, T=table, S=section

Continuation of Table 6.6. Used reagents and conditions[a] for the reactions in this chapter.

Exp.	$[PBu_4]X$ X=	mass $[PBu_4]Br$ grams	mmol	Promoter	amount of promoter grams/mL	mmol	mass $[Ru_3(CO)_{12}]$ grams	mmol Ru	Promoter/Ru	H_2/CO	Relevant To[b]
jhbr231	Cl	13.0210	44.1564	HCl 36% aq.	0.0017	0.0466	0.1254	0.5884	0.08	2	F 6.10
jhbr232	Cl	13.0065	44.1072	HCl 36% aq.	0.0034	0.0932	0.1248	0.5856	0.16	2	F 6.10
jhbr233	Cl	12.9909	44.0543	HCl 36% aq.	0.0054	0.1468	0.1254	0.5884	0.25	2	F 6.10
jhbr234	Cl	12.9488	43.9116	HCl 36% aq.	0.0106	0.2913	0.1253	0.5880	0.50	2	F 6.10
jhbr235	Cl	12.9056	43.7651	HCl 36% aq.	0.0161	0.4427	0.1246	0.5847	0.76	2	F 6.10
jhbr236	Cl	12.8616	43.6159	HCl 36% aq.	0.0212	0.5825	0.1255	0.5889	0.99	2	F 6.10
jhbr237	Cl	12.7747	43.3212	HCl 36% aq.	0.0323	0.8855	0.1249	0.5861	1.51	2	F 6.10
jhbr238	Cl	12.6894	43.0319	HCl 36% aq.	0.0429	1.1767	0.1252	0.5875	2.00	2	F 6.10
jhbr239	Cl	12.5162	42.4446	HCl 36% aq.	0.0641	1.7593	0.1254	0.5884	2.99	2	F 6.10
jhbr240	Cl	12.4297	42.1512	HCl 36% aq.	0.0748	2.0506	0.1252	0.5875	3.49	2	F 6.10
jhbr274	Br	14.7014	43.3242	HBr 48% aq.	0.0713	0.8810	0.2502	1.1740	0.75	2	S 6.12
jhbr277	Br	14.9998	44.2035	-	-	-	0.2496	1.1712	0.00	2	S 6.12
jhbr279	Br	14.7007	43.3221	HBr 48% aq.	0.0713	0.8810	0.2497	1.1717	0.75	2	S 6.12

[a] Reaction conditions 200 ^oC, 250 bar total constant pressure, 4 hrs. [b] F= figure, T=table, S=section

Continuation of Table 6.6. Used reagents and conditions[a] for the reactions in this chapter.

Exp.	[PBu4]X X=	mass [PBu4]Br grams	mmol	Promoter	amount of promoter grams/mL	mmol	mass [Ru3(CO)12] grams	mmol Ru	Promoter/Ru	H2/CO	Relevant To[b]
Jhbr322	Br	14.9998	44.2035	-	-	-	0.25	1.173	-		F 6.30
Jhbr323	Br	14.7016	43.3248	HBr 48% aq	0.099	0.8810	0.2497	1.172	0.752		F 6.30
Jhbr324	I	17.0769	44.2023	-	-	-	0.2499	1.173	-		F 6.28
Jhbr325	Cl	13.0352	44.2046	-	-	-	0.2501	1.174	-		F 6.28
Jhbr337	Br	14.4026	42.4436	HBr 48% aq	0.099	1.7619	0.2497	1.172	1.504		F 6.31
Jhbr348	Br	15.0000	44.2041	HBr 48% aq	0.099	0.8810	0.25	1.173	0.751		F 6.31
Jhbr349	Br	14.9998	44.2035	HBr 48% aq	0.198	1.7619	0.25	1.173	1.502		F 6.31
jhbr353	Br	14.7020	43.3259	HBr 48% aq.	0.0713	0.8810	0.2503	1.1745	0.75	2	F 6.25
jhbr354	I	16.6238	43.0295	HI 55% aq.	0.1497	1.1702	0.2500	1.1731	1.00	2	F 6.7
jhbr356	I	16.8510	43.6176	HI 55% aq.	0.0748	0.5851	0.2501	1.1736	0.50	2	F 6.7
jhbr357	I	16.7381	43.3253	HI 55% aq.	0.1123	0.8777	0.2502	1.1740	0.75	2	F6.7
jhbr358	I	17.0776	44.2041	-	-	-	0.2497	1.1717	0.00	2	F 6.7
jhbr359	I	16.9646	43.9116	HI 55% aq.	0.0374	0.2926	0.2498	1.1722	0.25	2	F 6.7

[a] Reaction conditions 200 ^{o}C, 250 bar total constant pressure, 4 hrs. [b] F= figure, T=table, S=section.

Table 6.7. Recovered material after the reaction (given in mmol).

Exp.	Methanol	Ethanol	Propanol	Butanol	EG	2-methoxy ethanol	2-ethoxy ethanol	methyl acetate	Dimethoxymethane
jhbr92	4.2074	0.1703	nd	0.0045	0.0413	nd	0.0095	nd	nd
jhbr93	22.4157	5.5844	0.4257	0.0691	1.5351	nd	0.1939	0.1374	0.1991
jhbr94	20.0891	3.6857	0.2641	0.0114	1.0962	0.2776	0.0628	0.1751	0.1985
jhbr95	15.6868	1.8477	0.1410	0.0072	0.7675	0.1613	0.0260	0.1203	0.1146
jhbr96	13.1470	1.3677	0.1101	0.0061	0.6120	0.1344	0.0245	0.0814	0.0789
jhbr97	10.7830	0.8604	0.0682	0.0039	0.2989	0.0969	0.0188	0.0719	nd
jhbr98	10.0021	0.8996	0.0742	0.0051	0.5319	0.0949	0.0211	nd	nd
jhbr99	10.0895	0.6330	0.0470	0.0046	0.3219	0.0687	0.0100	nd	nd
jhbr100	24.4405	7.0310	0.4645	0.0010	1.7059	0.4204	0.1387	0.1781	0.1618
jhbr101	7.3960	0.4116	0.0327	0.0040	0.3132	0.0475	0.0187	nd	nd
jhbr210	25.6514	6.7841	0.3115	0.0810	1.9939	0.3262	0.1412	nd	nd
jhbr92	4.2074	0.1703	nd	0.0045	0.0413	nd	0.0095	nd	nd
jhbr221	41.4916	12.2317	1.1989	0.1755	6.0814	1.4134	0.3129	nd	nd
jhbr222	41.5727	16.2487	1.8594	0.2403	4.2137	1.7419	0.3953	nd	nd
jhbr226	21.6134	16.0570	0.8641	0.1632	0.6646	0.3653	0.0284	nd	0.1661
jhbr227	11.7113	15.4483	0.9648	0.1736	1.3016	0.0158	0.0446	nd	nd
jhbr228	12.4342	18.2413	0.9957	0.1378	0.2972	0.0121	0.0314	0.4138	nd
jhbr229	11.9151	17.9666	1.2252	0.1783	0.7396	0.0146	0.0297	0.4080	nd
jhbr230	11.2601	18.4778	1.3078	0.1806	0.2458	0.2937	0.0245	0.4486	nd

Continuation of Table 6.7 Recovered material after the reaction (mmol).

Exp.	Methanol	Ethanol	Propanol	Butanol	EG	2-methoxy ethanol	2-ethoxy ethanol	methyl acetate	Dimethoxymethane
jhbr232	35.5068	9.8753	1.2586	0.1904	2.9401	0.9874	0.2535	0.0785	nd
jhbr233	35.5935	10.4181	0.7913	0.1727	3.4578	1.0542	0.2653	nd	0.2334
jhbr234	35.2946	11.1662	0.9799	0.2131	3.2374	1.1117	0.2982	nd	0.4037
jhbr235	35.2779	12.3172	1.1476	0.2131	4.3886	1.2362	0.3244	nd	0.2574
jhbr236	35.2970	12.6636	1.2622	0.2119	3.9832	1.2782	0.3158	nd	0.2490
jhbr237	31.5942	13.2100	1.6555	0.2281	2.9359	1.1944	0.3385	nd	0.1965
jhbr238	27.2128	13.3818	1.7103	0.2332	2.1510	1.0416	0.3058	nd	0.1546
jhbr239	18.3084	9.5338	1.7343	0.2284	2.1033	0.7493	0.2865	nd	nd
jhbr240	14.9207	7.9759	1.5674	0.1978	0.5891	0.5901	0.2348	nd	nd

Continuation of Table 6.7 Recovered material after the reaction (mmol).

Exp.	Methanol	Ethanol	Propanol	Butanol	EG	2-methoxy ethanol	2-ethoxy ethanol	methyl acetate	Dimethoxymethane
jhbr274	0.6324	0.6187	0.0724	0.0203	0.0221	0.0329	nd	0.0327	nd
jhbr277	14.4817	12.4976	0.6940	0.0500	0.6748	0.2238	nd	0.4939	0.0344
jhbr279	0.9067	1.2163	0.1331	0.0377	0.0241	0.0491	nd	0.0913	nd
Jhbr337	5.2219	6.6220	0.6218	0.1957	0.0166	0.1164	nd	0.4165	0.4341
Jhbr348	5.4879	9.8973	1.0129	0.2409	0.3304	0.1465	nd	0.5694	0.2923
Jhbr354	10.9490	2.5422	0.3373	0.3371	0.2350	0.0998	nd	nd	0.0119
Jhbr337	5.2219	6.6220	0.6218	0.1957	0.0166	0.1164	nd	0.4165	0.4341
Jhbr348	5.4879	9.8973	1.0129	0.2409	0.3304	0.1465	nd	0.5694	0.2923
Jhbr354	10.9490	2.5422	0.3373	0.3371	0.2350	0.0998	nd	nd	0.0119
jhbr353	18.2166	11.7988	0.8029	0.2298	0.6238	0.3876	nd	0.7309	0.1116
jhbr354	10.9490	2.5422	0.3373	0.3371	0.2350	0.0998	nd	nd	0.0119
jhbr356	34.0807	2.9012	0.1769	0.2711	0.4792	0.1344	nd	nd	0.0465
jhbr357	30.2091	3.2490	0.1390	0.2974	0.1323	0.1282	nd	nd	0.0209
jhbr358	25.7900	1.2282	0.0935	0.2537	0.1953	0.0756	nd	nd	0.0330
jhbr359	30.5327	1.8170	0.1057	0.3159	0.1756	0.1072	nd	nd	0.0346

6.18 Conclusion

In this chapter we have tried to expand our knowledge on how the catalytic system behaves by addition of various promoters, changing the halide in the solvent and by changing the concentration of bromide in the system by replacing it with triflate.

Reducing the concentration of bromide in the system is not beneficial to catalysis, the halide must play an essential role in catalysis. Quite possibly an important catalyst contains one or more halide ions as ligands.

Exchanging bromide for chloride and iodide, significantly alters the behaviour of the catalysts. Using the iodide as a halide leads to a system that is particularly selective for the methanol synthesis, but not for the methanol homologation step. The bromide halide system is the most selective for the methanol homologation step. The chloride halide system is by far the most productive catalytic system, where both the rate for methanol formation and the rate for methanol homologation are very high.

The system containing iodide seems very susceptible to the presence of HI. However, this does not lead to a very significant increase in the levels of ethanol formed. However, it does lead to an improvement of the overall reaction rates.

In contrast, using HCl in $[PBu_4]Cl$ does not rapidly lead to the expected change in the catalytic composition from $[HRu_3(CO)_{11}]^-$ to $[RuCl_3(CO)_3]^-$. As a result, the reaction rates are not influenced as much. However, using higher levels of HCl will eventually result in promotion of the system. IR studies showed that good conversion to $[RuCl_3(CO)_3]^-$ is reached upon addition of 3.5 eq. of HCl to ruthenium. Yet, the homologation step is not increased as much as in the HBr series.

In addition, we have studied the change in spectroscopic properties of each catalytic mixture after catalysis and compared them to the activity for CO conversion. Because $[HRu_3CO)_{11}]^-$ does not contain any halides, it must be $[RuX_3(CO)_3]^-$ that leads to the biggest difference in catalysis. The CO absorptions of the carbonyls in this complex shows that the for the chloride complex there is the least amount of backbonding. This makes the carbonyls both more labile and subject to lesser "umpolung". Studies on changing the partial pressures of CO and H_2 could show more

insight, because if the CO pressure is higher this should change the effective "lability" of these carbonyls.

Furthermore, the effect of the presence of phosphate during catalysis was studied. In similar, but not the same, systems this promoter has proven to be very effective in promoting homologation and ethanol formation. We have reproduced those results and we have shown that the system needs a threshold minimum of 0.5 equivalents of phosphate to ruthenium to be effective. Interestingly, IR studies on the product liquids have not shown changes in catalytic composition. However, ^{1}H NMR spectra of the hydride region have shown that indeed the nature of the hydride species has changed and we can relate the increase in homologation with the rise of an unknown compound that has different chemical shifts upon changing the halide in the system. Future investigations into the homologation step should involve studies into the identity and action of this species.

Furthermore, we have tried to understand the action of trimethylphosphate or phosphoric acid on the catalytic system by testing compounds with similar structural features as promoters in our system. We have found that we could not imitate the action of trimethylphosphate by the addition of dimethylsulfate or dimethylcarbonate. However, we have found that the system is able to cope with the presence of sulfate ions even though many other catalysts for syngas conversion cannot.

In the final section the focus was on the conversion of methanol. We have demonstrated that, by the addition of primary and secondary alcohols, homologation can occur with higher alcohols, and also secondary alcohols, but the product is the linear 1-C_{n+1} alcohol.

Our next efforts went to determining the amount of methane formed in the system. Using a microGC for our analysis we have found that the selectivity for methane formation is the highest for the bromide system and the lowest for the iodide system and intermediate for the chloride system. Furthermore, we have tried to establish the methane formation in context to the methanol homologation step. Unfortunately, we have not achieved a good analysis technique capable of doing so, so we have focussed on the liquid product formation.

A system that has a near excess of HBr causes the reaction rate of the system for methanol to come to a halt. However, the system is still active for methanol homologation, as predicted by measuring the rate constants for homologation throughout the HBr series in Chapter 5. We have discovered that this system is also very active for methane synthesis, as it appears the selectivity for methane is much higher than for ethanol. This is not the case for a system where less HBr is added and this suggest that because we do not change the actual catalytic species, but rather the composition, the species that catalyses methane formation is different from the species that catalyses ethanol formation.

We have further shown that using instead of HBr, a mixture of mainly $[RuBr_2(CO)_3]_2$ and a little of $[Ru_3(CO)_{12}]$ also leads to an active system for homologation with comparable results in ethanol formation.

In the final section, we have used DME instead of methanol as a starting material for homologation. This also leads to the production of ethanol.

Chapter 7
Conclusions and Future work

In the first chapter we present an overview of the current literature of the field of homogeneous syngas conversion towards alcohols.

To start our investigations we first invested time and effort to overcoming reproducibility problems, which were solved by the use of methanol as a washing solvent. We then proceeded to develop a good GC technique for analysing the liquid components of the product mixtures. The choice for our internal standard was a difficult one because of the crowded nature of the GC spectrum, we established that acetonitrile was a good choice. Further, we identified most of the components by GC MS techniques and then enabled quantification by using the same column with FID detection. We performed initial NMR and IR analysis on the catalytic species. We found that the use of $[Ru_3(CO)_{12}]$ and RuO_2 lead to the same spectrum of products, however with minor differences in the amounts of product made. We found that RuO_2 has increased formation of C_{4+} alcohols and that these alcohols are all made from gas phase CO, and not via free methanol or degradation of $[PBu_4]Br$. While methanol incorporation leads to the formation of the lower alcohols. The primary product of $Ru/[PBu_4]Br$ syngas synthesis is methanol which is incorporated into nearly every other product that is formed during catalysis, except for ethylene glycol. We further found that the homologation of methanol to ethanol leads to conservation of the methanol carbon into the methyl group of ethanol. However, in going from ethanol to propanol, scrambling of the label occurs between C_2 and C_3, indicating that a Ru-alkyl species is an intermediate towards the CO inserted product. The alkyl species can undergo β-hydride abstraction and alkenene rotation about the bond axis before the hydride is added again and migration onto CO occurs. The stepwise formation of products in the $Ru/[PBu_4]Br$ system with free methanol as an intermediate leads to a possible way to dissect the set of reactions and investigate each reaction independently. Furthermore, it enables individual optimisation and overall flexibility in tuning the product outcome of the set of reactions that coincide in the $Ru/[PBu_4]Br$ system.

In chapter 3 we investigated parts of the gas phase behaviour of the Ru/[PBu_4]Br system. Increasing the pressure by addition of N_2 did not increase the rate of catalysis. However, addition of CO_2 did lead to an increase of the rate of catalysis, although we do not understand why this is the case. Subsequently, the WGS reaction activity of the Ru/[PBu_4]Br system was examined by running reactions with a starting gas phase composition at various points along the WGS equilibrium. We found that all reaction reached equilibrium positions before the end of the 4 hour reaction time. To get a better insight into how fast the equilibrium was reached we repeated one example and sampled the gas phase composition over time. After one hour the equilibrium had been reached. Interestingly, we still saw methanol formation, even though the partial pressure of CO was close to 6 bar in one of the reactions. If we start from a system with only CO_2 and H_2 we achieve the 6 bar of CO (equilibrium position) fairly quickly and still form methanol (methanol from H_2 and CO_2). In addition to syngas and CO_2, the presence of significant levels of methane was detected after the reaction. Subsequent labelling studies showed that at least a part of this methanol must be generated by the conversion of free methanol.

In the following chapter, we moved on to establishing the order in CO and H_2 for both the methanol formation and homologation reaction. In order to do so we developed such tool for quantifying the rates of methanol formation and homologation. Even though the method relies heavily on crude assumptions (i.e. the rate constants of each reaction remain equal over time, the homologation reaction is first order in methanol/ethanol and the gas phase composition remains constant over time) it gives consistent results and a good starting point for assessing the relative rates of the individual reactions. We find that some of the initial assumptions do not hold up. For instance, the reaction rates do not remain constant over time, but this effect is less significant if the reaction times are shorter than 6 hours.

We used the kinetic model to estimate the rates of each reaction and compared them with the changing partial pressures of CO and H_2 to establish the orders. The rate of methanol formation is mostly dependent on p_{H2} and therefore increasing the hydrogen partial pressure leads to higher rates. The homologation reaction is highly dependent on the p_{CO} and this leads to "conflicting interests" between the two reactions.

The results suggest that the best method of operation would be to use two consecutive reactors for the tandem operation of turning syngas into ethanol. In the first reactor the system is optimised for methanol formation by the use of high H_2 pressures and low CO pressures to increase the rate. In the second reactor the methanol from the first reactor is converted into ethanol under relatively high CO pressures, using lower H_2 pressure. Using the WGS reaction as a driving force the generation of ethers with the release of water can be promoted. This process may also be used for product separation. Alternatively, rather than using methanol, the C_1 source can be dimethyl ether which can be converted to either ethanol or diethylether depending on the process requirements. One notable advantage for this is that per two conversions of methanol two molecules of water are formed while per single conversion of DME only one molecule of water is formed.

In the process of developing and testing the kinetic tool we also found an inconsistency in the overall activity of the Ru/$[PBu_4]$Br system upon changing batches of $[PBu_4]$Br. We traced this inconsistency back to the presence of $[HPBu_4]$Br in the $[PBu_4]$Br. We subsequently found a method for removing the impurity and determine how the levels of $[HPBu_3]$Br affect the rates of catalysis. The levels of $[HPBu_3]$Br promote methanol formation only if the concentration of it remains in between 0 and 0.8 equivalents to the amount of ruthenium in the system. From this we can infer that a change in the catalyst takes place by the addition of $[HPBu_3]$Br to the system. Furthermore, there is a colour change in the product mixture and the IR spectra show a change in composition of the catalysts. By IR analysis of the product mixtures we conclude that in the CO hydrogenation reactions, $[HPBu_3]$Br acts to convert $[HRu_3(CO)_{11}]^-$ into $[Ru(CO)_3Br_3]^-$ and both of these ruthenium complexes are required for active catalysis. By examining more closely the action of $[HPBu_3]$Br and the effect it has on the catalytic species. We find that $[HPBu_3]$Br breaks up during catalysis and acts as a phosphine and HBr source. The phosphine has little action on the catalysis other than reacting with $[RuBr_3(CO)_3]^-$ or a precursor to $[RuBr_3(CO)_3]^-$, rendering it inactive and removing ruthenium away from an active form in the catalytic cycle. Excess PBu_3 may also react with methyl bromide to form $[MePBu_3]$Br.

The HBr shifts the composition of the ruthenium species towards more $[RuBr_3(CO)_3]^-$. Based on the correlation between the presence of this species and the rate of homologation we assume that this species plays an important role in the homologation reaction. However, when we promote the formation of this species by the addition of an excess of HBr we can see the catalytic activity of the system drop significantly due to a lack of $[HRu_3(CO)_{11}]^-$. This supports Dombek's finding that there is a hydride donor and a hydride acceptor needed for intermolecular hydrogenation of CO, and for the homologation.

We then moved on to examine the effect of the halide anion in the solvent (and ligand for $[RuX_3(CO)_3]^-$). We find that using the chloride anion significantly increases the overall activity of the system. However, addition of HCl does not change the catalyst composition as dramatically as adding HBr or HI does. On the other hand, using iodide and HI as a promoter does not lead to a very significant increase in the homologation reaction rate, while addition of HBr does. This can be related to the activity of $[RuBr_3(CO)_3]^-$ compared to $[RuI_3(CO)_3]^-$. The iodide version is much less active for homologation than the bromide version. For chloride the picture is more complicated as ruthenium seems less reactive towards HCl than it is to HBr. This leads to a higher presence of "free HCl" in the promoted reactions, which can cloud any measurements relating species to rates. We feel that the presence of free protons in the solution may significantly influence the reaction mechanism.

In the following section, we decided to look more closely to the homologation reaction. We have assessed how the system responds to the presence of phosphate during catalysis. In similar, but not the same, systems this promoter has proven to be very effective in promoting homologation and ethanol formation. We have found the same results and we have shown that the system needs a threshold minimum of 0.5 equivalents of phosphate to ruthenium to be effective. Interestingly, IR studies on the product liquids have not shown changes in catalytic composition. However, ^1H NMR spectra of the hydride region have shown that indeed the nature of the hydride species has changed and we can relate the increase in homologation with the rise of an unknown compound that has different chemical shifts upon changing the halide in the system. We have tried to understand the action of trimethylphosphate or phosphoric acid on the

catalytic system by testing compounds with similar structural features as promoters in our system. We have found that we could not imitate the action of trimethylphosphate by the addition of dimethylsulfate or dimethylcarbonate. However, we have found that the system is able to cope with the presence of sulfur even though many other catalysts for syngas conversion cannot. We have concluded the studies by suggesting a possible mechanism wherein the phosphate ion plays a central role in activation of the methyl group by ruthenium and subsequent CO activation for insertion into the ruthenium methyl group. Finally, we have shown that, by the addition of primary and secondary alcohols, homologation can occur with higher alcohols, and also secondary alcohols, but the product is the linear 1-C_{n+1} alcohol.

We have further shown that using instead of HBr, a mixture of mainly $[RuBr_2(CO)_3]_2$ and a little of $[Ru_3(CO)_{12}]$ also leads to an active system for homologation with comparable results in ethanol formation. Finally, we tried the conversion of dimethyl ether as a precursor of methanol towards ethanol and we find that the system is also active for this reaction. In this way we limit the amount of water that is present during catalysis and this reduces "loss" of CO towards CO_2.

7.1 Future work

Because the CO conversion catalysed by $[Ru_3(CO)_{12}]$ in phosphonium halides leads to a stepwise production of oxygenates it will be necessary to investigate each reaction separately. The first step is the synthesis of free methanol or formaldehyde, followed by rapid reduction. The second catalytic step is the conversion of methanol to I) ethanol, II) methane and III) ethanoic acid. Except for methane, the compounds are further derivatised towards ethers (from alcohols) and esters (from alcohols and carboxylic acids) by the medium under the standard reaction conditions. The synthesis of methanol from syngas is well-developed using CuZnO catalysts, under much cheaper conditions. Therefore, economic reasons for the development of this chemistry for methanol production do not really exist at the current time. However, scientifically speaking the formation of methanol by homogeneous catalysts is very interesting. First of all, we suggest to complete a full analysis mass balance of the reaction products including all the gas phase components. This could be very difficult but well

worthwhile. From there, the identity of all the unknown inorganic species would be desired in order to come closer to identifying active species in the catalytic cycle.

It would be very good to relate catalytic species to the rate of methane formation, and to establish the orders in all reactants for the methane formation. At the same time, they can be established more elaborately for the ethanol formation step and this may lead to ways to favour the ethanol formation step over methane formation.

Possibly, a combination of MS techniques and generation and assessment of all organometallic species present during catalysis should help with this. Furthermore, for methanol formation we suggest performing experiments to determine more precisely the rate constants and orders in each species that is identified and present during catalysis. This would enable an improvement of the model of the system and more accurately pinpointing where theory does not agree with practice. Establishing the reaction order in: p_{CO}, p_{CO2}, p_{H2}, water $[HRu_3(CO)_{11}]^-$ and $[RuX_3(CO)_3]^-$ and the unknown species for methanol formation may be very useful for determining which species plays a role in the mechanistic cycles of catalysis.

Additionally, we suggest determining the rate of diffusion of each gas into the phosphonium ionic liquids. Where the diffusion is very slow, surface kinetics may need to be modelled. Furthermore, it may be interesting to develop the methanol formation reaction on silica, alumina or other suitable surfaces (SILP). In this case the surface area of the ionic liquid may be greatly enhanced. To prevent leaching of the liquid phase it may be necessary to adjust the hydrophobicity of the phosphonium salt. We suggest establishing the same parameters for the synthesis of EG. Most likely, the kinetic parameters and factors can be determined in the same set of experiments.

The use of SILP has been investigated by Wasserscheid for the catalysis of the WGSR using very similar systems. We suggest expanding upon this set reactions by using phosphonium salts. It would be desirable to determine more accurately the rate constants and orders for the WGS reaction so to achieve better accuracy for modelling.

For the homologation reaction, it would be particularly interesting to verify one of the suggested mechanisms, or alternatively to reject them on the basis of

experimental analysis. Therefore, we also suggest establishing the kinetic parameters and orders for p_{CO}, p_{CO2}, p_{H2}, water, $[HRu_3(CO)_{11}]^-$, $[RuX_3(CO)_3]^-$, MeBr and/or or other methyl halides and even methylphosphates. It may be advantageous to prepare a set of ruthenium compounds and react them step by step with reagents such as methanol, MeBr, trimethylphosphate, CO and H_2 to see if they react. Furthermore, it may be interesting to determine the rate of formation of methyl bromide or other methyl halides from methanol or dimethyl ether in phosphonium halides, with or without the presence of phosphoric acid or trimethylphosphate. Determination of the full catalytic cycle may point to slow steps (for instance CO migration) which could be improved upon using suitable promoters. The catalytic cycle should be in accordance with the orders and kinetic constants found in the rate order studies. This should also lead to clarification of the mechanism of promotion by phosphoric acid.

Not of direct interest for most companies, but nonetheless important in this system is also the elucidation of the mechanism of formation of methane. If any of these applications are to be used on a large scale the synthesis of methane should be minimised in order to prevent loss of the methanol. We suggest the same approach as with all of the above mentioned research topics.

All of these suggestions should lead to full kinetic understanding of the methanol formation, the methanol homologation and the methane formation in this system. This enables full modelling of the reactions and constrain the optimisation time of each reaction. Furthermore, this information will lead to better understanding of the mechanism and possibly lead to improvements in the catalysts and the catalytic cycle.

List of Abbreviations

BPR	back pressure regulator
BuOH	butanol
CO	carbon monoxide
EG	ethylene glycol
EtOH	ethanol
FID	flame ionisation detector
F-T	Fischer-Tropsch
GC	gas chromatography
HexOH	hexanol
IR	Infrared (spectroscopy)
MeOH	methanol
MFC	mass flow controller
MS	mass spectrum
NMP	N-methylpyrrolidinone
NMR	Nuclear Magnetic Resonance
PeOH	pentanol
PPN	bis(triphenylphosphine)iminium
PrOH	propanol
RWGS	reversed water-gas-shift
SILP	supported ionic liquid phase
TG	tetraglyme
THF	tetrahydrofuran
WGS	water-gas-shift

References

1. W. Keim, *Pure Appl. Chem.*, 1986, **58**, 825-832.
2. V. Subramani and S. K. Gangwal, *Energy & Fuels*, 2008, **22**, 814-839.
3. E. I. A. US Department of Energy, http://tonto.eia.gov/dnav/pet/hist/LeafHandler.ashx?n=PET&s=RBRTE&f=D.
4. J. S. Bradley, *J. Am. Chem. Soc.*, 1979, **101**, 7419-7421.
5. J. S. Bradley, G. B. Ansell and E. W. Hill, *J. Am. Chem. Soc.*, 1979, **101**, 7417-7419.
6. J. S. Bradley, G. B. Ansell and E. W. Hill, *J. Organomet. Chem.*, 1980, **184**, C33-C35.
7. B. D. Dombek, *J. Am. Chem. Soc.*, 1980, **102**, 6855-6857.
8. B. D. Dombek, *Abstr. Am. Chem. Soc.*, 1980, **180**, 208-INOR.
9. B. D. Dombek, *Abstr. Am. Chem. Soc.*, 1981, **182**, 19-Inde.
10. B. D. Dombek, *J. Am. Chem. Soc.*, 1981, **103**, 6508-6510.
11. J. F. Knifton, *J. Am. Chem. Soc.*, 1981, **103**, 3959-3961.
12. W. Keim, M. Berger and J. Schlupp, *J. Catal.*, 1980, **61**, 359-365.
13. W. Keim, M. Berger, A. Eisenbeis, J. Kadelka and J. Schlupp, *J. Mol. Catal.*, 1981, **13**, 95-106.
14. J. W. Rathke and H. M. Feder, *J. Am. Chem. Soc.*, 1978, **100**, 3623-3625.
15. J. R. Blackborow, R. J. Daroda and G. Wilkinson, *Coord. Chem. Rev.*, 1982, **43**, 17-38.
16. W. F. Gresham,DuPont de Nemours, 1951, GB 655-237.
17. W. F. Gresham,DuPont de Nemours, 1955, CA 516932.
18. P. Chini, G. Longoni, V. G. Albano, F. G. A. Stone and W. Robert, in *Advances in Organometallic Chemistry*, Academic Press, 1976, pp. 285-344.
19. E. L. Muetterties, *Angew. Chem., Int. Ed. Engl.*, 1978, **17**, 545-558.
20. E. L. Muetterties, *Science*, 1977, **196**, 839-848.
21. E. L. Muetterties, W. R. Pretzer, M. G. Thomas, B. F. Beier, D. L. Thorn, V. W. Day and A. B. Anderson, *J. Am. Chem. Soc.*, 1978, **100**, 2090-2096.
22. K. G. Caulton, M. G. Thomas, B. A. Sosinsky and E. L. Muetterties, *Proc Natl Acad Sci U S A*, 1976, **73**, 4274-4276.
23. E. L. Muetterties, *Bull. Soc. Chim. Belg.*, 1976, **85**, 451-470.
24. F. A. Cotton and R. M. Wing, *Inorg. Chem.*, 1965, **4**, 314-317.
25. *CRC Handbook of Chemistry and Physics*, CRC Press, Boca Raton, 2008.
26. E. L. Muetterties, *Pure Appl. Chem.*, 1978, **50**, 941-950.
27. M. G. Thomas, B. F. Beier and E. L. Muetterties, *J. Am. Chem. Soc.*, 1976, **98**, 1296-1297.
28. K. Jonas, D. J. Brauer, C. Krueger, P. J. Roberts and Y. H. Tsay, *J. Am. Chem. Soc.*, 1976, **98**, 74-81.
29. J. S. Bradley, G. B. Ansell and E. W. Hill, *J. Organomet. Chem.*, 1980, **184**, C33-C35.
30. B. F. G. Johnson, J. Lewis, S. W. Sankey, K. Wong, M. McPartlin and W. J. H. Nelson, *J. Organomet. Chem.*, 1980, **191**, C3-C7.
31. G. C. Demitras and E. L. Muetterties, *J. Am. Chem. Soc.*, 1977, **99**, 2796-2797.
32. R. L. Pruett, *Science*, 1981, **211**, 11-16.
33. R. L. Pruett, *Proc Natl Acad Sci U S A*, 1977, **295**, 239-248.

34. R. L. Pruett and W. E. Walker,Union Carbide, 1974, 3-833-634.
35. L. Kaplan,Union Carbide Corporation, 1976, US 3-944-588.
36. L. Kaplan,1979, US 1-537-850.
37. J. L. Vidal and W. E. Walker, *Inorg. Chem.*, 1980, **19**, 896-903.
38. A. Fumagalli, T. F. Koetzle, F. Takusagawa, P. Chini, S. Martinengo and B. T. Heaton, *J. Am. Chem. Soc.*, 1980, **102**, 1740-1742.
39. J. V. Doorn and C. Masters,1977.
40. M. J. Doyle, A. P. Kouwenhoven, C. A. Schaap and B. van Oort, *J. Organomet. Chem.*, 1979, **174**, C55-C58.
41. W. Keim, M. Anstock, M. Roper and J. Schlupp, *C1 Mol. Chem.*, 1984, **1**, 22-32.
42. D. R. Fahey, *J. Am. Chem. Soc.*, 1981, **103**, 136-141.
43. R. C. Williamson and T. P. Kobylinski,Gulf.
44. L. C. Costa, *Catalysis Reviews-Science and Engineering*, 1983, **25**, 325-363.
45. C. P. Casey, M. A. Andrews and D. R. McAlister, *J. Am. Chem. Soc.*, 1979, **101**, 3371-3373.
46. B. D. Dombek, *J. Am. Chem. Soc.*, 1979, **101**, 6466-6468.
47. R. Whyman, *J. Organomet. Chem.*, 1973, **56**, 339-343.
48. J. F. Knifton,Texaco, GB2024811

49. B. D. Dombek, *J. Organomet. Chem.*, 1983, **250**, 467-483.
50. J. D. Cotton, M. I. Bruce and F. G. A. Stone, *J. Chem. SOC. (A)*, 1968, 2162.
51. M. J. Cleare and W. P. Griffith, *J. Chem. Soc. A*,, 1969, 372 - 380.
52. S. H. Han, G. L. Geoffroy, B. D. Dombek and A. L. Rheingold, *Inorg. Chem.*, 1988, **27**, 4355-4361.
53. C. E. Kampe, N. M. Boag, C. B. Knobler and H. D. Kaesz, *Inorg. Chem.*, 1984, **23**, 1390-1397.
54. J. W. Koepke, J. R. Johnson, S. A. R. Knox and H. D. Kaesz, *J. Am. Chem. Soc.*, 1975, **97**, 3947-3952.
55. G. Lavigne and H. D. Kaesz, *J. Am. Chem. Soc.*, 1984, **106**, 4647-4648.
56. S. D. Barratt and D. J. Cole-Hamilton, *J. Chem. Soc.*, 1985, 1559.
57. J. P. Collman, J. N. Cawse and J. I. Brauman, *J. Am. Chem. Soc.*, 1972, **94**, 5905-5906.
58. W. F. Edgell and J. Lyford, *J. Am. Chem. Soc.*, 1971, **93**, 6407-6414.
59. K. P. Schick, N. L. Jones, P. Sekula, N. M. Boag, J. A. Labinger and H. D. Kaesz, *Inorg. Chem.*, 1984, **23**, 2204-2207.
60. B. N. Chaudret, D. J. Cole-Hamilton, R. S. Nohr and G. Wilkinson, *J. Chem. Soc., Dalton Trans.*, 1977, 1546 - 1557.
61. S. D. Barrat and D. J. Cole-Hamilton, *J. Chem. Soc.*, 1985, 458.
62. S. D. Barrat and D. J. Cole-Hamilton, *J. Chem. Soc.*, 1984, 1209.
63. G. Smith and D. J. Cole-Hamilton, *J. Chem. Soc., Dalton Trans.*, 1984, 1209.
64. J. P. Collman and S. R. Winter, *J. Am. Chem. Soc.*, 1973, **95**, 4089-4090.
65. D. S. Barratt and D. J. Colehamilton, *J. Organomet. Chem.*, 1986, **306**, C41-C44.
66. C. P. Casey and S. M. Neumann, *J. Am. Chem. Soc.*, 1977, **99**, 1651-1652.
67. K. M. Doxsee and R. H. Grubbs, *J. Am. Chem. Soc.*, 1981, **103**, 7696-7698.
68. J. F. Knifton,Texaco, 1981, US4265828.
69. J. F. Knifton,Texaco, 1982, US4356332.

70. J. F. Knifton, *J. Chem. Soc., Chem. Commun.*, 1983, 729-730.
71. B. D. Dombek, *Organometallics*, 1985, **4**, 1707-1712.
72. B. K. Warren and B. D. Dombek, *J. Catal.*, 1983, **79**, 334-347.
73. H. Ono, K. Fujiwara, M. Hashimoto, E. Sugiyama and K. Yoshida, *J. Mol. Catal.*, 1989, **57**, 113-123.
74. H. Ono, K. Fujiwara, M. Hashimoto, H. Watanabe and K. Yoshida, *J. Mol. Catal.*, 1990, **58**, 289-297.
75. J. F. Knifton, *Platinum Met. Rev.*, 1985, **29**, 63-72.
76. D. J. Cole-Hamilton, M. F. Sellin and P. B. Webb, *Chem. Comm.*, 2001, 781-782.
77. D. J. Cole-Hamilton and P. B. Webb, *Chem. Comm.*, 2004, 612-613.
78. D. J. Cole-Hamilton, P. B. Webb, M. F. Sellin, T. E. Kunene, S. Williamson and A. M. Z. Slawin, *J. Am. Chem. Soc.*, 2003, **125**, 15577-15588.
79. D. J. Cole-Hamilton, M. F. Sellin, I. Bach, J. M. Webster, F. Montilla, V. Rosa, T. Aviles and M. Poliakoff, *J. Chem. Soc., Dalton*, 2002, 4569-4576.
80. J. R. Zoeller, *Catalysis Today*, 2009, **140**, 118-126.
81. J. M. S. S. EsperancÌ§a, J. N. Canongia Lopes, M. Tariq, L. s. M. N. B. F. Santos, J. W. Magee and L. s. P. N. Rebelo, *J. Chem. Eng. Data*, 2009, **55**, 3-12.
82. B. D. Dombek and A. M. Harrison, *J. Am. Chem. Soc.*, 1983, **105**, 2485-2486.
83. S.-H. Chun, T. B. Shay, S. E. Tomaszewski, P. H. Laswick, J.-M. Basset and S. G. Shore, *Organometallics*, 1997, **16**, 2627-2630.
84. E. A. Seddon and K. R. Seddon, *The chemistry of Ruthenium*, Elsevier, Amsterdam, 1984.
85. D. Worsley and A. Mills, *Ultrasonics*, 1992, **30**, 333-341.
86. J. F. Knifton, R. A. Grigsby and J. J. Lin, *Organometallics*, 1984, **3**, 62-69.
87. J. F. Knifton,Texaco, 1982, US4315993 (A).
88. D. J. Cole-Hamilton, U. Hintermair, Z. X. Gong, A. Serbanovic, M. J. Muldoon and C. C. Santini, *Dalton Transactions*, 2010, **39**, 8501-8510.
89. S. Werner, N. Szesni, A. Bittermann, M. J. Schneider, P. HÃ¤rter, M. Haumann and P. Wasserscheid, *Appl. Catal., A*, **377**, 70-75.
90. S. Werner, N. Szesni, A. Bittermann, M. J. Schneider, P. Härter, M. Haumann and P. Wasserscheid, *Appl. Catal., A*, **377**, 70-75.
91. S. Werner, N. Szesni, M. Kaiser, R. W. Fischer, M. Haumann and P. Wasserscheid, *ChemCatChem*, **2**, 1399-1402.
92. T. W. Dekleva, D. Forster, H. P. D.D. Eley and B. W. Paul, in *Adv. Catal.*, Academic Press, 1986, pp. 81-130.
93. D. Forster, *J. Chem. Soc., Dalton*, 1979, 1639-1645.
94. N. Yoneda, S. Kusano, M. Yasui, P. Pujado and S. Wilcher, *Appl. Catal., A*, 2001, **221**, 253-265.
95. A. Haynes, P. M. Maitlis, G. E. Morris, G. J. Sunley, H. Adams, P. W. Badger, C. M. Bowers, D. B. Cook, P. I. P. Elliott, T. Ghaffar, H. Green, T. R. Griffin, M. Payne, J. M. Pearson, M. J. Taylor, P. W. Vickers and R. J. Watt, *J. Am. Chem. Soc.*, 2004, **126**, 2847-2861.
96. I. Wender, *Fuel Proc. Tech.*, 1996, **48**, 189-297.
97. J. S. Bradley,Exxon, 1983, US4421862.
98. H. Dumas, J. Levisalles and H. Rudler, *J. Organomet. Chem.*, 1980, **187**, 405-412.
99. J. L. Vidal,Union Carbide, 1990, US4954665

100. J. C. Slaa, J. G. van Ommen and J. R. H. Ross, *Catalysis Today*, 1992, **15**, 129-148.
101. G. A. Mills, ed. U. D. o. Energy, 1993.
102. M. G.Alex, *Fuel*, 1994, **73**, 1243-1279.
103. M. Hidai and H. Matsuzaka, *Polyhedron*, 1988, **7**, 2369-2374.
104. N. Isogai and K. Tanaka, *J. Organomet. Chem.*, 1990, **397**, 101-107.
105. J. Pursiainen, K. Karjalainen and T. A. Pakkanen, *J. Organomet. Chem.*, 1986, **314**, 227-230.
106. K. G. Moloy and R. W. Wegman, *J. Chem. Soc., Chem. Comm.*, 1988, 820-821.
107. J. F. Knifton,Texaco, 1986, US4605677 (A).
108. K. Watanabe, K. Kudo and N. Sugita, *Bull. Chem. Soc. Jpn.*, 1985, **58**, 2029-2037.
109. E. Lindner, a. Scheytt and P. Wegner, *J. Organomet. Chem.*, 1986, **308**, 311-323.
110. D. F. Gill, B. E. Mann and B. L. Shaw, *J. Chem. Soc., Dalton*, 1973, 311-317.
111. H. Ono, K. Fujiwara, M. Hashimoto, H. Watanabe and K. Yoshida, *J. Mol. Catal*, 1990, **58**, 289-297.
112. D. S. Barratt and D. J. Cole-Hamilton, *J. Chem. Soc.*, 1985, 1559-1560.
113. M. R. Netherton and G. C. Fu, *Org. Lett.*, 2001, **3**, 4295-4298.
114. A. A. Nunez-Magro, L. M. Robb, P. J. Pogorzelec, A. M. Z. Slawin, G. R. Eastham and D. J. Cole-Hamilton, *Chem. Sci.*, 2010, **1**, 723-730.
115. D. J. Cole-Hamilton, A. J. Rucklidge, G. E. Morris and A. M. Z. Slawin, *Helv. Chim. Acta*, 2006, **89**, 1783-1800.
116. H. Ono, M. Hashimoto, K. Fujiwara, E. Sugiyama and K. Yoshida, *J. Organomet. Chem.*, 1987, **331**, 387-395.
117. D. S. Barratt, C. Glidewell and D. J. Cole-Hamilton, *J. Chem. Soc., Dalton*, 1988, 1079-1081.
118. Y. Kiso, M. Tanaka, H. Nakamura, T. Yamasaki and K. Saeki, *J. Organomet. Chem.*, 1986, **312**, 357-364.
119. P. Jaunky, H. W. Schmalle, M. Alfonso, T. Fox and H. Berke, *J. Organomet. Chem.*, 2004, **689**, 801-810.
120. W. F. Gresham,DuPont, 1953, US2636046.
121. W. Desloges, A. A. Neverov and R. S. Brown, *Inorg. Chem.*, 2004, **43**, 6752-6761.
122. M. J. Belousoff, M. B. Duriska, B. Graham, S. R. Batten, B. Moubaraki, K. S. Murray and L. Spiccia, *Inorg. Chem.*, 2006, **45**, 3746-3755.
123. T. C. Forschner and A. R. Cutler, *Organometallics*, 1985, **4**, 1247-1257.
124. M. J. Wax and R. G. Bergman, *J. Am. Chem. Soc.*, 1981, **103**, 7028-7030.